IAEA-TECDOC-949

Thermophysical properties of materials for water cooled reactors

INTERNATIONAL ATOMIC ENERGY AGENCY IAEA

June 1997

The IAEA does not normally maintain stocks of reports in this series. However, microfiche copies of these reports can be obtained from

INIS Clearinghouse
International Atomic Energy Agency
Wagramerstrasse 5
P.O. Box 100
A-1400 Vienna, Austria

Orders should be accompanied by prepayment of Austrian Schillings 100,— in the form of a cheque or in the form of IAEA microfiche service coupons which may be ordered separately from the INIS Clearinghouse.

The originating Section of this publication in the IAEA was:

Nuclear Power Technology Development Section
International Atomic Energy Agency
Wagramerstrasse 5
P.O. Box 100
A-1400 Vienna, Austria

THERMOPHYSICAL PROPERTIES OF MATERIALS FOR WATER COOLED REACTORS
IAEA, VIENNA, 1997
IAEA-TECDOC-949
ISSN 1011-4289

© IAEA, 1997

Printed by the IAEA in Austria
June 1997

FOREWORD

The IAEA Co-ordinated Research Programme (CRP) to establish a thermophysical properties data base for light and heavy water reactor materials was organized within the framework of the IAEA's International Working Group on Advanced Technologies for Water Cooled Reactors. The work within the CRP started in 1990. The objective of the CRP was to collect and systematize a thermophysical properties data base for light and heavy water reactor materials under normal operating, transient and accident conditions. The important thermophysical properties include thermal conductivity, thermal diffusivity, specific heat capacity, enthalpy, thermal expansion and others. These properties as well as the oxidation of zirconium-based alloys, the thermophysical characteristics of high temperature concrete-core melt interaction and the mechanical properties of construction materials are presented in this report. The thermophysical properties of a broad spectrum of reactor and construction materials, such as fuel cladding, absorber, structural materials, concretes, light and heavy water and gases, are presented over a wide range of temperature. Experimental methods and the test facilities used for the thermophysical property measurements are described in supplements.

It is hoped that this report will serve as a useful source of thermophysical properties data for water cooled reactor analyses. The properties data are maintained on the THERSYST system at the University of Stuttgart, Germany and are internationally available.

The IAEA staff members responsible for this activity were V. Krett and J. Cleveland of the Nuclear Power Technology Development Section, Division of Nuclear Power and the Fuel Cycle.

EDITORIAL NOTE

In preparing this publication for press, staff of the IAEA have made up the pages from the original manuscript(s). The views expressed do not necessarily reflect those of the governments of the nominating Member States or of the nominating organizations.

Throughout the text names of Member States are retained as they were when the text was compiled.

The use of particular designations of countries or territories does not imply any judgement by the publisher, the IAEA, as to the legal status of such countries or territories, of their authorities and institutions or of the delimitation of their boundaries.

The mention of names of specific companies or products (whether or not indicated as registered) does not imply any intention to infringe proprietary rights, nor should it be construed as an endorsement or recommendation on the part of the IAEA.

CONTENTS

1. INTRODUCTION

The Co-ordinated Research Programme (CRP) on "Thermophysical Properties Data Base for Light and Heavy Water Reactor Materials" was organized in the framework of the IAEA's International Working Group on Advanced Technologies for Water Cooled Reactors (IWGATWR).

This IWG serves as a forum for exchange of information on national programmes, provides advice to the IAEA on international cooperative activities in advanced technologies in water cooled reactors, and supports the conduct of these activities.

Institutes which have participated in this CRP are:

- Institute of Atomic Energy, Beijing, China
- Nuclear Research Institute, Řež, Czech Republic
- University of Stuttgart, Stuttgart, Germany
- Bhabha Atomic Research Centre, Mumbai, India
- High Energy Density Research Centre, Russian Academy of Science, Moscow, Russian Federation
- Institute of Physics and Power Engineering, Obninsk, Russian Federation
- Boris Kidrič Institute of Nuclear Sciences, Yugoslavia (through 1991).

The report developed by the CRP has been independently reviewed in a collaborative effort between the IAEA and the US DOE's International Nuclear Safety Center at Argonne National Laboratory (ANL), and between the IAEA and the Atomic Energy of Canada, Ltd. (AECL). These independent technical reviews have been carried out to ascertain that there are no inconsistencies in related parameters and that the presented properties are consistent with accepted data. Furthermore, additional data have been provided to the CRP by ANL and by AECL.

The data base on reactor materials presented in this report, except for the data base for light and heavy water, is incorporated into the existing THERSYST data base system established at Stuttgart University in Germany. This database is described in Supplement S5. This data base can be obtained through a special request addressed to the Stuttgart University.

The description of the Chinese data base TPSYS is presented in Supplement S6.

Regarding future nuclear power, a key conclusion of the IAEA Symposium on Advanced Nuclear Power Systems (Republic of Korea, October 1993) was that advanced water cooled reactors currently undergoing development and design review will, in the short and medium term, be the main contributor to any revival of nuclear power. While the early development of nuclear power was conducted to a large extent on a national basis, the cooperation demonstrated by institutes contributing to establishment of this thermophysical properties data base is an example of the increased level of international cooperation in reactor technology.

2. PURPOSE, OBJECTIVES AND SCOPE OF THE CO-ORDINATED RESEARCH PROGRAMME

The objective of the CRP has been to collect and systematize a thermophysical properties data base for light and heavy water reactor materials under normal operating, transient and accident conditions. The materials properties considered include those needed for light and heavy water reactor operational and safety assessments. The materials have been grouped within the following categories:

- nuclear fuels,
- cladding materials,
- absorber materials,
- structural materials,
- coolants,
- gases.

The thermophysical properties included in the database are:

- thermal conductivity,
- thermal diffusivity,
- specific heat,
- enthalpy,
- heat of melting,
- coefficient of thermal expansion (linear for solids, volume coefficient for fluids),
- emittance,
- density (and porosity, as a parameter defining sintered materials),
- equation of state.

The data on thermal conductivity, thermal diffusivity, coefficient of thermal expansion, and emittance of solid materials were collected from room temperature to their melting points. The specific heat, enthalpy, and density for the same category of materials are also important and were collected from room temperature to a temperature exceeding their melting temperatures by approximately 100 K.

The THERSYST database system developed at the University of Stuttgart in Germany for storage, handling, and presentation of thermophysical properties data was adopted as the system for maintaining the reactor materials thermophysical properties database. The data base on reactor materials documented in this report, except for the data base for light and heavy water, is included in the THERSYST system. This data base can be obtained through a special request addressed to the University of Stuttgart.

The CRP was carried out through research agreements with institutes in Russian Federation and research contracts with China, Czech Republic, Germany, India and the former Yugoslavia. The research contract with the institute in Yugoslavia was cancelled in 1992 due to the UN restrictions.

The chief Scientific Investigators from the participating countries/institutes have been:

- Hanming Xu, Institute of Atomic Energy, China
- J. Jakab, Nuclear Research Institute, Czech Republic
- G. Neuer, G. Jaroma-Weiland, Universität Stuttgart, IKE, Germany
- V. Venkat Raj, Bhabha Atomic Research Centre, India
- V. Fortov, High Energy Density Research Center, Russian Academy of Sciences, Russian Federation
- V. Bobkov, Russian Research Center, Institute of Physics and Power Engineering, HEMATIC, Russian Federation
- K. Maglic, Boris Kidrič Institute of Nuclear Sciences, Yugoslavia.

3. ACTIVITIES AND CONTRIBUTIONS OF PARTICIPATING INSTITUTIONS

This chapter contains a summary of activities and contributions of the participating institutions.

3.1. ACTIVITIES OF PARTICIPATING INSTITUTIONS

The ***China Institute of Atomic Energy (CIAE), Beijing, China*** was founded in 1950, and has played an important role in the Chinese nuclear industry. CIAE consists of 7 departments with a total staff of about 4,000. The major research areas are briefly described as follows:

- Nuclear reactor design and safety analysis, which includes reactor physics, thermal hydraulics, nuclear fuel cycle management, severe accident analysis, Probabilistic Safety Analyses (PSA), and nuclear materials.
- Nuclear physics research with accelerator.
- Nuclear waste management.
- Application of isotopes and medical isotopes production.
- Scientific computing for reactor design.
- Development and production of various nuclear equipment.
- Health physics research.

A working group consisting of five people was set up since 1990 for the research work which has been contributed to this CRP.

The ***Nuclear Research Institute (NRI), Řež***, since its foundation in 1955, has played a leading role in nuclear research in former Czechoslovakia and now in the Czech Republic. At present the work of NRI Řež is mainly concerned with:

- technical research and development work in the field of nuclear power and technology,
- co-ordination of projects involving research work on nuclear safety, integrity of reactor components, reactor materials, reactor physics and technology, radioactive waste management, development and production of radio-pharmaceuticals and selected aspects of the utilization of ionizing radiation,
- function as the Central Analytical Laboratory for the inspection of nuclear materials for guarantee purposes,
- function as the Technical-Economical Information Center for nuclear research.

Research work is performed in five divisions of:

- nuclear power and safety
- reactor materials
- fuel cycle chemistry
- reactor physics
- radionuclides

and in the central analytical laboratory and the research reactor laboratory.

From January 1993 the NRI became a joint-stock company, owned by the largest Czech energy and nuclear industry companies and by the State. At present the total staff strength is approximately 690 persons, of which nearly 300 are university graduates.

The ***Institute for Nuclear Technology and Energy Systems (IKE), Universität Stuttgart, Germany*** is engaged in teaching as well as in interdisciplinary research on nuclear and non-nuclear energy, with emphasis on energy technology economics. IKE is comprised of 7 divisions with a staff of 156, including 98 scientists. The major areas of research and development in the various divisions are:

- integrated systems for planning and simulation of complex plants and systems; design, simulation and optimization of heat supply systems and components,

- reactor safety analysis; safety technology; modelling, simulation and analysis of severe hypothetical reactor accidents,
- sampling and processing of experimental data; information and data management systems; expert systems; computer networks
- research and development of heat transfer and storage systems; thermophysical properties of solids: measurements, data base.

The thermophysical research group (part of the Division of Energy and Heat Transfer Technology) consists of seven scientists and two technicians. Its main task is the study of thermal conductivity, specific heat capacity and emissivity of solid materials. Experimental investigations and literature evaluations are carried out in order to make reliable data available for thermal calculations by means of the data base THERSYST which has been developed for storage, handling and presentation of thermophysical properties data of solid materials. Data published in the literature as well as measured at IKE are stored in the data base. The structure and features of THERSYST are described in Supplement S5.

The ***Bhabha Atomic Research Centre (BARC), Mumbai, India*** is the major nuclear energy research centre in India. It is a Government organization located in Mumbai, conducting research related to various facets of nuclear energy and employs more than 13,000 engineers, scientists and technicians. While the major thrust is related to R&D for nuclear power programmes, particularly thermal reactors, research related to isotope applications, physical and chemical sciences, materials sciences, electronics and instrumentation, biology, medicine and agriculture is also being carried out. The work relevant to thermal reactors deals mainly with pressurized heavy water reactors (PHWRs) and encompasses areas such as design analysis, development of computer codes, materials research, nuclear fuel cycle, development and testing of components, safety research, ageing and qualification studies, waste management. An advanced heavy water reactor with passive safety features is also being designed. The safety research work includes experimental and theoretical studies in thermal hydraulics, plant dynamics, PSA, development of simulators, operator support systems, studies related to Design Basis Accidents and Beyond Design Basis Accidents.

At the ***High Energy Density Research Center (HEDRC), Moscow*** of the Russian Academy of Sciences experimental investigations of thermophysical and mechanical properties of reactor materials are carried out over a wide range of temperatures and pressures, up to extremely high values which occur in severe accidents in nuclear power plants (NPP) as in the case of a core melt accident, or steam and gas explosions or high-velocity impact on structural elements of the reactor. The HEDRC has ~500 employees, of which ~350 are university graduates. The HEDRC has a number of experimental facilities which make it possible to carry out investigations on the thermophysical and mechanical properties of fuel materials, absorbing and structural reactor materials, including concretes, in liquid and solid phases. At the HEDRC the physical models and computer codes for the protective containment of the nuclear reactor, the effect of the melt of reactor materials and the impact and detonation effects are being developed. The calculation of nuclear reactor behaviour during normal operation and accident conditions is based on thermophysical and mechanical properties data of reactor materials obtained from the facilities at the centre.

The ***Institute of Physics and Power Engineering (IPPE)***, Obninsk, Russia is involved in work related to nuclear power stations. One of main tasks of IPPE is the safety of nuclear power stations with water cooled and liquid metal-cooled reactors and the technology of construction materials. The institute has a broad data base on the thermophysical properties of materials for advanced water cooled reactors.

3.2. CONTRIBUTIONS OF PARTICIPATING INSTITUTIONS TO THE CRP

The *China Institute of Atomic Energy* has contributed to the project mainly in the following aspects:

- Collection of thermophysical properties of uranium-aluminium alloy.
- Collection of data on thermal conductivity and diffusivity of uranium.
- Collection of data on thermal conductivity and diffusivity of uranium dioxide fuel.

- Collection of data on melting heat and normal total emittance of zirconium +2.5% niobium.
- Development of a personal-computerized thermophysical properties data base management system TPSYS.

Data under these items are collected through the following ways:

- From literature and publications.
- From experiments performed within China.
- Arranging special new experiments during the period of the research contract for some data.
- By theoretical prediction or extrapolation.

The work performed at the *Nuclear Research Institute (NRI) Řež*, within the scope of this CRP has been oriented towards the collection of data characterizing the oxidation properties of zirconium based alloys in a high temperature steam environment. This CRP is in close connection with the wider research programme of NRI, dealing with the programme of assessing safety aspects of reactors in situations beyond normal operational conditions. The programme covers topics such as the behaviour of fuel elements in an accident situation up to fuel melting and analyses of severe accidents.

The contributions of NRI to the CRP consist of:

- collection of data on zirconium based alloys oxidation properties for temperatures above ~900°C. These data have been obtained from literature sources covering the last two decades.
- development of a mathematical model for zirconium alloys oxidation kinetics. This model has been verified on a wide variety of oxidation experiments - from simple "isothermal" oxidation to complex transient oxidation with varying temperatures.
- providing oxidation properties for Zr-1%Nb alloy-cladding material of WWER-type fuel elements. Experiments on this alloy oxidation have been performed in the Institute of Nuclear Fuels, Zbraslav near Prague under contracts with NRI, Řež.

Within the framework of the CRP, the thermophysical properties of nuclear materials have been collected and stored in THERSYST, developed in the *Institute for Nuclear Technology and Energy Systems (IKE)*, Stuttgart, Germany.

In order to find the data published so far, a computer search in the bibliographic data banks Chemical Abstracts, INIS and METADEX was carried out. The properties covered were:

- thermal conductivity and thermal diffusivity,
- specific heat capacity and enthalpy,
- linear thermal expansion and density
- emittance.

The search was carried out for the following material groups:

- fuels: U, U-Al-alloy, UO_2, $(U,Gd)O_2$, $(U,Pu)O_2$,
- cladding: Zircaloy-2, Zircaloy-4, ZrO_2-layers on Zircaloy, Inconel 718 and other Ni-base alloys,
- absorber materials: B_4C and Ag-Cd-In alloys,
- structural materials: austenitic stainless steels; Zr-2.5%Nb-alloy.

Altogether 145 publications were found. They have been evaluated and the data have been stored in THERSYST. To find the newest publications, a computer search of the literature data bases has been made every year during the CRP. The bibliographic information on evaluated papers is listed in Chapter 4.

The work within this CRP at the *Bhabha Atomic Research Centre* was carried out at the Reactor Safety Division. The responsibility of BARC was in the area of thermophysical properties of light and heavy water. An extensive literature survey was carried out and over 75 publications were studied. It was found that over the last few years substantial advances have been made in the measurement of thermophysical properties of light and heavy water.

Wide ranging formulations have evolved for these properties based on the published data and the work of the International Formulation Committees. In 1984, the International Association for Properties of Steam (IAPS), adopted the IAPS-1984 formulations for the thermodynamic properties of ordinary water for scientific and general use and the IAPS-1984 formulations for the thermodynamic properties of heavy water. In the years 1982 and 1985 the IAPS released the formulations and amended formulations for the viscosity and thermal conductivity of both heavy and light water.

These IAPS formulations, which cover the entire range of interest, have the advantage of avoiding the combination of piecewise limited range equations. Also they ensure consistency of all thermodynamic properties over the entire range of validity. These formulations have been adopted for developing computer programmes, in FORTRAN-77, for the prediction of thermodynamic and thermophysical properties of light and heavy water. In the case of heavy water, the upper limit of the range of validity of IAPS formulations is around 800 K. These formulations have been used to predict the properties over the extended range up to 800°C.

The *High Energy Density Research Center, Moscow* contributed to the CRP in the following aspects:

- Thermophysical properties of refractory concretes-zirconium dioxide concrete and alumina concrete.
- Thermophysical properties of silicate concrete.
- Concrete-core melt interaction.
- Mechanical properties of steels.

Data have been collected from literature and by experimental investigations.

The investigations were carried out in the following facilities:

- Facilities for investigating the thermal expansion of electrically conducting and insulating materials up to 2600 K, using high-frequency induction heating and resistance furnace heating.
- Facilities for investigating radiant and optical properties at high temperatures, using electrical heating.
- A facility for investigating electrical resistance, enthalpy, heat and temperature of phase transitions, and specific volume of metals, alloys and graphite by means of the fast electrical explosion of samples.
- A facility for investigating heat capacity, melting points and heat of melting, emissivity of materials in solid and liquid phases by means of the slow electrical explosion of samples.
- A facility for investigating the interaction between the melts of reactor materials and concretes, using induction heating.
- Benches with metallic and ferrum-concrete explosion chambers.
- A powder gun bench.

The *Institute of Physics and Power Engineering, Obninsk, Russia* has submitted experimental data to the CRP on thermophysical properties of

- light water and steam,
- gases: hydrogen, helium, xenon, krypton,
- gaseous mixture,
- metallic uranium,
- zirconium dioxide,
- boron carbide.

4. THERMOPHYSICAL PROPERTIES OF SOLID MATERIALS

Recommended data for the thermophysical properties of nuclear materials have been published in the MATPRO-publications. The last issue of MATPRO-data [RT000063][1], from 1990, contains descriptions of material properties subroutines available in that data base. The adequacy of the available data on the appropriate physical and chemical properties of some nuclear materials has been reviewed in the report EUR-12404 [RT000062][2] published by the Commission of European Communities. Furthermore, a variety of other recommendations have been made for the thermal conductivity and specific heat capacity of fuels. All these recommendations are listed as relations in the original form given by the author.

All data stored in THERSYST are the originally published data relative to the temperature scale in use at the time of the measurements. There has been no conversions from the 1948 International Practical Temperature Scale (IPTS) to the 1968 IPTS or to the 1990 IPTS. The data are represented in this chapter in graphical form showing the thermophysical property as a function of temperature. To each figure belongs a table in which the parameters of influence (descriptors) for that property are listed. The actual status of the data base for reactor material is presented in Table 4.1. A complete list of descriptors used in this chapter is given in Table 4.2.

Furthermore the experimental data on the thermophysical properties of metallic uranium have been evaluated in the Material Properties Data Base Center HEMATIC (IPPE, Obninsk). The recommended relations are given in Section 4.1.1. and Supplement S7. Additional relations for ZrO_2 and B_4C have been supplied by HEMATIC and they are listed in the corresponding sections. Data for accident conditions on some physical properties of uranium are given in Supplement S7.

Experimental and additional data from the literature on uranium-aluminium alloy and zirconium-based alloys were supplied by CIAE (Beijing, China). These data are listed in corresponding sections.

---

[1] RT000063 HOHORST J. K. (Editor), "SCDAP/RELAP5/MOD2 Code Manual, vol.4: MATPRO- a library of materials properties for light-water-reactor accident analysis", NUREG/CR-5273 (1990)

[2] RT000062 HARDING J. H., MARTIN D. G., POTTER P. E., "Thermophysical and thermochemical properties of fast reactor materials", EUR 12402EN (1989), 1-90

Table 4.1 ACTUAL STATUS OF DATA BASE FOR REACTOR MATERIALS (THERSYST 15.04.94)

MATERIAL NAME	PROPERTIES						SUM
	THC	CP	ENT	LEX	DEN	EMI	
uranium	66	6	3	24	-	21	120
aluminium-uranium alloy	3	-	-	4	-	-	7
uranium dioxide	142	15	11	19	-	5	192
plutonium-uranium dioxide	101	21	13	15	-	-	150
gadolinium-uranium oxide	12	7	2	3	3	-	27
silver-indium-cadmium	2	2	-	2	1	-	7
boron carbide	23	11	3	8	1	-	46
Zircaloy-2, zirconium-tin alloy	7	4	-	13	1	3	28
Zircaloy-4, zirconium-tin alloy	6	2	-	17	1	3	29
zirconium dioxide, zirconia	11	2	-	6	1	8	28
Hasteloy X, 2.4603	2	1	1	2	-	-	6
Inconel 600, 2.4816, NiCr 15 Fe	1	1	-	2	-	-	4
Inconel X-750, Inconel X	2	-	-	2	-	1	5
Inconel 617	3	4	-	4	1	-	12
Inconel 718, 2.4668	6	1	-	2	-	-	9
AISI 420, 1.4021, 20Kh13, EZh-2	3	-	-	3	-	6	12
AISI 430, 1.4016	4	-	-	2	-	-	6
AISI 403, 1.4000	1	-	-	-	-	-	1
AISI 347, FCBC, 1.4550	5	-	-	2	-	-	7
AISI 316, 1.4401/1.4436	7	2	1	7	-	1	18
AISI 304, X 5 CrNi 18 9, 1.4301	13	5	2	6	-	-	26
X10NiCrMoTiB 15 15, 1.4970	1	1	-	-	-	-	2
	421	85	36	143	9	48	742

THC	thermal conductivity
CP	specific heat capacity
ENT	enthalpy
LEX	thermal expansion
DEN	density
EMI	emissivity
SUM	total number of data sets

Table 4.2 LIST OF THERSYST DESCRIPTORS USED IN CHAPTER 4; CODES AND THEIR DESIGNATIONS

EKEY	data set number in THERSYST
MNAM	material name
CCOM	chemical composition
CCOMA	amount of element
DEN	density (g/cm^3)
TD	theoretical density (g/cm^3)
POR	porosity (%)
MELTT	melting temperature (K)
MELTH	enthalpy of fusion (J/g)
TRATXT	phase transition
TRAT	temperature of phase transition (K)
TRAH	enthalpy of phase transition (J/g)
TREATT	thermal treatment of a specimen
TRTEM	temperature of thermal treatment
TRTIM	time of thermal treatment
TRPR	pressure of thermal treatment
YSPEC	spectral range (for emissivity measurements)
DIR	measurement direction
VAL	valuation of the data
DONO	document number
AU	author(s)

4.1. FUEL MATERIALS

4.1.1. Uranium

Those metals or alloys that can be used as nuclear fuel include the fissile materials U-233, U-235, Pu-239 and fertile materials that include U-238, Th-232. Only U can be used in the pure metallic form.

Metallic uranium and its alloys are mainly used as nuclear fuel in low temperature, low burn-up research reactors rather than in commercial power reactors. Primarily it is included here for comparison purposes only. The crystal structure of uranium is shown in Table 4.1.1.1.

Enthalpy

Six data-sets have been found on the enthalpy of uranium metal (Figure 4.1.1.1). The phase transition temperatures and the heat of transition are given in Table 4.1.1.2.

MATPRO equations for enthalpy of uranium were calculated by integration of the specific heat equations piecewise over α, β, and γ temperature ranges. A constant of integration was determined to force an enthalpy of zero at 300 K.

for $300\ \text{K} < T < 938\ \text{K}$

$$H_u = -3.255468\times10^{4} + T\left[1.0466\times10^{2} + T\left(2.685\times10^{-3} + 3.389\times10^{-5}\ T\right)\right] \qquad (4.1.1\text{-}0)$$

for $938\ \text{K} \leq T < 1049\ \text{K}$

$$H_u = -5.1876776\times10^{4} + 1.7092\times10^{2}\ T \qquad (4.1.1\text{-}1)$$

for $1049\ \text{K} \leq T < 1405.6\ \text{K}$

$$H_u = -2.0567496\times10^{-4} + 1.602\times10^{2}\ T \qquad (4.1.1\text{-}2)$$

for $T \geq 1405.6\ \text{K}$

$$H_u = 6.177850\times10^{5} + 1.602\times10^{2}\ T \qquad (4.1.1\text{-}3)$$

where H_u is the enthalpy (J/kg), and T is the temperature (K). Note that these enthalphy equations are not thermodynamically consistent with the MATPRO heat capacity equations (4.1.1-7) through (4.1.1-9).

The evaluation of the literature data at the HEMATIC Institute in Obninsk gives:

for $300\ \text{K} < T < 940\ \text{K}$

$$H_u = -6.4668 + 0.0597T + 7.0576\times10^{-5}T^{2} - \frac{1.232\times10^{3}}{T} \qquad (4.1.1\text{-}4)$$

for $940\ \text{K} < T < 1050\ \text{K}$

$$H_u = -32.53 + 0.17776\ T \qquad (4.1.1\text{-}5)$$

for $1050\ \text{K} < T < 1405\ \text{K}$

$$H_u = -5.622 + 0.1619\ T \tag{4.1.1-6}$$

where H_u is the enthalpy (kJ/kg), and T is the temperature (K). The reference temperature is 298.15 K.

The Root Mean Square Error (RMSE) of equations (4.1.1-4) to (4.1.1-6) against the experimental data is 11% for the temperature range from 300 K to 1405 K.

Specific heat capacity

Data on the specific heat capacity of uranium metal found in literature are presented in Figure 4.1.1.2, the sources of the data and the density of the specimen are given in Table 4.1.1.3.

The MATPRO-recommendation is calculated using following expressions:

for $300\ \text{K} < T < 938\ \text{K}$

$$C_P = 104.82 + 5.3686\times10^{-3}\ T + 10.1823\times10^{-5}\ T^2 \tag{4.1.1-7}$$

for $938\ \text{K} \leq T < 1049\ \text{K}$

$$C_P = 176.41311 \tag{4.1.1-8}$$

for $1049\ \text{K} \leq T < 1405.6\ \text{K}$

$$C_P = 156.80756 \tag{4.1.1-9}$$

where C_P is the specific heat capacity (J/(kg·K)), and T is the temperature (K). Note that these heat capacities are not consistent with the MATPRO enthalpy equations (4.1.1-0) to (4.1.1-3); i.e. they are not the temperature derivatives of the enthalpy equations.

Recommendation made at HEMATIC are:

for $300\ \text{K} < T < 940\ \text{K}$

$$C_P = 0.0597 + 14.11\times10^{-5}T + \frac{1.232\times10^3}{T^2} \tag{4.1.1-10}$$

for $940\ \text{K} < T < 1050\ \text{K}$

$$C_P = 0.178$$

for $1050\ \text{K} < T < 1405\ \text{K}$

$$C_P = 0.162$$

where C_P is in kJ/(kg·K).

Thermal conductivity

66 data-sets on the thermal conductivity of uranium metal have been found. Experimental results obtained for specimens of a different chemical purity and of different thermal treatment are presented in Figure 4.1.1.3. The key to the data presented is given in Table 4.1.1.4.

The MATPRO-recommended curve has been obtained from a polynomial fit of the selected experimental data [RT000070, RT000071, RT000074] taken from TPRC-data collection [TPM01000].

$$\lambda = 20.457 + 1.2047\times10^{-2}\ T - 5.7368\times10^{-6}\ T^2 \qquad (4.1.1\text{-}11)$$

where λ is the thermal conductivity (W/(m·K)) and T is the temperature (K).

At the HEMATIC Institute in Obninsk the following formula has been obtained:

for 300 K < T < 1405 K

$$\lambda = 22.356 - 0.0161\ T + 0.000123\ T^2 - 1.346\times10^{-7}\ T^3 + 3.756\times10^{-11}\ T^4 \qquad (4.1.1\text{-}12)$$

The RMSE does not exceed 15% in the temperature range 300 K to 1405 K.

The thermal diffusivity of uranium recommended by TPRC is presented in Table 4.1.1.5.

Thermal expansion

Thermal expansion data on polycrystalline uranium found in the literature are presented in Figure 4.1.1.4. The crystal structure of the specimens and the data sources are given in Table 4.1.1.6.

MATPRO-recommended data have been calculated for a reference temperature of 300 K using the following expressions for the thermal expansion strains ε:

for 300 K< T < 942 K

$$\varepsilon = \frac{-0.30033 + T\,(7.1847\times10^{-4} + 1.0498\times10^{-6}\ T)}{100} \qquad (4.1.1\text{-}13)$$

for 942 K ≤ T < 1045 K

$$\varepsilon = \frac{-0.28340 + 1.9809\times10^{-3}\ T}{100} \qquad (4.1.1\text{-}14)$$

for 1045 K ≤ T ≤ 1405.6 K

$$\varepsilon = \frac{-0.27120 + 2.2298\times10^{-3}\ T}{100} \qquad (4.1.1\text{-}15)$$

where ε is the thermal strain (m/m) and T is the temperature (K).

HEMATIC proposed the following relation for the thermal expansion coefficient over the temperature range 300 K to 1405 K:

$$\alpha = 6.82 + 0.04714\ T - 8.187\times10^{-5}\ T^2 + 6.737\times10^{-8}\ T^3 - 1.929\times10^{-11}\ T^4 \qquad (4.1.1\text{-}16)$$

where α is the mean thermal expansion coefficient (10^{-6} 1/K) and T is the temperature (K).

The RMSE does not exceed 10% for the experimental data used in the evaluation.

Emissivity

One publication on the emissivity of uranium metal was found [RT000083], in which the influence of the ambient atmosphere and of the oxide layer on the measured property was investigated in detail. Based on these data Touloukian proposed the so called "recommended" data for three different surface characterizations, a polished sample and specimens with 700 and 1000 μg O_2/cm^2. The emissivity data are presented at Figure 4.1.1.5.

Nomenclature for Section 4.1.1

C_P - specific heat capacity, J/(kg·K),
other units: 1 kJ/(kg·K) = 10^3 J/(kg·K),
1 J/(g·K) = 10^3 J/(kg·K);
H_u - enthalpy, (J/kg),
other units: 1 kJ/kg = 10^3 J/kg,
1 J/g = 10^3 J/kg;
T - temperature (K);
α - thermal expansion coefficient, (1/K);
ε - thermal strain, (m/m),
other unit: %
λ - thermal conductivity, (W/(m·K)).

Table 4.1.1.1 THE CRYSTAL STRUCTURE OF URANIUM [RT000250]

PARAMETER **PHASE**	***α*-U**	***β*-U**	***γ*-U**
Crystal structure	orthorhombic	tetragonal	body-centered-cubic
Temperature range (K)	<942	942-1049	1049-1408
Crystal constant (Å)			
a	2.853	10.759	3.525
b	5.865		
c	4.955	5.656	
Density (g/cm^3), measured by x-ray diffraction	19.05	18.11	18.06

Table 4.1.1.2 ENTHALPY OF URANIUM

EKEY	**DEN**	**MELTT**	**MELTH**	**TRATXT**	**TRAT**	**TRAH**	**DONO**	**AU**
E5001248	19.05	1406	82.35	α/ß	938	12.50	RT000063	MATPRO
				ß/γ	1049	20.0		
E5001306	-	-	-	α/ß	941	11.85	JT000175	Ginnings
				ß/γ	1047	19.05		
E5001312	-	1405	29.32	α/ß	940	10.74	JT000176	Marchidan
				ß/γ	1048	17.57		
E5001544	-	-	-	ß/γ	1050	24.6	RT000084	Affortit
E5001763	-	-	-				JT000188	Mulford
E5002036	-	1408	38.43	α/ß	942	11.7	RT000113	Oetting
				ß/γ	1049	19.98		

Descriptors, units

DEN	density (g/cm^3)	TRATXT	phase transition
MELTT	melting temperature (K)	TRAT	temperature of phase transition (K)
MELTH	enthalpy of fusion (J/g)	TRAH	heat of phase transition (J/g)

Table 4.1.1.3 SPECIFIC HEAT OF URANIUM

EKEY	**DEN**	**YEAR**	**DONO**	**AU**
E5001197	-	1980	JT000131	Nakamura
E5001247	19.05	1990	RT000063	MATPRO
E5001305	-	1956	RT000077	North
E5001313	-	1976	JT000176	Marchidan
E5001543	-	1967	RT000084	Affortit
E5002037	-	1976	RT000113	Oetting

Descriptor, unit: DEN density (g/cm^3)

Table 4.1.1.4 THERMAL CONDUCTIVITY OF URANIUM

EKEY	DEN	DONO	AU
E0000098	-	TPM01000	Touloukian
E0005113	-	R0000105	Lucks
E5001205	-	JT000170	Garlick
E5001206	-	JT000170	Garlick
E5001207	-	JT000170	Garlick
E5001208	-	JT000170	Garlick
E5001209	-	JT000170	Garlick
E5001210	-	JT000170	Garlick
E5001211	-	JT000170	Garlick
E5001212	-	JT000170	Garlick
E5001213	-	JT000170	Garlick
E5001214	-	JT000170	Garlick
E5001215	-	JT000170	Garlick
E5001216	-	JT000170	Garlick
E5001217	-	JT000170	Garlick
E5001218	-	JT000170	Garlick
E5001219	-	JT000170	Garlick
E5001220	-	JT000170	Garlick
E5001221	-	JT000170	Garlick
E5001222	-	JT000170	Garlick
E5001223	-	JT000170	Garlick
E5001224	-	JT000170	Garlick
E5001249	19.0	RT000063	MATPRO
E5001252	-	RT000069	Bell
E5001254	-	RT000070	Bates
E5001255	-	RT000070	Bates
E5001256	14.7	RT000072	Plott
E5001257	17.2	RT000072	Plott
E5001258	16.2	RT000072	Plott
E5001259	15.7	RT000072	Plott
E5001260	18.0	RT000072	Plott
E5001261	18.5	RT000072	Plott
E5001265	-	RT000073	Kratz
E5001268	-	RT000075	Chiotti
E5001269	-	RT000075	Chiotti
E5001270	-	RT000068	Tyler
E5001272	-	RT000067	Kratz
E5001273	-	RT000067	Kratz
E5001274	-	RT000071	Babbitt
E5001275	-	RT000071	Babbitt
E5001276	-	RT000071	Babbitt
E5001277	-	RT000071	Babbitt
E5001278	-	RT000071	Babbitt
E5001279	-	RT000071	Babbitt
E5001280	-	RT000071	Babbitt
E5001281	-	RT000071	Babbitt
E5001282	-	RT000071	Babitt
E5001283	-	RT000071	Babbitt
E5001284	-	RT000071	Babbitt
E5001285	-	RT000071	Babbitt
E5001286	-	RT000071	Babbitt
E5001287	-	RT000071	Babbitt
E5001288	-	RT000071	Babbitt
E5001289	-	RT000071	Babbitt
E5001290	-	RT000071	Babbitt
E5001291	-	RT000071	Babbit
E5001292	-	RT000071	Babbitt
E5001293	-	RT000071	Babbitt
E5001294	-	RT000071	Babbitt
E5001295	18.8	RT000076	Deem
E5001296	18.9	RT000076	Deem
E5001297	18.8	RT000076	Deem
E5001298	18.8	RT000076	Deem
E5001299	-	RT000076	Deem
E5001303	-	RT000074	Droher
E5001304	-	RT000074	Droher

Table 4.1.1.5 THERMAL DIFFUSIVITY (a) OF URANIUM RECOMMENDED IN TPRC

T (K)	*a* (cm^2/s)
300	0.125
400	0.126
500	0.127
600	0.125
700	0.122
800	0.119
900	0.116
938	0.114
938	0.118
1000	0.134
1049	0.139
1049	0.156
1100	0.162
1200	0.172

Remarks:

1. T.P. (orthorh.-tetragonal) 938 K
   T.P. (tetragonal-b.c.c.) 1049 K
2. Data from: page 206 of TPRC Volume 10 "Thermal Diffusivity", ed. Y. S. Touloukian, R. W. Powell, C. Y. Ho, and M. C. Nicolaou, IFI/Plenum, New York, 1973

Table 4.1.1.6 THERMAL EXPANSION OF POLYCRYSTALLINE URANIUM

EKEY	CSTR	DONO	AU
E0000458	ORTH	TPM12000	Touloukian
E5001250	-	RT000063	MATPRO
E5001317	ORTH	JT000172	Bridge
E5001322	ORTH	RT000079	Laguer
E5001326	-	RT000082	Saller
E5001335	TETR	RT000081	Kelpfer
E5001336	BCC	RT000081	Kelpfer

Descriptors		Codes	
EKEY	data-set number	ORTH	orthogonal
CSTR	crystal structure	TETR	tetragonal
DONO	document number	BCC	body centered cubic
AU	author(s)		

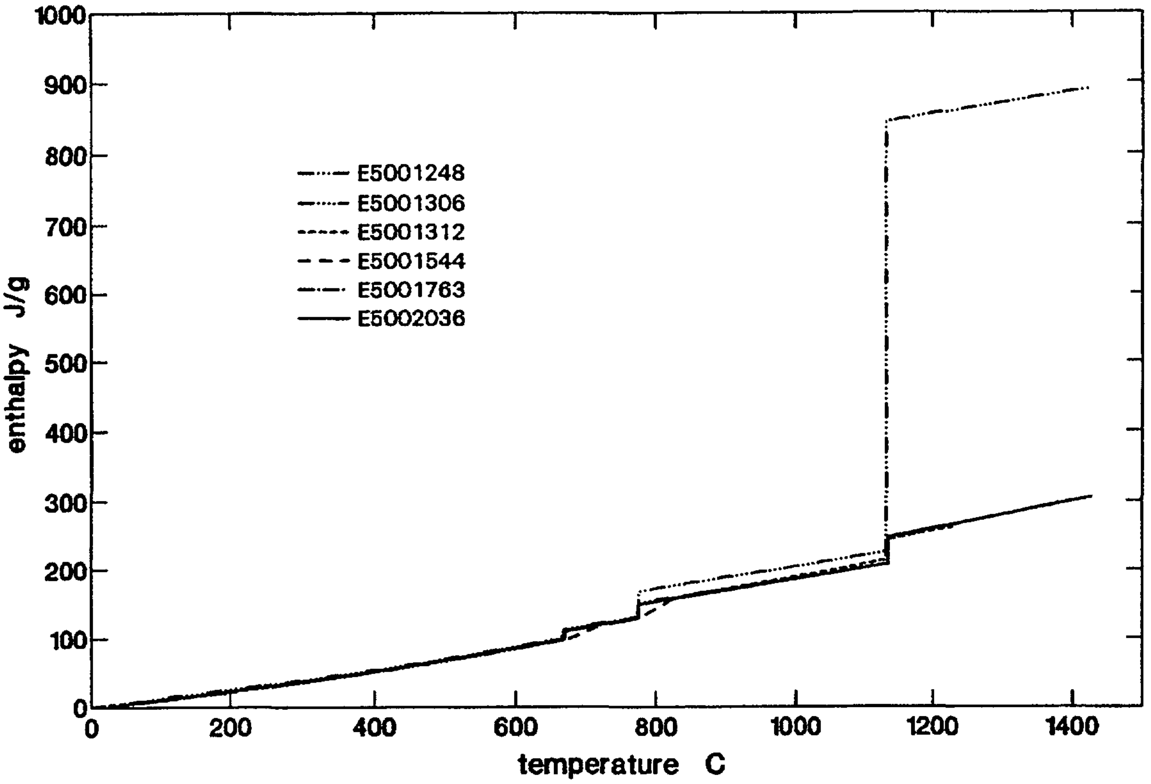

Figure 4.1.1.1 Enthalpy of uranium

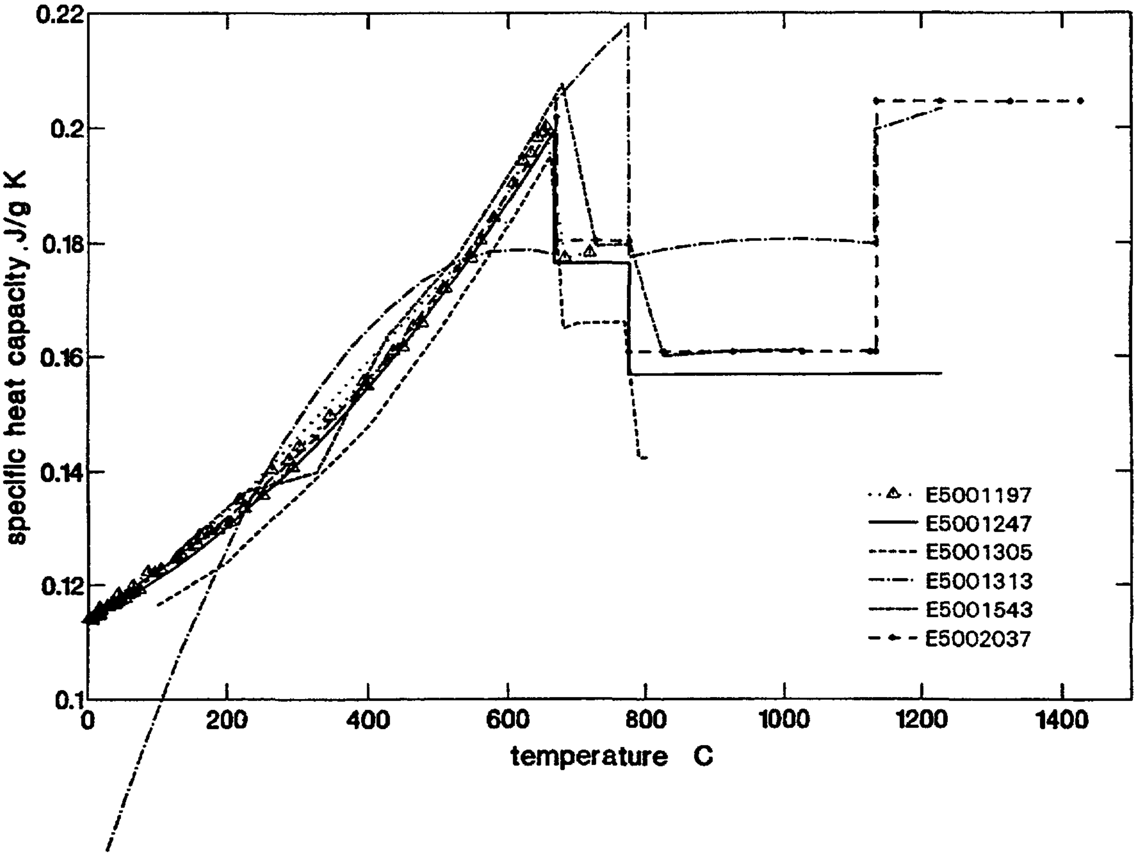

Figure 4.1.1.2 Specific heat capacity of uranium

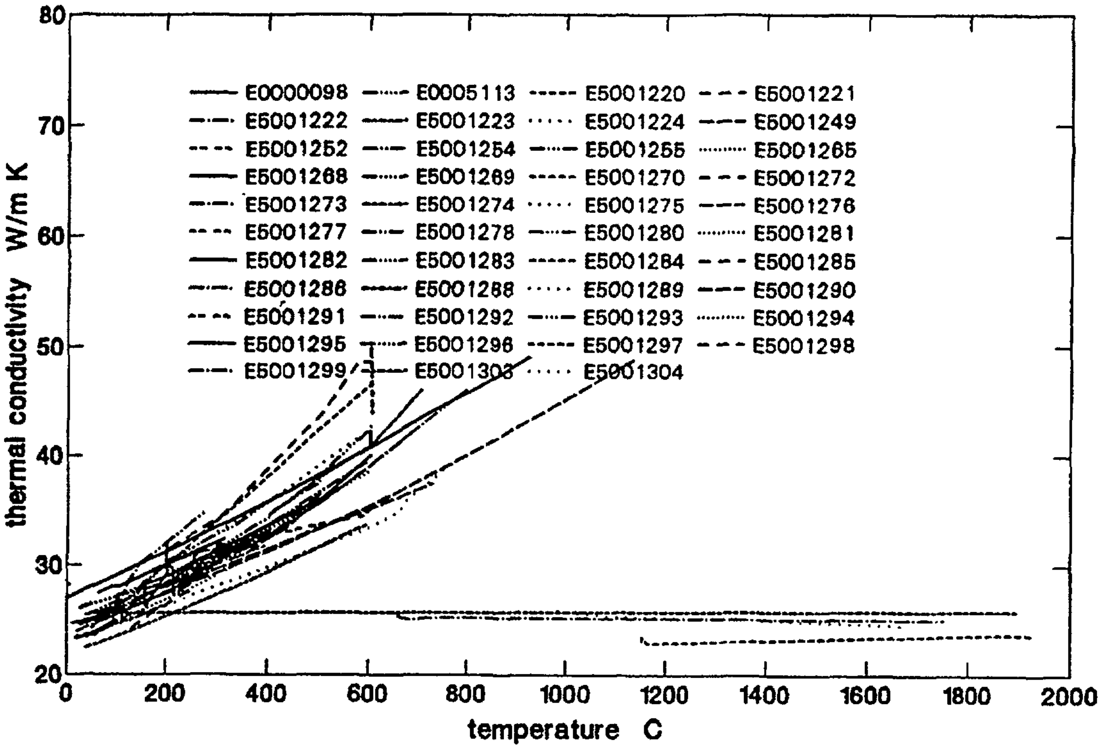

Figure 4.1.1.3 Thermal conductivity of uranium

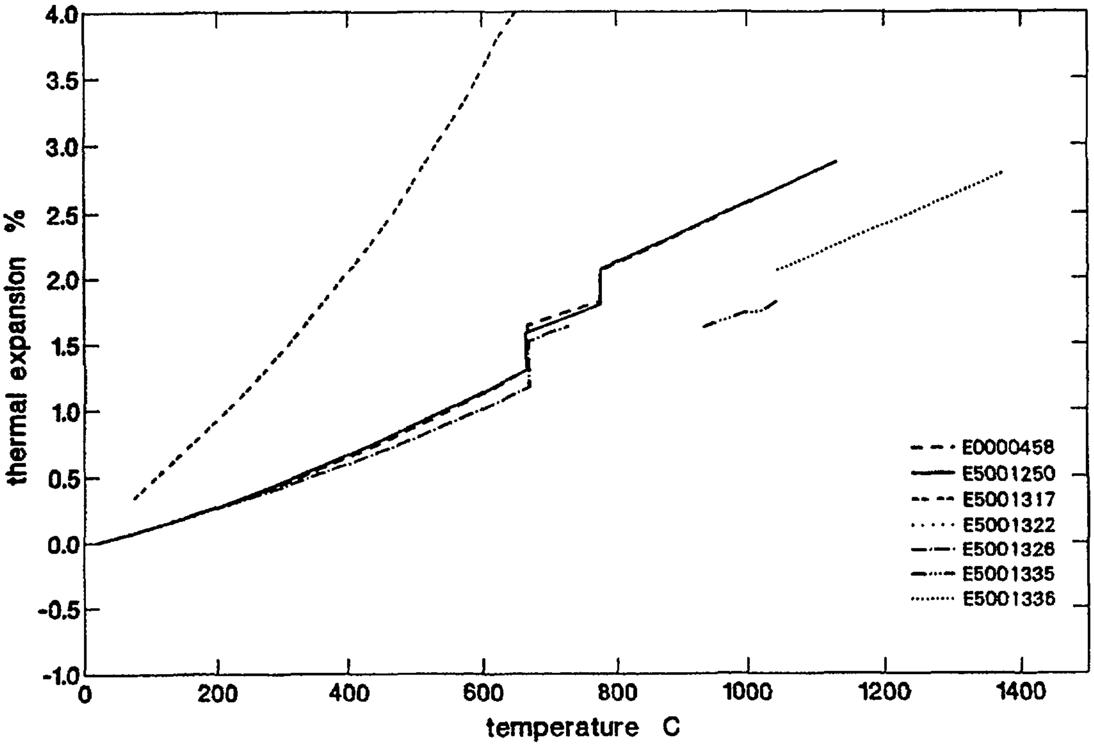

Figure 4.1.1.4 Thermal expansion of uranium

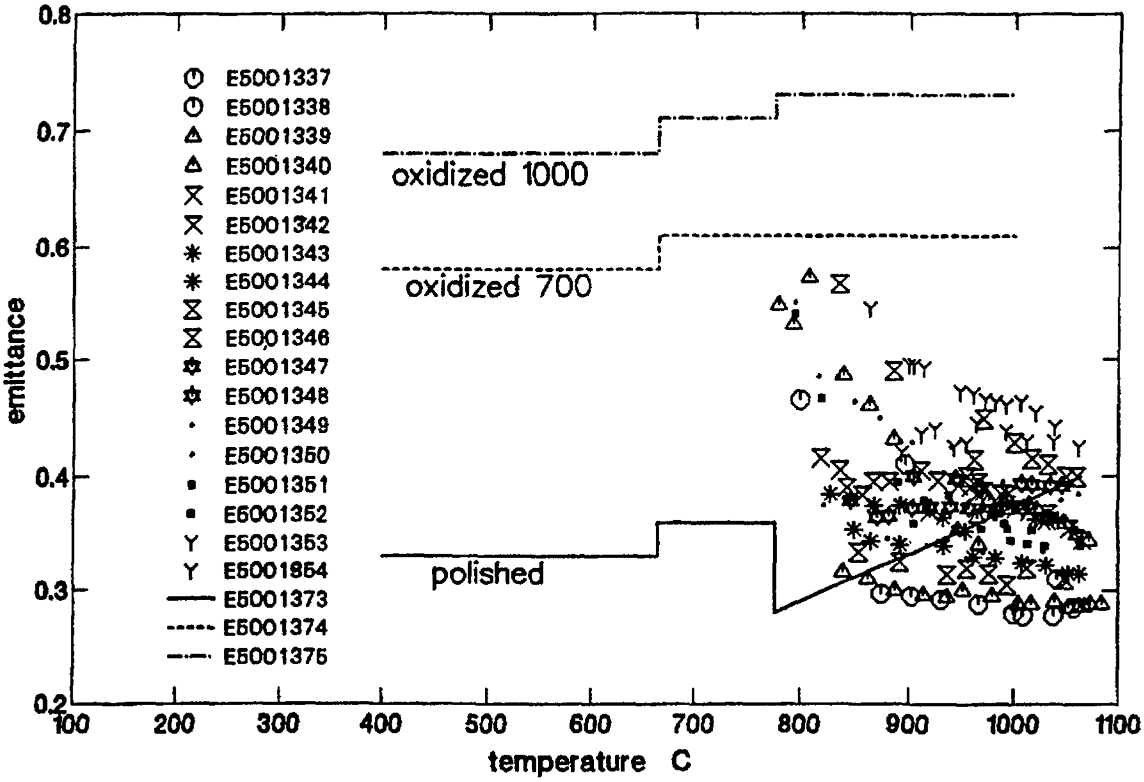

Figure 4.1.1.5 Total hemispherical emissivity of uranium

References to Section 4.1.1

Note: literature, stored in THERSYST is referenced by document number, e.g. JT000131, etc.

JT000131 NAKAMURA J., TAKAHASHI Y., IZUMI S., "Heat capacity of metallic uranium and thorium from 80 to 1000 K", J. Nucl. Mater. 88 (1980), 64-72

JT000169 FLOTOW H. E., OSBORNE D. W., "Heat capacity of alpha uranium from 1.7 to 25 K", Phys. Rev. 151 (1966), 564-570

JT000170 GARLICK A., SHAW D., "The thermal conductivity of irradiated uranium", J. Nucl. Mater. 16 (1965), 333-339

JT000172 BRIDGE J. R., SCWARTZ C. M., VAUGHAN D. A., "X-ray diffraction determination of the coefficient of expansion of alpha uranium", J. Metals 206 (1956), 1282-1285

JT000175 GINNINGS D. C., CORRUCCINI R. J., "Heat capacities at high temperatures of uranium, uranium trichloride, and uranium tetrachloride", JNBS 39 (1947) 309-316

JT000176 MARCHIDAN D. I., CIOPEC M., "Enthalpy of uranium to 1500 K by drop calorimetry", J. Chem. Thermodynamics 8 (1976), 691-701

JT000188 MULFORD R. N. R., SHELDON R. I., "Density and heat capacity of liquid uranium at high temperature", J. Nucl. Mater., 154 (1988), 268-275

R0000105 LUCKS C. F., DEEM H. W., "Progress relating to civilian applications during June 1958: Thermal conductivity of uranium and UO_2", USAEC Rept. BMI-1273, 1-62 (1958)

RT000063 HOHORST J. K. (Editor), "SCDAP/RELAP5/MOD2 Code Manual, vol.4: MATPRO-a library of materials properties for light-water-reactor accident analysis", NUREG/CR-5273 (1990)

RT000067 KRATZ H. R., RAETH C. H., "Thermal conductivity of uranium", USAEC CP-2315 (1945), 1-14

RT000068 TYLER W. W., WILSON A. C., WOLGA G. J., "Thermal conductivity, electrical resistivity and thermoelectric power of uranium", USAEC KAPL-802 (1952), 1-25

RT000069 BELL I. P., "Fast reactor: physical properties of materials of construction", UKAEA R&DB(C)TN-127 (1955), 1-10

RT000070 BATES J. C., "A comparison of the thermal conductivity of irradiated and unirradiated uranium", UKAEA R&DB(W)TN-78 (1953), 1-5

RT000071 BABBITT J. D., DAUPHINEE T. M., ARMSTRONG L. D., PERIA W., "Thermal conductivity of metals at high temperatures. II Thermal conductivity of uranium: preliminary study", AECL-326 CRR-438 (1956),1-37

RT000072 PLOTT R. F., RAETH C. H., "Determination of the thermal conductivity and density of tubaloy and some of its compounds", USAEC CP-228 (1942), 1-8

RT000073 KRATZ H. R., "Metallurgical project", USAEC CT-861 (1943), 1-15

RT000074 DROHER J. J., DOMINGO F. A.; INMAN G. M. (Eds.), "Thermal conductivity of uranium", NAA-SR-878 (1954), 1-118

RT000075 CHIOTTI P., CARLSON O. N., "Thermal conductivity of uranium", USAEC ISC-314 (1953), 1-26

RT000076 DEEM H. W., NELSON H. R., "Thermal conductivity of powder-metallurgy uranium", BMI-745 (1952), 1-15

RT000077 NORTH J. M., "A high temperature adiabatic calorimeter for the specific heat of uranium between 100 and 800 C°", AERE, Rep. M/R-1016 (1956), 1-9

RT000078 LLOYD L. T., "Thermal expansion of alpha-uranium single crystals", ANL-5972 (1959), 1-48

RT000079 LAQUER H. L., SCHUCH A. F., "Low temperature calorimetry of uranium", LAMS-1358 (1952), 1-14

RT000080 none given, "Metallurgy of tuballoy", USAEC-CT-2144 (1944), 214-230

RT000081 KELPFER H. H., CHIOTTI P., "Characteristics of the solid state transformations in uranium", USAEC-ISC-893 (1957), 1-113

RT000082 SALLER H. A., ROUGH F. A., CHUBB W., "The property of uranium containing minor additions of chromium, silicon, or titanium", BMI-1068(Del.) (1956), 1-32

RT000083 LEMMON A. W. Jr., "The reaction of steam with uranium and with various *uranium-niobium-zirconium* alloys at high temperatures", BMI-1192 (1957), 1-74

RT000084 AFFORTIT C., "Mesure de la chaleur specifique des metaux jusqu'a leur temperature de fusion", CEA-R 3287 (1967), 60

RT000113 OETTING F. L., RAND M. H., ACKERMANN R. J., "The chemical thermodynamic of actinide elements and compounds. Part 1: The actinide elements", IAEA, Vienna (1976)

RT000250 CORDFUNKE E. H. P., KONINGS R. J. M., "Thermodynamical data for reactor materials and fission products" (1990), Elsvier, Holland

TPM01000 TOULOUKIAN Y. S., POWELL R. W., HO C. Y., KLEMENS P. G., "Thermophysical Properties of Matter. Vol. 1: Thermal Conductivity - Metallic Elements and Alloys", IFI/Plenum, New York-Washington (1970)

TPM07000 TOULOUKIAN Y. S., DEWITT D. P., "Thermophysical Properties of Matter. Vol. 7: Thermal Radiative Properties - Metallic Elements and Alloys", TPRC vol. 7 (1970); IFI/Plenum New York-Washington (1970)

TPM12000 TOULOUKIAN Y. S., KIRBY R. K., TAYLOR R. E., DESAI P. D., "Thermophysical Properties of Matter. Vol. 12: Thermal Expansion - Metallic Elements and Alloys", IFI/Plenum, New York-Washington (1975)

Additional literature used in the HEMATIC evaluation

(1) SIBORG H. T., KATZ G. G., "Chemistry of active elements",- translation from English, Gosatomizdat (1960)

(2) VDOVENKO V. M., "Chemistry of uranium and transuranic elements", Academy of Sciences of the USSR (1960); "Modern Radiochemistry", Gosatomizdat (1969)

(3) FOOT F. J., in book "Reports of International Conference on Peaceful Application of Nuclear Power; Geneva, 1955", Gosgeologizdat (1968), v. 9, p. 51

(4) TCHIRKIN V. S., "Thermophysical properties of materials for nuclear power industry, Gosatomizdat (1968)

(5) EMEL'IANOV V. S., EVSTIUKHIN A. I., "Metallurgy of nuclear fuel", Gosatomizdat (1969)

(6) HOLDENN A. A., "Metallurgy of uranium", Metallurgizdat (1962)

(7) SCHEVTCHENKO V. B., SUDARIKOV B. N., "Technology of uranium", Gosatomizdat (1961)

(8) "Materials for nuclear reactors", - transl. from Engl., Ed., SOKURSKIY JU. N., Gosatomizdat (1963)

(9) STERLIN I. M., "Metallurgy of uranium", Gosatomizdat (1960)

(10) SERGEEV G. IA., TITOVA V. V., BORISOV K. A., "Metallurgy of uranium and some materials of nuclear reactors", Atomizdat (1960)

(11) ZINOV'EV V. E., "Thermoph. properties", Metallurgy (1989)

(12) WICKS K. E., BLOCK F. E.: "Thermodynamical properties of 65 elements, their oxides, halogenides, carbides and nitrides", - transl. from Engl., Metallurgy (1965)

(13) Nuclear Materials. Book 1. Nuclear fuel materials. Red. SKOROV D.M., Gosatomizdat (1961)

(14) ZINOV'EV V. E., "Kinetic properties of metals under high temperatures", Handbook: Metallurgy (1984), 200 pp

(15) DAS D., DHARWADKAR S. R., CHANDRASEKHARAIAH M. S., "Thermodynamics of liquid uranium vaporization", Journal of Nuclear Materials v. 130 (1985), p.217-224

(16) "Properties of elements", Handbook, Ed.: DRITZ M. E., Metallurgy (1985), 671 pp

(17) SAMSONOV G. V., "Physico-chemical properties of elements", Handbook, Kiev: Nauko Dumka

(18) KEJ D., LEBI G., "Tables of physical and chemical constants", Fizmatgiz (1962)

(19) MARCHIDAN D. I., CIOPEC M., "Enthalpy of Uranium to 1500 K by drop calorimetry", Chem. Thermodynamics (1978), 8, p. 691-701

4.1.2. Uranium-aluminium alloys

Only data on the specific heat capacity, thermal conductivity and thermal expansion were found in the literature for different compositions of U-Al-alloy.

Heat of fusion

The melting point values given in "The Chemical Thermodynamics of Actinide Elements and Compounds, Part 5: The Actinide Binary Alloys", by P. Chiotti et al., published by the IAEA, Vienna 1981, are as follows:

Al-22.2 wt%U	1173 K
Al-26.7 wt%U	1273 K

For Al-25.4 wt%U, the melting point can also be estimated from the available phase diagram. The estimated values are:

1238 K	(from Binary Alloy Phase Diagrams, by T.B. Massalski, ASME 1986)
1151 K	(from Uranium-Aluminium Constitutional Diagram in Reactor Handbook, Interscience Publishers (1960) p.174).

Li Wengdan and Li Yongjing of China Institute of Atomic Energy gave the following data by differential scanning calorimetry experimental method (data to be published as CIAE report):

Solidus temperature for Al-27.3 wt%U	916 K
Enthalpy of phase transition for αAl + $UAl_4 \rightarrow L + UAl_4$	193.4 J/g
Temperature of phase transition for $L + UAl_4 \rightarrow L + UAl_3$	1003 K
The corresponding enthalphy of phase transition	9.29 J/g
Measurement accuracy	± 3%

The above data can be used in estimation of heat of fusion with the U-Al alloys.

Thermal conductivity

Data on the thermal conductivity of U-Al alloy are presented in Fig. 4.1.2.1. The uranium concentration and the data sources are given in Table 4.1.2.1.

Results obtained in China for 25.4 wt% U can be approximated for temperatures between 356 K to 617 K by the equation:

$$\lambda = 180.26 - 2.29 \cdot 10^{-2} T \qquad (4.1.2\text{-}1)$$

where λ is the thermal conductivity (W/(m·K)) and T is the temperature (K).

The influence of thermal treatment on thermal conductivity is discussed in Supplement S3.

Specific heat capacity

The specific heat capacity of uranium-aluminium alloy has been measured in China for uranium content of 25.4 wt%. These data are presented in Table 4.1.2.2. In the temperature range from room temperature to 873 K the specific heat can be approximated by the equation:

$$C_P = 0.560 + 3.715\times10^{-4}T \qquad (4.1.2\text{-}2)$$

where C_P is the specific heat (J/(g·K)) and T is the temperature (K).

Thermal expansion

Classical experimental data on the thermal expansion of U-Al alloys have been obtained by Saller [RT000200]. These data are presented in Fig. 4.1.2.2. together with the provisional data of Touloukian. The composition of the alloys and the data sources are listed in Table 4.1.2.3.

Nomenclature to Section 4.1.2

C_P - specific heat capacity, (J/(g·K) = 10^3 (J/(kg·K));
T - temperature (K);
α - thermal expansion coefficient, (1/K);
ε - thermal strain, (m/m);
other unit: %;
λ - thermal conductivity, (W/(m·K)).

Table 4.1.2.1 THERMAL CONDUCTIVITY OF U-Al ALLOYS

EKEY	CCOM	CCOMA	DONO	AU
E0005106	U	96.0	R0000063	Francis
	Al	4.0		
E0005107	U	98.0	R0000063	Francis
	Al	2.0		
E5001225	Al	74.6	PT000018	Lili
	U	25.4		
E50001753	U	12.5	RT000200	Saller
E50001754	U	22.7	"	Saller
E50001755	U	30.5	"	Saller
Descriptor, unit:		**CCOMA Chemical composition (wt%)**		

Table 4.1.2.2 SPECIFIC HEAT CAPACITY C_p OF Al-25.4 U ALLOY

T (K)	C_P (J/(g·K))
359	0.6933
373	0.6988
473	0.7356
573	0.7729
673	0.8101
773	0.8474
873	0.8843 (extrapolated)

Table 4.1.2.3 THE THERMAL EXPANSION OF Al-U ALLOYS

EKEY	CCOM	CCOMA	DONO	AU
E0000689	Al	70.0	TPM12000	Touloukian
	U	30.0		
E0000691	Al	85.0	TPM12000	Touloukian
	U	15.0		
SAL4	U	12.5	RT000200	Saller
SAL5	U	22.7	"	Saller
SAL6	U	30.5	"	Saller
Descriptor, unit:		CCOMA Chemical composition (wt%)		

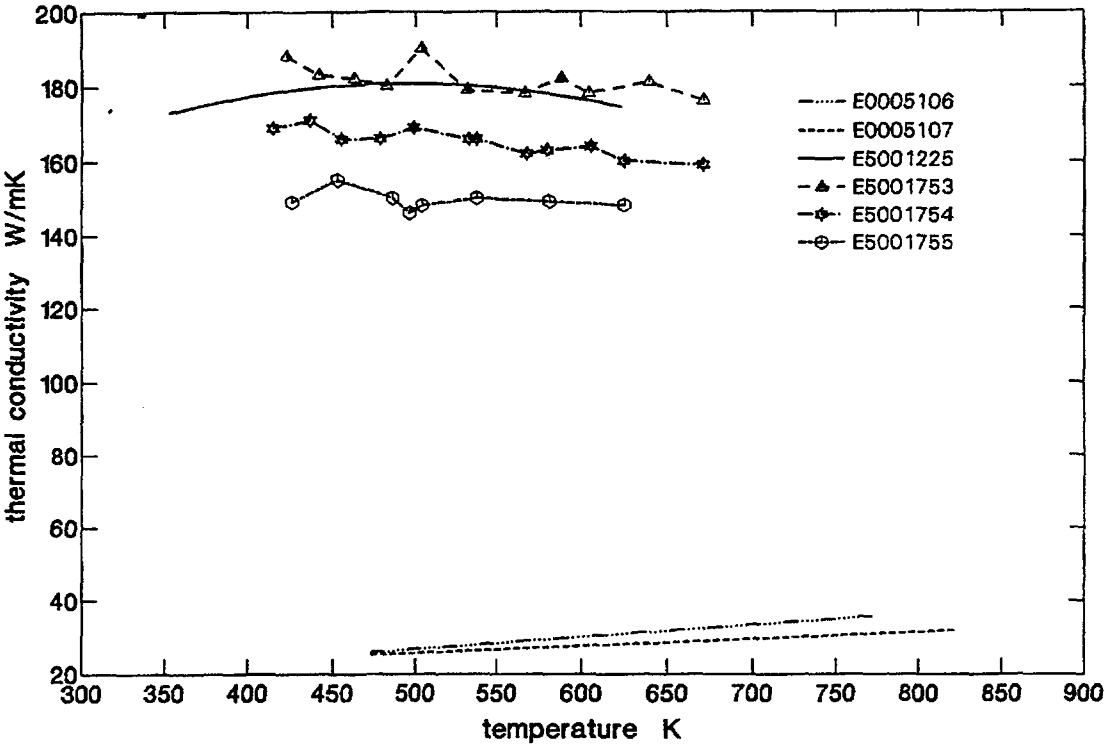

Figure 4.1.2.1 Thermal conductivity of U-Al alloys

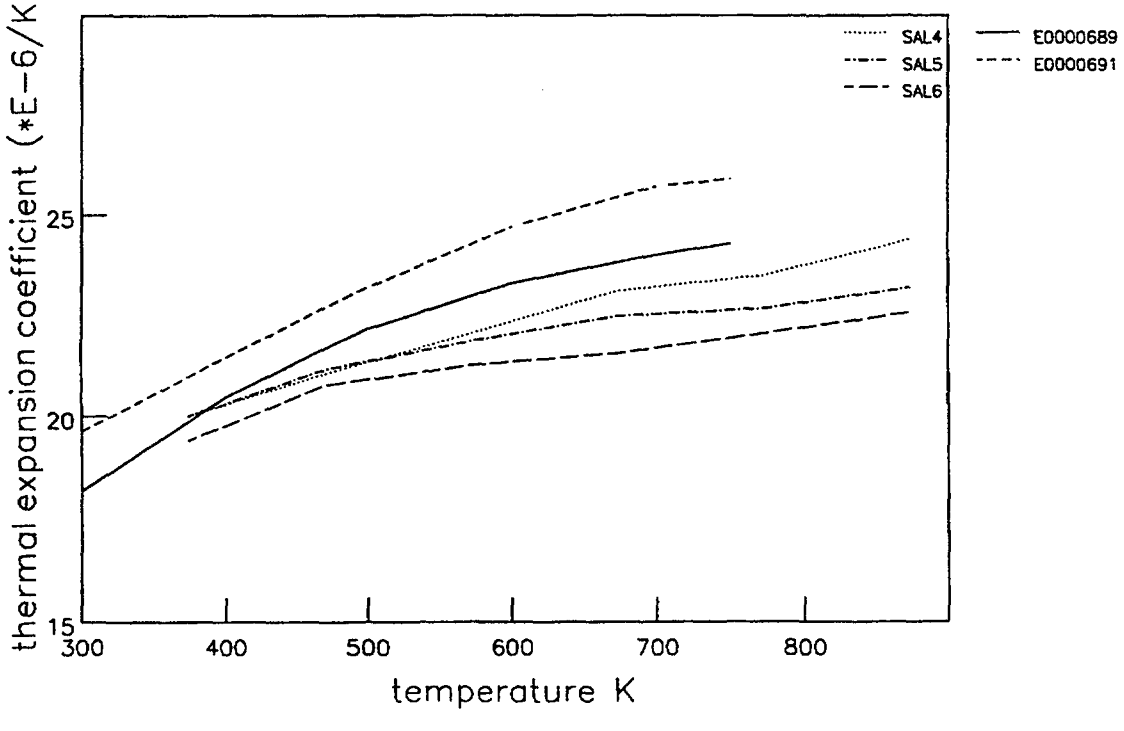

Figure 4.1.2.2 Thermal expansion of U-Al alloy

References to Section 4.1.2

Note: literature stored in THERSYST is referenced by document number, e.g. PT000018, etc.

PT000018	LILI Z., BIN L., "The measurement of thermal conductivity of nuclear fuels in China". Proc. 2nd Research Co-ordination Meeting on Establishment of Thermophysical Properties, 19-22 April (1993), IAEA, Vienna
R0000063	FRANCIS E. L., "Uranium data manual", UKAEA Rept. IGR-R/R-287 (1958) 1-51
RT000200	SALLER H. A., Proceedings of International Conference on the Peaceful Uses of Atomic Energy, Vol. 9 (1955), p. 562, 214-220
TPM12000	TOULOUKIAN Y. S. et al., "Thermophysical properties of matter. Vol. 12: Thermal Expansion - Metallic elements and alloys" IFI/Plenum, New York-Washington (1977)

4.1.3. Uranium dioxide

As it can be seen from Table 4.1 the actual experimental data on uranium dioxide have been stored in THERSYST. The thermophysical properties for this material have been subject of different assessments and evaluations. This section gives only the recommendations worked out by different authors. The list of all publications from which the data are collected in THERSYST is given at the end of this chapter.

Enthalpy

Recommended curves for the enthalpy of UO_2 are presented in Figure 4.1.3.1. In Table 4.1.3.1 recommended values for melting temperature and heat of fusion are listed.

The recommended equations are as follows:

Fink:

for 298.15 K < T < 2670 K

$$\begin{aligned} H_u = {} & 4.0386\times10^4\left[\left(\exp\left(\frac{516.12}{T}\right) - 1\right)^{-1} - \left(\exp\left(\frac{516.12}{298.15}\right) - 1\right)^{-1}\right] \\ & + 3.8609\times10^{-3}\left[T^2 - (298.15)^2\right] \\ & + 3.4250\times10^8 k_B\left[T\exp\left(\frac{-1.9105}{k_B T}\right) - 298.15\exp\left(\frac{-1.9105}{298.15 k_B}\right)\right] \end{aligned} \qquad (4.1.3\text{-}1)$$

for 2670 K < T < 3120 K

$$H_u = 167.04T - 218342 \qquad (4.1.3\text{-}2)$$

for 3120 K ≤ T ≤ 3530 K

$$H_u = 130.95T - 30911 \qquad (4.1.3\text{-}3)$$

where H_u is the enthalpy (J/mol), T is the temperature (K) and k_B is the Boltzmann constant, 8.6144×10^{-5} eV·K^{-1}.

Harding:

for $\tau \leq 0.856$

$$\begin{aligned} H_u = {} & -22528 + 201296\tau + 138884\tau^2 + 5498.6\tau^3 - 329758\tau^4 \\ & + 322837\tau^5 + 186.3\tau^{-1} \end{aligned} \qquad (4.1.3\text{-}4)$$

for $\tau > 0.856$

$$H_u = 521159\,\tau - 220041 \qquad (4.1.3\text{-}5)$$

where τ is the reduced temperature T/T_m and T_m is the melting temperature (3120 K) and the reference temperature is 298.15 K.

MATPRO:

for 300 K < T ≤ 3113 K

$$H_u = \frac{296.7 \cdot 535.285}{\exp\left(\frac{535.285}{T}\right) - 1} + \frac{2.43\times10^{-2} \cdot T^2}{2} + \frac{\gamma}{2}\left[8.745\times10^{7} \exp\left(\frac{-1.577\times10^{5}}{RT}\right)\right] + 32670 \qquad (4.1.3\text{-}6)$$

where H_u is the enthalpy (J/kg), T is the temperature (K), γ is the oxygen-to-metal ratio and R is the universal gas constant = 8.3141 (J/(mol·K)). MATPRO equations for enthalphy UO_2 were calculated by integration of the specific heat equation. A constant of integration was determined to force an enthalpy to zero at 300 K.

The report by Kerrisk and Clifton [JT000028] has recommended the following expression for enthalpy in the temperature range from 298 K to 1500 K:

$$H_u = 4.28778 \cdot 10^{4} \left(\left[\frac{1}{\exp(\frac{535.285}{T}) - 1} \right] - \left[\frac{1}{\exp(\frac{535.285}{298}) - 1} \right] \right) \qquad (4.1.3\text{-}7)$$

$$+ 3.28332 \cdot 10^{-3} (T^2 - 298^2) + 2.36134 \cdot 10^{7} \exp(-\frac{18969.5}{T})$$

where H_u is the enthalpy (J/mol), T is the temperature in (K), and the reference temperature is 298 K.

Specific heat capacity

The data of various authors for the specific heat capacity of UO_2 are presented in Figure 4.1.3.2. and Table 4.1.3.2.

They are calculated using the following equations:

Fink:

for 298 K ≤ T ≤ 2670 K

$$C_P = \frac{2.0835\times10^{7} \exp\left(\frac{516.12}{T}\right)}{T^2 \left[\exp\left(\frac{516.12}{T}\right) - 1\right]^2} + 7.7218\times10^{-3} T \qquad (4.1.3\text{-}8)$$

$$+ 3.4250\times10^{8} k_B \exp\left(-\frac{1.9105}{k_B T}\right)\left(1 + \frac{1.9105}{k_B T}\right)$$

for 2670 K ≤ T ≤ 3120 K

$$C_P = 167.0 \qquad (4.1.3\text{-}9)$$

for T > 3120 K

$$C_P = 131.0 \qquad (4.1.3\text{-}10)$$

where C_P is the specific heat (J/(mol·K)), T is the temperature (K) and k_B is the Boltzmann constant, 8.6144×10^{-5} eV·K^{-1}.

Harding:

for $\tau \leq 0.856$ ($T \leq 2670.7$ K)

$$C_P = \frac{1}{T_m}(201296 + 277767\tau + 16497\tau^2 - 1319031\tau^3 + 1614187\tau^4 - 186.27\tau^{-2}) \qquad (4.1.3\text{-}11)$$

for $0.856 < \tau < 1.0$ (2670.7 K $< T \leq$ 3120 K)

$$C_P = 167.03 \qquad (4.1.3\text{-}12)$$

for $T > 3120$ K (liquid)

$$C_P = 130.95 \qquad (4.1.3\text{-}13)$$

where τ is the reduced temperature T/T_m and T_m is the melting temperature (3120 K).

MATPRO:

for 300 K $< T \leq$ 3113 K

$$C_P = \frac{296.7\,(535.285)^2 \cdot \exp\left(\frac{535.285}{T}\right)}{T^2\left[\exp\left(\frac{535.285}{T}\right) - 1\right]^2} + 2.43\times10^{-2}T + \frac{\gamma \cdot 8.745\times10^7 \cdot 1.577\times10^5}{2RT^2}\exp\left(\frac{-1.577\times10^5}{RT}\right) \qquad (4.1.3\text{-}14)$$

for $T > 3113$ K

$$C_P = 503 \qquad (4.1.3\text{-}15)$$

where C_P is the specific heat (J/(kg·K)), T is the temperature (K), γ is the oxygen-to-metal ratio and R is the universal gas constant = 8.3141 (J/(mol·K)).

Differentiation of 4.1.3-7 over the temperature range 298 K to 1500 K gives the specific heat by Kerrisk et al.,as:

$$C_P(T) = 80.1027\left(\frac{535.285}{T}\right)^2 \frac{\exp\left(\frac{535.285}{T}\right)}{\left[\exp\left(\frac{535.285}{T}\right)-1\right]^2} + 6.56665\times10^{-3}T + \frac{4.47937\times10^{11}}{T^2}\exp\left(-\frac{18969.5}{T}\right) \qquad (4.1.3\text{-}16)$$

where C_P is the specific heat (J/(mol·K)) and T is the temperature (K).

Thermal conductivity

The recommended curves for the thermal conductivity of solid 100% dense stoichiometric UO_2 as a function of temperature, proposed by different authors, are presented in Figure 4.1.3.3. In Table 4.1.3.3 the recommended values for melting temperature, enthalpy of fusion and theoretical density are listed.

Analytically, the recommendations may be expressed as follows:

Fink:

For $298.15\ \mathrm{K} \le T \le 2670\ \mathrm{K}$,

$$\lambda = \frac{1}{6.8337\times10^{-2} + 1.6693\times10^{-4}T + 3.1886\times10^{-8}T^2} + 1.2783\times10^{-1}T \exp\left(-\frac{1.1608}{k_B T}\right) \tag{4.1.3-17}$$

where k_B is the Boltzmann constant, $8.6144\times10^{-5}\ \mathrm{eV\cdot K^{-1}}$.

For $2670\ \mathrm{K} \le T \le 3120\ \mathrm{K}$,

$$\lambda = 4.1486 - 2.2673\times10^{-4}T \tag{4.1.3-18}$$

Washington:

$$\lambda = \frac{1}{0.035 + 2.25\times10^{-4}T} + 83.0\times10^{-12}T^3 \tag{4.1.3-19}$$

Brandt:

$$\lambda = \frac{1}{0.0439 + 2.16\times10^{-4}T} + 11.2\times10^{-2}T \exp\left(-\frac{1.18}{k_B T}\right) - 4.18\times10^{5} \exp\left(-\frac{3.29}{k_B T}\right) \tag{4.1.3-20}$$

Ainscough, given in the paper by Martin [JT000079]:

$$\lambda = 9.851 - 8.803\times10^{-3}T + 3.301\times10^{-6}T^2 - 3.727\times10^{-10}T^3 \tag{4.1.3-21}$$

Killeen, given in the paper by Martin [JT000079]:

$$\lambda = \frac{1}{0.0375 + \dfrac{2.165\times10^{-4}}{T}} + 3.861\times10^{-3}T\exp\left(-\frac{1.07}{k_B T}\right)\left[1 + 0.36883\left(\frac{1.07}{k_B T} + 2\right)^2\right] \tag{4.1.3-22}$$

Harding:

$$\lambda = \left(0.0375 + 2.165\times10^{-4}T\right)^{-1} + 4.715\times10^{9}T^{-2} \exp\left(-\frac{1.41}{k_B T}\right) \tag{4.1.3-23}$$

where λ is the thermal conductivity (W/(m·K)), T is the temperature (K).

Hyland analysed in detail three contributions to thermal conductivity (lattice, electronic and radiation) at high temperature and recommended the following expression for the temperature range 2000 to 3120 K (T_m):

$$\lambda = 2.3 + \frac{2.25\times10^5}{T}\exp\left(-\frac{12.45\times10^3}{T}\right) \tag{4.1.3-24}$$

The *MATPRO* recommendation yields similar values for theoretically dense UO_2 although it is not so firmly based on physical principles.

$$\begin{aligned}\lambda = {} & \frac{C_V}{(0.339+0.06867T'')(1+3\varepsilon_{th})} \\ & + 5.2997\times10^{-3}T\exp\left(-\frac{13358}{T}\right)\left[1+0.169\left(\frac{13358}{T}+2\right)^2\right]\end{aligned} \tag{4.1.3-25}$$

where

C_V = phonon contribution to the specific heat at constant volume (J/(kg·K)). The first term of the MATPRO correlation for fuel specific heat capacity is used for this factor (4.1.3-14).

ε_{th} = linear strain caused by thermal expansion when temperature is > 300 K (unitless). The MATPRO correlation for fuel thermal expansion is used for this factor (4.1.3-37).

T = fuel temperature (K)

T'' = fuel temperature if < 1800 K. For temperatures > 2300 K, T'' is 2050 K; for temperatures in the range 1800 to 2300 K, T'' is found by interpolation, as explained in Subsection 2.3.3 of MATPRO.

In China the following relation is recommended for the temperature range 500 K to 3100 K:

$$\lambda = F\left[\frac{1}{A+BT} + DT\exp\left(-\frac{E_a}{k_BT}\right)\left[1+H\left(\frac{E_a}{k_BT}+2\right)^2\right]\right] \tag{4.1.3-26}$$

where $F = 1 - \alpha P$; $\alpha = 2.7 - 5.8\times10^{-4}\ T$;
$A = 3.68\times10^{-2}$ m·K/W; $B = 2.25\times10^{-4}$ m /W;
$D = 5.31\times10^{-3}$ W/(m·K^2); $E_a = 1.15$ eV;
$H = 0.264$; $k_B = 8.6144\times10^{-5}$ eV/K,
and P is the fractional porosity.

Standard deviation: ±3.6%.

Thermal conductivity of liquid UO_2 has been calculated from different thermal diffusivity measurements using the specific heat data of Leibowitz (Table 4.1.3.4).

MATPRO has recommended 11.5 W/(m·K) based on Kim's experiments.

Fink [JT000148] analysed the thermal diffusivity measurements of different authors and evaluated them by means of a transient heat transfer code. The new values are given below:

from Kim's experiment: 5.5 W/(m·K),
from Tasman's experiment: 4.5 W/(m·K),
from Otter's experiment: 6.75 W/(m·K),

and Fink recommended a new value of 5.6 W/(m·K).

Thermal conductivity depends significantly on the stoichiometry of the fuel, porosity produced during manufacture and created during irradiation within grains and at grain boundaries, and cracking of the fuel due both to temperature gradients and temperature changes produced during reactor operation.

The effect of porosity on thermal conductivity

The porosity correction proposed in MATPRO is based on the Maxwell-Eucken equation:

$$\lambda = \lambda_0 \frac{1-P}{1+\beta P} \tag{4.1.3-27}$$

where λ_0 is the thermal conductivity of fully dense fuel, P is the fractional porosity. Factor β is a linear function of temperature:

$$\beta = \beta_0 + \beta_1 T \tag{4.1.3-28}$$

For β_0 and β_1 the mean values of 6.5 and -0.00469, respectively have been proposed. This correction is limited to temperatures below 2050 K.

Many authors use the Loeb expression:

$$\lambda = \lambda_0 (1-\alpha P) \tag{4.1.3-29}$$

with different values for the coefficient α. Washington recommended $\alpha = 2.5$. Brandt proposed this factor as a linear function of temperature $\alpha = 2.6 - 0.5\times10^{-5}\cdot T$. This correction can be used up to 3100°C.

The recommendation of Harding takes into account the pore structure. He has proposed the relation:

$$\lambda = \lambda_0 (1-P_1)(1-P_2-P_3)^{2.5}(1-P_4-P_5)^{3.5} \tag{4.1.3-30}$$

where the various P's refer to volume fractions of different types of pores: P_1 -large spherical pores, P_2 - small spherical manufacturing pores, P_3 - spherical intragranular gas bubbles or pores, P_4 - lenticular grain face bubbles or pores, and P_5 - toroidal grain edge bubbles or pores.

The effect of nonstoichiometry on thermal conductivity

In MATPRO the influence of nonstoichiometry has been only considered in the term describing the effect of point defects on the phonon conductivity.

Other authors differentiate between hypostoichiometric (O/U ratio < 2.00) and hyperstoichiometric (O/U ratio > 2.00) fuels. In the case of $UO_{2-\eta}$ where η lies between 0 and 0.05, the thermal conductivity for stoichiometric UO_2 should be multiplied by a factor $(1+\eta)$ over the whole temperature range.

In case of hyperstoichiometric $UO_{2+\eta}$ for temperatures below 1800 K the correction proposed by Washington is also recommended by Harding and Martin [JT000029].

$$\lambda = \frac{1}{0.035+3.47\eta-7.26\eta^2+2.25\times10^{-4}T} + (83.0-537\eta+7610\eta^2)\times10^{-12}T^3 \qquad (4.1.3\text{-}31)$$

where η is stoichiometric excess $UO_{2+\eta}$.

For temperatures above 1800°K the Washington recommendation should be replaced by:

$$\lambda = \frac{1}{0.035+3.47\eta\phi-7.26\eta^2\phi+2.25\times10^{-4}T} + (83.0-537\eta\phi+7610\eta^2\phi)\times10^{-12}T \qquad (4.1.3\text{-}32)$$

where $\phi = (3120\text{-}T)/1347$, and T is temperature in K. These two relations are valid over the O/U range 2.00 to 2.02. Equation (4.1.3-31) can be used for the O/U range 2.02 to 2.10 over the temperature range 800 to 1300 K.

The effect of burnup on thermal conductivity

AECL, in collaboration with the European Institute of Transuranium Elements in Karlsruhe, Germany, have modelled the effect of burnup on thermal conductivity of UO2 through study of SIMFUEL (simulated high burnup fuel). SIMFUEL replicates the composition and the microstructure (without fission-gases and volatiles) of irradiated fuel by introducing 11 stable additives into the UO2, both those that are soluble in the fluorite-type lattice of the fuel and others that precipitate as second phases. The details on this work are contained in the references listed at the end of this section.

Thermal expansion

Recommended curves for the thermal expansion of UO_2 are presented in Figure 4.1.3.4. They have been calculated using the equations:

Fink:

for $298.15\text{ K} \le T \le 3120\text{ K}$

$$\varepsilon = -1.930412\times10^{-3} + 5.723\times10^{-6}T + 2.487\times10^{-9}T^2 + 1.140\times10^{-13}T^3 \qquad (4.1.3\text{-}33)$$

for $3120\text{ K} \le T \le 3400\text{ K}$

$$\varepsilon = 7.87\times10^{-2} + 3.775\times10^{-5}(T-3120) \qquad (4.1.3\text{-}34)$$

Harding:

for $273\text{ K} \le T \le 923\text{ K}$

$$\varepsilon = -2.66\times10^{-3} + 9.802\times10^{-6}T - 2.705\times10^{-10}T^2 + 4.391\times10^{-13}T^3 \qquad (4.1.3\text{-}35)$$

for $923\text{ K} \le T \le 3120\text{ K}$

$$\varepsilon = -3.28\times10^{-3} + 1.179\times10^{-5}T - 2.429\times10^{-9}T^2 + 1.219\times10^{-12}T^3 \qquad (4.1.3\text{-}36)$$

MATPRO:

for $300\text{ K} \le T \le 3113\text{ K}$

$$\varepsilon = 1.0\times10^{-5}T - 3.0\times10^{-3} + 4.0\times10^{-2}\exp\left(\frac{-6.9\times10^{-20}}{k_B T}\right) \qquad (4.1.3\text{-}37)$$

for $T > 3113$ K

$$\varepsilon = \varepsilon(T_m) + 0.043 + 3.6\times10^{-5}(T - T_m) \qquad (4.1.3\text{-}38)$$

where ε is the linear expansion (m/m), T is the temperature (K) and T_m is the melting temperature (3113 K) and k_B is Boltzmann constant.

Emissivity

Recommended curves for the spectral emissivity (ε_λ) of UO_2 are presented in Figure 4.1.3.5. They have been calculated from the relations:

Fink:

for $1000\ \text{K} < T \leq 3120$ K

$$\varepsilon_\lambda = 0.836 + 4.321\times10^{-6}(T - 3120) \qquad (4.1.3\text{-}39)$$

for $T > 3120$ K

$$\varepsilon_\lambda = 1 - 0.16096\exp\left[-3.7897\times10^{-4}(T-3120) - 3.2718\times10^{-7}(T - 3120)^2\right] \qquad (4.1.3\text{-}40)$$

Harding:

for $T \leq 3120$ K

$$\varepsilon_\lambda = 0.85 \qquad (4.1.3\text{-}41)$$

for $T > 3120$ K the recommendation of Fink is proposed.

where ε_λ - spectral emissivity for wave length, $\lambda = 0.63$ μm.

The *MATPRO* recommendation for total normal emissivity ε_t in solid state is:

$$\varepsilon_t = 0.7856 + 1.5263\times10^{-5}T \qquad (4.1.3\text{-}42)$$

Nomenclature to Section 4.1.3

C_P - specific heat capacity (J/(kg·K)
other units: 1 J/(g·K) = 10^3 J/(kg·K),
1 J/(mol·K) = 3.704 J/(kg·K) for UO_2
H_u - enthalpy (J/kg)
other units: 1 J/g = 10^3 J/kg,
1 J/mol = 3.704 J/kg for UO_2
T - temperature (K)
ε - thermal strain, (m/m)
other unit: %
λ - thermal conductivity, (W/(m·K))
ε_λ - spectral emissivity
ε_t - total emissivity.

Table 4.1.3.1 ENTHALPY: RECOMMENDED DATA FOR STOICHIOMETRIC UO_2

EKEY	DEN	MELTT	MELTH	YEAR	DONO	AU
E5000490	-	3120	277.1	1981	JT000080	Fink
E5002035	10.96	3120	283.0	1989	RT000062	Harding
E5001054	10.98	3113.15	274	1990	RT000063	MATPRO

- Descriptors, units	
DEN Density (g/cm^3)	MELTT Melting temperature (K)
MELTH Heat of fusion (J/g)	

Table 4.1.3.2 SPECIFIC HEAT CAPACITY: RECOMMENDED DATA FOR STOICHIOMETRIC UO_2

EKEY	MELTT	MELTH	AU	YEAR	DONO
E0006375	3113	274.0	MATPRO	1990	RT000063
E5000489	3120	277.1	Fink	1981	JT000080
E5001043	3120	283.0	Harding	1989	RT000062

Descriptors, units	
MELTT Melting temperature (K)	MELTH Enthalpy of fusion (J/g)

Table 4.1.3.3 THERMAL CONDUCTIVITY: RECOMMENDED DATA FOR STOICHIOMETRIC UO_2

EKEY	TD	MELTT	MELTH	YEAR	DONO	AU
E0006462	10.96	-	-	1976	R0000152	Brandt
E5000110	-	-	-	1973	RT000002	Washington
E5000187	10.95	-	-	1989	JT000029	Harding, Martin
E5000491	-	3120	277.1	1981	JT000080	Fink
E5001044	10.956	3120	283.0	1989	RT000062	Harding
E5001048	-	-	-	1983	JT000141	Hyland
E5001049	10.96	-	-	1982	JT000079	Killeen
E5001050	10.96	-	-	1982	JT000079	Ainscough
E5001058	10.98	3113	274.0	1990	RT000063	MATPRO
E5001178	10.96	-	-	1982	JT000079	Martin

Descriptors, units			
TD	Theoretical density (g/cm^3)	AU	Author(s)
MELTT	Melting temperature (K)	DONO	Document number
MELTH	Enthalpy of fusion (J/g)		

Table 4.1.3.4 THERMAL CONDUCTIVITY OF LIQUID UO_2

EKEY	THC	AU	DONO
E5001091	11	Kim	P0000052
E5001086	2.2	Tasman	JT000146
E5001090	8.5	Otter	JT000147

Descriptors, units			
EKEY	Data-set number	AU	Author(s)
THC	Thermal conductivity (W/(m·K))	DONO	Document number

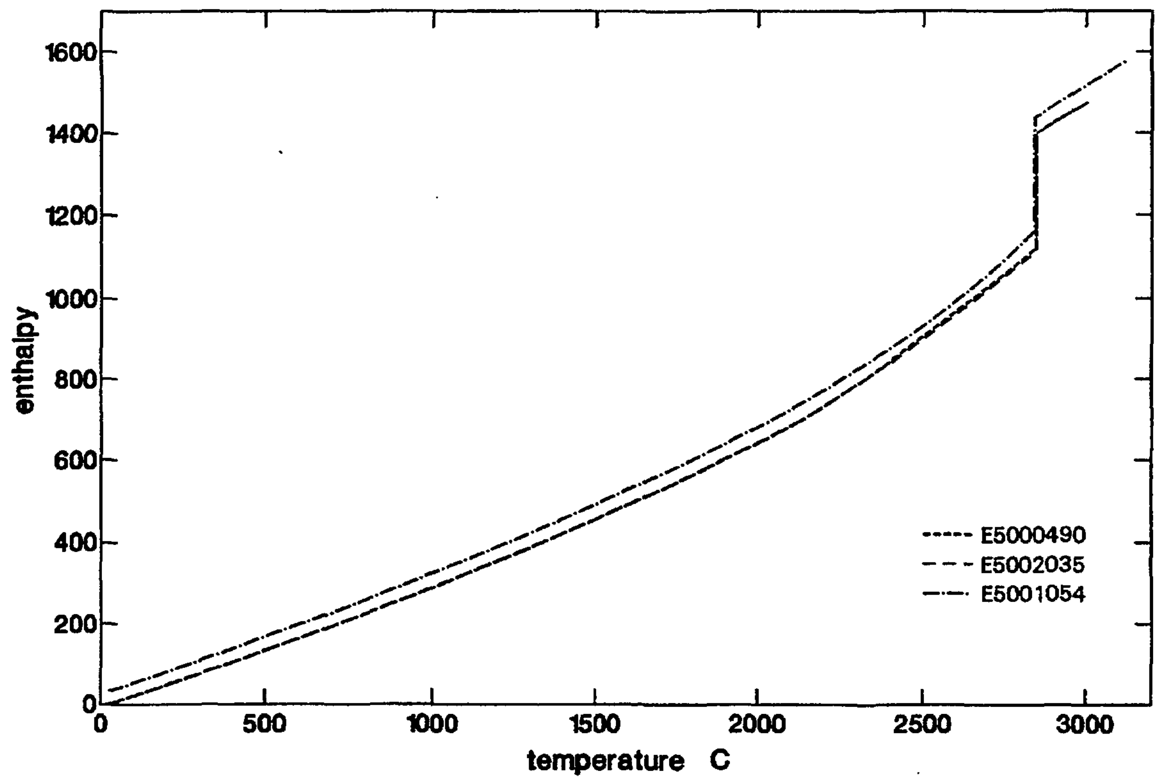

Figure 4.1.3.1 Enthalpy of UO_2

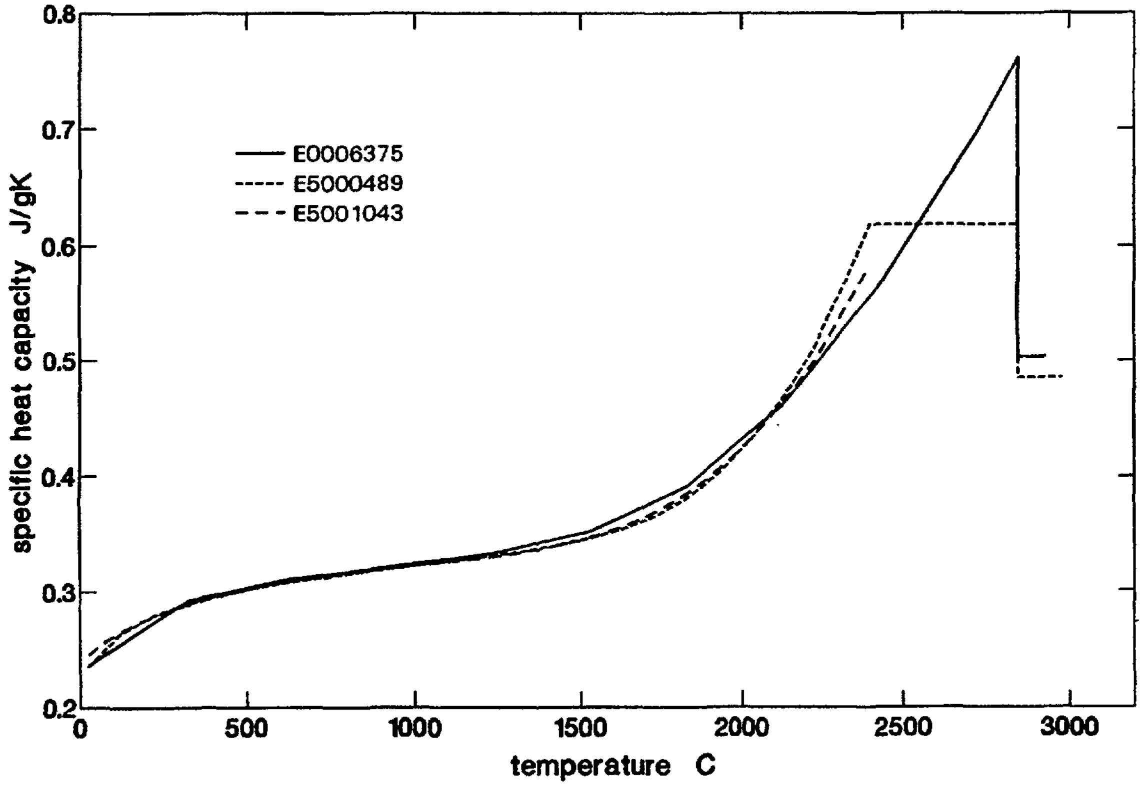

Figure 4.1.3.2 Recommended specific heat for UO_2

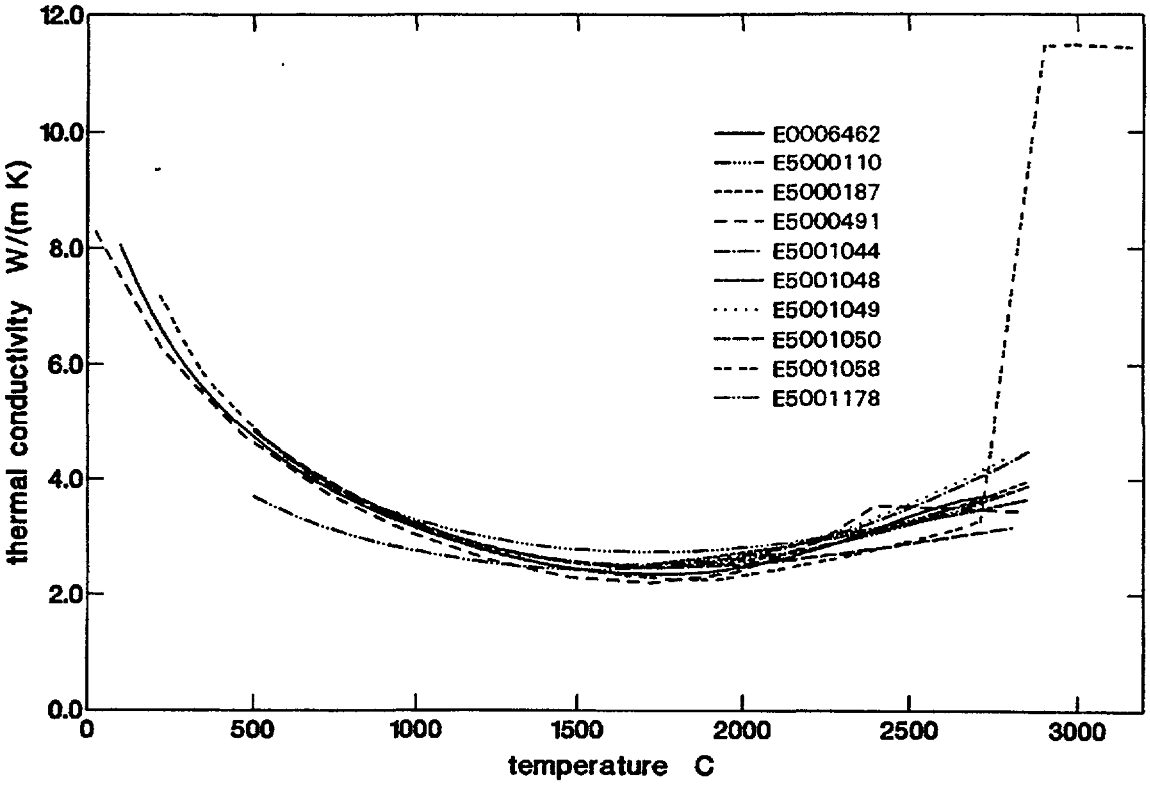

Figure 4.1.3.3 Recommended thermal conductivity of UO_2

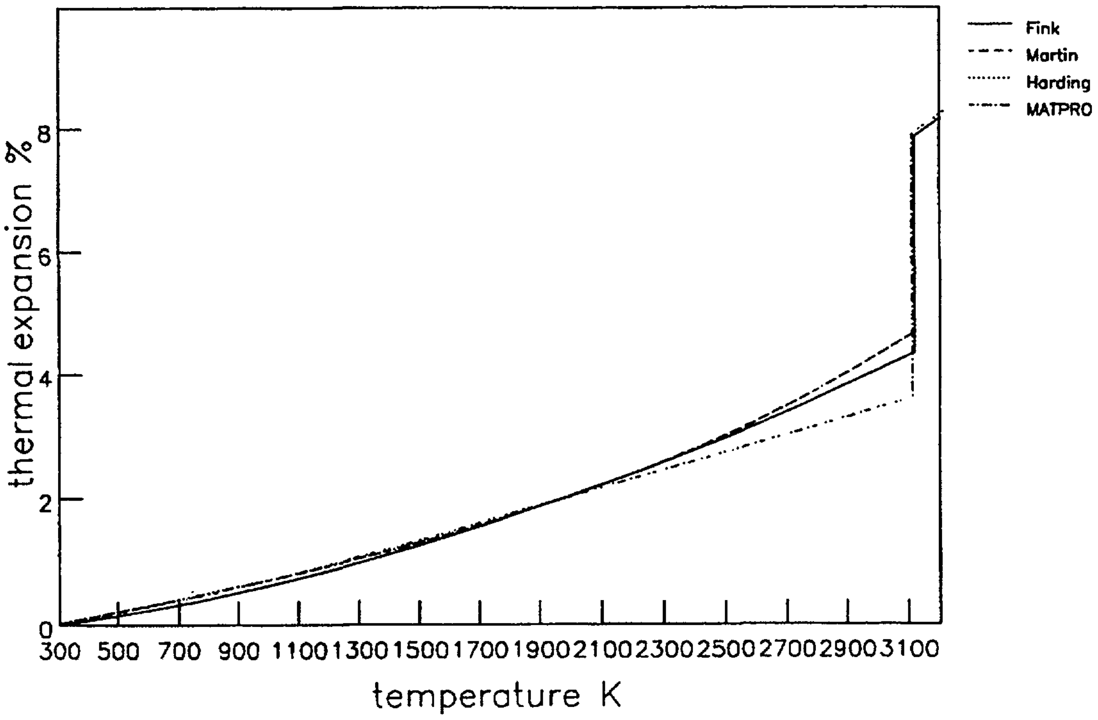

Figure 4.1.3.4 Recommended data for thermal expansion of UO_2

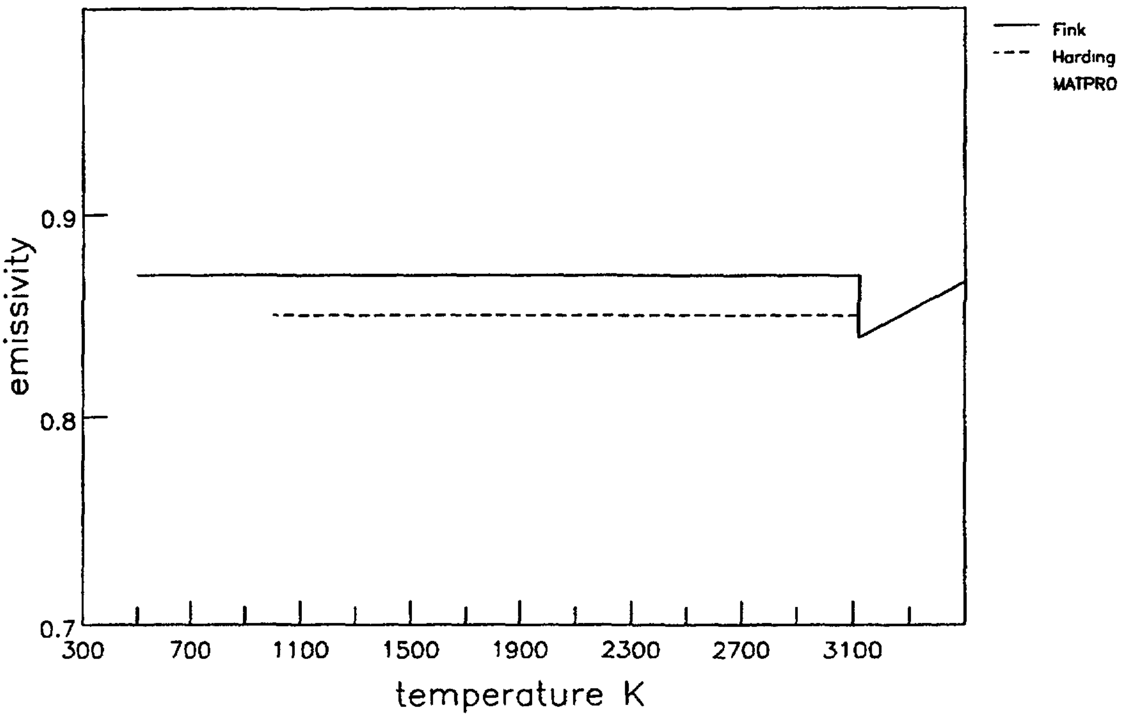

Figure 4 1 3 5 Recommended data for emissivity of UO_2

References to Section 4.1.3

Note: literature stored in THERSYST is referenced by document number, e.g. T000007, etc.

Enthalpy

JT000007 FINK J. K., "Enthalpy and heat capacity of the actinide oxides", Int. J. Thermophys. 3 (1982), 165-200

J0003099 LEIBOWITZ L., CHASANOV M. G., MISHLER L. W., FISCHER D. F., "Enthalpy of liquid uranium dioxide to 3500°C", J. Nucl. Mater. 39 (1971), 115-116

JT000028 KERRISK J. F., CLIFTON D. G., "Smoothed values of the enthalpy and heat capacity of UO_2", Nucl. Technol. 16 (1972), 531-535

JT000068 MILLS K. C., PONSFORD F. H., RICHARDSON M. J., ZAGHINI N., FASSINA P., "Heat capacity and enthalpy of UO_2 and gadolinia-doped UO_2", Thermochim. Acta 139 (1989), 107-120

JT000080 FINK, J. K., CHASANOV, M. G., LEIBOWITZ, L., "Thermophysical properties of uranium dioxide", J. Nucl. Mater. 102 (1981), 17-25

R0000148 HEIN R. A., FLAGELLA P. N., "Enthalpy measurements of UO_2 and tungsten to 3260 K", GEMP-578 (1968), General Electric, 21 p

RT000004 LEIBOWITZ, L., "Properties for LMFBR safety analysis", ANL-CEN-RSD-76-1 (1976)

RT000006 OGARD, A. E., LEARY J. A., "High temperature heat content and heat capacity of uranium dioxide and uranium dioxide-plutonium dioxide solid solution", LA-DC-8620 (1965), 1-26

RT000016 GIBBY R. L., "Enthalpy and heat capacity of $U_{0.75}Pu_{0.25}O_{2-x}$ (25-1490°C)", HEDL-TME 73-19 (1973), 1-29

RT000063 HOHORST J. K. (Editor), "SCDAP/RELAP5/MOD2 Code Manual, vol. 4: MATPRO-a library of materials properties for light-water-reactor accident analysis", NUREG/CR-5273 (1990)

Specific heat capacity

JT000007 FINK J. K., "Enthalpy and heat capacity of the actinide oxides", Int.J.Thermophys. 3 (1982), 165-200

JT000028 KERRISK J. F., CLIFTON D. G., "Smoothed values of the enthalpy and heat capacity of UO_2", Nucl. Technol. 16 (1972), 531-535

JT000068 MILLS K. C., PONSFORD F. H., RICHARDSON M. J., ZAGHINI N., FASSINA P., "Heat capacity and enthalpy of UO_2 and gadolinia-doped UO_2", Thermochim. Acta 139 (1989), 107-120

JT000074 AFFORTIT C., MARCON J.-P., "Chaleur specifique a haute temperature des oxydes d'uranium et de plutonium", Rev. Int. Haut. Temp. Refract. 7 (1970), 236-241

JT000080 FINK J. K., CHASANOV M. G., LEIBOWITZ L., "Thermophysical properties of uranium dioxide", J. Nucl. Mater. 102 (1981), 17-25

JT000144 INABA H., NAITO K., OGUMA M., "Heat capacity measurement of $U_{(1-y)}Gd_yO_2$ $0.00<y<0.142$) from 310 to 1500 K", J. Nucl. Mater. 149 (1987) 341-348

R0000148 HEIN R. A., FLAGELLA P. N. "Enthalpy measurements of UO_2 and tungsten to 3260 K", GEMP-578 (1968), General Electric, 21 p

RT000004 LEIBOWITZ, L., "Properties for LMFBR safety analysis", ANL-CEN-RSD-76-1 (1976)

RT000006 OGARD A. E., LEARY J. A., "High temperature heat content and heat capacity of uranium dioxide and uranium dioxide-plutonium dioxide solid solution", LA-DC-8620 (1965), 1-26

RT000062 HARDING J. H., MARTIN D. G., POTTER P. E., "Thermophysical and thermochemical properties of fast reactor materials", EUR 12402EN (1989), 1-90

RT000063 HOHORST J. K. (Editor), "SCDAP/RELAP5/MOD2 Code Manual, vol.4: MATPRO-a library of materials properties for light-water-reactor accident analysis", NUREG/CR-5273 (1990)

Thermal conductivity

JT000019 CRAYNEST VAN J. C.,STORA J. P., "Effet de la porosite sur la variation de conductibilite thermique du bioxyde d'uranium en fonction de la temperature. Application a l'oxyde mixte (U,Pu)O_2", J. Nucl. Mater. 37 (1970), 153-158

JT000021 GIBBY R. L., "The effect of plutonium content on the thermal conductivity of (U,Pu)O_2 solid solution", J. Nucl. Mater. 38 (1971), 163-177

JT000022 GOLDSMITH L. A., DOUGLAS J. A. M., "Measurements of the thermal conductivity of uranium dioxide at 670-1270 K", J. Nucl. Mater. 47(1973), 31-42 TRG Report 2103(W); UKAEA (1971), Addendum 1972

JT000023 SCHMIDT H. E., "Some considerations on the thermal conductivity of stoichiometric uranium dioxide at high temperatures", J. Nucl. Mater. 39 (1971), 234-237

JT000029 HARDING J. H., MARTIN D. G., "A recommendation for the thermal conductivity of UO_2", J. Nucl. Mater. 166 (1989), 223-226

JT000032 KAMIMOTO M., MURABAYASHI M., TAKAHASHI Y., MUKAIBO T., "Thermal conductivity of UO_2 and U_4O_9 from 100 to 300", J. Nucl. Mater. 46 (1973), 309-314

JT000043 FUKUSHIMA S., OHMICHI T., MAEDA A., HANDA M., "Thermal conductivity of near-stoichiometric (U,Nd)O_2, (U,Sm)O_2 and (U,Eu)O_2 solid solutions", J. Nucl. Mater. 114 (1983), 312-325

JT000045 FUKUSHIMA S., OHMICHI T., MAEDA A., WATANABE H., "The effect of yttrium content on the thermal conductivity of near-stoichiometric (U,Y)O_2 solid solutions", J. Nucl. Mater. 102 (1981), 30-39

JT000070 FUKUSHIMA S., OHMICHI T., MAEDA A., WATANABE H., "The effect of gadolinium content on the thermal conductivity of near-stoichiometric (U,Gd)O_2 solid solutions", J. Nucl. Mater. 105 (1982), 201-210

JT000079 MARTIN D. G., "A re-appaisal of the thermal conductivity of UO_2 and mixed (U,Pu)O_2 oxide fuels", J. Nucl. Mater. 110 (1982), 73-94

JT000080 FINK J. K., CHASANOV M. G., LEIBOWITZ L., "Thermophysical properties of uranium dioxide", J. Nucl. Mater. 102 (1981), 17-25

JT000110 HIRAI M., ISHIMOTO S., "Thermal diffusivities and thermal conductivities of UO_2-Gd_2O_3", J. Nucl. Sci. Technol. 28 (1991), 995-1000

JT000141 HYLAND G. J., "Thermal conductivity of solid UO_2: critique and recommendation", J. Nucl. Mater. 113 (1983), 125-132

JT000146 TASMAN H. A., PEL D., RICHTER J., SCHMIDT H.-E., "Measurement of thermal conductivity of liquid UO_2", High Temp. -High Pressures 15 (1983), 419-431

JT000147 OTTER C., DAMIEN D., "Mesure de la diffusivite thermique de UO_2 fondu", High Temp. -High Pressures 16 (1984), 1-6

JT000148 FINK J. K., LEIBOWITZ L., "An analysis of measurements of the thermal conductivity of liquid urania", High Temp. -High Pressures 17 (1985), 17-26

JT000149 PRESTON S. D., BARRETT C., FASSINA P., MILLS K. C., ZAGHINI N., "Thermal diffusivities and thermal conductivities of UO_2 and $U_{(1-x)}Gd_xO_2$ solid solutions", High Temp. -High Pressures 21 (1989), 287-295

P0000052 KIM C. S., et al., "Measurement of thermal diffusivity of molten UO_2", (Proceedings of the 7th Symposium on Thermophysical Properties), Gaithersburg, Maryland (1977)

PT000002 SCHMIDT H. E., RICHTER J., van den BERG M., "Eine neue Methode zur Messung der Wärmeleitfähigkeit", BMBW-FB K 70-01 (1970), 176-200

PT000018 LILI Z., BIN L., "The measurement of thermal conductivity of nuclear fuels in China", Proc.2nd Research Co-ordination Meeting of CRP (Establishment of a Data Base for Thermophysical Properties), 19-22 April (1993), Vienna, Austria

R0000095 GODFREY T. G., FULKERSON W., KOLLIE T. G. et al., "Thermal conductivity of uranium dioxide and Armco iron by an improved radial heat flow technique", ORNL-3556 (1964), 1-67

R0000149 STORA J.-P., de BERNARDY de SIGOYER B., DELMAS R., DESCHAMPSP., LAVAUD B., "Conductibilite thermique de l'oxyde d'uranium fritte dans les conditions d'utilisation en pile", CEA-R 2586, Commissariat a l'Energie Atomic, Paris (1964)

R0000150 ITAKI T., KITIHARA T., TSUTSUMI M., et al., "In-Core measurement of the thermal conductivity of Vipac UO_2 fuel (2)", PNCPU-report-040,(1969),105-113

R0000151 CONWAY J. B., FEITH A. D., "An interim report on a round robin experimental program to measure the thermal conductivity of stoichiometric uranium dioxide", GEMP-715(1969),Addendum (1970), General Electric Co.

R0000152 BRANDT R., HAUFLER G., NEUER G., "Thermal conductivity and emittance of solid UO_2", Ed.: Y. S. Touloukian, CINDAS, Purdue University (1976)

R0000153 VOGT J., GRANDELL L., RUNFORS U., "Determination of the thermal conductivity of unirradiated uranium dioxide", RMB-527 (1964)

R0000154 DANIEL J. L., MATOLICH JR. J., DEEM H. W., "Thermal conductivity of UO_2", HW-69945 (1962), General Electric, 42 p

RT000002 WASHINGTON A. B. G., "Preferred values for thermal conductivity of sintered ceramic fuel for fast reactor use", TRG-Report-2236(D) (1973), 1-61

RT000004 none given, "Properties for LMFBR safety analysis", ANL-CEN-RSD-76-1 (1976)

RT000013 HETZLER F. J., LANNIN T. E., PERRY K. J., ZEBROSKI E.L., "The thermal conductivity of uranium and uranium-plutonium oxides", GEAP-4879 (1967), 1-28

RT000014 LASKIEWICZ R. A., EVANS S. K., MELDE G. F., BOHABOY P. E., "Thermal conductivity of uranium-plutonium oxide", GEAP-13733 (1971), 1-26

RT000021 ASAMOTO R. R., ANSELIN F. L., CONTI A. E., "The effect of density on the thermal conductivity of uranium dioxide", GEAP-5493 (1968), 1-50

RT000026 HAGRMAN D. L., REYMANN G. A., MASON R. E. (Eds.), "MATPRO-version 11 (revision 2); A handbook of materials properties for use in the analysis of light water reactor fuel rod behavior", NUREG/CR-0479 TREE-1280,Rev.2 (1981), 1-529

RT000062 HARDING J. H., MARTIN D. G., POTTER P. E., "Thermophysical and thermochemical properties of fast reactor materials", EUR 12402EN (1989), 1-90

RT000063 HOHORST J. K. (Editor), "SCDAP/RELAP5/MOD2 Code Manual, vol. 4: MATPRO- a library of materials properties for light-water-reactor accident analysis", NUREG/CR-5273 (1990)

RT000076 DEEM H. W., NELSON H. R., "Thermal conductivity of powder-metallurgy uranium", BMI-745 (1952), 1-15

TT000001 WEILBACHER J. C., "Mesure de la diffusivite thermique des oxydes mixtes d'uranium et de plutonium. Influence de la stoechiometrie et de la teneur en plutonium", Thesis (1972)

Additional literature, collected in China

(1) S. YING and Z. JI, Nucl. Power Engineering, 1 (1980), 1-12

(2) W. LI et al., Nucl. Science and Engineering, 3 (1983), 251

(3) J. YU et al., Atomic Science and Technology, 3 (1981), 298

(4) S. YING and Z. JI, Proc. of 1st Asian Thermophysical Properties Conference (1986), 658-664

(5) J. SHEN and Z. LIANG, Proc. of Nuclear Mat. Conference, Private Communication (1983)

References on work with SIMFUEL

(1) LUCUTA P.G., MATZKE HJ., HASTINGS I.J., "A Pragmatic Approach to Modelling Thermal Conductivity of Irradiated UO_2 Fuel: Review and Recommendations", submitted to J. Nucl. Mater. 1996 April

(2) LUCUTA P.G., MATZKE HJ., VERRAL R.A., "Modelling of UO_2 Based SIUFUEL Thermal Conductivity - the Effect of Burnup", J. Nucl. Mater. 217 (1994) 279-286

(3) LUCUTA P.G., MATZKE HJ., VERRAL R.A., "Thermal Conductivity of Hyperstoichiometric SIMFUEL", J. Nucl. Mater. 223 (1995) 51-60

(4) LUCUTA P.G., MATZKE HJ., VERRAL R.A., TASMAN H.A., "Thermal Conductivity of SIMFUEL", J. Nucl. Mater. 188 (1992) 198-204

(5) MATZKE HJ., LUCUTA P.G., VERRAL R.A., HIERNAUT J.P., "Thermophysical Properties of UO_2 and SIMFUEL - Simulated High-Burnup Fuel", Thermal Conductivity 22 (1994) 904-912

(6) LUCUTA P.G., MATZKE HJ., VERRAL R.A., KLEMENS P.G., "Analysis of SIMFUEL Thermal Conductivity", Thermal Conductivity 22 (1994) 894-903

(7) LUCUTA P.G., VERRAL R.A., MATZKE HJ., HASTINGS I.J., "A Characterization and Thermal Properties of Hyperstoichiometric SIMFUEL", IAEA-TECDOC-697 (1993) 165-172.

Thermal expansion

JT000080 FINK J. K., CHASANOV M. G., LEIBOWITZ L., "Thermophysical properties of uranium dioxide", J. Nucl. Mater. 102 (1981), 17-25

JT000098 MARTIN D. G., "The thermal expansion of solid UO_2 and (U,Pu) mixed oxides - a review and recommendations", J. Nucl. Mater. 152 (1988), 94-101

JT000142 UNE K., "Thermal expansion of UO_2-Gd_2O_3 fuel pellet", J. Nucl. Sci. Technol. 23 (1986), 1020-1022

J0003089 CONWAY J. B., FINCEL Jr. R. M., HEIN R. A., "The thermal expansion and heat capacity of UO_2 to 2200 C°," Trans. Am. Nucl. Soc. 6 (1963), 153

PT000012 BRETT N. H., RUSSELL L.E., "The thermal expansion of PuO_2 and other actinide oxides between room temperature and 1000 C°", Proc.2nd Int. Conf. Plutonium Metallurgy; Grenoble 1960; Eds. E. Grison, W. B. H. Lord, R. D. Fowler; Cleaver-Hume Press Ltd., London (1961)

PT000030 DROTNING W. D., "Thermal expansion of molten uranium dioxide", Proceedings of 8th Symposium on Thermophysical Properties; NBS, Gaithersburg, Maryland (1981)

RT000004 LEIBOWITZ, L. "Properties for LMFBR safety analysis", ANL-CEN-RSD-76-1 (1976)

RT000008 ROTH J., HALTEMAN E. K., "Thermal expansion of coprecipitated $(U,Pu)O_2$ powders by X-ray diffraction techniques," NUMEC-2389-9 (1965), 1-63

RT000062 HARDING J. H., MARTIN D. G., POTTER P. E., "Thermophysical and thermochemical properties of fast reactor materials", EUR 12402EN (1989), 1-90

RT000063 HOHORST J. K. (Editor), "SCDAP/RELAP5/MOD2 Code Manual, vol. 4: MATPRO-a library of materials properties for light-water-reactor accident analysis", NUREG/CR-5273 (1990)

TPM13000 TOULOUKIAN Y. S., KIRBY R. K., TAYLOR R. E., LEE T. Y. R., "Thermophysical Properties of Matter. Vol. 13: Thermal Expansion - Nonmetallic Solids", IFI/Plenum, New York-Washington (1977)

Additional literature with new experimental data

(1) A. C. MOMIN et al., J. Nuclear Materials 185 (1990), 308-310

Emissivity

JT000039 BOBER M., KAROW H. U., MUELLER K., "Study of the spectral reflectivity and emissivity of liquid ceramics", High Temp. -High Pressures 12 (1980), 161-168

JT000080 FINK J. K., CHASANOV M. G., LEIBOWITZ L., "Thermophysical properties of uranium dioxide", J. Nucl. Mater. 102 (1981), 17-25

RT000062 HARDING J. H., MARTIN D. G., POTTER P. E., "Thermophysical and thermochemical properties of fast reactor materials", EUR 12402EN (1989), 1-90

RT000063 HOHORST J. K. (Editor), "SCDAP/RELAP5/MOD2 Code Manual, vol. 4: MATPRO-a library of materials properties for light-water-reactor accident analysis", NUREG/CR-5273 (1990)

4.1.4. UO_2-PuO_2 mixture

Enthalpy

Data on the enthalpy of the mixed oxide $(U_{0.8}Pu_{0.2})O_2$ are presented in Figure 4.1.4.1, the identification of the curves is given in Table 4.1.4.2.

The MATPRO-recommendation for the solid phase was determined by combining the contribution from each constituent in the proportion to its weight fraction. For the enthalpy of UO_2 the equation (4.1.3-6) should be used. For PuO_2 the following expression is recommended:

$$H_u = \frac{347.4 \times 571}{\exp\left(\frac{571}{T}\right) - 1} + \frac{3.95 \times 10^{-4} T^2}{2} + \frac{3.860 \times 10^7}{2} \exp\left(\frac{-1.967 \times 10^5}{RT}\right) \tag{4.1.4-1}$$

For molten fuel the enthalpy is calculated using the expression:

$$H_u = H_u(T_m) + H_m + (T - T_m) \cdot C_P(T_m) \tag{4.1.4-2}$$

where $H_u = H(T) - H(300)$ is the enthalpy (J/kg), T is the temperature (K), H_m is the heat of fusion (J/kg), $H_u(T_m)$ and $C_P(T_m)$ is the enthalpy and specific heat at melting temperature T_m, respectively.

Fink analyzed the experimental data of Gibby [RT000016], Leibowitz [JT000156], [RT000016], Ogard and Leary [RT000006], and Clifton [RT000024] and recommended for the enthalpy of $(U_{0.8}Pu_{0.2})$ O_2 the following expressions:

$298.15 \text{ K} \le T \le 2750 \text{ K}$

$$\begin{aligned} H_u = {} & 50998.52\left\{\left[\exp\left(\frac{585.49}{T}\right) - 1\right]^{-1} - \left[\exp\left(\frac{585.49}{298.15}\right) - 1\right]^{-1}\right\} \\ & + 8.0048 \times 10^{-4}\left[T^2 - (298.15)^2\right] \\ & + 2.6863 \times 10^6 k_B\left[T\exp\left(-\frac{0.75748}{k_B T}\right) - 298.15\exp\left(-\frac{0.75748}{298.15 k_B}\right)\right] \end{aligned} \tag{4.1.4-3}$$

where k_B is the Boltzmann constant = 8.6144×10^{-5} eV·K^{-1}

$2750 \text{ K} < T < T_m$

$$H_u = 161.80T - 205940 \tag{4.1.4-4}$$

where $H_u = H(T) - H(298.15)$ is the enthalpy (J·mol^{-1}) and T is the temperature (K).

Harding has used the mole average technique to determine the enthalpy of mixed oxide. By plotting the enthalpy against the reduced temperature $\tau = T/T_m$ (T_m is melting temperature) he was able to divide the solid state temperature range into two parts: below and above $\tau = 0.856$. For the enthalpy of UO_2 he recommended equations (4.1.3-4 and 4.1.3-5), and for PuO_2 the following relations:

For $\tau \le 0.856$ ($298 \text{ K} < T \le 2312 \text{ K}$)

$$H_u = -32481 + 228656\tau + 43346\tau^2 - 11270\tau^3 + 987.72\tau^4 + 1970.7\tau^5 + 744.21\tau^{-1} \tag{4.1.4-5}$$

For $\tau > 0.856$ ($T > 2312$ K)

$$H_u = 352544\tau - 109876 \qquad (4.1.4\text{-}6)$$

where H_u is the enthalpy (J/mol), and T is the temperature (K). The reference temperature is 298 K.

For molten mixed oxide he used the recommendation of Rand et al.,for all compositions of $(U,Pu)O_2$:

$$H_u = 130.95T - 30911.4 \qquad (4.1.4\text{-}7)$$

The enthalpy of fusion H_f for mixed oxide is given by:

$$H_f = 76537.9 + 3581.5y \qquad (4.1.4\text{-}8)$$

where y - fraction of PuO_2.

The error on the enthalpy below $\tau = 0.856$ is about 2% and above rises to 5%. The error for molten fuel is approximately 10%.

Specific heat capacity

The specific heat capacity of solid mixture of $(U,Pu)O_2$ is determined in MATPRO by combining the contribution from each constituent in the proportion to its weight fraction. It is calculated using equation (4.1.3-14) for UO_2 and the following relation for PuO_2:

$$C_P = \frac{347.4\times 571^2 \exp\left(\frac{571}{T}\right)}{T^2\left[\exp\left(\frac{571}{T}\right) - 1\right]^2} + 3.95\times 10^{-4}T + \frac{3.860\times 10^7 \cdot 1.967\times 10^5}{RT^2}\exp\left(\frac{-1.965\times 10^5}{RT}\right) \qquad (4.1.4\text{-}9)$$

For molten mixed oxide MATPRO proposed the same value as for UO_2:

$$C_P = 503 \qquad (4.1.4\text{-}10)$$

where C_P is the specific heat capacity (J/(kg·K)), and T is the temperature (K). The standard error for solid material is between 6 and 10 (J/kg·K) depending on the fraction of PuO_2.

Fink analyzed the experimental data of Gibby [RT000016], Leiboewitz [JT000156], [RT000016], Ogard and Leary [RT000006], and Clifton [RT000024] and recommended for the enthalpy of $(U_{0.8}\,Pu_{0.2})O_2$ the following expressions:

For 298.15 K $\leq T \leq$ 2750 K

$$C_P = \frac{2.9859\times 10^7 \exp\left(\frac{585.49}{T}\right)}{T^2\left[\exp\left(\frac{585.49}{T}\right) - 1\right]^2} + 1.6010\times 10^{-3}T + 2.6863\times 10^6 k_B \exp\left(-\frac{0.75748}{k_B T}\right)\left(1 + \frac{0.75748}{k_B T}\right) \qquad (4.1.4\text{-}11)$$

where k_B is the Boltzmann constant = 8.6144×10^{-5} eV·K^{-1}

For 2750 K $\leq T \leq T_m$

$$C_P = 161.80 \tag{4.1.4-12}$$

where C_P is specific heat in J/(mol·K)

Harding proposed using the mole average technique. He plotted the specific heat against reduced temperature $\tau = T/T_m$ (T_m - melting temperature) and divided the solid state temperature range in two parts: below and above $\tau = 0.856$. For the specific heat of UO_2 equations (4.1.3-11) and (4.1.3-12) should be used. For PuO_2 he proposed:

For $\tau \leq 0.856$

$$C_P = \frac{1}{T_m}(228656 + 86692\tau - 33810\tau^2 + 3950.5\tau^3 + 9853.53\tau^4 - 744.21\tau^{-2}) \tag{4.1.4-13}$$

For $\tau > 0.856$

$$C_P = 130.54 \tag{4.1.4-14}$$

where C_P is the specific heat capacity (J/(mol·K)), and T is the temperature (K).

The errors for the solid state are 5% and 10% below and above $\tau = 0.856$, respectively.

For molten (U, Pu)O_2 he proposed the value:

$$C_P = 130.95 \tag{4.1.4-15}$$

The available experimental data together with recommended curves are presented in Figure 4.1.4.2.

Thermal conductivity

According to Harding, the conductivity of $(U_{0.8}Pu_{0.2})O_2$ is 5% lower than that of UO_2 over the whole temperature range and is given by the relation

$$\lambda = \frac{1}{0.037 + 2.37\times10^{-4}T} + 78.9\times10^{-12}T^3 \tag{4.1.4-16}$$

This equation is valid for all plutonium compositions between 12 and 30%. Below 12% the reduction in conductivity from that of the UO_2 value is proportionately less. This also applies to the hypo- and hyperstoichiometric mixed oxide fuel recommendations discussed below.

For hypostoichiometric mixed oxide fuel (O/M ratio = $2 - \chi$)

$$\lambda = 0.037 + 3.33\chi + 2.37\times10^{-12}T^3 \tag{4.1.4-17}$$

over the range $0.00 \leq \chi \leq 0.10$ and $773 < T \leq 3120 - 470y$

where y is the fraction of plutonium.

For hyperstoichiometric mixed oxide fuel (O/M ratio = $2 + \chi$)

$$\lambda = \frac{1}{0.037 + 1.67\chi + 2.37\times10^{-4}T} + 78.9\times10^{-12}T^3 \qquad (4.1.4\text{-}18)$$

over the range $0.00 \le \chi \le 0.12$ and $773 \le T \le 3120 - 470y$.

where λ is the thermal conductivity (W/(m·K)) and T is the temperature (K).

The thermal conductivity is presented in Figure 4.1.4.3.

Weilbacher [TT00001] measured the thermal diffusivity of uranium-plutonium mixed oxides. These data will be added to the data base at a later date.

Thermal expansion

The MATPRO equation for the thermal expansion of solid UO_2 and PuO_2 is

$$\varepsilon = K_1T - K_2 + K_3 \exp\left(-\frac{E_D}{k_BT}\right) \qquad (4.1.4\text{-}19)$$

where ε - linear strain (equal to zero at 300 K) (m/m), T is the temperature (K) and k_B is Boltzmann's constant (1.38×10^{-23} J/K). The other parameters are given in Table 4.1.4.1.

For solid mixed oxide the thermal expansion may be found by combining the contribution from each constituent in proportion to its weight fraction.

During melting an expansion equal to a linear strain of 0.043 occurs.

The uncertainty of the pooled data was found to be temperature-dependent, increasing approximately linearly with temperature. Therefore, a ±10% error is given rather than a fixed value.

The linear thermal expansion data are presented in Figure 4.1.4.4.

Nomenclature to Section 4.1.4

C_p	- specific heat capacity, (J/(kg·K),	other units: 1 J/(g·K) = 10^3 J/(kg·K), 1 J/(mol·K) = 3.623 J/(kg·K) for PuO_2, 1 J/(mol·K) = 3.687 J/(kg·K) for $(U_{0.8}Pu_{0.2})O_2$
H_u, H_f	- enthalpy, (J/kg),	other units: 1 J/g = 10^3 J/kg, 1 J/mol = 3.623 J/kg for PuO_2, 1 J/mol = 3.687 J/kg for $(U_{0.8}Pu_{0.2})O_2$;
T	- temperature (K);	
ε	- thermal strain, (m/m),	other unit: %
λ	- thermal conductivity, (W/(m·K)).	

Table 4.1.4.1 PARAMETERS USED IN UO_2 AND PuO_2 SOLID PHASE THERMAL EXPANSION CORRELATIONS

Constant	UO_2	PuO_2	Units
K_1	1.0×10^{-5}	9.0×10^{-6}	K^{-1}
K_2	3.0×10^{-3}	2.7×10^{-3}	Unitless
K_3	4.0×10^{-2}	7.0×10^{-2}	Unitless
E_D	6.9×10^{-20}	7.0×10^{-20}	J

Table 4.1.4.2 ENTHALPY OF $(U_{0.8}Pu_{0.2})O_2$

```
  EKEY    I CCOM   I MELTT I MELTH   I TRATXT    I TRAT   I DONO     I AU
---------I-------I-------I--------I----------I-------I----------I---------
E5000041 I 2.00  I ---   I ---    I solidus  I 2998   I RT000004 I Leibowitz
         I       I ---   I ---    I liquidus I 3043   I          I
E5000079 I 2.00  I ---   I ---    I          I        I JT000007 I Fink
E5000131 I 2.00  I ---   I ---    I          I        I RT000006 I Ogard
E5000132 I 1.98  I ---   I        I          I        I RT000006 I Ogard
E5000169 I 1.98  I ---   I ---    I          I        I RT000010 I Gibby
E5000198 I 1.97  I 3025  I ---    I          I        I RT000012 I Leibowitz
E5001855 I 1.97  I 3025  I ---    I          I        I RT000012 I Leibowitz
E5000225 I 1.98  I ----  I ---    I          I        I RT000016 I Gibby
E5000226 I 1.95  I ---   I ---    I          I        I RT000016 I Gibby
E5000351 I 2.00  I ---   I ---    I          I        I RT000024 I Clifton
E5001204 I 2.00  I ---   I ---    I          I        I RT000066 I Baker
E5001194 I 1.971 I ---   I ---    I          I        I JT000156 I Leibowitz
E5001195 I 1.971 I ---   I ---    I          I        I JT000156 I Leibowitz
E5001378 I 2.00  I ---   I 285.3  I solidus  I 3001   I RT000062 I Harding
         I       I       I        I liquidus I 3004   I
E5001647 I 2.00  I ---   I ---    I          I        I RT000006 I Ogard
E5001649 I 1.98  I ---   I ---    I          I        I RT000006 I Ogard
E5001856 I 1.92  I 3025  I ---    I          I        I RT000012 I Leibowitz
E5002038 I 2.00  I ---   I ---    I solidus  I 3112.1I RT000063 I MATPRO
         I       I       I        I liquidus I 3112.5I
```

```
Signification of descriptors
----------------------------
CCOM    O/(U+Pu) ratio               MELTT   melting temperature [K]
MELTH   heat of fusion [J/g]         TRATXT  phase transition
TRAT    temperature of phase transition [K]
```

Table 4.1.4.3 SPECIFIC HEAT OF $(U_{0.8}Pu_{0.2})O_2$

```
  EKEY     I CCOMA    I DONO     I AU
---------I---------I----------I------------
E5000001 I 2.000    I JT000001 I Schmidt
E5000002 I 1.990    I JT000001 I Schmidt
E5000003 I 1.980    I JT000001 I Schmidt
E5000004 I 1.960    I JT000001 I Schmidt
E5000005 I 1.945    I JT000001 I Schmidt
E5000006 I 1.930    I JT000001 I Schmidt
E5000040 I 1.980    I RT000004 I Leibowitz
E5000080 I 2.000    I JT000007 I Fink
E5000133 I 2.000    I RT000006 I Ogard
E5000134 I 1.980    I RT000006 I Ogard
E5000199 I 1.970    I RT000012 I Leibowitz
E5000227 I 1.980    I RT000016 I Gibby
E5000228 I 1.950    I RT000016 I Gibby
E5000409 I 1.980    I JT000074 I Affortit
E5000410 I 2.000    I JT000074 I Affortit
E5000411 I 2.045    I JT000074 I Affortit
E5000412 I 2.080    I JT000074 I Affortit
E5000413 I 1.830    I JT000074 I Affortit
E5000414 I 2.050    I JT000074 I Affortit
E5001196 I 1.971    I JT000156 I Leibowitz
E5001379 I 2.000    I RT000062 I Harding

CCOMA       oxygen/(U+Pu) ratio
```

Table 4.1.4.4 THERMAL CONDUCTIVITY OF $(U_{0.8}Pu_{0.2})O_2$

EKEY	CCOM	DEN	POR	DONO	AU
E5000008	2.00	---	5.0	JT000001	Schmidt
E5000010	1.99	---	5.0	JT000001	Schmidt
E5000012	1.98	---	5.0	JT000001	Schmidt
E5000014	1.96	---	5.0	JT000001	Schmidt
E5000016	1.945	---	5.0	JT000001	Schmidt
E5000018	1.93	---	5.0	JT000001	Schmidt
E5000042	2.00	---	5.0	RT000004	Leibowitz
E5000043	1.95	---	5.0	RT000004	Leibowitz
E5000044	1.90	---	5.0	RT000004	Leibowitz
E5000087	2.00	---	5.0	RT000002	Washington
E5000088	2.00	---	5.0	RT000002	Washington
E5000089	2.00	---	4.0	RT000002	Washington
E5000090	2.00	---	4.0	RT000002	Washington
E5000091	2.00	---	3.0	RT000002	Washington
E5000092	2.00	---	3.0	RT000002	Washington
E5000093	2.00	---	2.0	RT000002	Washington
E5000094	2.00	---	2.0	RT000002	Washington
E5000095	2.00	---	1.0	RT000002	Washington
E5000096	2.00	---	1.0	RT000002	Washington
E5000097	2.00	---	0	RT000002	Washington
E5000098	2.00	---	0	RT000002	Washington
E5000125	2.00	10.90	---	JT000021	Gibby
E5000142	2.00	---	5.0	PT000003	Schmidt
E5000143	1.995	---	5.0	PT000003	Schmidt
E5000144	1.990	---	5.0	PT000003	Schmidt
E5000145	1.980	---	5.0	PT000003	Schmidt
E5000146	1.960	---	5.0	PT000003	Schmidt
E5000147	1.945	---	5.0	PT000003	Schmidt
E5000148	1.930	---	5.0	PT000003	Schmidt
E5000194	1.990	10.60	4.0	RT000011	Gibby
E5000195	1.990	10.60	4.0	RT000011	Gibby
E5000196	2.00	10.57	4.6	RT000011	Gibby
E5000197	2.00	10.57	4.6	RT000011	Gibby
E5000200	2.00	---	4.8	RT000013	Hetzler
E5000201	2.00	---	4.5	RT000013	Hetzler
E5000202	1.982	---	5.2	RT000013	Hetzler
E5000203	1.982	---	5.7	RT000013	Hetzler
E5000204	1.982	---	3.4	RT000013	Hetzler
E5000205	2.048	---	6.9	RT000013	Hetzler
E5000206	2.048	---	7.9	RT000013	Hetzler
E5000216	1.986	---	9.0	RT000014	Laskiewicz
E5000217	1.940	---	9.0	RT000014	Laskiewicz
E5000218	1.950	---	9.0	RT000014	Laskiewicz
E5000219	1.950	---	9.0	RT000014	Laskiewicz
E5000220	1.960	---	16.0	RT000014	Laskiewicz
E5000221	1.965	---	14.5	RT000014	Laskiewicz
E5000222	1.965	---	13.1	RT000014	Laskiewicz
E5000223	1.980	---	9.0	RT000014	Laskiewicz
E5000224	2.00	---	9.0	RT000014	Laskiewicz
E5000462	1.980	---	5.0	RT000050	Philipponn
E5000486	2.00	10.50	---	RT000051	Craynest
E5000487	1.980	10.44	---	RT000051	Craynest
E5000488	1.930	10.30	---	RT000051	Craynest
E5000705	1.980	10.50	---	RT000042	Yokouchi
E5000969	2.00	10.59	4.1	JT000002	Fukushima
E5001028	1.940	---	8.3	JT000015	Evans
E5001029	1.950	---	8.3	JT000015	Evans
E5001030	1.980	---	8.3	JT000015	Evans
E5001031	2.00	---	8.3	JT000015	Evans
E5001180	2.00	---	0	JT000079	Martin
E5001181	1.900	---	0	JT000079	Martin
E5001182	2.120	---	0	JT000079	Martin
E5001376	2.00	11.06	0	RT000062	Harding

Units of descriptors

CCOM	O/(U+Pu) ratio	DEN	density [g/cm^3]
POR	porosity [%]		

Table 4.1.4.5 THERMAL EXPANSION OF $(U_{0.8}Pu_{0.2})O_2$

```
EKEY      I CCOM I DEN      I POR   I DONO      I AU
---------I------I--------I------I----------I----------
E5000151 I 2.10 I 10.72  I 3.1   I RT000008 I Roth
E5001377 I 2.00 I 11.06  I 0     I RT000062 I Harding

Units of descriptors
--------------------
CCOM     O/(U+Pu) ratio
DEN      density  [g/cm^3]
POR      porosity [%]
```

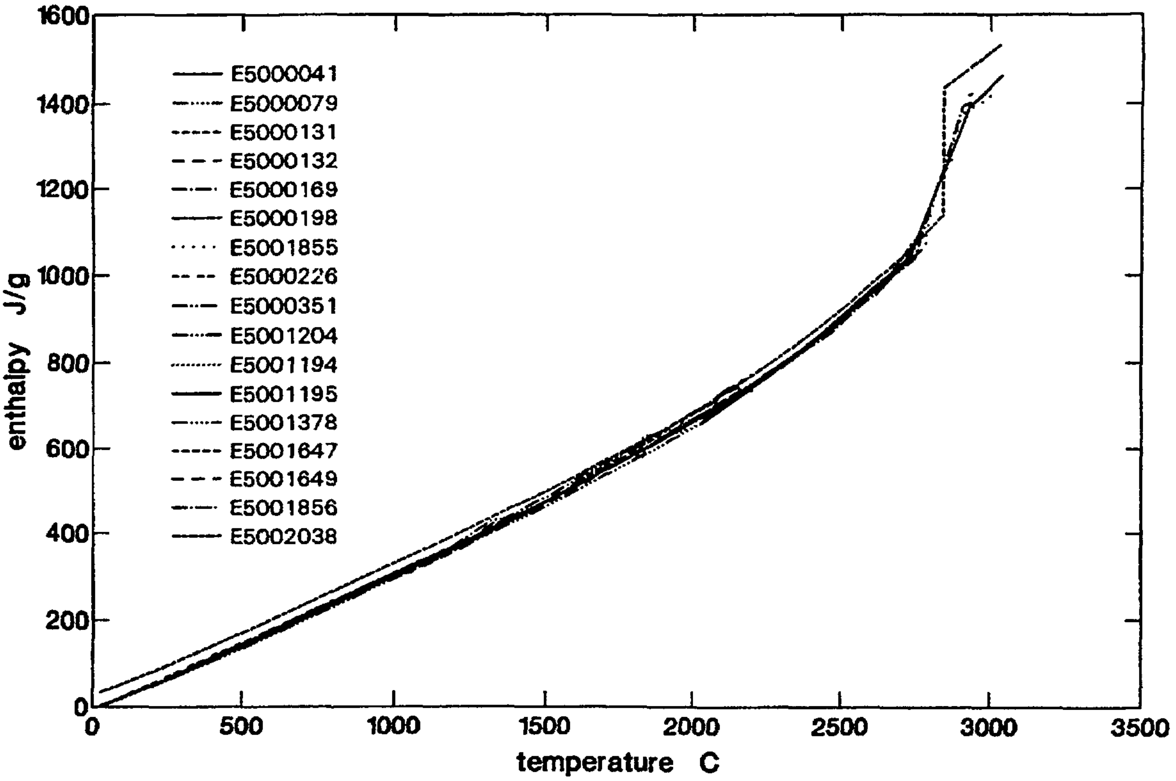

Figure 4.1.4.1 Enthalpy of (U,Pu)O_2

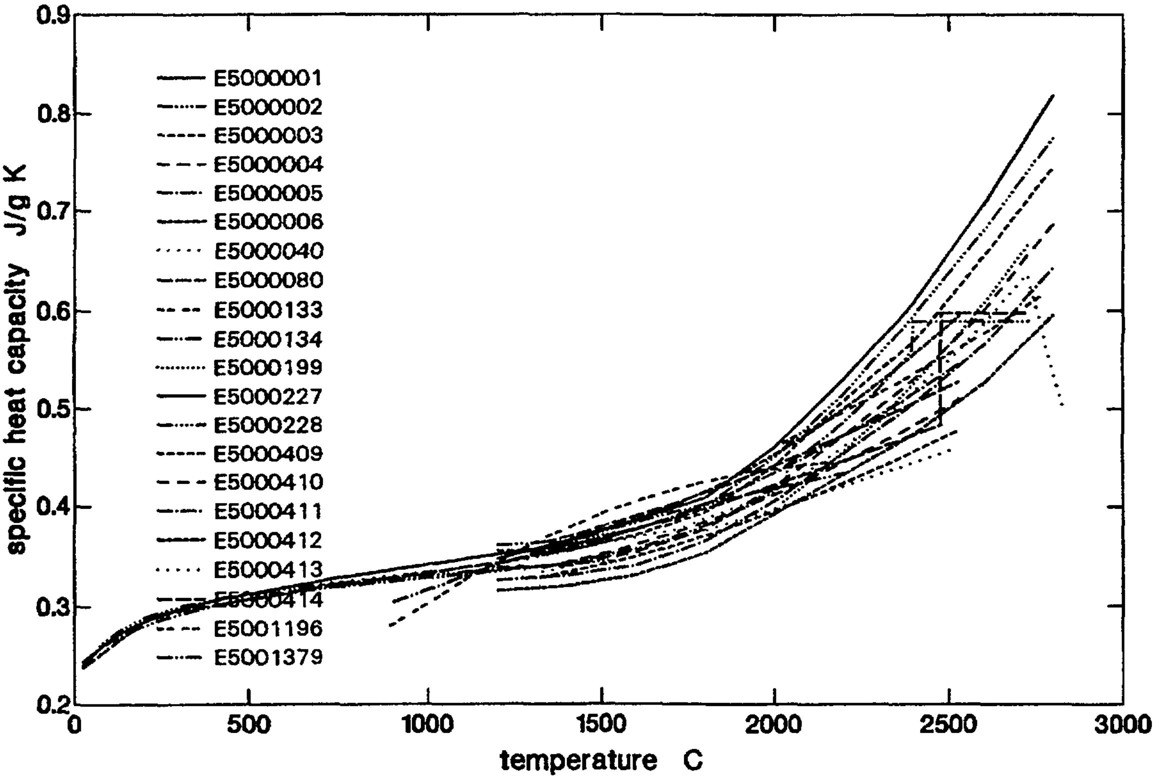

Figure 4.1.4.2 Specific heat capacity of (U,Pu)O_2

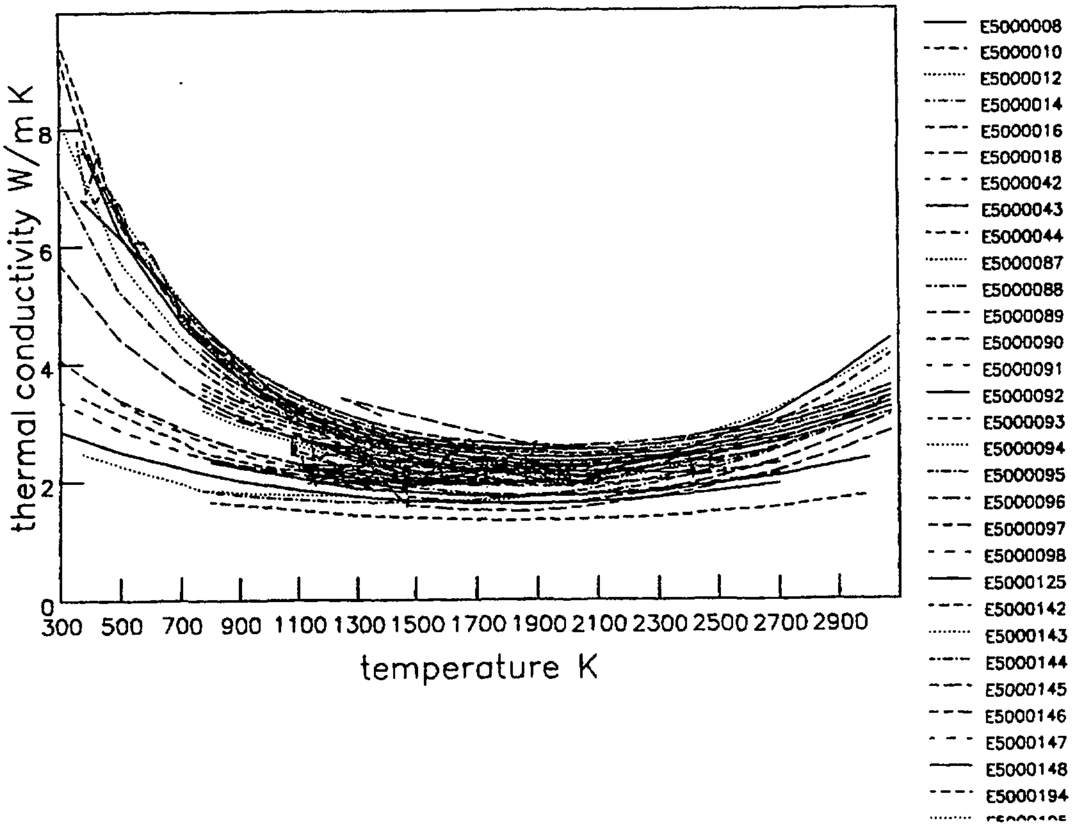

Figure 4.1.4.3 Thermal conductivity of (U,Pu)O_2

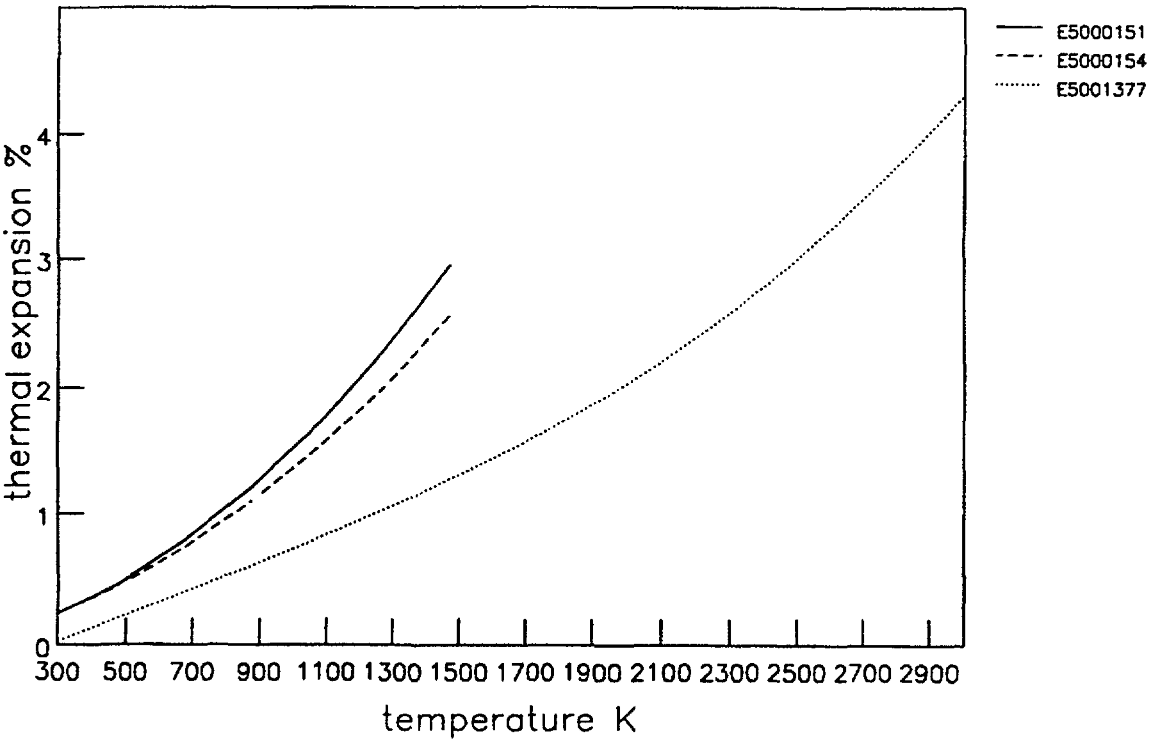

Figure 4.1.4.4 Thermal expansion of (U,Pu)O_2

References to Section 4.1.4

Note: Literature stored in THERSYST is references by document number, e.g. JT000001.

JT000001 SCHMIDT H. E., "Die Waermeleitfaehigkeit von Uran-Dioxyd und Uran-Plutonium-Dioxyd bei hohen Temperaturen", High Temp. -High Pressures 3 (1971), 345-353

JT000002 FUKUSHIMA S., OHMICHI T., HANDA M., "The effect of rare earths on thermal conductivity of uranium, plutonium and their mixed oxide fuels", J. Less-Common Metals 121 (1986), 631-636

JT000005 SENGUPTA A. K., ARORA K. S., KUMAR A., GANGULY C., "Thermal conductivity of titania-doped UO_2-4%PuO_2", High. Temp. -High Pressures 19 (1987), 509-512

JT000007 FINK J. K., "Enthalpy and heat capacity of the actinide oxides", Int. J. Thermophys. 3 (1982), 165-200

JT000015 EVANS S. K., BOHABOY P. E., "Thermal conductivity of physically mixed $(U_{0.8}Pu_{0.2})O_{2-x}$", Trans. Am. Nucl. Soc. 13 (1970), 571-572

JT000021 GIBBY R. L., "The effect of plutonium content on the thermal conductivity of $(U,Pu)O_2$ solid solution.", J. Nucl. Mater. 38 (1971), 163-177

JT000031 LORENZELLI R., EL SAYED ALI M., "Dilatation thermique d'oxydes mixtes $(UPu)O_{2-x}$ en fonction de l'ecart a la stoechimetrie", J. Nucl. Mater. 68 (1977), 100-103

JT000074 AFFORTIT C., MARCON J.-P., "Chaleur specifique a haute temperature des oxydes d'uranium et de plutonium", Rev. Int. Haut. Temp. Refract. 7 (1970), 236-241

JT000079 MARTIN D. G. "A re-appaisal of the thermal conductivity of UO_2 and mixed (U Pu)O_2 oxide fuels", J. Nucl. Mater. 110 (1982), 73-94

JT000098 MARTIN D. G., "The thermal expansion of solid UO_2 and (U,Pu) mixed oxides - a review and recommendations.", J. Nucl. Mater. 152 (1988), 94-101

JT000156 LEIBOWITZ L., FISCHER D. F., CHASANOV M. G., "Enthalpy of uranium-plutonium oxides: $(U_{0.8}Pu_{0.2})O_{1.97}$ from 2350 to 3000 K", J. Nucl. Mater. 42 (1972), 113-116

JT000159 CALZA-BINI A., COSOLI G., FILACCHIONI G., LANCHI M., NOBILI A., ROCCA U., ROTOLONI P., "In-pile thermal conductivity of fuel oxide: UO_2 pellets and Vipac UO_2-PuO_2 pellets and sol-gel.", Nucl. Technol. 21 (1974), 208-216

PT000003 SCHMIDT H. E., CALIGARA F., "Waermeleitfaehigkeit und Waermeleitungs-Integrale von Uran-Plutonium-Mischoxiden", Reaktortagung Berlin,Deutsches Atomforum (1970), 566-569

PT000012 N. H., RUSSELL L. E., "The thermal expansion of PuO_2 and other actinide oxides between room temperature and 1000 C°", Proc. 2nd Int. Conf. Plutonium Metallurgy; Grenoble 1960; Eds. E. Grison, W. B. H. Lord, R. D. Fowler; Cleaver-Hume Press Ltd., London 1961

PT000028 ELBEL H., SCHMIDT H. E., "Characterisation of mixed oxide fuel pellets with respect to their thermal conductivity.", Proc. Conf. on Nuclear Fuel Performance, 25-29 March 1985, Stratford-on-Avon, UK; British Nuclear Energy Society, London(1985), vol. 1, 357-361

RT000001 YAMAGUCHI T., KANEKO H.,HONDA Y., "Measurements of thermal conductivity for $(U_{0.7},Pu_{0.3})O_{2-x}$ fuels", PNCT831-80-01 (1980), 11-21

RT000002 WASHINGTON A. B. G., "Preferred values for thermal conductivity of sintered ceramic fuel for fast reactor use", TRG-Report-2236(D) (1973), 1-61

RT000004 LEIBOWITZ L., "Properties for LMFBR safety analysis", ANL-CEN-RSD-76-1 (1976)

RT000005 GIBBY R. L., LAWRENCE L. A., "Fabrication, microstructure and thermal conductivity in UO_2-25 wt.%PuO_2 sintered pellets", HEDL-SA-270 (1971), 1-11

RT000006 OGARD A.E.,LEARY J. A., "High temperature heat content and heat capacity of uranium dioxide and uranium dioxide-plutonium dioxide solid solution", LA-DC-8620 (1965), 1-26

RT000007 GIBBY R. L., "The effect of oxygen stoichiometry on the thermal diffusivity and conductivity of $(U_{0.75}Pu_{0.25})O_{2-x}$", BNWL-927 (1969), 1-49

RT000008 ROTH J., HALTEMAN E. K., "Thermal expansion of coprecipitated $(U,Pu)O_2$ powders by X-ray diffraction techniques", NUMEC-2389-9 (1965), 1-63

RT000010 GIBBY R. L., LEIBOWITZ L., KERRISK J. F., CLIFTON D. G., "Analytical expressions for enthalpy and heat capacity for uranium-plutonium oxide", HEDL-TME 73-60 (1973), 1-20

RT000011 GIBBY R. L., "The thermal diffusivity and thermal conductivity of stoichiometric $(U_{0.8}Pu_{0.2})O_2$", BNWL-704 (1968), 1-38

RT000012 LEIBOWITZ L., FISHER D.F., CHASANOV M.G., "Enthalpy of molten uranium-plutonium oxides", ANL-8082 (1974), 1-15

RT000013 HETZLER F. J., LANNIN T. E., PERRY K. J., ZEBROSKI E. L., "The thermal conductivity of uranium and uranium-plutonium oxides", GEAP-4879 (1967), 1-28

RT000014 LASKIEWICZ R. A., EVANS S. K., MELDE G. F., BOHABOY P. E., "Thermal conductivity of uranium-plutonium oxide", GEAP-13733 (1971), 1-26

RT000016 GIBBY R. L., "Enthalpy and heat capacity of $U_{0.75}Pu_{0.25}O_{2-x}$ (25-1490°C)", HEDL-TME 73-19 (1973), 1-29

RT000017 BONNEROT J. M., "Proprietes thermiques des oxydes mixtes d'uranium et de plutonium", CEA-R-5450 (1988), 1-190

RT000020 PALLMER P. G., "Lattice expansion of UO_2-PuO_2", BNWL-1349-1 (1970), 2.27-2.39

RT000024 Clifton D. G, Brewer R., "High temperature calorimetry of irradiated oxides", LA-4993-PR (1972), 18

RT000029 GIBBY R. L., "Fabrication, microstructure and thermal conductivity in UO_2-25 wt.%PuO_2 sintered pellets", HEDL-TME 72-88 (1972), 1-28

RT000042 YOKOUCHI Y., MASUYAMA S., MATSUMOTO K., "Thermal diffusivity measurements of PuO_2-UO_2 fuel simulated to pellets irradiated at high burnup", PNCT-9006 (1969), 134-149

RT000050 PHILIPPONNEAU Y., "Thermal conductivity of mixed oxide fuel; review and recommendation", CEA-DECPu Note Technique SEFCA no.157 (1990), 1-22

RT000051 CRAYNEST VAN J. C., WEILBACHER J. C., "Etude de la conductibilite thermique des oxydes mixtes d'uranium et de plutonium", CEA-R-3488 (1968), 1-18

RT000062 HARDING J. H., MARTIN D. G., POTTER P. E., "Thermophysical and thermochemical properties of fast reactor materials", EUR 12402EN (1989),1-90

RT000063 HOHORST J. K. (Editor), "SCDAP/RELAP5/MOD2 Code Manual, vol.4: MATPRO-a library of materials properties for light-water-reactor accident analysis", NUREG/CR-5273 (1990)

RT000066 BAKER R. D. (compiler), "High temperature calorimetry of irradiated oxides", LA-4749-MS (1971), 29

RT000089 GIBBY R. L., "Thermal conductivity of (Pu,U)O", BNWL-1349-1 (1970), 2.9-2.19

RT000094 SERIZAWA H., YOKOUCHI Y., KOIZUMI M., "Thermal diffusivity measurement of UO_{2-x} and PuO_2-UO_2 by the modulated electron beam heating technique", PNCPU-Report-040 (1969), 96-104

TT000001 WEILBACHER J. C., "Mesure de le diffusivite termique des oxydes mixes d'uranium et de plutonium. Influence de la teneur en plutonium", Thesis (1972)

4.1.5. UO_2-Gd_2O_3 mixture

The measurements of accurate properties on irradiated fuel is very difficult because of the heterogeneity of the material and its out-of-pile evolution after irradiation. The influence of the fission products may be simulated by the addition an oxide of a rare earth element (Gd_2O_3, Eu_2O_3, Nd_2O_3 or Sm_2O_3) to the UO_2 fuel.

The experimental data on the thermophysical properties of the mixed oxide UO_2-Gd_2O_3 were collected and they are presented at Figure 4.1.5.1 to 4.1.5.4. The Gd_2O_3 content in each specimen, its density and data sources are listed in Tables 4.1.5.1 to 4.1.5.4.

As can be seen from Figure 4.1.5.3 the addition of fission products diminishes the thermal conductivity, this effect decreases when the temperature increases. The reduction of the conductivity at 1800 K would be about 1% for each mol% of fission product added. The thermal conductivity data presented have been calculated from thermal diffusivity measurements. Before reference values for the thermal conductivity can be proposed, accurate data on specific heat capacity are necessary. The experimental data on specific heat of UO_2-Gd_2O_3 differ especially at high temperatures (Figure 4.1.5.2).

Nomenclature to Section 4.1.5

C_P - specific heat capacity, (J/(kg·K), other units: 1 J/(g·K) = 10^3 J/(kg·K),
H_u - enthalpy, (J/kg), other units: 1 J/g = 10^3 J/kg,
T - temperature (K);
ε - thermal strain, (m/m), other unit: %
λ - thermal conductivity, (W/(m·K)).

Table 4.1.5.1 ENTHALPY OF UO_2-Gd_2O_3

EKEY	CCOM	DEN	DONO	AU
E5001174	Gd_2O_3 3 wt% O/(U+Gd) ratio 2.042	10.3	JT000068	Mills
E5001175	Gd_2O_3 5 wt% O/(U+Gd) ratio 2.042	9.61	JT000068	Mills

Table 4.1.5.2 SPECIFIC HEAT CAPACITY OF UO_2-Gd_2O_3

EKEY	CCOM	DEN	DONO	AU
E5001080	Gd_2O_3 8.06 wt% O/(U+Gd) ratio 2.001	-	JT000143	Bruet
E5001082	Gd_2O_3 3 wt% O/(U+Gd) ratio 2.000	-	JT000144	Inaba
E5001083	Gd_2O_3 7 wt% O/(U+Gd) ratio 2.001	-	JT000144	Inaba
E5001084	Gd_2O_3 10 wt% O/(U+Gd) ratio 1.998	-	JT000144	Inaba
E5001085	Gd_2O_3 5 wt% O/(U+Gd) ratio 1.998	-	JT000145	Inaba
E5001176	Gd_2O_3 3 wt% O/(U+Gd) ratio 2.042	10.3	JT000068	Mills
E5001177	Gd_2O_3 5 wt% O/(U+Gd) ratio 2.042	9.61	JT000068	Mills

Table 4.1.5.3 THERMAL CONDUCTIVITY OF UO_2-Gd_2O_3

EKEY	CCOM	DEN	POR	DONO
E5000796	Gd_2O_3 1.98 wt% O/(U+Gd) ratio 1.998	10.43	-	JT000070
E5000797	Gd_2O_3 4.06 wt% O/(U+Gd) ratio 1.997	10.37	-	JT000070
E5000798	Gd_2O_3 8.08 wt% O/(U+Gd) ratio 2.000	10.21	-	JT000070
E5000799	Gd_2O_3 12.06 wt% O/(U+Gd) ratio 2.002	10.17	-	JT000070
E5000800	Gd_2O_3 12.20 wt% O/(U+Gd) ratio 2.003	10.21	-	JT000070
E5000801	Gd_2O_3 12.66 wt% O/(U+Gd) ratio 1.998	10.15	-	JT000070
E5001035	Gd_2O_3 3 wt% O/(U+Gd) ratio 2.002	-	5	JT000110
E5001037	Gd_2O_3 5 wt% O/(U+Gd) ratio 2.000	-	5	JT000110
E5001039	Gd_2O_3 7 wt% O/(U+Gd) ratio 2.002	-	5	JT000110
E5001041	Gd_2O_3 10 wt% O/(U+Gd) ratio 2.000	-	5	JT000110
E5001096	Gd_2O_3 2.96 wt% O/(U+Gd) ratio 2.042	10.3	-	JT000149
E5001097	Gd_2O_3 4.80 wt% O/(U+Gd) ratio 2.031	9.61	-	JT000149

Table 4.1.5.4 THERMAL EXPANSION OF UO_2-Gd_2O_3

EKEY	CCOM	POR	DONO	AU
E5001073	Gd_2O_3 5 wt%	4.5	JT000142	Une
E5001074	Gd_2O_3 8 wt%	4.5	JT000142	Une
E5001075	Gd_2O_3 10 wt%	4.5	JT000142	Une

Descriptors/Unit	
CCOM	Chemical composition (wt%)
DEN	Density (g/cm^3)
POR	Porosity (%)

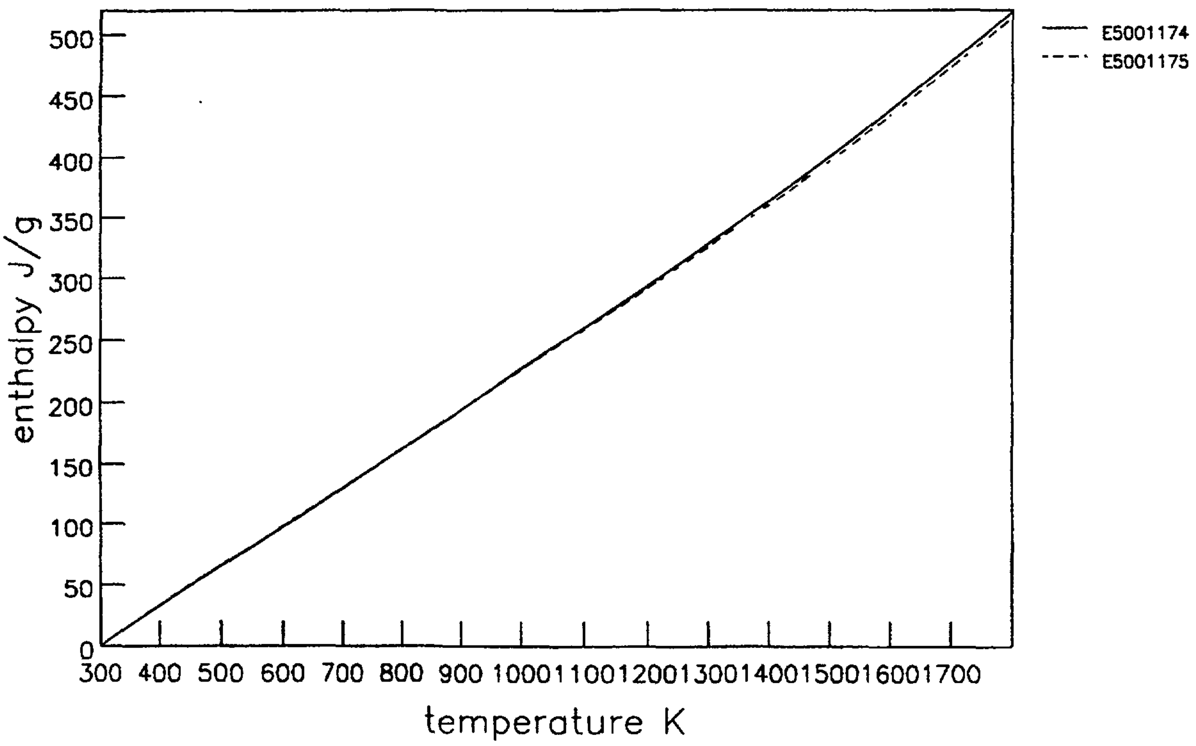

Figure 4.1.5.1 Enthalpy of UO_2-Gd_2O_3

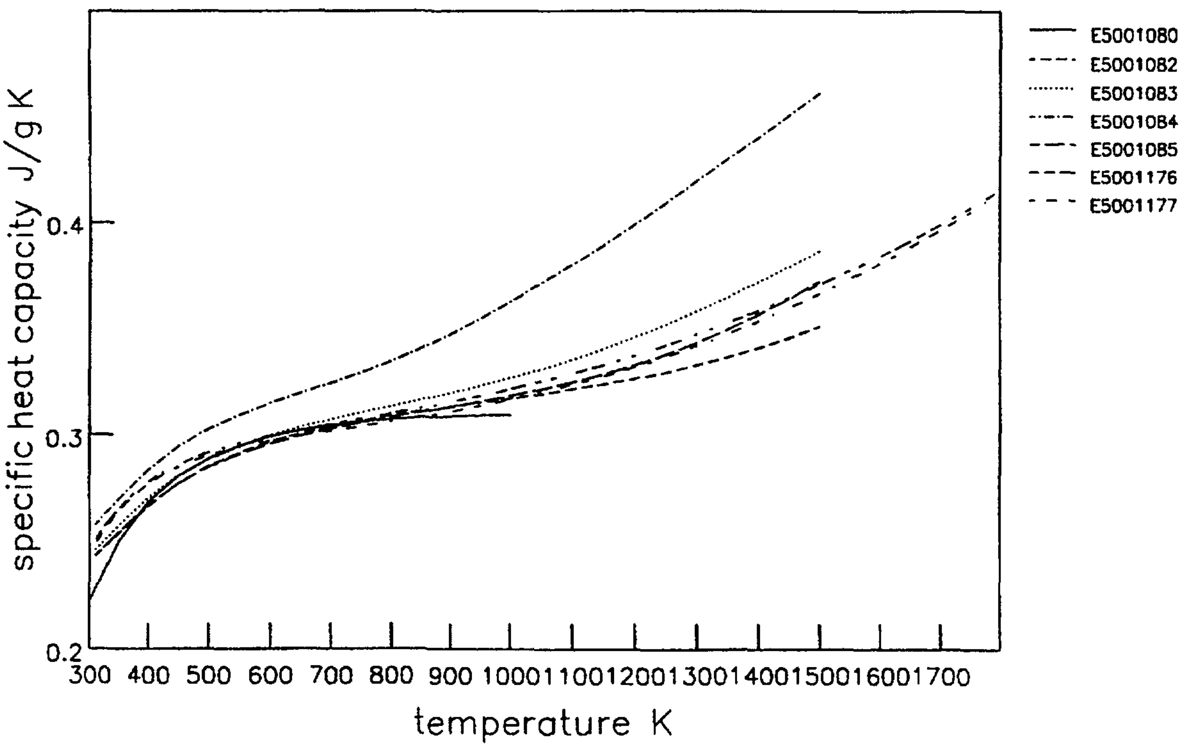

Figure 4.1.5.2 Specific heat capacity of UO_2-Gd_2O_3

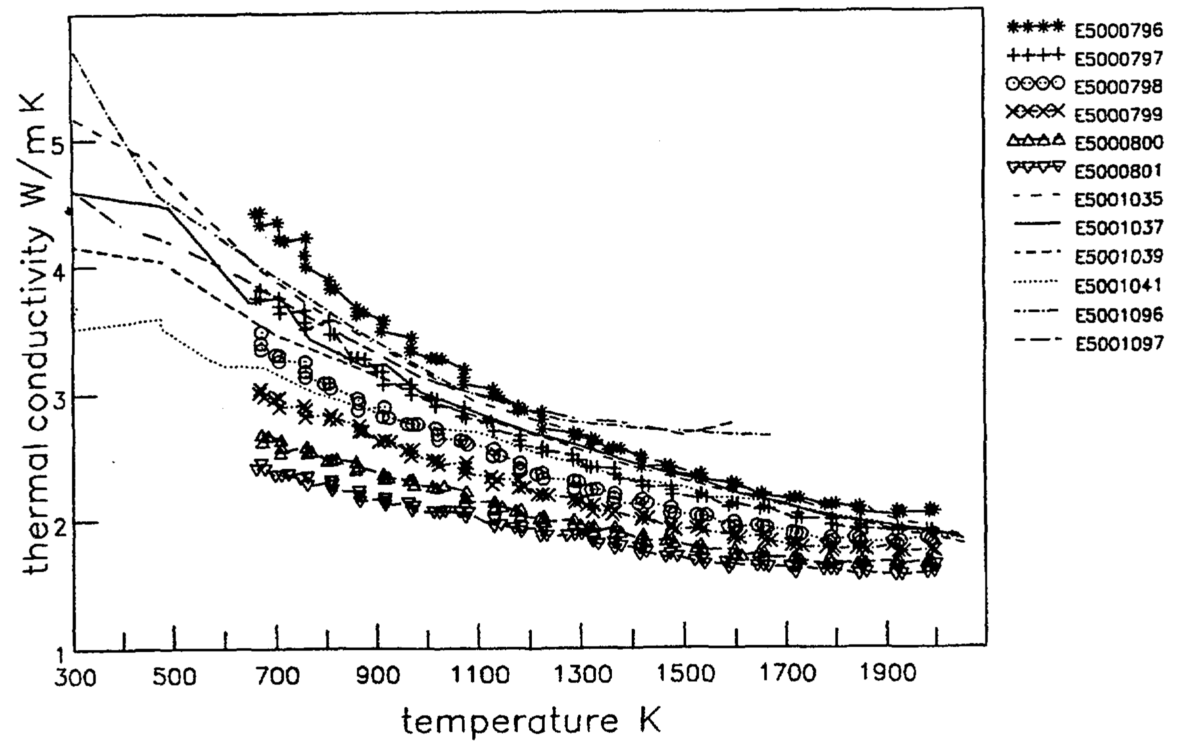

Figure 4.1.5.3 Thermal conductivity of UO_2-Gd_2O_3

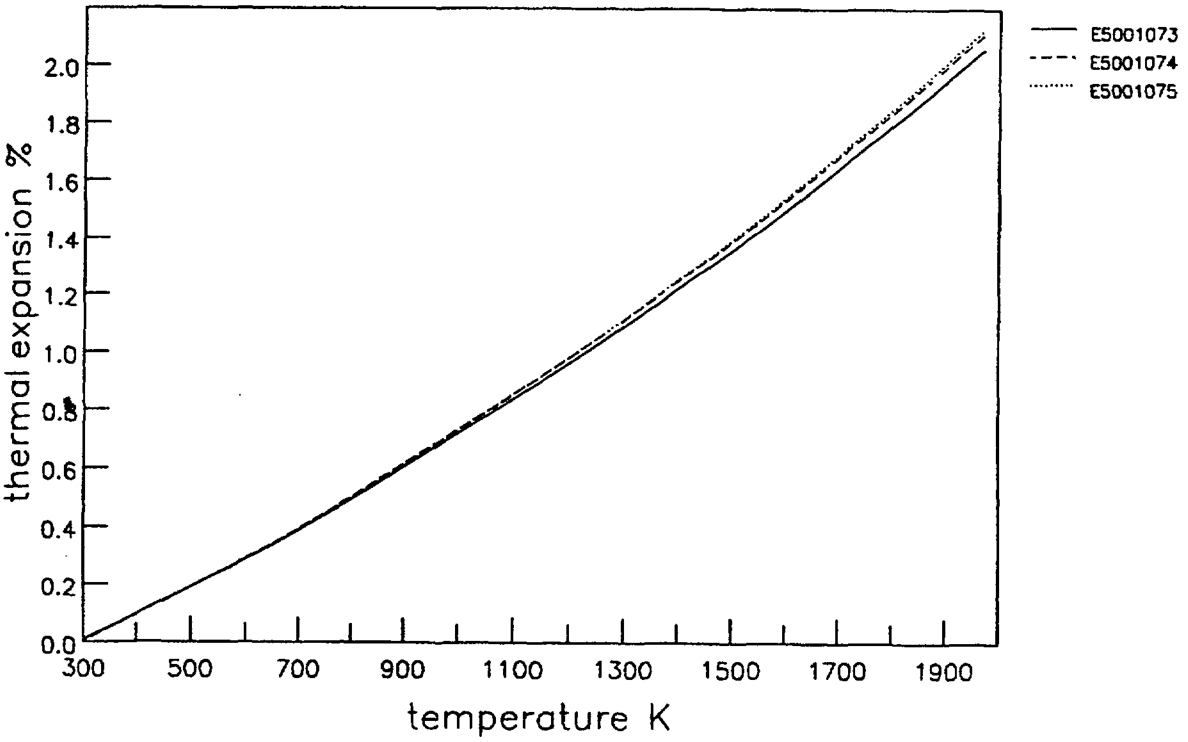

Figure 4.1.5.4 Thermal expansion of $(U,Gd)O_2$

References to Section 4.1.5

Note: Literature stored in THERSYST is references by document number, e.g. JT000008.

JT000008 MUNIR Z. A., "The electrical conductivity of doped and undoped uranium oxide", Int. J. Thermophys. 2 (1981), 177-186

JT000068 MILLS K. C., PONSFORD F. H., RICHA, "Heat capacity and enthalpy of UO_2 and gadolinia-doped UO_2", Thermochim. Acta 139 (1989), 107-120

JT000070 FUKUSHIMA S., OHMICHI T., MAEDA, "The effect of gadolinium content on the thermal conductivity of near-stoichiometric $(U,Gd)O_2$ solid solutions", J. Nucl. Mater. 105 (1982), 201

JT000110 HIRAI M., ISHIMOTO S., "Thermal diffusivities and thermal conductivities of UO2-Gd2O", J. Nucl. Sci. Technol. 28 (1991), 995-1000

JT000139 HIRAI M., "Thermal diffusivity of UO_2-Gd_2O_3 pellets", J. Nucl. Mater. 173 (1990), 247

JT000142 UNE K., "Thermal expansion of UO_2-Gd_2O_3 fuel pellet", J. Nucl. Sci. Technol. 23 (1986), 1020-1022

JT000143 BRUET M., BERGERON J., BERNARD F, MELIN P. et al., "Analytical out-of-pile and in-pile experiments", ENC 86 Trans., Geneva, June 1-6 (1986); Vol. 4 ENC-4, Topic VI, 269-278

JT000144 INABA H., NAITO K., OGUMA M., "Heat capacity measurement of $U_{(1-y)}Gd_{(y)}O_2$ ($0.00 < y < 0.142$) from 310 to 1500 K", J. Nucl. Mater. 149 (1987) 341-348

JT000145 INABA H., NAITO K., OGUMA M., "Heat capacity measurement of gadolinia-doped (7.3 Mol%) UO_2 from 310 to 1370 K", J. Nucl. Mater. 137 (1986) 176-178

JT000149 PRESTON S. D., BARRETT C., FASSIN, "Thermal diffusivities and thermal conductivities of UO_2 and $U_{(1-x)}Gd_{(x)}O_2$ solid solutions", High Temp. -High Pressures 21 (1989), 287-295

4.2. CLADDING MATERIALS

4.2.1. Zirconium based alloys

Thermophysical properties of Zr-2.5%Nb alloy

Some Russian and German data, including some data on the Zr-1.0%Nb alloy, are given in the following:

(1) V. E. MIKRYUKOV, Vestnik Moskov Univ. Ser. Mat. Mekhan., Astron. Fiz. I Khim 12 (5), 73 -80 (1957); as referenced in Y. S. TOULOUKIAN, R. W. POWELL, C. Y. HO, and P. G. KLEMENS, "Thermophysical Properties of Matter Vol. 1, Thermal Conductivity Metallic Elements and Alloys", pp. 461-467, 886, Plenum Press, N. Y. (1970)

(2) B. R. BRODSKIY, "Thermal Expansion of Zr Alloys with 1% and 2.5% Nb", Russian Metallurgy 6, 119 -122 (1977) [pages refer to English translation]

(3) B. BEYER and R. JUKNAT, "Physical and Mechanical Properties of Zirconium-Niobium alloys Containing 1 and 2.5 wt% Niobium" AEC German Democratic Republic AEC Report CONG-6610549 (Vol 1), 55 -75 (1966)

(4) V. I. SOLYANYI, F. P. BURTRA, V. N. KONEV, A. I. LYSENKO, and V. S. YAMNIKOV, "Anisotropy of the Thermal Expansion Coefficient of Fuel-Element Jackets Made of Zr-1%Nb Alloy", Atominaya Energiya, Vol. 50 No. 3, 207-209 (March 1981); [English Translation pp. 196-199]

(5) P. F. PRASOLOV, V. E. SHESTAK, P. A. PLATONAV, O. K. CHUGNOV, and V. F. VIKTOROV, "Anisotropy of the Elastic Modulus and Thermal Expansion Coefficient of Textured Zirconium Alloys N - 1 and N - 2.5", Atominaya Energiya, vol. 68 No. 2, 98-101 (February 1990); [English Translation pp 113-118]

The data presented here will fall into two classes:

(a) that obtained during the implementation of this IAEA Co-ordinated Research Programme, and

(b) that generated largely for Atomic Energy of Canada Ltd. (AECL).

Due to the lack of data in the literature on Zr-2.5%Nb alloys, thermophysical properties measurements were carried out by the Chinese Institute of Atomic Energy. Part of the results are given below. The whole data are contained in the THERSYST and TPSYS data base.

The Zr-2.5%Nb alloy used in the experiment was prepared by the China Northwest Research Institute of Non-ferrous Metals by vacuum melting, forging, extruding and annealing after cold working. The chemical composition is Nb (2.4-2.55 wt%), Cr (0.014 wt%), Fe (0.084 wt%), C (240 ppm). N (40 -60 ppm), Ni 0.0038 wt%), rest Zr. The as-machined samples have a density of 6533 kg/m3 at room temperature. The melting temperature of Zr-2.5%Nb measured by CIAE is 2083 ± 15 K, which can be used in the estimation of the heat of fusion of Zr-2.5%Nb.

Data generated for AECL are for both heat-treated and cold-worked material. All of this material was prepared by Teledyne Wah Chang of Albany, Oregon, USA, and met the AECL specification for Zr-2.5%Nb viz. Nb (2.4-2.8%), Cr (200 ppm max.), Fe (1500 ppm max.), C (270 ppm max.), N (65 ppm max.), Ni (70 ppm max.), O (900-1300 ppm.). The material was hot extruded, then either cold-worked about 25%, (the cold-worked material), or quenched from the $(\alpha+\beta)$-phase and cold-worked about 15%, (the heat treated material). The density of the materials was in the range 6511-6521 kg/m^3 at room temperature.

New information

Thermal conductivity

Three sets of thermal conductivity data for cold-worked Zr-2.5%Nb pressure tube (axial) annealed at different temperatures were obtained. These are shown in Table 4.2.1.1. The texture and other characteristics of the samples were given in the paper: W. Li, Lili Zhang et al., "Thermal Diffusivity and Conductivity of Zirconium Alloy", Proceedings of the first Asian Thermal Physical Properties Conference (1986) pp. 665-670.

Specific heat capacity

The specific heat capacity of Zr-2.5%Nb was measured by the laser pulse comparative method using pure Fe as the reference sample. The data obtained are listed in Table 4.2.1.2.

Linear thermal expansion

The coefficient of linear thermal expansion along the axial direction of 19%-cold-worked Zr-2.5%Nb pressure tube was determined using a standard dilatometric method. Part of the data are given in Table 4.2.1.3.

Normal total emissivity

The normal total emissivity was measured by the Chinese Nonferrous Metals and Electric Materials Test Center on two as-machined specimens with the surface oxide removed (see Table 4.2.1.4).

AECL data

Thermal conductivity

The thermal conductivity data are shown in Table 4.2.1.5 and thermal diffusivity data in Table 4.2.1.6. Further details of the work are presented in references [1,2].

Specific heat capacity

The specific heat capacity was measured with a differential scanning calorimeter, the measurements standardized with a sapphire sample. The data obtained are listed in Table 4.2.1.7, further details can be found references [1,2].

Linear thermal expansion

Thermal expansion was determined using standard dilatometric methods. For specimens cut from cold-worked tubing the values were found to be [3]:

Longitudinal: $\Delta L/L = -\,0.38\times10^{-4} + 5.86\times10^{-6}\Delta T + 3.72\times10^{-9}\,\Delta T^2$

Transverse: $\Delta L/L = 7.9\times10^{-6}\Delta T$

For specimens cut from heat-treated pressure tubing:

Longitudinal: $\Delta L/L = 6.0\times10^{-6}\Delta T$

Transverse: $\Delta L/L = 6.0\times10^{-6}\Delta T$

the equations valid from 273 K to 773 K.

Emissivity

Both the Normal Total Emissivity and the Total Hemispherical Emissivity were measured by standard techniques described in reference [4]. Data obtained are listed in Tables 4.2.1.8 and 4.2.1.9.

Thermophysical properties of Zircaloy-2 and 4

Specific heat capacity

Specific heat capacity data on Zircaloy-2 and Zircaloy-4 are presented in Figure 4.2.1.1. The melting temperature, the heat of fusion and the transition temperatures are listed in Table 4.2.1.10.

The MATPRO recommended values for the specific heat of Zircaloy-2 and Zircaloy-4 are listed in Table 4.2.1.11, with additional AECL data in Table 4.2.1.13 from references [1], [2].

For the MATPRO data the standard error is temperature dependent: ± 10 J/(kg·K), for 300 K < T < 1090 K: ± 25 J/(kg·K), for 1090 K < T < 1300 K and ± 100 J/(kg·K) for T > 1300 K.

Thermal conductivity

The thermal conductivity of Zircaloy-2 and Zircaloy-4 are presented in Figure 4.2.1.2. Additional information on the curves is given in Table 4.2.1.13.

MATPRO recommend the following relations:

For 300 K < T < 2098 K

$$\begin{aligned} \lambda &= 7.51 + 2.09\times10^{-2}T - 1.45\times10^{-5}T^2 + 7.67\times10^{-9}T^3 \\ \sigma &= \pm1.01 \end{aligned} \tag{4.2.1-1}$$

For $T \geq 2098$ K

$$\begin{aligned} \lambda &= 36 \\ \sigma &= \pm5 \end{aligned} \tag{4.2.1-2}$$

where λ is the thermal conductivity (W/(m·K)), T is the temperature (K) and σ is the uncertainty (W/(m·K)).

Additional experimental data on the thermal conductivity of Zircaloy-2 and Zircaloy-4 were supplied by China. They are presented in Table 4.2.1.14 and Table 4.2.1.15.

Zircaloy-2 was prepared with the chemical composition Sn (1.30-1.68 wt%), Fe (0.18-0.24 wt%), Cr (0.019-0.130 wt%), Ni (<0.0007). The radial thermal conductivity was measured on a tube sample with a diameter of 10 mm and a thickness of 0.65 mm.

Zircaloy-4 was prepared with the chemical composition Sn (1.30-1.68 wt.%), Cr (0.019-0.130 wt.%), Ni (< 0.0007 wt.%). The axial thermal conductivity of the rod sample was measured by the laser pulse method.

Thermal conductivity data on Zircaloy-2 obtained by AECL are presented in Table 4.2.1.16, and thermal diffusivity data in Table 4.2.1.17. The experiments were done using standard commercial grade material [1,2].

Linear thermal expansion

Thermal expansion data on both Zircaloy alloys are presented in Figure 4.2.1.3, the direction of measurement and data sources are given in Table 4.2.1.18. AECL found for cold-worked (15-25%) Zircaloy-2 [3].

Longitudinal: $\Delta L/L = 5.0\times10^{-6}\Delta T$

Transverse: $\Delta L/L = 7.9\times10^{-6}\Delta T$

and for annealed Zircaloy-2 and Zircaloy-4

Longitudinal: $\Delta L/L = 5.2\times10^{-6}\Delta T$

the equations valid from 273 K to 773 K.

A total of six equations are recommended by MATPRO to find the single crystal thermal strain, basal plane symmetry ($\varepsilon_{11} = \varepsilon_{22}$) is assumed.

The single-crystal thermal strain relations are:

For 300 K < T < 1083 K

$$\varepsilon_{11} = 4.95\times10^{-6}T - 1.485\times10^{-3} \tag{4.2.1-3}$$

$$\varepsilon_{33} = 1.26\times10^{-5}T - 3.78\times10^{-3} \tag{4.2.1-4}$$

where ε_{11} is the circumferential thermal expansion (m/m), ε_{33} is the axial thermal expansion (m/m), and T is temperature (K).

For 1083 K $\leq T \leq$ 1244 K

$$\varepsilon_{33} = \left[8.76758 + 1.09822\cos\left(\frac{T - 1083}{161}\pi\right)\right]\times10^{-3} \tag{4.2.1-6}$$

$$\varepsilon_{11} = \left[2.77763 + 1.09822\cos\left(\frac{T - 1083}{161}\pi\right)\right]\times10^{-3} \tag{4.2.1-5}$$

where the arguments of the cosines are in radian.

For 1244 K $\leq T \leq$ 2098 K

$$\varepsilon_{11} = 9.7\times10^{-6}T - 1.04\times10^{-2} \tag{4.2.1-7}$$

$$\varepsilon_{33} = 9.7\times10^{-6}T - 4.4\times10^{-3} \tag{4.2.1-8}$$

For T > 2098 K (liquid)

$$\varepsilon_{p} = \frac{2}{3}\varepsilon_{11} + \frac{1}{3}\varepsilon_{33} + 0.0067 \tag{4.2.1-9}$$

where ε_{11} is the circumferential thermal expansion strain of a single crystal of Zircaloy at 2098 K (m/m), ε_{33} is the axial thermal expansion strain of a single crystal of Zircaloy at 2098 K (m/m), and ε_{p} is the thermal expansion of molten Zircaloy (m/m).

To obtain cladding strains from these single-crystal strains, it is necessary to do a volume-weighted averaging over the entire cladding section. The predicted Zircaloy thermal strains have an expected standard error near 10% for temperature below 1090 K and 50% for higher temperatures.

Emissivity

Data on the normal total emissivity of Zircaloy-2 and Zircaloy-4 recommended by MATPRO are represented in Figure 4.2.1.4 with the data sources listed in Table 4.2.1.19. This property depends on the surface of the materials: its roughness and the thickness of the oxide layer. AECL data on emissivity of Zircaloy-4 is presented in Figures 4.2.1.5 and 4.2.1.6 from references [4,5], with data on Zircaloy-2 in Tables 4.1.1.20 and 4.2.1.21 from reference [7]. Some dependence of emissivity on the thickness of the oxide layer on Zircaloy-2 is shown in the AECL data; this topic is covered in more detail in Section 4.2.4 (Zirconium dioxide). Note that the emissivity data shown in Figures 4.2.1.5 and 4.2.1.6 are for sub-stoichiometric oxides black in colour.

Nomenclature to Section 4.2.1

C_p - specific heat capacity, (J/(kg·K), other units: 1 J/(g·K) = 10^3 J/(kg·K)
T - temperature (K)
α - thermal expansion coefficient, (1/K)
ε_i - thermal strain, (m/m), i = 11-circumferential, i = 33-axial, i = p-liquid, other unit: %
λ - thermal conductivity, (W/(m·K))
a - thermal diffusivity (mm^2/s)

Table 4.2.1.1 THERMAL CONDUCTIVITY λ (W/(m·K)) OF Zr-2.5%Nb ALLOY; T = TEMPERATURE (K)

Sample 1: pressure tube (axial) annealed at 673 K

T	λ
372	23.1
489	21.8
520	20.8
586	19.5
632	19.8
737	20.0
827	21.1
927	22.5
1021	24.3
1130	27.3

Sample 2: pressure tube (axial) annealed at 1073 K

T	λ
352	15.9
426	17.0
439	18.0
559	19.0
593	19.1
642	18.9
672	19.2
684	19.5
774	20.4
969	23.2
1068	25.3
1130	27.9

Sample 3: pressure tube (axial) annealed at 1123 K

T	λ
438	17.0
533	18.4
559	18.5
617	19.0
773	19.8
817	20.1
872	20.6
971	22.9
1117	27.1

Table 4.2.1.2 SPECIFIC HEAT CAPACITY C_P (J/(kg·K)) OF Zr-2.5%Nb; T=Temperature (K)

T	C_P
323	276.3
373	279.3
423	286.4
473	292.7
523	298.9
573	305.2
629	310.7
673	316.5
723	321.5
773	326.6
823	331.2
873	335.8
923	340.0
1073	347.5

Table 4.2.1.3 COEFFICIENT OF LINEAR THERMAL EXPANSION α (10^{-6}/K) ALONG AXIAL DIRECTION OF Zr-2.5%Nb PRESSURE TUBE; T=Temperature (K)

T	α
323	4.36
373	4.76
473	4.71
573	4.91
673	5.22
773	5.36
873	4.75
923	3.90
973	2.99

Table 4.2.1.4 NORMAL TOTAL EMISSIVITY ϵ OF Zr-2.5%Nb; T=Temperature (K)

T	ϵ
1259	0.411
1403	0.393
1469	0.382
1574	0.346
1664	0.338
1737	0.376
1909	0.365
1976	0.394

Table 4.2.1.5 THERMAL CONDUCTIVITY λ (W/(m·K)) OF Zr-2.5%Nb ALLOY; T=TEMPERATURE (K)

Sample 1		Sample 2		Sample 3		Sample 4		Sample 5	
T	λ	T	λ	T	λ	T	λ	T	λ
322	17.6	423	20.2	326	17.0	328	17.3	319	17.0
375	17.5	473	20.6	374	17.1	370	17.1	401	17.2
478	18.4	523	20.8	465	17.8	475	17.8	446	17.4
562	18.6	573	21.3	569	18.2	558	17.9	581	17.9
679	19.8	623	21.7	687	19.5	690	19.4	663	18.8

Sample 1: Cold-worked pressure tube, axial
Sample 2: Cold-worked rod, longitudinal
Sample 3: Heat-treated pressure tube, axial
Sample 4: Cold-worked pressure tube, circumferential
Sample 5: Heat treated pressure tube, circumferential

Table 4.2.1.6 THERMAL DIFFUSIVITY a (mm^2/s) OF Zr-2.5%Nb ALLOY; T=TEMPERATURE (K)

Sample 1		Sample 2		Sample 3	
T	a	T	a	T	a
296	9.36	294	9.33	423	10.3
383	9.10	375	8.97	473	10.2
475	8.84	472	8.75	523	10.2
574	8.84	569	8.61	573	10.1
673	8.91	673	8.72	623	10.1

Sample 1: Cold-worked pressure tube
Sample 2: Heat-treated pressure tube
Sample 3: Cold-worked rod

Table 4.2.1.7 SPECIFIC HEAT CAPACITY OF Zr-2.5%Nb

Temperature (K)	Specific heat capacity (J/kg·K))		
	Cold-worked [1]	Cold-worked [2]	Heat- treated [1]
340	286.5		286.4
350	287.7		287.7
375	290.0		290.9
400	291.3		293.1
425	294.0	293	296.8
450	294.5		299.6
475	295.3	310	301.0
500	296.7		299.6
525	298.0	318	301.1
550	300.5		305.6
575	303.4	310	306.6
600	307.1		310.7
625	311.1	322	314.1
650	316.2		318.7
675	328.0	339	323.5

The numbers [1] and [2] in the headings refer to the references at the end of the section.

Table 4.2.1.8 NORMAL TOTAL EMISSIVITY OF Zr-2.5%Nb, T=Temperature (K), Sam. =Sample

T	Sam. 1	Sam. 2	Sam. 3	Sam. 4	Sam. 5
373	0.168			0.496	0.552
423	0.181	0.416	0.459	0.498	0.550
473	0.184			0.503	0.553
523	0.210			0.507	0.546
573	0.230				0.558
623	0.233			0.497	
673	0.303			0.502	0.544

Table 4.2.1.9 TOTAL HEMISPHERICAL EMISSIVITY OF Zr-2.5%Nb
T = Temperature (K), Sam. = Sample

T	Sam. 1	Sam. 2	Sam. 3	Sam. 4	Sam. 5
373	0.180			0.455	0.512
423	0.186	0.397	0.447	0.464	0.513
473	0.184			0.475	0.520
523	0.208			0.475	0.508
573	0.226				0.522
623	0.232			0.462	
673	0.303			0.466	0.606

Sample description for Tables 4.2.1.8 and 4.2.1.9

Sample No.	Metallurgical Condition and Oxide Thickness
1	Steel wool polished
2	Pickled + 2 hours steam at 673 K and 10.4 MPa., 0.46 μm
3	Pickled + 5 hours steam at 673 K and 10.4 MPa., 1.1 μm
4	Pickled + 12 hours steam at 673 K and 10.4 MPa., 1.8 μm
5	Pickled + 60 hours steam at 673 K and 10.4 MPa., 2.0 μm

Table 4.2.1.10 SPECIFIC HEAT CAPACITY OF Zircaloy

```
EKEY     I MNAM         I DEN  I MELTT I MELTH I TRATXT I TRAT I DONO     I AU        I
---------I--------------I------I-------I-------I--------I------I----------I-----------I
E0006241 I Zircaloy-2   I ---  I ---   I ---   I        I      I J0003003 I Casey     I
E0006379 I Zircaloy-2   I 6.51 I ---   I ---   I        I      I J0000926 I Gilchrist I
E0006468 I Zircaloy-2   I ---  I ---   I ---   I        I      I J0000943 I Maglic    I
E0006533 I Zircaloy-2,4 I 6.49 I   2098I   225.I α/α+ß  I 1090 I RT000063 I MATPRO    I
         I              I      I       I       I α+ß/ß  I 1250 I          I           I

Units of descriptors
--------------------
DEN            density [g/cm^3]
MELTT          melting temperature [K]
MELTH          heat of melting [J/g]
TRAT           temperature of transition [K]
```

Table 4.2.1.11 Zircaloy SPECIFIC HEAT CAPACITY (Zircaloy-2 and Zircaloy-4)

Temperature (K)	Specific Heat Capacity (J kg^{-1} K^{-1})
300	281
400	302
640	331
1090	375
1093	502
1113	590
1133	615
1153	719
1173	816
1193	770
1213	619
1233	469
1248	356
2098	356
2099	356

Table 4.2.1.12 SPECIFIC HEAT CAPACITY OF Zircaloy-2

Temperature (K)	Specific heat capacity (J/(kg.K))		
	Annealed [1]	Annealed [2]	Cold-worked [1]
340	285.8		288.9
350	286.0		289.2
375	289.2		292.8
400	290.9		294.0
425	292.4	293	295.8
450	291.7		296.8
475	292.8	293	299.2
500	294.7		300.9
525	296.4	308	301.7
550	299.1		304.4
575	300.3	314	306.4
600	307.0		310.2
625	311.3	310	313.7
650	316.2		317.9
675	315.5	331	325.9

The numbers [1] and [2] in the headings refer to the references at the end of the section.

Table 4.2.1.13 THERMAL CONDUCTIVITY OF Zircaloy ALLOYS

```
EKEY      I MNAM          I DEN   I DONO      I AU            I
---------I--------------I-------I----------I--------------I
E0005081 I Zircaloy 2    I  6.55 I R0000110 I Scott         I
E0005112 I Zircaloy-2    I ---   I R0000105 I Lucks         I
E0006255 I Zircaloy-2    I ---   I P0000030 I Chirigos      I
E0006378 I Zircaloy-2    I  6.51 I J0000926 I Gilchrist     I
E0006467 I Zircaloy-2    I ---   I J0000943 I Maglic        I
E0006411 I Zircaloy-2    I ---   I J0003057 I Murabayashi   I
E0006514 I Zircaloy-2,4  I  6.49 I RT000063 I MATPRO        I
E0005082 I Zircaloy 4    I ---   I R0000110 I Scott         I
E0005083 I Zircaloy 4    I ---   I R0000109 I Feith         I
E0006254 I Zircaloy-4    I ---   I P0000030 I Chirigos      I
E0006413 I Zircaloy-4    I ---   I J0003057 I Murabayashi   I

Units of descriptors
--------------------
DEN       density  [g/cm^3]
```

Table 4.2.1.14 Thermal conductivity of Zircaloy-2 alloy

Temperature (K)	λ (W/(m·K))
293	13.91
323	13.81
373	13.72
423	13.72
473	13.82
523	14.01
573	14.29
623	14.66
673	15.13
723	15.69
773	16.35
823	17.09
873	17.93
923	18.86
973	19.89
1023	21.01
1073	22.22
1123	23.54
1173	24.26
1223	25.82
1273	26.36
1300	26.83
1400	29.43

Table 4.2.1.15 Thermal conductivity of Zircaloy-4 alloy

Temperature (K)	λ (W/(m·K))
293	13.18
323	13.32
373	13.59
423	13.90
473	14.26
523	14.66
573	15.11
623	15.61
673	16.15
723	16.73
773	17.37
823	18.04
873	18.77
923	19.53
973	20.35
1023	21.21
1073	22.11
1123	23.06
1173	24.06
1223	25.10
1273	26.19
1300	26.50
1400	27.89

Table 4.2.1.16 THERMAL CONDUCTIVITY λ (W/(m·K)) OF Zircaloy-2 ALLOY; *T*=TEMPERATURE (K)

Sample 1

T	λ
318	13.7
378	14.3
454	15.4
576	16.4
687	17.9

Sample 2

T	λ
339	13.8
376	14.1
486	15.7
574	16.8
668	18.7

Sample 3

T	λ
330	13.4
381	14.0
463	15.1
569	16.6
673	17.8

Sample 4

T	λ
328	17.3
370	17.1
475	17.8
558	17.9
690	19.4

Sample 5

T	λ
330	14.2
381	14.9
459	16.0
574	17.6
664	19.3

Sample 6

T	λ
328	14.3
375	14.8
470	16.2
567	17.5
678	19.7

Sample 7

T	λ
423	16.5
473	17.1
523	17.7
573	18.1
623	18.7

Sample 1: Cold-worked pressure tube, axial
Sample 2: Annealed strip, rolling direction
Sample 3: Stress-relieved thin wall tube, axial
Sample 4: Cold -worked pressure tube, circumferential
Sample 5: Annealed strip, transverse
Sample 6: Stress-relieved thin wall tube, circumferential
Sample 7: Annealed rod, axial

Table 4.2.1.17 THERMAL DIFFUSIVITY *a* (mm^2/s) OF Zircaloy ALLOY; T=TEMPERATURE (K)

Sample 1

T	a
292	7.30
379	7.35
472	7.42
571	7.65
673	7.75

Sample 2

T	a
296	7.01
389	7.04
473	7.08
573	7.22
673	7.42

Sample 3

T	a
423	8.6
473	8.6
523	8.7
573	8.8
623	8.8

Sample 1: Cold-worked pressure tube, radial
Sample 2: Annealed strip, through thickness
Sample 3: Annealed rod, axial

Table 4.2.1.18 THERMAL EXPANSION OF Zircaloy ALLOYS

EKEY	MNAM	DIR	DONO	AU
E0004502	Zircaloy-2	axial	J0001456	Peggs
E0004503	Zircaloy-2	axial	J0001456	Peggs
E0004504	Zircaloy-2	diametral	J0001456	Peggs
E0004505	Zircaloy-2	axial	J0001456	Peggs
E0004506	Zircaloy-2	diametral	J0001456	Peggs
E0004507	Zircaloy-2	axial	J0001456	Peggs
E0006527	Zircaloy-2,4	liquid	RT000063	MATPRO
E0007369	Zircaloy-2	axial	J0002043	Bunnel
E0007370	Zircaloy-2	diametral	J0002043	Bunnel
E0007371	Zircaloy-2	axial	J0002043	Bunnel
E0007372	Zircaloy-2	diametral	J0002043	Bunnel
E0002291	Zircaloy-4	polycrystal	J0000250	Slattery
E0002292	Zircaloy-4	polycrystal	J0000250	Slattery
E0002293	Zircaloy-4	polycrystal	J0000250	Slattery
E0002294	Zircaloy-4	polycrystal	J0000250	Slattery
E0002295	Zircaloy-4	polycrystal	J0000250	Slattery
E0002296	Zircaloy-4	polycrystal	J0000250	Slattery
E0004498	Zircaloy-4	axial	J0001456	Peggs
E0004499	Zircaloy-4	axial	J0001456	Peggs
E0007378	Zircaloy-4	axial	J0002043	Bunnel
E0007379	Zircaloy-4	diametral	J0002043	Bunnel
E0007380	Zircaloy-4	axial	J0002043	Bunnel
E5000284	Zircaloy-2,4	direction-11	RT000063	MATPRO
E5000285	Zircaloy-2,4	direction-33	RT000063	MATPRO

Table 4.2.1.19 EMISSIVITY OF Zircaloy-2 AND -4

EKEY	REMARKS	DONO	AU
E5000281	no oxide layer	RT000063	MATPRO
E5000282	oxide layer <3.88E-6m	RT000063	MATPRO
E5000283	oxide layer >3.88E-6m	RT000063	MATPRO

Table 4.2.1.20 NORMAL TOTAL EMISSIVITY OF Zircaloy-2,
T = Temperature (K), Sa. = Sample

T	Sa. 1	Sa. 2	Sa. 3	Sa. 4	Sa. 5	Sa. 6	Sa.7
373	0.141	0.424	0.521				
423	0.148	0.414	0.542	0.582	0.748	0.132	0.450
473	0.154	0.416	0.557	0.599		0.137	
523	0.167						
573	0.175	0.434	0.588	0.620			
673	0.289	0.433					

Table 4.2.1.21 TOTAL HEMISPHERICAL EMISSIVITY OF Zircaloy-2,
T = Temperature (K), Sa. = Sample

T	Sa. 1	Sa. 2	Sa. 3	Sa. 4	Sa. 5	Sa. 6	Sa.7
373	0.142	0.384	0.520				
423	0.143	0.376	0.547	0.584	0.688	0.149	0.458
473	0.148	0.393	0.558	0.587		0.150	
523	0.163						
573	0.169	0.410	0.571	0.615			
673	0.303						

Sample description for Tables 4.2.1.20 and 4.2.1.21

Sample No.	Metallurgical Condition and Oxide Thickness
1	Pickled
2	Pickled + 2 days in air at 673 K, 0.9 μm
3	Pickled + 10 days in air at 673 K, 1.48 μm
4	Pickled + 55 days in steam at 673 K and 10.4 MPa., 2.3 μm
5	Pickled + air 30 days 673 K then 73 days 773 K, 94 μm
6	Machined to roughness of 1.9 x 10^{-6} m CLA.
7	Machined + 13 days in air at 673 K, 1.61 μm

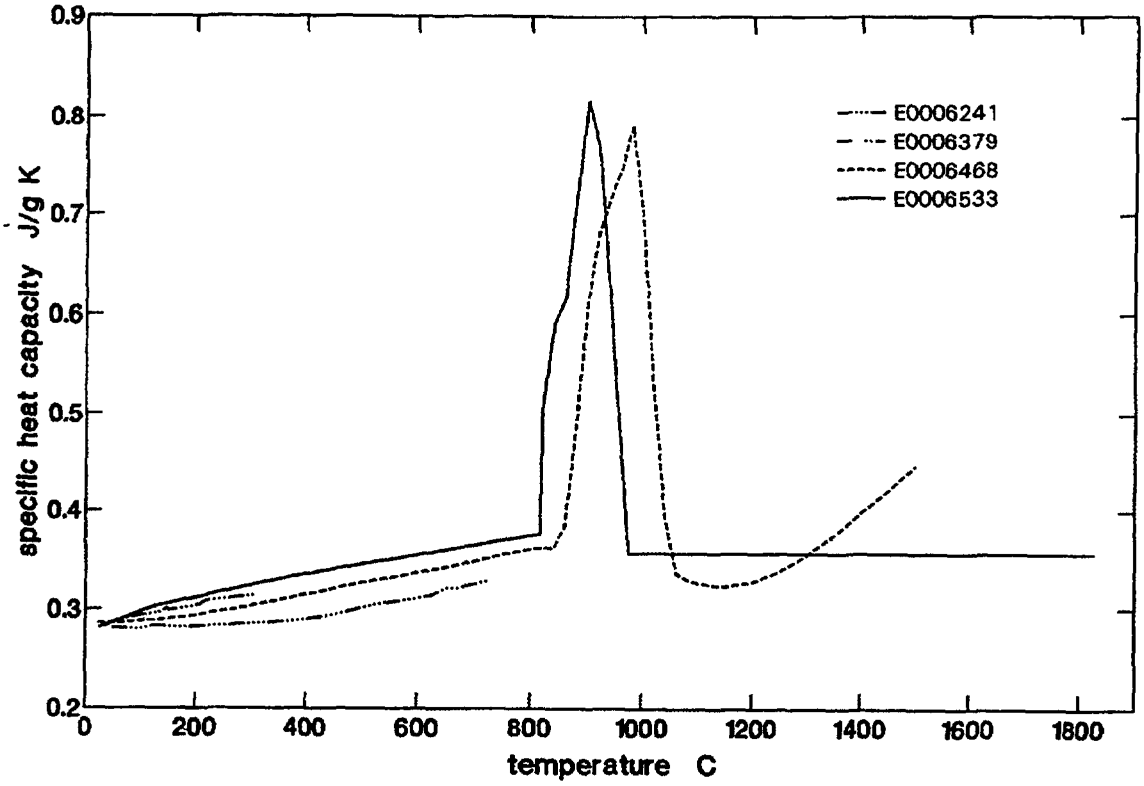

Figure 4.2.1.1 Specific heat capacity of Zircaloy

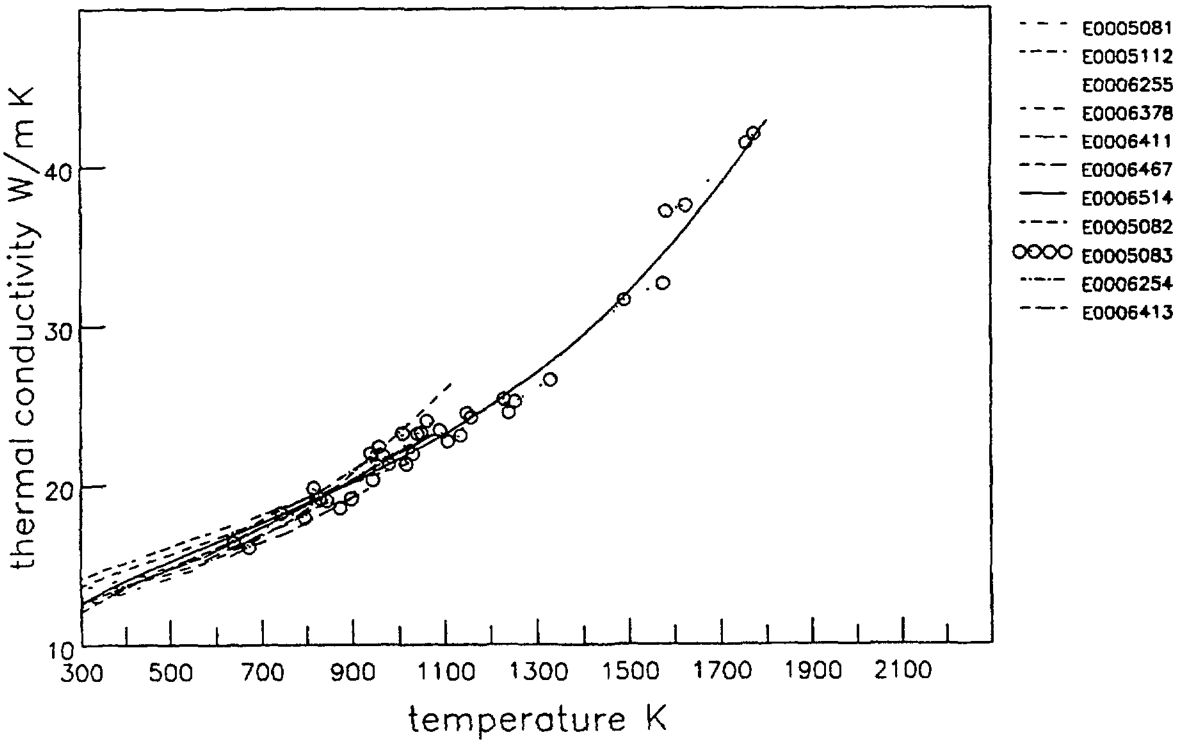

Figure 4.2.1.2 Thermal conductivity of Zircaloy

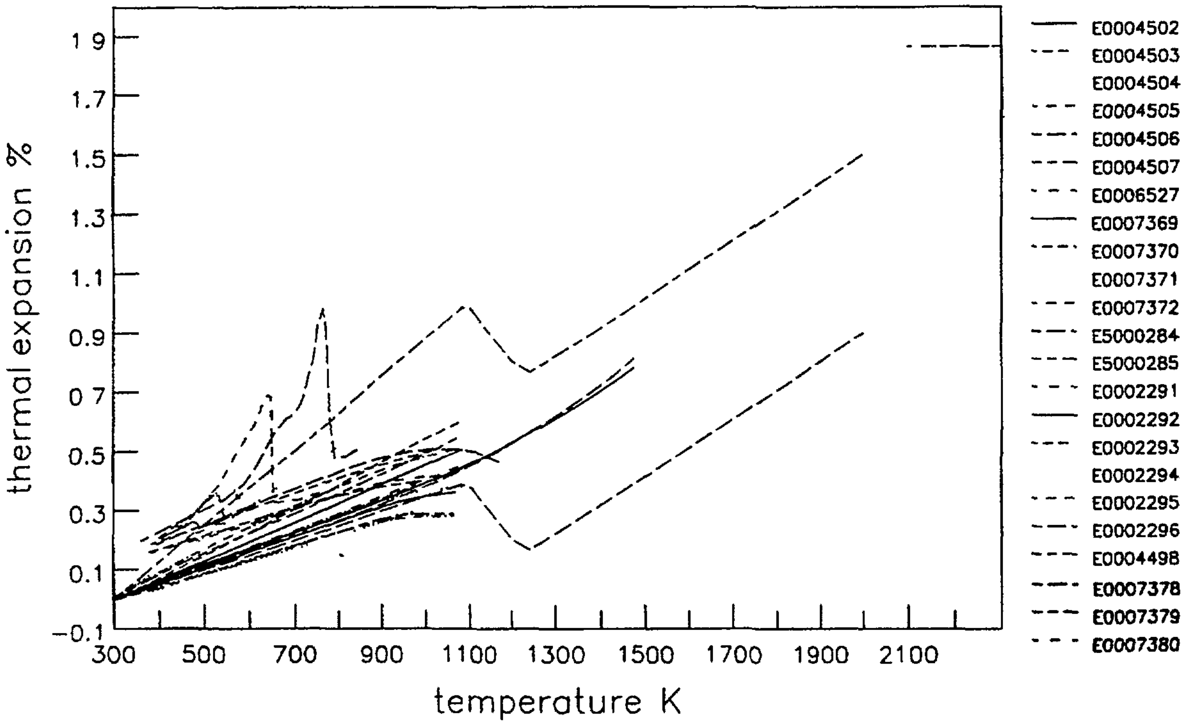

Figure 4.2.1.3 Thermal expansion of Zircaloy

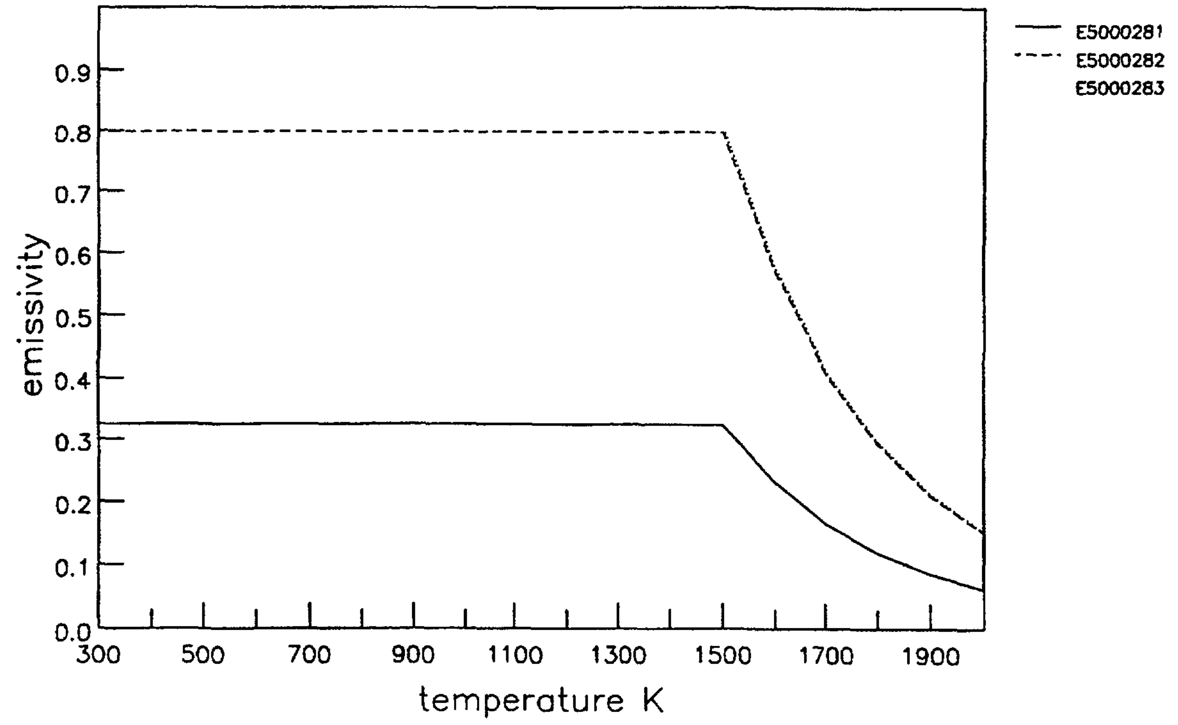

Figure 4.2.1.4 Emissivity of Zircaloy

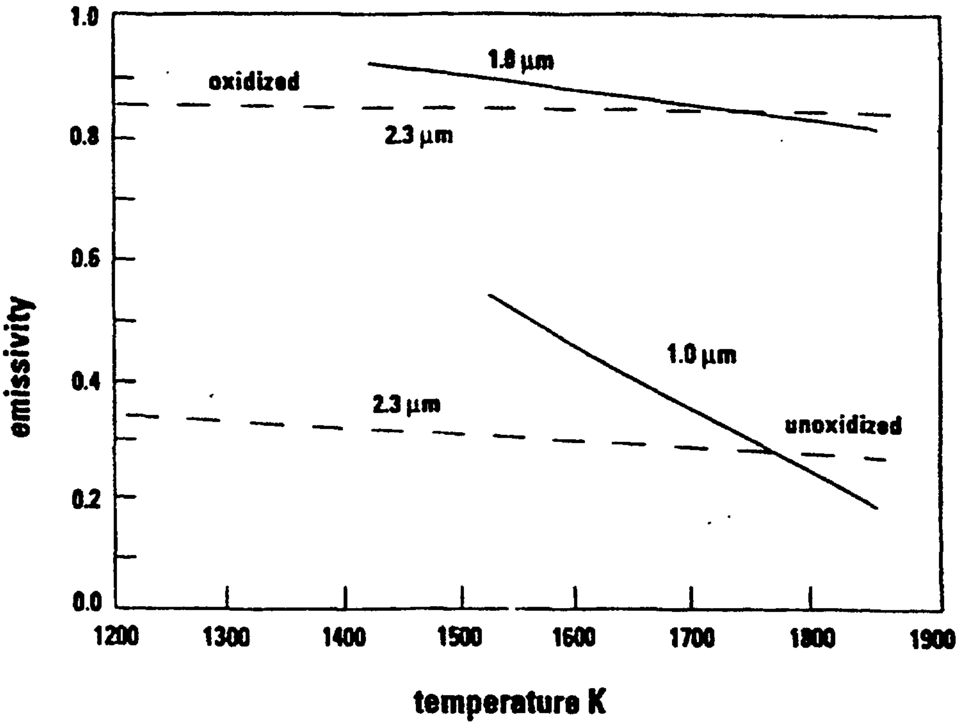

Figure 4.2.1.5 Spectral emissivity at 1.0 and 2.3 µm for unoxidized and oxidized Zircaloy-4 as a function of temperature [4].

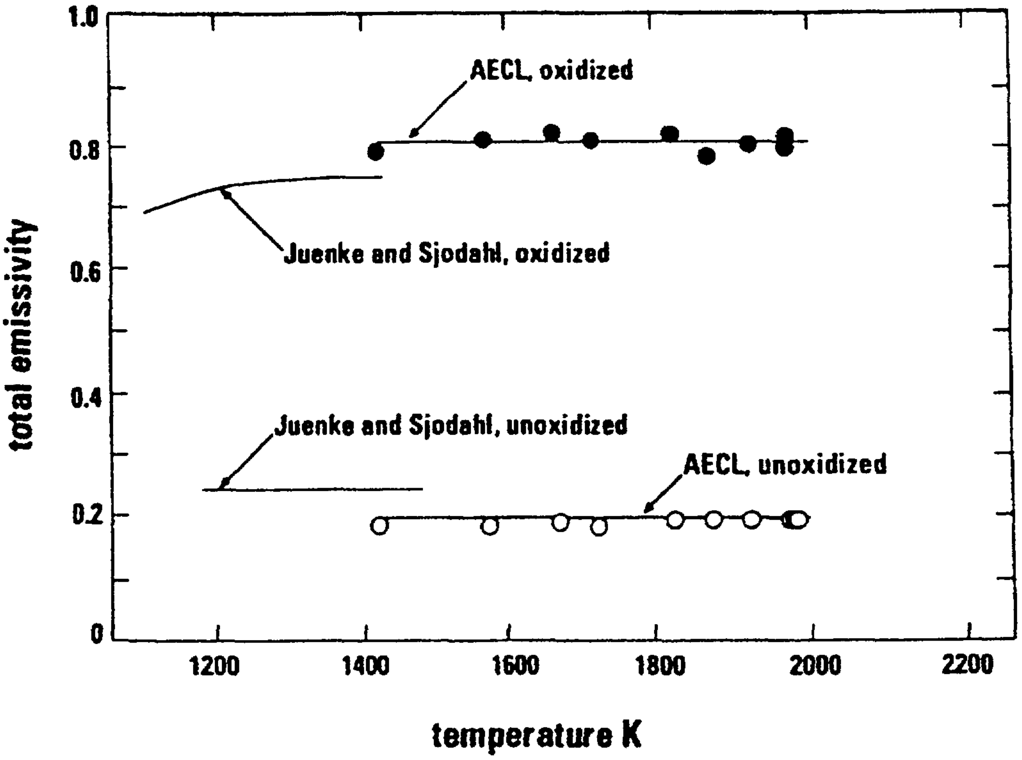

Figure 4.2.1.6 Total emissivity of Zircaloy-4 as a function of temperature [5]. Some data from [6] are shown.

References to Section 4.2.1

Note:Literature stored in THERSYST is referenced by document number, e.g. J0000250, etc.

J0000250 SLATTERY G. F., "The effect of hydride on the thermal expansivity of zirconium alloys", J. Less-Common Met. 11 (1966), 89-98

J0000926 GILCHRIST K. E., "Thermal property measurements on Zircaloy-2 and associated oxide layers up to 1200°C", J. Nucl. Mat. 62 (1976), 257-264

J0000943 MAGLIC K., PEROVIC N. L., Stanimirovic A., "Calorimetric and transport properties of Zircaloy 2, Zircaloy 4 and Inconel 625", Int. J. Thermophys. 15 (1994), 741-756

J0001456 PEGGS, I. D., STADNYK, A. M., GODIN, D. P., "Thermophysical properties of zirconium-alloy fuel-channel components", High Temp. -High Pressures 8 (1976), 441-450

J0002043 BUNNEL L. R., BATESS J. L., MELLINGER G. B., "Some high-temperature properties of Zircaloy-oxygen alloys", J. Nucl. Mater. 116 (1983), 219-232

J0003003 CASEY D. N., YATES B., "The specific heat capacities of boron-containing alloys and cermets of Zircaloy-2, and related thermodynamic properties of zirconium", High Temp. -High Pressures 6 (1974), 33-46

J0003057 MURABAYASHI M., TANAKA S., TAKAHASHI Y., "Thermal conductivity and heat capacity of Zircaloy-2, -4 and unalloyed zirconium", J. Nucl. Sci. Technol. 12 (1975), 661-662

P0000030 CHIRIGOS J. N., KASS S., KIRK W. W., SALVAGGIO G. J., "Fuel element fabrication with special emphasis on cladding materials. Development of Zircaloy-4", Proc. Symposium held in Vienna, May 10-13,1960; Ed. IAEA; Academic Press London, New York, 1961

R0000105 LUCKS C. F., DEEM H. W., "Progress relating to civilian applications during June 1958: Thermal conductivity of uranium and UO_2", USAEC Rept. BMI-1273, 1-62 (1958)

R0000109 FEITH A. D., "High-temperature materials program: Property measurements", USAEC Rept. GEMP-61, 153-155 (1966)

R0000110 SCOTT D. B., "Physical and mechanical properties of Zircaloy 2 and 4", USAEC Rept. WCAP-3269-41, 1-13 (1965)

RT000063 HOHORST J. K. (Editor), "SCDAP/RELAP5/MOD2 Code Manual, vol.4: MATPRO-a library of materials properties for light-water-reactor accident analysis", NUREG/CR-5273 (1990)

Additional references to Section 4.2.1

[1] PRICE E. G.,"Thermal Conductivity, Electrical Resistivity,and Specific Heat of CANDU Constructional Alloys and AISI Type 403 End Fitting", TDVI-368, 1980

[2] MILLS R. W., SCHANKULA M. H., LANGE B. A., "The Thermal Conductivity of Zirconium, Zircaloy-2 and Zirconium-2.5 wt.% Niobium and Some of Their Hydrides from 150°C to 350°C", AECL internal document

[3] PRICE E. G., AECL internal document

[4] MATHEW P. M., KRAUSE M., DEAN M., "Emittance of Zircaloy-4 Sheath at High Temperatures in Argon and Steam Atmospheres", Proc. 10th Annual CNA/CNS Conf. (1989) p. 9-12-9-17

[5] MATHEW P. M., GEORGE I. M., "Total Emissivity of Zircaloy-4 at High Temperatures", to appear in Proc. 17th Annual CNA/CNS Conf. (1996)

[6] JUENKE E. F., SJODAHL L. H., "Physical and Mechanical Properties: Emittance Measurements", AEC Fuels and Materials Development Program, GEMP-1008 (1968) p. 239 -246.

[7] MURPHY E. V., HAVELOCK F., "Emissivity of Zirconium Alloys in Air in the Temperature Range 100-400°C", J. Nucl. Mater. 60 (1976) p. 167-176.

4.2.2. Oxidation properties of zirconium based alloys

Owing to the extreme importance of zirconium based cladding material oxidation under accident conditions and the close relationship of this phenomenon to various safety issues of light and heavy water reactors, it was decided to collect appropriate information on oxidation parameters and incorporate this data into the THERSYST system.

Oxidation kinetics

The reaction of zirconium (pure or as a basic constituent of fuel element cladding alloys) with steam is described by the following relation

$$Zr + 2H_2O = 2H_2 + (Zr + 2O) + heat \qquad (4.2.2\text{-}1)$$

At temperatures above the $(\alpha + \beta)/\beta$ allotropic transformation temperature three layers are formed:

- superficial layer of zirconium dioxide ZrO_2,
- intermediate layer of oxygen stabilized alpha phase α-*Zr*(O),
- β-phase zirconium, containing dissolved oxygen.

The governing mechanism for reaction (4.2.2-1) is the diffusion of oxygen anions through the anion-deficient ZrO_2 lattice. Under this assumption, and under isothermal conditions with unlimited steam supply to the reaction surface, the reaction rate can be described by a parabolic expression of the form

$$\delta^2 = K_\delta t \qquad (4.2.2\text{-}2)$$

the so called "parabolic law" of oxidation kinetics. In expression (4.2.2.2) the quantity δ is a measure of the reaction extent, expressed per unit area of reaction surface. In this equation, t is the time and quantity δ can be measured as

- mass increase due to oxygen uptake per unit area,
- thicknesses of oxide, alpha or combined oxide-alpha layers,
- amount of hydrogen, generated in the reaction.

A frequently used measure of the reaction extent is the "mass of zirconium reacted", equivalent to the mass of zirconium in the stoichiometric ZrO_2 oxide formed. Another definition of this quantity, which cannot be measured directly, is the mass of zirconium reacted determined from the oxygen uptake, assuming that all the oxygen consumed forms ZrO_2.

With the exception of the "zirconium reacted" all the other quantities can be measured directly; mass increase by gravimetric method, thicknesses of layers by metallographical examination and hydrogen by oxidizing atmosphere analysis.

The most important parameter of oxidation kinetics is the reaction rate constant K_δ. From a series of experimental results for the specimens, exposed in an oxidizing environment (steam, steam - gas mixtures) for different time intervals, this parameter can be obtained by regression methods, or, by plotting the measured quantity against $t^{1/2}$.

The reaction rate constant is related to temperature by an Arrhenius equation

$$K_\delta(T) = A\exp\left(-\frac{Q}{RT}\right) \qquad (4.2.2\text{-}3)$$

where A is a pre-exponential term, Q is the activation energy, R is the gas constant and T the absolute temperature.

A more detailed description of the oxidation kinetics, mechanisms governing the oxidation process and a mathematical model for zirconium oxidation is given in Supplement S1.

Collected data on oxidation kinetics parameters

A total of 858 data items have been collected from the referenced literature for the oxidation parameters: giving the parabolic reaction rate constant K_δ for the following oxidation reaction extent parameters:

mass increase : 22 data sets, 159 items
ZrO_2 layer : 16 data sets, 122 items
$\alpha Zr(O)$ layer : 8 data sets, 63 items
$ZrO_2+\alpha Zr(O)$ layers : 10 data sets, 78 items
Zr reacted : 20 data sets, 163 items

Total : 76 data sets, 585 items

The majority of the data points for K_δ were only presented in the referenced literature in graphical form. From cases where the results were presented in both graphical and tabular form we have concluded that the error of extracting data from the graphs is typically in the 2-4% range, which is far below the experimental uncertainties.

After collection, all data have been transformed to the most commonly used units:

the parabolic reaction rate constant [$g^2/(cm^4 \cdot s)$], and
the oxide plus alpha-zirconium combined layer growth constant [cm^2/s].

The most important parameters, describing the experimental conditions from the referenced literature sources [1-31] are summarized in Table 4.2.2.1. These parameters are:

Specimen material and shape

Oxidation has been widely studied for the Zircaloy-4 cladding material of fuel elements. Only a limited number of experiments have been performed for other materials: Zircaloy-2, pure zirconium and zirconium-niobium alloys. The majority of specimens had a tubular form, with dimensions (diameter, wall thickness) typical for light water reactors. Other forms of specimens were adopted for special reasons, e.g. a disk shaped specimen was used in experiment [17] which continuously monitored the specimen mass increase and in experiment [23] where the specimen was heated by a defocused CO_2 laser beam.

External/internal heating

There are two ways of heating a specimen to a desired temperature, according to the location of heat source:

- external, provided by resistance, infrared furnace or by a laser beam,
- internal, when the specimen is heated directly (resistance, inductive).

Oxidizing environment

Most of the experiments have been performed by oxidation in pure steam under "unlimited" steam supply condition. Uetsuka and co-workers performed a series of experiments for studying the influence of different oxidizing media and steam supply conditions: oxidation under very limited steam supply (effect of the "steam starvation") [19,20], oxidation in oxygen/argon mixture [18,21] and steam/hydrogen and steam/argon mixtures [22]. Steam starvation can be achieved by a very low content of steam in a mixture. This effect has been studied at very high temperatures in steam/hydrogen environments with up to 95% hydrogen content [23].

Temperature range

Most of the referenced experiments have been carried out in the temperature range 900 to 1500°C. At temperatures above 900°C most experiments obey the parabolic law of oxidation kinetics, as observed in experiments [3,4,7,10-12,15,24,27]. Experiments above 1500°C are accompanied by difficulties in controlling and measuring the temperature of the reacting surface. Nevertheless, oxidation kinetics at very high temperatures are of importance for severe accidents.

Measured oxidation parameters

The most frequently presented oxidation parameter is the rate of mass increase, given by the oxygen uptake in the oxide and alpha layers. This parameter is measured by a gravimetric method (simply: specimen weighing) after oxidation. Arrangement of the apparatus [17] allows the mass increase to be continuously measured during oxidation. This parameter was obtained indirectly in experiments [13,14] by checking the amount of hydrogen generated by the reaction ("hydrogen evolution method"). The remaining three parameters, thicknesses of ZrO_2 layer, oxygen stabilized α-Zr(O) layer and combined oxide-alpha Zr layer were determined from metallographic examinations. The mass of reacted zirconium is not a directly measured parameter.

Complete descriptions of the parameters, consisting of details on:

- literature source,
- sample specification (material, shape, specimen pre-treatment, chemical composition, etc.),
- experimental conditions (details on apparatus, heating mode, oxidation type, etc.),
- oxidizing environment (composition of oxidizing media, pressure, reaction time, temperature range, etc.)
- and other experimental parameters have been prepared to the extent required for incorporation into THERSYST data base system.

Collected data are illustrated in Figures 4.2.2.1-4.2.2.5 in Arrhenius form (1/temperature dependence). These data sets represent the "raw material" for further evaluation, in topics such as:

- experimental techniques and methods (temperature measurement, sample heating mode, post-exposure examination method of the sample),
- factors affecting the oxidation process (steam supply, effect of the sample shape and dimensions),
- chemical composition of the sample and the oxidizing environment, etc.

that should be taken into account. An important part of the experimental results assessment will be a computer simulation of the experiments (see description of code FRAOXI in Supplement S1). Using such a simulation the reliability of the experimental results and the lack of experimental data (e.g. reaction rate constant K_w for weight gain at temperatures above 1600°C) can be assessed.

In the scope of a wider programme consisting of fuel rod behaviour analysis under normal operating and accident conditions a great effort was spent in NRI Řež collecting data on Zr-1%Nb cladding material properties. Oxidation properties of this alloy, represented by the weight gain rate constant are illustrated in Figure 4.2.2.6. Other oxidation properties (oxide and alpha layer thickness, effect of oxidizing atmosphere pressure) have also been studied. The majority of this study has been performed under contract between NRI Řež and the Institute of Nuclear Fuels (INF) at Zkrozlov near Prague.

For practical use in solving problems connected with cladding oxidation a simple form of the Arrhenius formula (4.2.2-3) for the reaction rate constant is often very valuable. In Tables 4.2.2.2 and 4.2.2.3, a selected set of the most reliable parameters are presented for the two important measures of oxidation: weight gain and oxide layer thickness. For Zircaloy-4 and temperatures below ~1525°C (the transition temperature from tetragonal to cubic structure) all of the A, Q values present have approximately the same degree of reliability. For temperatures above 1525°C the A, Q values from reference [23] are recommended for the oxide layer thickness growth rate constant. No A, Q values for weight gain rate constant, based on experimental results, have been found in referenced literature. For Zr-1%Nb A, Q values from [24] are recommended.

There is only one set of values for Zr-2.5%Nb [36]. Note that there is a large literature on the corrosion of Zr-2.5%Nb at reactor operating temperatures (see for instance, IAEA TECDOC-684), which demonstrates significant differences between the behaviour of this material and the Zircaloys; at the elevated temperatures of interest to this report differences in oxidation are much less apparent.

Another aspect in solving problems connected with the cladding oxidation is the geometrical form of the layers. In a number of studies [4,37,38,39] penetrating "fingers" of αZr(O) have been found, in post oxidation examinations at room temperature, in the transformed β-phase, at depths up to 100% of the otherwise uniform layer of αZr(O). These brittle regions can have a major impact on the possibility of cladding fracture following quenching during a transient. Other irregularities in the oxygen-containing layers originate when straining the cladding during oxidation [11,40], causing points of weakness in the cladding. A further practical problem arises from the assumption that the observation of parabolic kinetics implies anion diffusion through the anion-deficient ZrO_2 lattice [11,14,36]. A growing porous oxide layer can still give parabolic kinetics since rate limitation by gaseous diffusion through the porous oxide can still give an oxidation rate inversely proportional to oxide thickness [41]. This may only show up as a region of low slope in the Arrhenius plot but the full implications have yet to be established. In the experimental work thus far the values of K_δ have been obtained at heating rates slower than those which might occur in a fast transient in-reactor, and the possibility of different values of K_δ under these conditions should be considered [42].

Nomenclature to Section 4.2.2

A - constant ((g/cm^2)^2/s),
K - reaction rate constant,
Q - active energy (kJ/mol),
R - gas constant (J(mol·K)),
t - time (s),
T - temperature (K)

Table 4.2.2.1 SUMMARY OF EXPERIMENTAL CONDITIONS IN THE REFERENCED EXPERIMENTS

Reference	Specimen		Heating mode	Oxidizing environment	Temperature range (°C)	Oxidation parameters
	Material	Shape				
[1]	Zry-4	T	I	ST	860-1480	M
[2]	Zry-4	T	E	ST	1000-1330	M,O,OA
[3]	Zry-4	T	I	ST	700-1490	R
[4]	Zry-4	T	I	ST	700-1490	R
[5]	Zry-4	T	E	ST	900-1500	M,O,A
[6]	Zr	T	E	ST	1000-1420	M,O,A
[7]	Zry-4	T	E,I	ST	700-1300	M,O,A,OA
[8]	Zry-4	T	E	ST	1350-1600	M
[9]	Zry-4	T	E	ST	1350-1600	M,O
[10]	Zry-4	T	E	ST	600-1300	M
[11]	Zry-4	T	E	ST	600-1600	M
[12]	Zry-4	T	E	ST	600-1600	M,O
[13]	Zry-4,2	C	I	ST	1000-1850	O,A
[14]	Zry-4,2	C	I	ST	1050-1850	O,A,OA,R
[15]	Zry-4	T	E	ST	690-990	M,O,OA
[16]	Zry-4	T	E	ST	1600-1880	M,O
[17]	Zry-4	D	E	ST	1100-1500	M
[18]	Zry-4	T	E	O_2 + Ar	900-1500	M,O,OA
[19]	Zry-4	P	E	Dil. ST	1000-1400	M
[20]	Zry-4	P	E	Dil. ST	1000-1490	M
[21]	Zr-4	T	E	O_2 + Ar	900-1500	M,O,OA
[22]	Zry-4	P	E	O_2 + Ar/H_2	1000-1500	M
[23]	Zry-4	D	E	ST,ST + H_2	1300-2400	O,OA
[24]	Zr1Nb	T	E	ST	600-1200	M,O,A
[25]	Zr1Nb	T	E	ST	1200-1450	M
[26]	Zr1Nb	T	E	ST	1300-1600	M
[27]	Zr1Nb	T	E	ST	700-1200	M,O,A
[28]	Zry-4	a)	E	ST	1000-1330	R
[29]	Zr	a)	E	ST	1000-1500	R
[30]	Zry-2	a)	E	ST	1000-1400	R
[31]	Zry-4	a)	I	ST	970-1250	R
[36]	Zr2.5Nb	C	I	ST	1000-1600	M,O,OA,R

Legend to Table 4.2.2.1

Specimen material

Zr	pure zirconium
Zry-2	Zircaloy-2
Zry-4	Zircaloy-4
Zr1Nb	Zirconium alloy with 1% Nb - cladding material of WWER-440 and WWER-1000 type reactors
Zr2.5Nb	Zirconium alloy with 2.5% Nb

Specimen shape

T	tubular-shaped specimen
D	disk-shaped specimen
P	plate-like specimen
C	cylindrical bar stack specimen

Heating of the specimen

I	internally heated specimen (inductive or resistance)
E	externally heated specimen (resistance or infra-red furnace, unfocused laser beam)

Incomplete information

a)	information on experimental condition is missing or incomplete

Oxidizing environment

ST	pure steam
O_2+Ar	25% oxygen + 75% Argon mixture (mol %)
Dil.ST	diluted steam-oxidation under limited steam supply
O_2+Ar/H_2	oxygen-argon or oxygen-hydrogen mixtures
ST+H_2	oxygen-hydrogen mixture with various content (5-95%) of the hydrogen

Measured oxidation parameters

M	mass increase (oxygen uptake)
O	ZrO_2 layer thickness
A	oxygen stabilized α-Zr(O) layer thickness
OA	double ZrO_2 + αZr(O) layer thickness
R	mass of Zr reacted - not directly measured quantity

Table 4.2.2.2 PARAMETERS *A* AND *Q* IN THE ARRHENIUS FORMULA FOR THE PARABOLIC RATE CONSTANTS K_W FOR WEIGHT GAIN. VALUES OF *A* ARE EXPRESSED IN ((g/cm^2)^2/s) AND VALUES OF *Q* IN (kJ/mol)

Reference	Material	Range of temperatures (°C)	*A*	*Q*
[2]	Zry-4	900-1350	0.468	170.3
[3][4]	Zry-4	950-1500	0.467	158.2
[5]	Zry-4	900-1500	0.362	167.1
[6]	Zr	1000-1450	0.990	187.3
[7][10][12]	Zry-4	900-1600	0.524	174.2
[21][22]	Zry-4	1000-1500	0.439	170.4
[25]	Zr-1%Nb	600-1400	0.561	178.1
[26]	Zr-1%Nb	900-1300	0.846	173.1
[36]	Zr-2.5%Nb	1000-1500	0.329	168.6
[36]	Zr-2.5%Nb	1500-1600	0.612	133.0

Table 4.2.2.3 PARAMETERS *A* AND *Q* IN THE ARRHENIUS FORMULA FOR THE PARABOLIC RATE CONSTANTS K_0 FOR OXIDE LAYER THICKNESS. *A* IS IN (cm^2/s), *Q* IN (kJ/mol)

Reference	Material	Range of temperatures (°C)	*A*	*Q*
[2]	Zry-4	900-1350	0.0215	150.0
[5]	Zry-4	900-1500	0.0225	150.2
[6]	Zr	1000-1450	0.0872	176.5
[7][10][12]	Zry-4	900-1600	0.0782	168.1
[13][14]	Zry-42	1050-1580	0.0013	113.0
[13][14]	Zry-42	1580-1850	0.0207	133.1
[23]	Zry-4	1300-1510	1.01	203.4
[23]	Zry-4	1510-2400	29.8	236.3
[25]	Zr-1%Nb	600-1200	0.0313	161.1

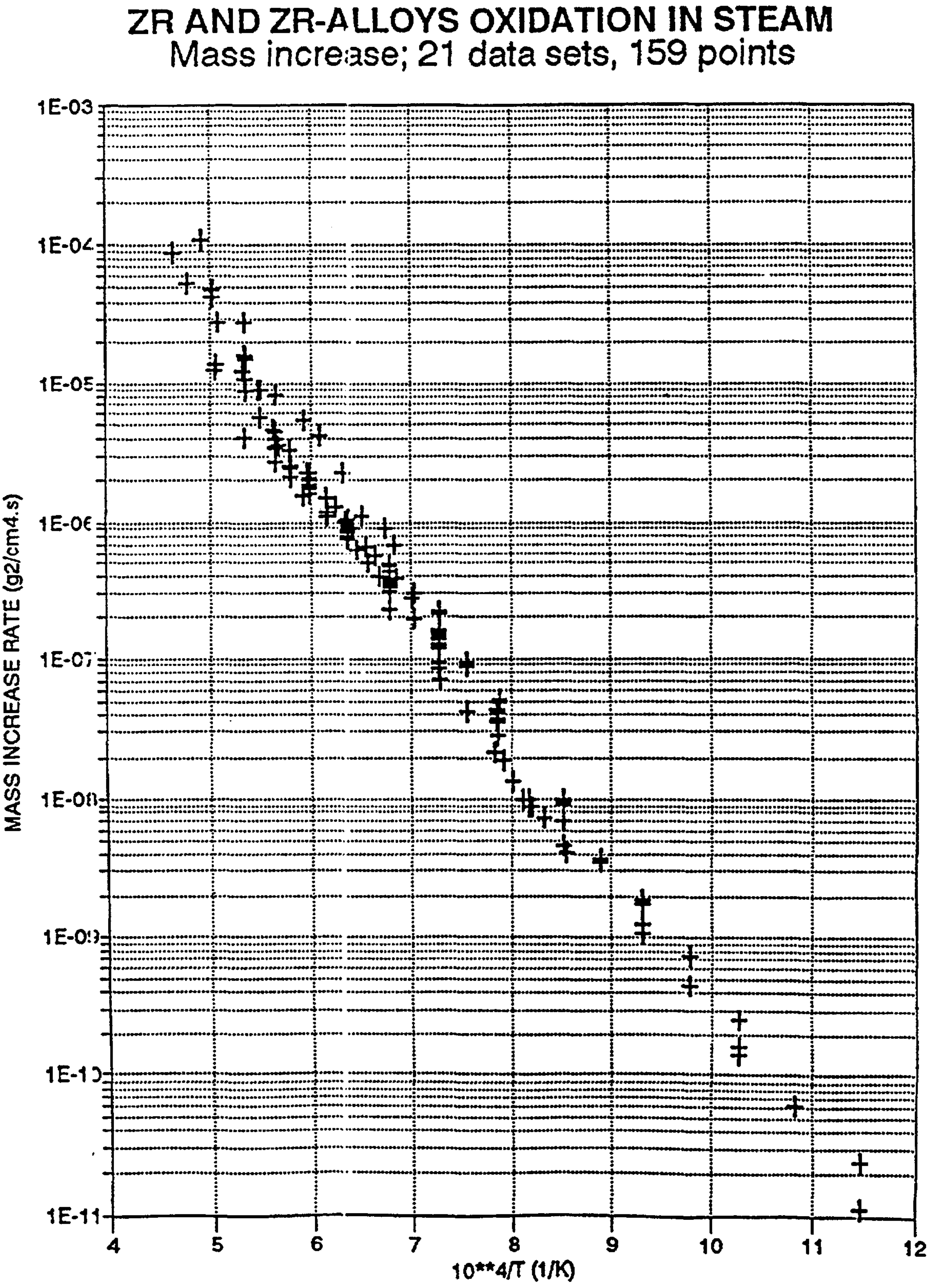

Figure 4.2.2.1 Oxidation kinetics parameter - mass increase rate - dependence on temperature

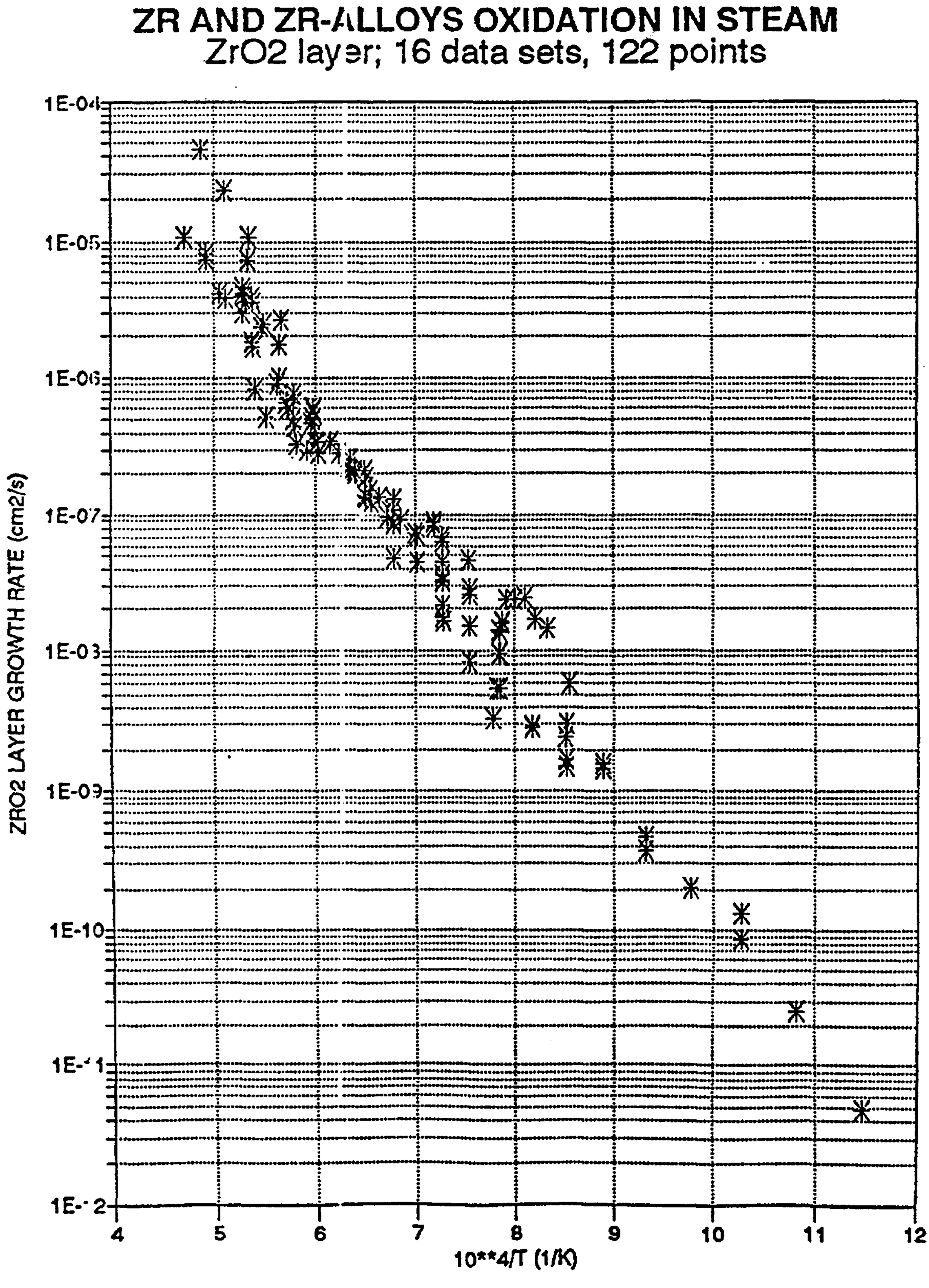

Figure 4.2.2.2 Oxidation kinetics parameter - oxide (ZrO_2) layer thickness growth rate - dependence on temperature

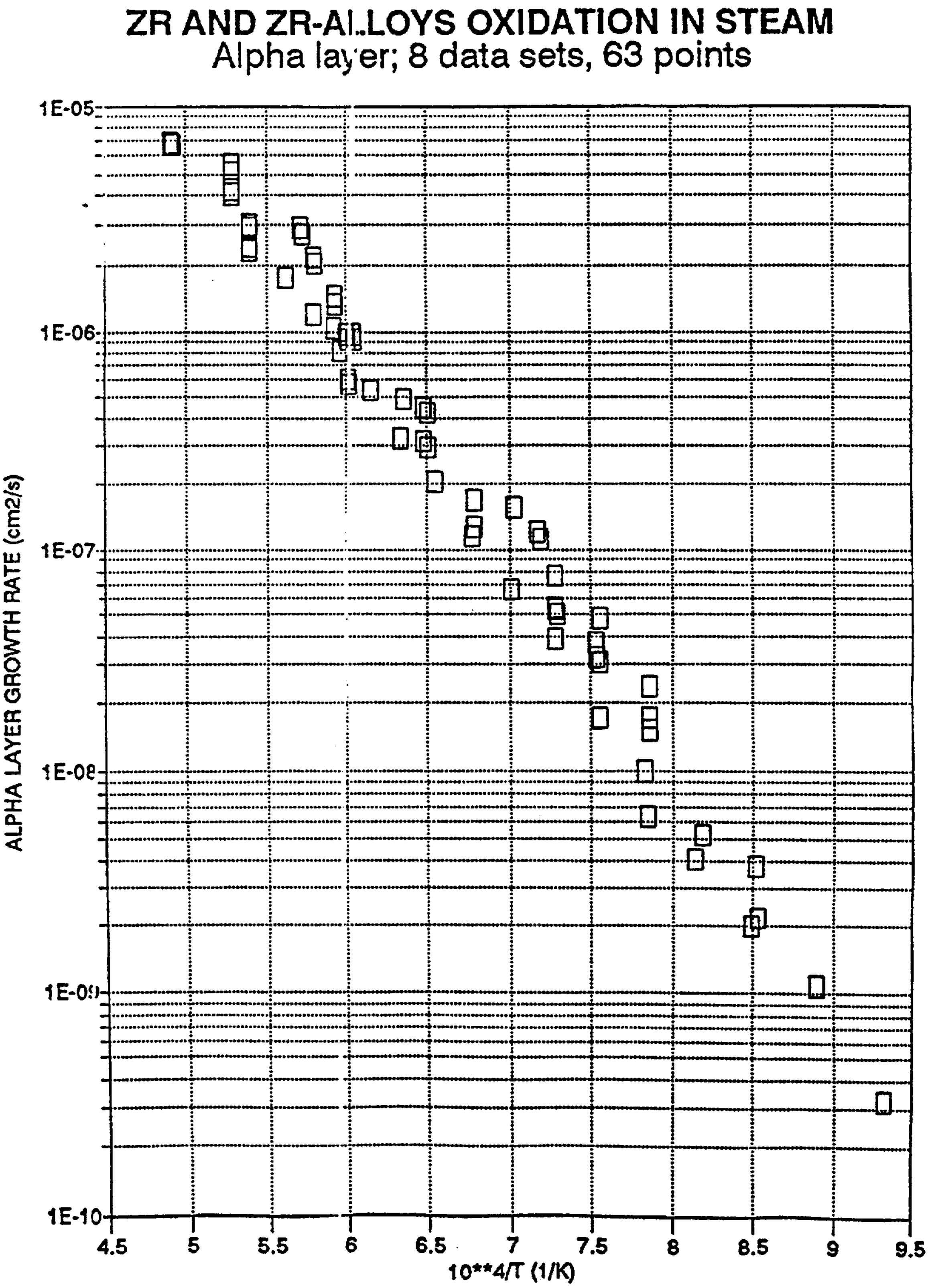

ZR AND ZR-ALLOYS OXIDATION IN STEAM
Alpha layer; 8 data sets, 63 points

Figure 4.2.2.3 Oxidation kinetics parameter - oxygen stabilized alpha Zr(0) layer thickness - dependance on temperature

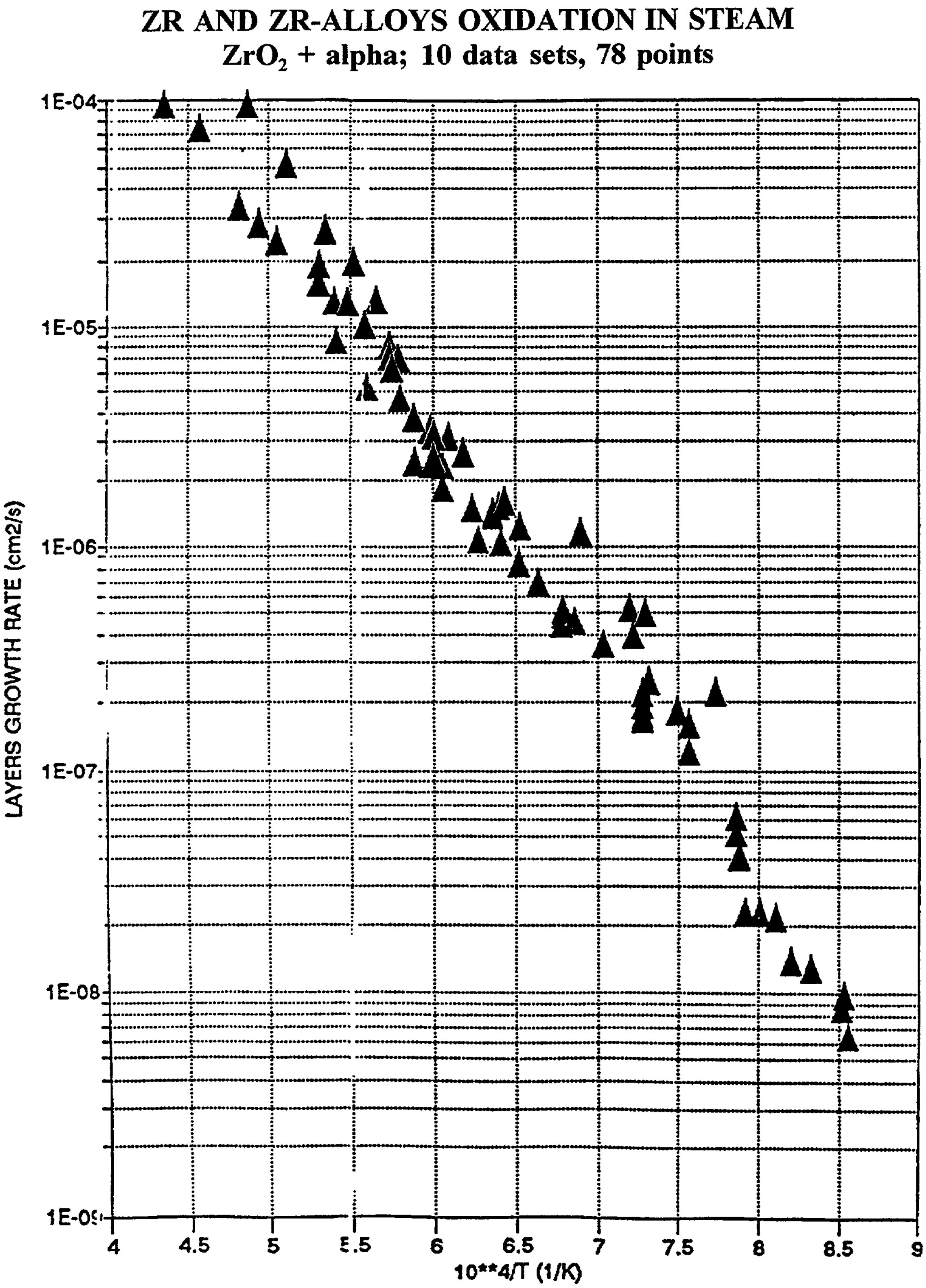

Figure 4.2.2.4 Oxidation kinetics parameter - combined oxide and alpha layer thickness growth rate - dependance

ZR AND ZR-ALLOYS OXIDATION IN STEAM

Zr reacted; 20 data sets, 163 points

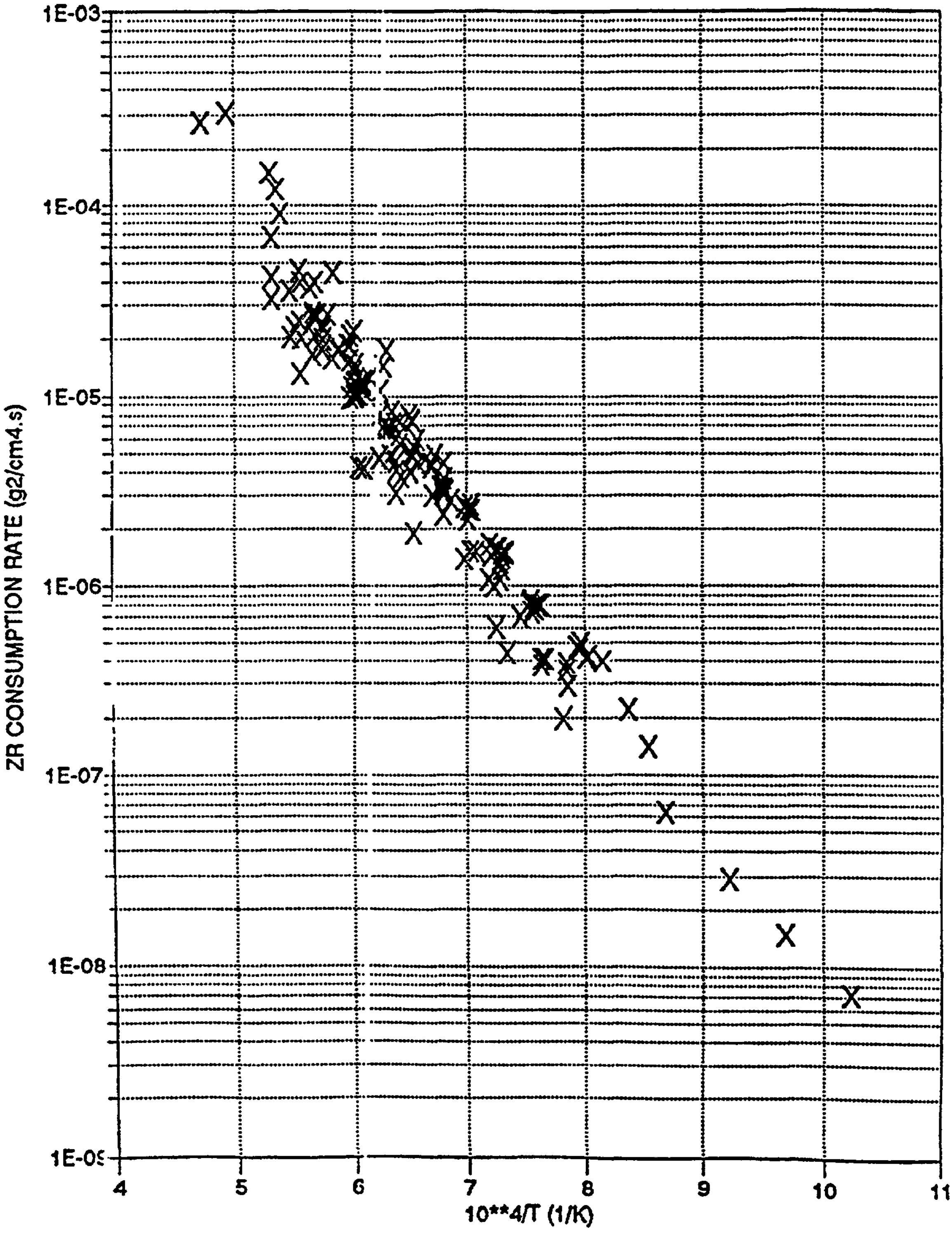

Figure 4.2.2.5 Consumption rate of zirconium reacted in oxidation: temperature dependance

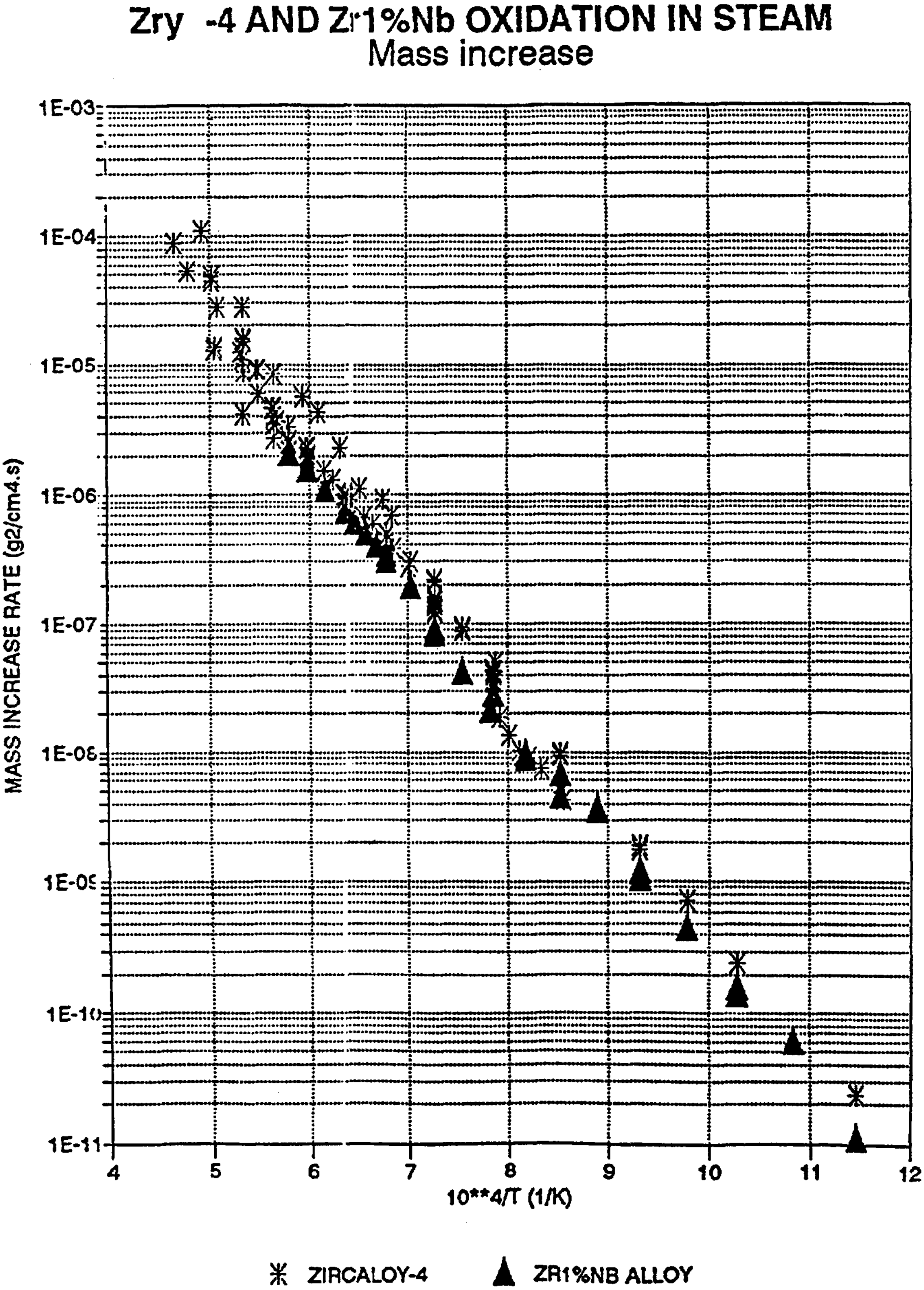

Figure 4.2.2.6 Comparison of oxidation kinetics parameter (mass increase) of Zircaloy-4 and Zr-1%Nb alloy. Data for Zr-1%Nb are from references [24,25,27].

References to Section 4.2.2

[1] BALLINGER, R. G., et al., "Oxidation reaction kinetics of Zircaloy-4 in an unlimited steam environment", J. Nucl. Mat. 62, 213-220 (1976)

[2] KAWASAKI,S., et al., "Oxidation of Zircaloy-4 under high temperature steam atmosphere and its effect on ductility of cladding", J. Nucl. Sci. Technol., 15, 589-596 (1978)

[3] OCKEN, H., et al., "Evaluation of models for Zircaloy oxidation in light of recent experiments", ASTM-STP-681 (1979), p. 514-536

[4] OCKEN, H., "An improved evaluation model for Zircaloy oxidation", Nucl. Technology 47, 343-357 (1980)

[5] PAWEL, R. E., et al., "The kinetics of oxidation of Zircaloy-4 in steam at high temperatures", El. Chem. Sci. Technol. 126, 1105-1111 (1979)

[6] PAWEL, R. E., CATHCART, J. J., "The oxidation of pure zirconium in steam from 1000 to 1416°C", J. Eletrochem. Soc. 128, 1999-2005 (1981)

[7] LEISTIKOW, S., et al., "Kinetik und Morphologie der isotherm Dampf-Oxidation on Zircaloy-4 bei 700-1300°C", KfK-2587, Mar. (1978)

[8] ATEF E. ALY, "Oxidation of Zircaloy-4 tubing in steam at 1350 to 1600°C". KfK-3358, May (1982)

[9] LEISTIKOW, S., et al., "Untersuchung des Wasserdampf-Oxidation-sverhaltens von Zircaloy-4 Hüllrohren bei 1350-1600°C", In "Projekt Nukleare Sicherheit", Jahresbericht 1982, KfK-3350, Jul. (1983), p. 4200.175-4200.195

[10] LEISTIKOV, D., et al., "Comparison of high temperature steam oxidation behaviour of Zircaloy-4 versus austenitic and ferritic steels under light water reactor safety aspects", KfK-3994, Dec. (1985)

[11] LEISTIKOW, S., SCHANZ, G., "The oxidation behaviour of Zircaloy-4 in steam between 600 and 1600°C". Werkstoffe und Korrosion, 36, 105-116 (1985)

[12] LEISTIKOW, S., "Hochtemperatur-Oxidation von Zircaloy Hüllrohren in Wasserdampf" In "Projekt Nukleare Sicherheit", Abschlusskolloquim, 1986 KfK-4170, Aug. (1986), p. 201-250

[13] URBANIC, V. F., "Method for estimating the exposure time and temperature for Zircaloy oxidation in steam", J. Nucl. Mat.,59, 90-94 (1976)

[14] URBANIC, V. F., HEIDRICK, T. R., "High-temperature oxidation of Zircaloy-2 and Zircaloy-4 in steam", J. Nucl. Mat., 75, 251-261 (1978)

[15] OLSEN,CH. S., "Temperature estimates from Zircaloy oxidation kinetics and microstructures", NUREG/CR-2807, Oct. (1982)

[16] PARSONS, P. D., et al., "The deformation, oxidation and embrittlement of PWR fuel cladding in a loss of coolant accident", ND-R-1351(S), Sep. (1986)

[17] MOALEM, M., OLANDER, D. R., "Oxidation of Zircaloy by steam", J. Nucl. Mat., 182, 170-194 (1991)

[18] UETSUKA, M., HOFMANN, P., "Reaction kinetics of Zircaloy-4 in a 25% O_2/75% Ar gas mixture from 900 to 1500°C under isothermal conditions", KfK-3917, May (1985)

[19] UETSUKA, et al., "Oxidation of Zircaloy-4 under limited steam supply from 1000 to 1400°C", J. Nucl. Sci. Technol., 23, 928-930 (1986)

[20] UETSUKA, H., OTOMO, T., "High-temperature oxidation of Zircaloy-4 in diluted steam", J. Nucl. Sci. Techn. 26, 240-248 (1989)

[21] UETSUKA, H., HOFMANN, P., "High-temperature oxidation kinetics of Zircaloy-4 in oxygen/argon mixtures", J. Nucl. Mat. 168, 47-57 (1989)

[22] UETSUKA, H., et al., "Zircaloy-4 oxidation behaviour in steam-hydrogen and steam-argon mixtures from 1000 to 1500°C", IAEA-SM-296/63, IAEA (1989)

[23] PRATER, J. T., COURTRIGHT, E. L., "High-temperature oxidation of Zircaloy-4 in steam and steam-hydrogen environments", NUREG/CR-4476, Feb. (1986)

[24] VRTÍLKOVÁ, V., "Statistical evaluations of oxidation formulae" (in Czech), ÚJP-631, Oct. (1988)

[25] VRTÍLKOVÁ, V., MOLIN, L., "Oxidation kinetics of Zr1%Nb cladding tube in 0.1 MPa steam at temperatures 1200-1400°C" (in Czech), ÚJP-673, Dec. (1989)

[26] BIBILASHVILI, Y. K., et al., "Interaction between cladding (Zr 1% Nb alloy) and steam at 1300-1600°C and atmospheric pressure", Bilateral Soviet-Czechoslovak Seminar on "Fuel rod behaviour modelling nuclear accident conditions", Moscow, Dec. (1990)

[27] BÖHMERT, J., LINEK, J., "Investigation of high temperature water-steam oxidation of Zr1Nb". ZfK-743, May (1991)

[28] SUZUKI, M., et al., "Zircaloy-steam reaction and embrittlement of the oxidized Zircaloy tube under postulated loss-coolant accident conditions", JAERI-M-6879, Jan. (1977), Referenced in [3], [4]

[29] CATHCART, J. V.,, et al., "Zirconium metal-water oxidation kinetics. IV: Reaction rate studies", ORNL/NUREG-17, Aug. (1977), Referenced in [3], [4]

[30] BROWN, A. F., HEALEY, T., "The kinetics of total oxygen uptake in steam oxidized Zircaloy-2 between 1000-1400°C". RD/BN4117, Sep. (1977), Referenced in [3], [4]

[31] WESTERMAN, R. E., HESSON, R. M., "Zircaloy cladding ID/OD oxidation studies". EPRI-NP-525, Nov. (1977), Referenced in [3], [4]

[32] VRTÍLKOVÁ, V., MOLIN, L., "Influence of steam pressure on zirconium based alloys in the temperature range 600-900°C" (in Czech). ÚJP-712, Dec. (1991)

[33] BĚLOVSKÝ, L., "FRAOXI-1: A computer model for calculating the external and internal oxidation of Zircaloy cladding" ÚJV-9326-T, Feb. (1991)

[34] PAWEL, R. E., CAMBELL, J. J., "The observation of effects of finite specimen geometry on the oxidation kinetics of Zircaloy-4", J. Electrochem. Soc., 127, 2188 (1980)

[35] VRTÍLKOVÁ, V., MOLIN, L., "Oxidation kinetics of Zr1%Nb fuel cladding under transient conditions" (in Czech), ÚJP-698, Institute of Nuclear Fuels, Prague, Zbraslav (1990)

[36] URBANIC, V. F., "Oxidation of Zirconium Alloys in Steam at 1000 to 1850 °C", Zirconium in the Nuclear Industry, Proceedings of the Third International Conference at Quebec City, Canada, 10-12 Aug. 1976, pp. 168-181, ASTM Philadelphia, PA (1977)

[37] DOBSON, W. G., BIEDERMAN, R. R., BALLINGER, R. G., "Zircaloy-4 Oxidation in Steam Under Transient Oxidizing Conditions", Zirconium in the Nuclear Industry, Proceedings of the Third International Conference at Quebec City, Canada, 10-12 Aug. 1976, pp. 150-167, ASTM Philadelphia, PA (1977)

[38] IGLESIAS, F. C., SAGAT, S., SILLS, H. E., "High Temperature Oxidation of Zircaloy", Res. Mech. 17, 125-143 (1986)

[39] BOHMERT, J., DIETRICH, M., LINEK, J., "Comparative Studies on High-Temperature Corrosion of ZrNb1 and Zircaloy-4", Nuc. Eng. Design 147, 53-62 (1993)

[40] BRADHURST, D. H., HEUER, P. M., "The Effects of Deformation on the High-Temperature Steam Oxidation of Zircaloy-2", J. Nuc. Mat. 55, 311-326 (1975)

[41] COX, B., JOHNSTON, T., "The Oxidation and Corrosion ofNiobium (Columbium)", AIME Trans. Met. Soc., 227, 36-47 (1963)

[42] COX, B., "A Method for Calculating the Transient Oxidation of Zircaloys", AECL-6784, March (1980)

Additional references on oxidation of zirconium based alloys

[43] BAKER, L. and JUST, L. C., Studies of metal-water reactions at high temperature III, Experimental and theoretical studies of zirconium-water reactions, ANL-6548 May (1962)

[44] WANKLYN, J. K, BRITTON, C. F., SILVESTER, D. R., WILKINS, N. J. M., Influence of Environment on the Corrosion of Zirconium and its Alloys in High-temperature Steam, J. of the Electrochemical Society 110, 856-866 (1963)

[45] COX, B., Some Effects of Pressure on the Oxidation of Zircaloy-2 in Steam and Oxygen, J. Of Less-common Metals 5, 325-336 (1963)

[46] COX B., Pore Structure in Oxide Films on Irradiated and Unirradiated Zirconium Alloys, J. of Nuclear Materials 148, 332-343 (1987)

[47] SHANG-SHIANG HSU and CHUEN-HORNG TSAI., Transient Oxidation of Zircaloy Fuel Cladding in High Temperature Steam, J. of Nuclear Materials 158, 217-223 (1988)

[48] URBANIC, V. F., WARR, B. D., MANOLESCU, A., CHOW, C. K., SHANAHAN, M. W., Oxidation and Deuterium Uptake of Zr-2.5Nb Pressure Tubes in CANDU-PHW Reactors, Zirconium in the Nuclear Industry, Proceedings of the Eighth International Symposium at San Diego, 1988, pp. 20-34, ASTM, Philadelphia, PA (1989)

[49] HILLNER, E., Corrosion of Zirconium-Base Alloys - An Overview, Zirconium in the Nuclear Industry, Proceedings of the Third International Conference at Quebec City, Canada, 10-12 Aug. 1976, pp. 211-235, ASTM, Philadelphia, PA (1977)

4.2.3. Ni-Cr-based alloys

There are some Ni-Cr-based alloys used as cladding materials in both light and heavy water cooled reactors. Their nominal chemical composition is listed in Table 4.2.3.1.

Specific heat capacity

The data available on the specific heat capacity of different Ni-Cr-based alloys are presented in Figure 4.2.3.1. In Table 4.2.3.2 the industrial name of the alloy, its density and data sources are listed.

Thermal conductivity

The thermal conductivity of different Ni-Cr-based alloys is presented in Figure 4.2.3.2. In Table 4.2.3.3 the thermal treatment of the specimens and data sources are listed.

Curve E0000107 represents recommended data for Inconel X-750, obtained at CINDAS, Purdue University. This curve can be used as representative for this group of alloys, the numerical values are listed in Table 4.2.3.4. The estimated error is 10% below 100 K, 5% from 200 to 1000 K and 10% above 1400 K.

Thermal expansion

Data on the thermal expansion of Ni-Cr-based alloys are presented in Figure 4.2.3.3. Data sources are listed in Table 4.2.3.5.

Curves E0001004, E0001012 and E0001014 represent provisional values for the thermal expansion of Hastelloy, Inconel 600 and Inconel X-750 respectively. They are valid for well-annealed alloys and are considered accurate to within 7% over entire temperature range. These data can be represented approximately by the following equations:

For Hastelloy type alloy (curve E0001004) in the temperature range from 20 K to 1600 K:

$$\frac{\Delta L}{L_o} = -0.275 + 6.475\times10^{-4}T + 1.064\times10^{-6}T^2 - 2.672\times10^{-10}T^3 \qquad (4.2.3\text{-}1)$$

For alloys of type Inconel 600 and Inconel X-750 (curves E0001012 and E0001014) in the temperature range from 20 K to 1300 K:

$$\frac{\Delta L}{L_o} = -0.277 + 7.105\times10^{-4}T + 8.451\times10^{-7}T^2 - 1.548\times10^{-10}T^3 \qquad (4.2.3\text{-}2)$$

Nomenclature to Section 4.2.3

T - temperature (K);
α - thermal expansion coefficient, (1/K);
ε - thermal strain, (m/m), other unit: %
λ - thermal conductivity, (W/(m·K)).

Table 4.2.3.1 CHEMICAL COMPOSITION (IN WEIGHT %) OF SOME Ni-Cr-BASED ALLOYS

alloy	Ni	Cr	Co	Mo	Fe	Nb	C	others
Hastelloy X	Bal.	22.0	1.50	9.0	18.5	-	0.10	Mn 0.65, W 0.60, Si 0.60
Inconel X-750	73.0	15.5	-	-	7.0	1.0	0.04	Ti 2.5, Al 0.70, Cu<0.50,Si<0.35 Mn<0.35
Inconel 600	75.0	15.5	-	-	8.0	-	0.05	
Inconel 617	54.0	22.0	12.5	9.0	-	-	0.07	Al 1.0
Inconel 625	61.0	21.5	-	9.0	2.5	3.65	0.05	Al<0.40,Mn<0.5 Ti<0.40,Si<0.50

Table 4.2.3.2 SPECIFIC HEAT CAPACITY OF Ni-Cr-BASED ALLOYS

```
EKEY     I MNAM        I DEN   I DONO     I AU
---------I-------------I-------I----------I----------
E0001898 I Hastelloy X I  8.24 I P0000041 I Maglic
E9000712 I Inconel 600 I ---   I AK000027 I Richter
E9000419 I Inconel 617 I  8.36 I AK000021 I Richter
E0006414 I Inconel 718 I ---   I J0003001 I Brooks
E0006465 I Inconel 625 I ---   I J0000943 I Maglic

Units of descriptors
--------------------
DEN      density [g/cm^3]
```

Table 4.2.3.3 THERMAL CONDUCTIVITY OF Ni-Cr-BASED ALLOYS

```
EKEY     I MNAM          I DEN   I TREATT I TRTEM  I TRTIM  I DONO
---------I---------------I-------I--------I-------I-------I---------
E0001897 I Hastelloy X   I   8.24I        I ---    I ---    I P0000041
E0004590 I Hastelloy X   I ---   I ANNE   I ---    I ---    I J0001900
E0007215 I Inconel 600   I ---   I        I ---    I ---    I J0003167
E0000107 I Inconel X-750I ---    I FUHT   I ---    I ---    I TPM01000
E0005232 I Inconel X     I ---   I        I ---    I ---    I R0000129
E9000422 I Inconel 617   I   8.36I UNTR   I ---    I ---    I AK000021
E9000425 I Inconel 617   I   8.36I ANNE   I  1433  I 20 secI AK000021
E9000434 I Inconel 617   I   8.36I ANNE   I  1433  I 20 secI AK000021
E0004413 I Inconel 718   I ---   I AGED   I   942  I  8 h   I J0001425
         I               I       I SCOO   I        I        I
E0004591 I Inconel 718   I ---   I        I ---    I ---    I J0001900
E0005665 I Inconel 718   I   8.26I ANNE   I  1308  I  1 h   I R0000141
E0005845 I Inconel 718   I ---   I        I ---    I ---    I J0001778
E0005853 I Inconel 718   I   8.24I ANNE   I  1320  I ---    I J0001778
         I               I       I AGED   I   985  I  8 h   I
         I               I       I AGED   I   895  I  8 h   I
E0005880 I Inconel 617   I ---   I SOHT   I  1338  I  1 h   I J0002809
         I               I       I QUEN   I        I        I
         I               I       I AGED   I  893   I 22.5h  I
         I               I       I AGED   I  993   I 21 h   I
E0006464 I Inconel 625   I ---   I        I ---    I ---    I J0000943

Units of descriptors
-----------------------------------------------------------------------
DEN    density [g/cm^3]          TRTEM   temperature of thermal treatment [K]

Signification of Codes
-----------------------------------------------------------------------
ANNE   annealed                  FUHT    fully heat treated
QUEN   quenched                  SCOO    slowly cooled
UNTR   untreated

Inconel X is a previous designation of Inconel X-750.
```

Table 4.2.3.4 RECOMMENDED THERMAL CONDUCTIVITY OF INCONEL X-750 [TPM01000]

Property: λ thermal conductivity [W/m K]
Variable: T temperature [K]

T	λ	T	λ
0	0	400	13.5
1	0.024	450	14.3
3	0.145	500	15.2
5	0.33	600	17.0
10	0.96	700	18.8
25	3.4	800	20.5
50	6.6	900	22.3
75	8.0	1000	24.0
100	8.7	1100	25.8
150	9.6	1200	27.6
200	10.3	1300	29.3
250	11.0	1400	31.1
273	11.3	1500	32.8
300	11.7	1600	34.6
350	12.6	1665	35.8

Table 4.2.3.5 THERMAL EXPANSION OF Ni-Cr-BASED ALLOYS

EKEY	MNAM	DONO	AU
E0001004	Hastelloy X	TPM12000	Touloukian
E0001012	Inconel 600	TPM12000	Touloukian
E0001014	Inconel X-750	TPM12000	Touloukian
E9000417	Inconel 617	AK000021	Richter
E9000429	Inconel 617	AK000021	Richter
E0005856	Inconel 718	P0000014	McElroy

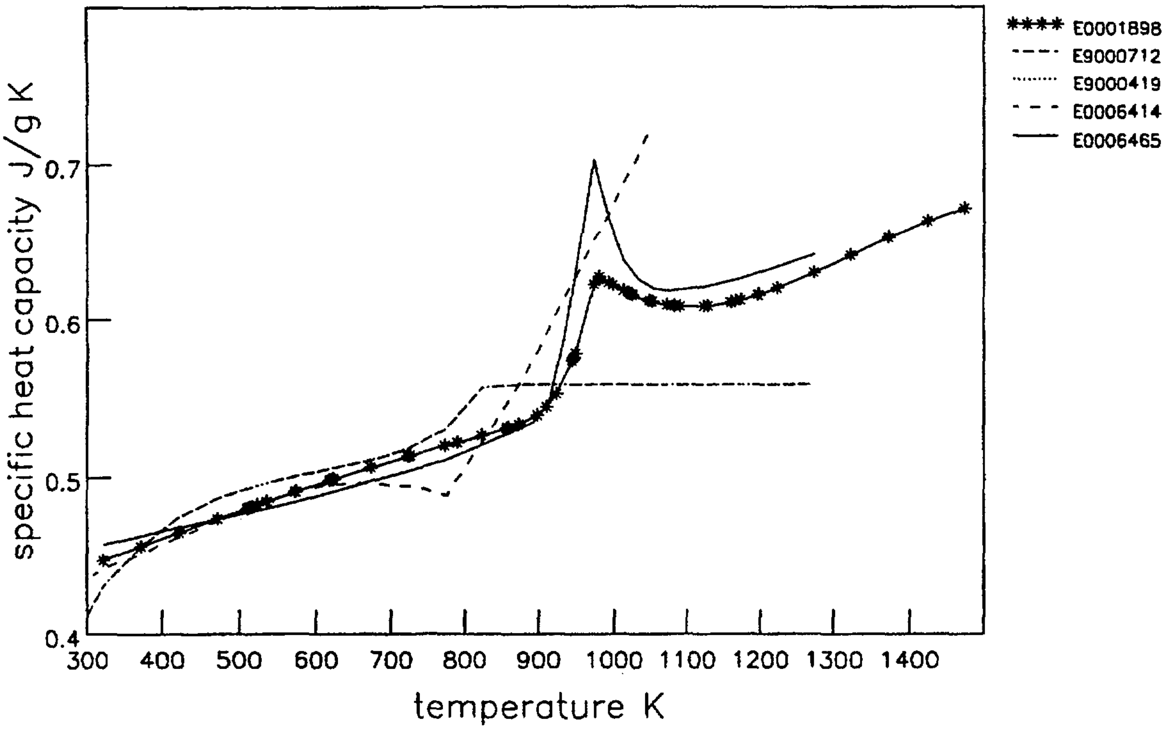

Figure 4.2.3.1 Specific heat capacity of Ni-Cr-based alloys

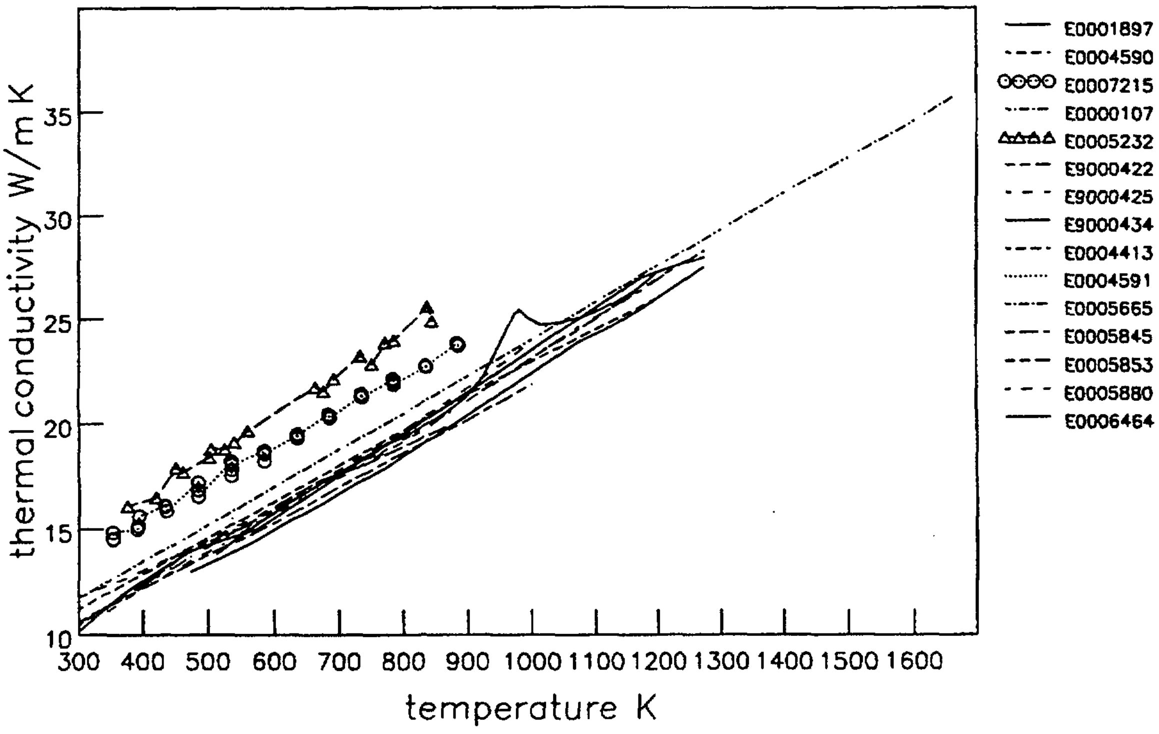

Figure 4.2.3.2 Thermal conductivity of Ni-Cr-based alloys

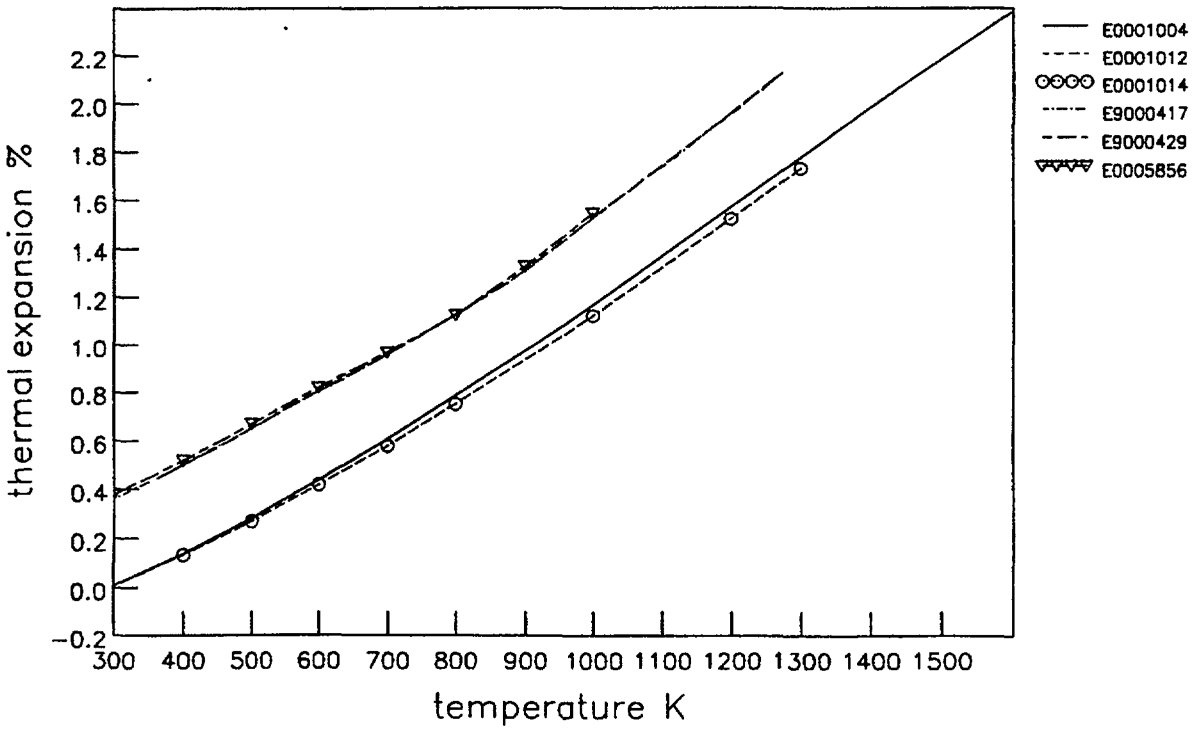

Figure 4.2.3.3 Thermal expansion of Ni-Cr-based alloys

Reference to Section 4.2.3

Note: Literature stored in THERSYST is referenced by document number, e.g. AK000021.

AK000021 RICHTER F., "Thermophysikanlische Eigenschaften des hochwarmfesten Werkstoffes NiCr22Co 12Mo (Inconel 617)", Mat.-wiss. u. Werkstofftech. 19 (1988), 55-61

AK000027 RICHTER F., BORN L., "Die spezifische Waermekapazitaet von metallischen Werkstoffen. Teil III", Z. Werkstoffterch. 17 (1986), 233-237

J0000943 MAGLIC K., PEROVIC N. L., STANIMIROVIC A., "Calorimetric and transport properties of Zircaloy 2, Zircaloy 4 and Inconel 625", Int. J. Thermophys. 15 (1994), 741-756

J0001425 TYE R. P., HAYDEN R. W., SPINNYE S. C., "The thermal conductivity of a number of alloys at elevated temperatures", High Temp. -High Pressures 4 (1972), 503-511

J0001778 FILONI L., ROCCHINI G., "Thermal conductivity of iron, plain carbon and stainless steel, and Inconel 718 from 360 K to 900 K", High Temp.-High Pressures 19 (1987), 381-387

J0001900 HUST J. G., WEITZEL D. H., POWELL R. L., "Thermal conductivity,electrical resistivity and thermopower of aerospace alloys from 4 to 300 K", J. Res. Nat. Bur. Stand 75A (1971), 269-277

J0002809 SWEET J. N., ROTH E. P., MOSS M., "Thermal conductivity of Inconel 718 and 304 stainless steel", Int. J. Thermophys. 8 (1987), 593-606

J0003001 BROOKS C. R., CASH M., GARCIA A., "The heat capacity of Inconel 718 from 313 to 1035 K", J. Nucl. Mater. 78 (1978), 419-421

J0003167 FILONI L., ROCCHINI G., "Thermal conductivity of Inconel 600 and Ti-6Al-4V from 360 K to 900 K", High Temp. -High Pressures 21 (1989), 373-376

P0000014 MCELROY D. L., WILLIAMS R. K., MOORE J. P., GRAVES R. S., WEAVER, "The physical properties of Inconel alloy 718 from 300 to 1000 K", Thermal Conductivity 15, Ed. V. V. Mirkovich, Plenum Press, New York, London (1978), 149-151

P0000041 MAGLIC K. D., PEROVIC N. L., Stanimirovic A. M., "Transport and calorimetry properties of Hastelloy X by pulse thermal diffusivity and calorimetry method", Pro c. 13th ECTP (European Conf. on Thermophysical Properties), Lisboa 1993, Ed. R. Taylor, Pion Limited, London (1993) 257-262

R0000129 EVANS J. E. Jr., "Thermal conductivity of 14 metals and alloys up to 1100 F", NACA-RM-E50L07, 1-15 (1951)

R0000141 HUST J. G., SPARKS L. L., "Thermal conductivity, electrical resistivity, and thermopower of aerospace alloys from 4 to 300 K III Annealed Inconel 718", NBS Rept. 9775, 1-35 (1970)

TPM01000 TOULOUKIAN Y. S., POWELL R. W., HO C. Y., KLEMENS P. G., "Thermophysical Properties of Matter Vol.1: Thermal Conductivity - Metallic Elements and Alloys", IFI/Plenum, New York-Washington (1970)

TPM12000 TOULOUKIAN Y. S., KIRBY R. K., TAYLOR R. E., DESAI P. D., "Thermophysical Properties of Matter. Vol. 12: Thermal Expansion - Metallic Elements and Alloys", IFI/Plenum, New York-Washington (1975)

4.2.4. Zirconium dioxide

Zirconium oxide exists in three phases: monoclinic, tetragonal and cubic. Assuming that the oxide layer on Zircaloy is slightly substoichiometric and that it may be under stress, MATPRO recommend temperatures of 1478 K and 2558 K for the monoclinic/tetragonal and tetragonal/cubic transitions, respectively.

Cordfunke and Konings [RT0000250] give transition temperatures of 1478 K, 1675 K, and 2630 K for the α (monoclinic)/β (tetragonal), β (tetragonal)/β+γ (tetragonal + cubic), and β+γ (tetragonal + cubic)/γ (cubic) transitions. They give 2983 K for the melting temperature of zirconium dioxide.

According to the HEMATIC evaluation ZrO_2 exists in the monoclinic phase below T_{ph} and as a polymorphic phase between T_{ph} and T_{melt}. The phase transition temperature T_{ph} is given as 1420 K by [1] and 1423 K by [2].

Enthalpy

The enthalpy of Zircaloy oxide was calculated by MATPRO by integrating the equations for specific heat capacity (equations 4.2.4-13 to 4.2.4-16).

For 300 K < T < 1478 K (monoclinic ZrO_2):

$$H_u = 565T + 3.055\times10^{-2}T^2 + 1.14\times10^7T^{-1} - 2.102495\times10^5 \qquad (4.2.4\text{-}1)$$

For 1478 K ≤ T ≤ 2000 K (tetragonal ZrO_2)

$$H_u = 604.5T - 1.46\times10^5 \qquad (4.2.4\text{-}2)$$

For 2000 K < T < 2558 K (tetragonal and cubic ZrO_2),

$$H_u = 171.7T + 0.1082T^2 + 2.868\times10^5 \qquad (4.2.4\text{-}3)$$

For 2558 K ≤ T < 2973 K,

$$H_u = 171.7T + 0.1082T^2 + 3.888\times10^5 \qquad (4.2.4\text{-}4)$$

For T ≥ 2973 K (liquid ZrO_2),

$$H_u = 815T + 1.39\times10^5 \qquad (4.2.4\text{-}5)$$

where H_u is the enthalpy $H(T)$ - $H(300)$ (J/kg) and T is the temperature (K). A relatively large standard error of 20% is expected. The recommended curve is presented in Figure 4.2.4.1. Table 4.2.4.1 lists the phase transitions and the transition temperature.

Cordfunke and Konings [RT0000250] recommended the following equations:

298.15 K ≤ T ≤ 1478 K

$$H_u = 69.622\ T + 3.766\times10^{-3}\ T^2 + 14.06\times10^5\ T^{-1} - 25773 \qquad (4.2.4\text{-}6)$$

1478 K < T < 1675 K

$$H_u = 74.475\ T - 17853 \tag{4.2.4-7}$$

1675 K < T < 2630 K

$$H_u = -66.530\ T + 42.07\times10^{-3}\ T^2 + 100290 \tag{4.2.4-8}$$

2630 K < T < 2983 K

$$H_u = 130.959\ T - 122047 \tag{4.2.4-9}$$

where $H_u = H(T) - H\,(298.15\ \text{K})$ is the enthalpy in J/mol, T = temperature in K.

HEMATIC propose the following relations for enthalpy:

for 300 K < T < 1400 K

$$H_u = -154.7 + 0.503T + 5.42\times10^{-5}T^2 \tag{4.2.4-10}$$

for 1400 K < T < 3000 K

$$H_u = -199.4 + 0.6T \tag{4.2.4-11}$$

for 3021 K < T < 4527 K

$$H_u = 170 + 0.818T \tag{4.2.4-12}$$

where H_u is the enthalpy $H(T)$-$H(298)$ (kJ/kg) and T is the temperature (K). The RMSE is less than 0.5%.

Specific heat capacity

Specific heat capacity data are presented in Figure 4.2.4.2. The sample density, melting temperature, heat of fusion and data sources are listed in Table 4.2.4.2.

MATPRO recommend the following expressions:

For 300 K < $T \leq$ 1478 K (monoclinic ZrO_2),

$$C_P = 565 + 6.11\times10^{-2}T - 1.14\times10^{7}T^{-2} \tag{4.2.4-13}$$

For 1478 K $\leq T \leq$ 2000 K (tetragonal ZrO_2),

$$C_P = 604.5 \tag{4.2.4-14}$$

For 2000 K < T < 2973 K (tetragonal and cubic ZrO_2),

$$C_P = 171.7 + 0.2164T \tag{4.2.4-15}$$

For $T \geq$ 2973 K (molten ZrO_2),

$$C_P = 815 \tag{4.2.4-16}$$

where C_P is the specific heat capacity (J/kg·K) and T is the temperature (K). A standard error of 20% is expected.

The expressions for the specific heat capacity can be also obtained from the recommendation of Cordfunke and Koning for the enthalpy by differentiation of equations (4.2.4-6 to 4.2.4-9).

HEMATIC propose the following relations:

For $300\ \text{K} < T \leq 1400\ \text{K}$

$$C_P = 0.503 + 10.84\times10^{-5}\,T \tag{4.2.4-17}$$

For $1400\ \text{K} < T < 3000\ \text{K}$

$$C_P = 0.6 \tag{4.2.4-18}$$

For $3000\ \text{K} < T < 4527\ \text{K}$

$$C_P = 0.818 \tag{4.2.4-19}$$

where C_P is the specific heat capacity (J/g·K) and T is the temperature (K). The root mean square error (RMSE) is less than 1%.

Thermal conductivity

The thermal conductivity data are presented in Figure 4.2.4.3. Explanations to the curves are listed in Table 4.2.4.3.

MATPRO recommend the following expressions based on the experimental data of Gilchrist [J0003084]. These data are the most representative of the oxide found on cladding.

For $300\ \text{K} < T \leq 2973\ \text{K}$

$$\lambda = 0.835 + 1.81\times10^{-4}\,T \tag{4.2.4-20}$$

For $T > 2973$ K

$$\lambda = 1.4 \tag{4.2.4-21}$$

where λ is the thermal conductivity (W/(m·K)) and T is the temperature (K). The expected standard error is 0.75.

HEMATIC proposed the following recommendation for ZrO_2 containing 13% porosity:

$$\lambda = 1.369 + 8.88\times10^{-5}\,T + 1.267\times10^{-7}\,T^2 \tag{4.2.4-22}$$

For fully dense material:

$$\lambda = 1.82 + 3.04\times10^{-4}\,T + 4.176\times10^{-8}\,T^2 \tag{4.2.4-23}$$

where λ is the thermal conductivity (W/(m·K)) and T is the temperature (K). Both relations are valid over the temperature range 300 to 2500 K. The RMSE is less than 10%.

Thermal expansion

Thermal expansion data are presented in Figure 4.2.4.4, additional information are given in Table 4.2.4.4.

MATPRO recommend the following expressions:

For 300 K < T < 1478 K (monoclinic ZrO_2),

$$\varepsilon = 7.8\times10^{-6}T - 2.34\times10^{-3} \qquad (4.2.4\text{-}24)$$

For 1478 K ≤ T < 2973 K (tetragonal and cubic ZrO_2),

$$\varepsilon = 1.302\times10^{-5}T - 3.338\times10^{-2} \qquad (4.2.4\text{-}25)$$

For $T = 2973$ K (solid to molten ZrO_2)

$$\varepsilon = -1.1\times10^{-2} \qquad (4.2.4\text{-}26)$$

where ε is the appropriate linear or volume expansion (m/m) and T is the temperature (K). The expected standard error of $\pm$ 5×10^{-3} is large (almost half the predicted value) because the equations (4.2.4-25) to (4.2.4-.26) are based on Zircaloy oxide data. Zircaloy oxide is substoichiometric and is severely stressed on cooling due to the difference in expansion between the oxide and the clad.

The thermal expansion equations can be used to calculate the density of Zircaloy oxide. MATPRO recommend the following:

$$\rho = \rho_0(1 - 3\varepsilon) \qquad (4.2.4\text{-}27)$$

where ρ is the density at a given temperature (kg/m^3), ρ_o is a density of 5800 kg/m^3 at 300 K and T is the temperature (K).

HEMATIC propose the following relation for the coefficient of thermal expansion α over the temperature range 500 to 2000 K:

$$\alpha = 5.754\times10^{-6} + 0.00239\times10^{-6}T \qquad (4.2.4\text{-}28)$$

where α is in unit of 1/K and T is in K. The RMSE is less than 15%.

Emissivity

Data on the spectral and total emissivity of ZrO_2 as a function of temperature are presented in Figure 4.2.4.5. Information on the experimental condition are given in Table 4.2.4.5.

Surface emissivities are significantly affected by oxidation of the cladding. An important parameter for these thin coatings is oxide thickness. For thin oxide coatings, the oxide may be only a few wavelengths of near infra-red radiation thick and appears partly transparent. Thick oxide layers are opaque, so thickness is less important than the nature of the outer oxide surface, which is affected by temperature and the chemical environment. MATPRO have therefore recommended several equations for the emissivity of Zircaloy cladding.

For cladding surface temperatures less than 1500 K, emissivities are modeled by equations (4.2.4-29) and (4.2.4-30). For oxide layer thickness less than 3.88×10^{-6} m,

$$\varepsilon_1 = 0.325 + 0.1246\times10^6 d \qquad (4.2.4\text{-}29)$$

For oxide layer thicknesses of 3.88×10^{-6} m or greater,

$$\varepsilon_1 = 0.808642 - 50.0d \qquad (4.2.4\text{-}30)$$

where ε_1 is the hemispherical emissivity (unitless) and d is the oxide layer thickness (m).

For cladding temperature above 1500 K, emissivity is taken to be the larger of 0.325 and

$$\varepsilon_2 = \varepsilon_1 \exp\left(\frac{1500 - T}{300}\right) \qquad (4.2.4\text{-}31)$$

where ε_1 is the value of emissivity obtained from equation (4.2.4-29) and T is the maximum cladding temperature (K).

Both equations are plotted in Figure 4.2.4.6 for temperature of 1500 K (curve E0001916) and 1673 K (curve E0001917).

The standard error expected from the use of equation (4.2.4-29) to predict emissivity in a reactor where the cladding surface temperature has never exceeded 1500 K is $\sigma_1 = \pm 0.1$.

When the cladding surface temperature has exceeded 1500 K, the expected standard error is estimated by

$$\sigma_2 = \pm\ 0.1 \exp\left(\frac{T - 1500}{300}\right) \qquad (4.2.4\text{-}32)$$

If equations (4.2.4-26) and (4.2.4-27) predict values of $\varepsilon_2 \pm \sigma_2$ that fall inside the range of physically possible values of emissivity (0.0-1.0), the value σ_2 is returned as the expected standard error. If the prediction $\varepsilon_2 + \sigma_2$ is greater than 1 or if $\varepsilon_2 - \sigma_2$ is less than 0, the standard error of equation (4.2.4-27) is modified to limit $\varepsilon_2 + \sigma_2$ at 1 and/or $\varepsilon_2 - \sigma_2$ at 0.

HEMATIC have reported the following additional data for emissivity. At a wavelength of 0.665μm the spectral emissivity of ZrO_2 given in [4] in 0.38 at 1000 K and 0.64 at 2000 K. The total emissivity [4] is 0.42 at 1000 K and 0.44 at 2000 K.

The emissivity of the zirconium dioxide used in [10] varies from 0.615 to 0.574 over the temperature range 79 to 951 K.

Nomenclature to Section 4.2.4

C_P - specific heat capacity, (J/(kg·K), other units: 1 J/(g·K) = 10^3 J/(kg·K);
H_u - enthalpy, (J/kg), other units: 1 J/g = 10^3 J/kg;
T - temperature (K);
α - thermal expansion coefficient, (1/K);
ε - thermal strain, (m/m), other unit: %
ε_1, ε_2 - emissivity, (-);
λ - thermal conductivity, (W/(m·K));
ρ - density, (kg/m^3).

Table 4.2.4.1 ENTHALPY OF ZrO_2

```
EKEY     I DEN I TRATXT    I TRAT  I TRAH  I DONO     I AU
---------I-----I-----------I-------I-------I----------I--------
E0001913 I 5.80I mono/tetr I   1478I   48.2I RT000063 I MATPRO
         I     I tertr/cub I   2558I   102.I          I
         I     I melting   I   2973I   706 I          I
E0007526 I -   I polymorph I   1423I   67.3I J0003247 I Chekhovskoi
E0003397 I -   I tetr/mono I   1420I   63.0I J0001160 I Kirillin

Units of descriptors
---------------------------------------------------------
DEN                density [g/cm^3]
TRATXT             phase transition
TRAT               temperature of phase transition [K]
TRAH               enthalpy of phase transition [J/g]
mono               monoclinic
tertr              tetragonal
cub                cubic
```

Table 4.2.4.2 SPECIFIC HEAT CAPACITY OF ZrO_2

```
  EKEY   I DEN   I TRATXT    I TRAT  I TRAH  I DONO     I AU
---------I-------I-----------I-------I-------I----------I----------
E0001912 I   5.80I mono/tetr I   1478I   48.2I RT000063 I MATPRO
         I       I tertr/cub I   2558I   102.I          I
         I       I melting   I   2973I   706 I          I
E0006382 I   5.20I           I       I       I J0000926 I Gilchrist
E0007527 I ---   I polymorph I   1423I   67.3I J0003247 I Chekhovskoi
E0007528 I ---   I           I       I       I J0003248 I Arthur

  Units of descriptors
  ---------------------------------------------------------
  DEN                density [g/cm^3]
  TRATXT             phase transition
  TRAT               temperature of phase transition [K]
  TRAH               enthalpy of phase transition [J/g]
  mono               monoclinic
  tertr              tetragonal
  cub                cubic
```

Table 4.2.4.3 THERMAL CONDUCTIVITY OF ZrO_2

EKEY	DEN	POR	LAYER	DONO	AU
E0006273	-	-	39.5	J0002988	Dua
E0006380	5.20	-	135	J0000926	Gilchrist
E0006381	5.80	-	20	J0000926	Gilchrist
E0006389	-	-	63	J0003084	Gilchrist
E0006390	-	-	50	J0003084	Gilchrist
E0006391	-	-	20	J0003084	Gilchrist
E0006392	-	-	20	J0003084	Gilchrist
E0006393	-	-	22	J0003084	Gilchrist
E0001915	5.80	-	-	RT000063	MATPRO
E0006619	4.92	20	-	J0003026	Faucher
E0006632	-	5	-	J0003027	Vishnevskii

Descriptors, units			
DEN density	(g/cm^3)	POR porosity	(%)
LAYER oxide layer thickness	(μm)		

Table 4.2.4.4 THERMAL EXPANSION OF ZrO_2

EKEY	DEN	DIR	DONO	AU
E0001359	5.890	parallel to c-axis	TPM13000	Touloukian
E0001360	5.890	parallel to a-axis	TPM13000	Touloukian
E0001361	5.890	parallel to b-axis	TPM13000	Touloukian
E0001363	5.890	polycrystalline	TPM13000	Touloukian
E0001917	5.800	polycrystalline	RT000063	MATPRO

Descriptors, unit	
DEN density	(g/cm^3)
DIR measuring direction	

Table 4.2.4.5. EMISSIVITY OF ZrO_2

EKEY	DEN	YSPEC	DONO	AU	REMARKS
E5000283	-	TOT	RT000026	MATPRO	oxide on Zircaloy
E0003766	-	TOT	J0001722	Zhorov	-
E0003767	-	TOT	J0001722	Zhorov	annealed at 1625 K
E0003768	-	TOT	J0001722	Zhorov	annealed at 1920 K
E0003795	-	TOT	R0000144	Whitson	-
E0006621	4.92	SPEL	J0003026	Faucher	-

Descriptors, units		Codes	
DEN density	(g/cm^3)	TOT	total
DEN density	(g/cm^3)	SPEL	spectral

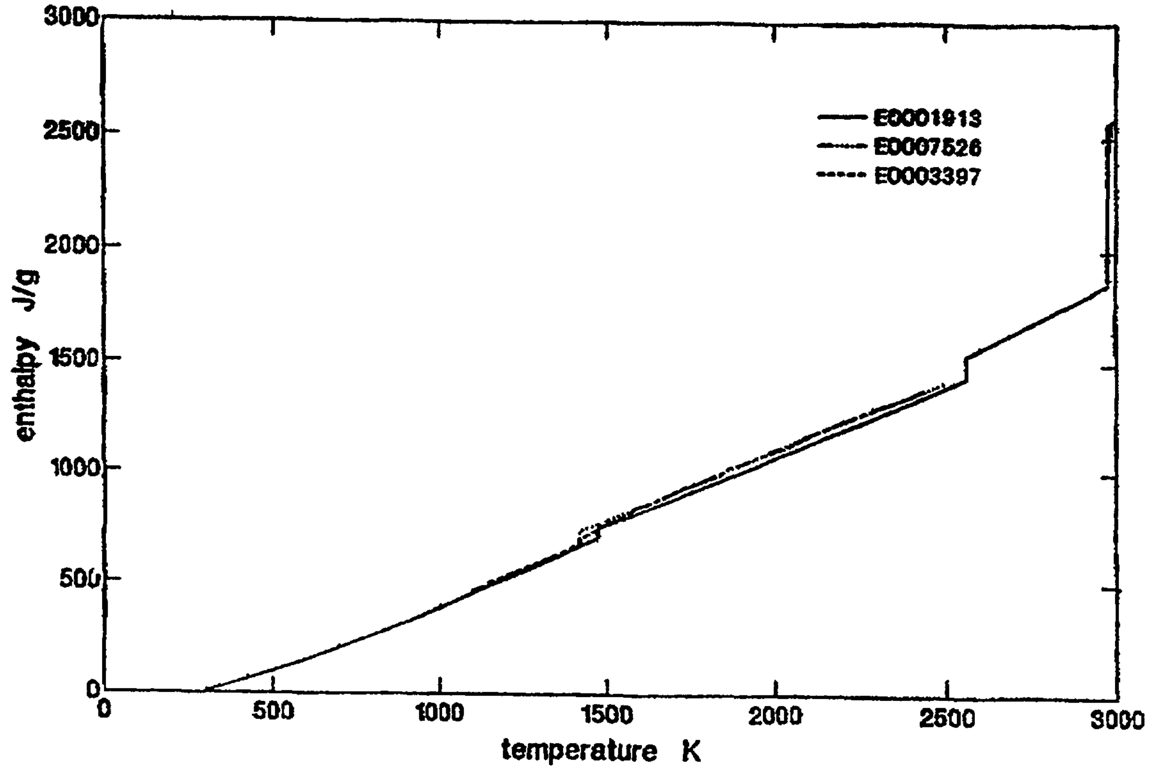

Figure 4.2.4.1 Enthalpy of ZrO_2

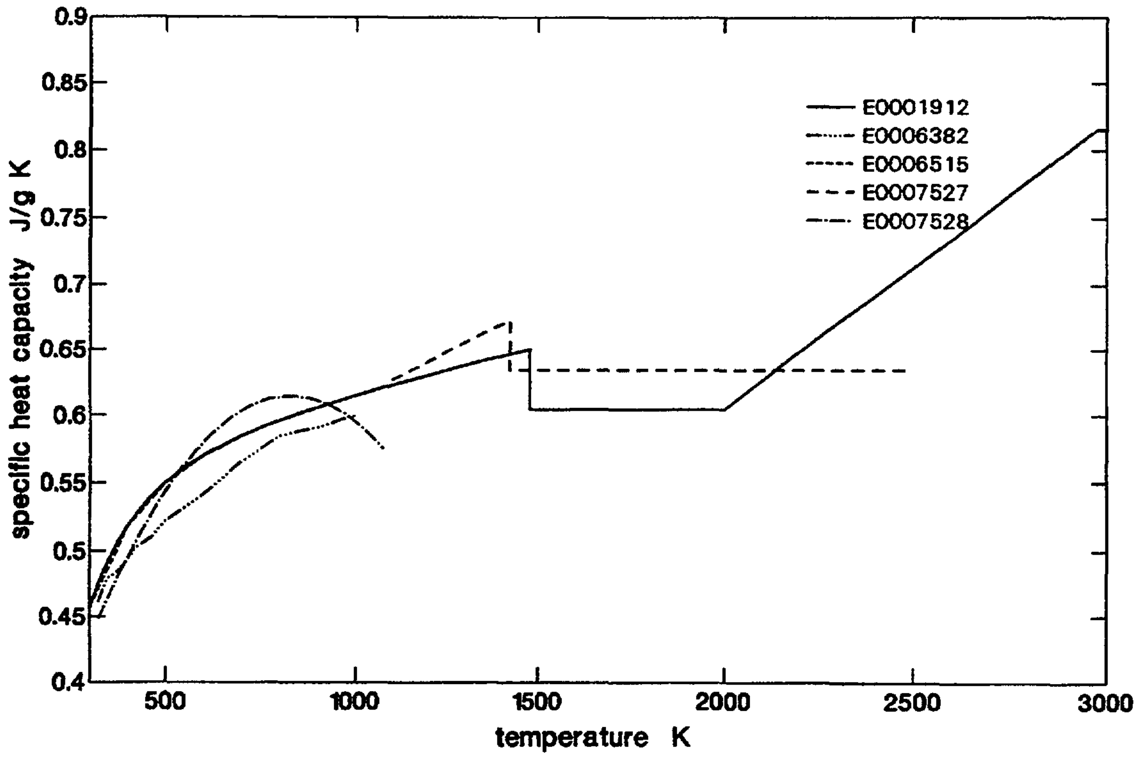

Figure 4.2.4.2 Specific heat capacity of ZrO_2

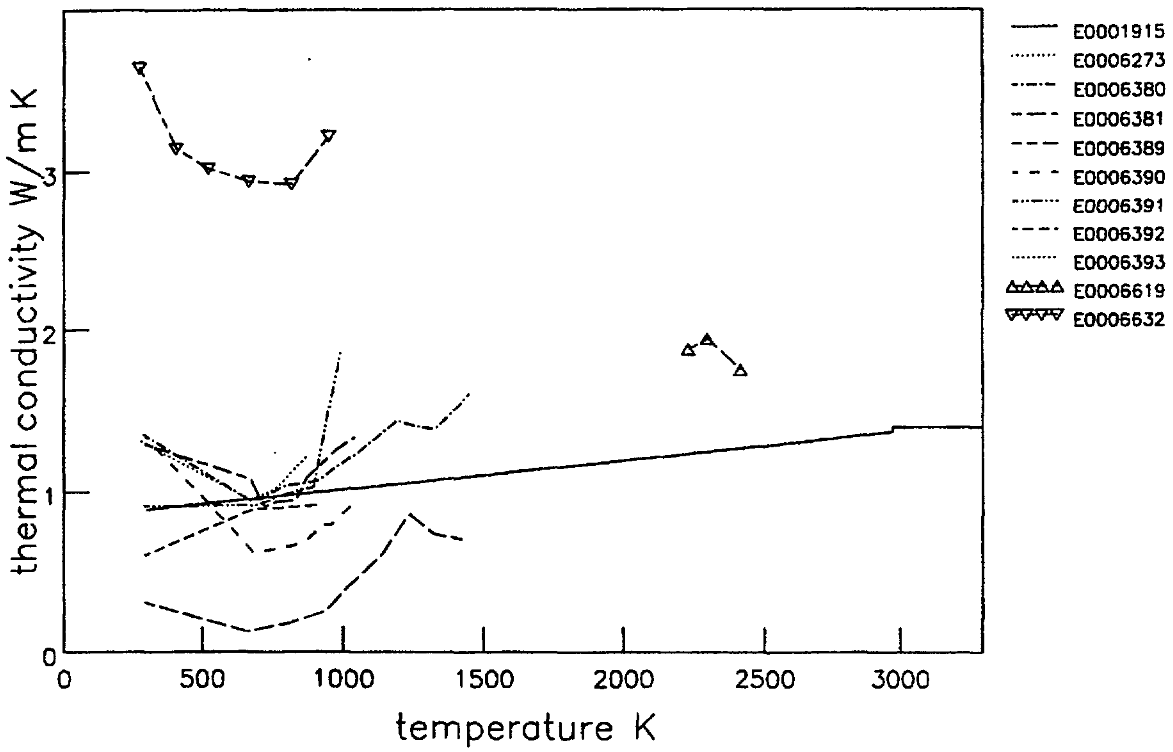

Figure 4.2.4.3 Thermal conductivity of ZrO_2

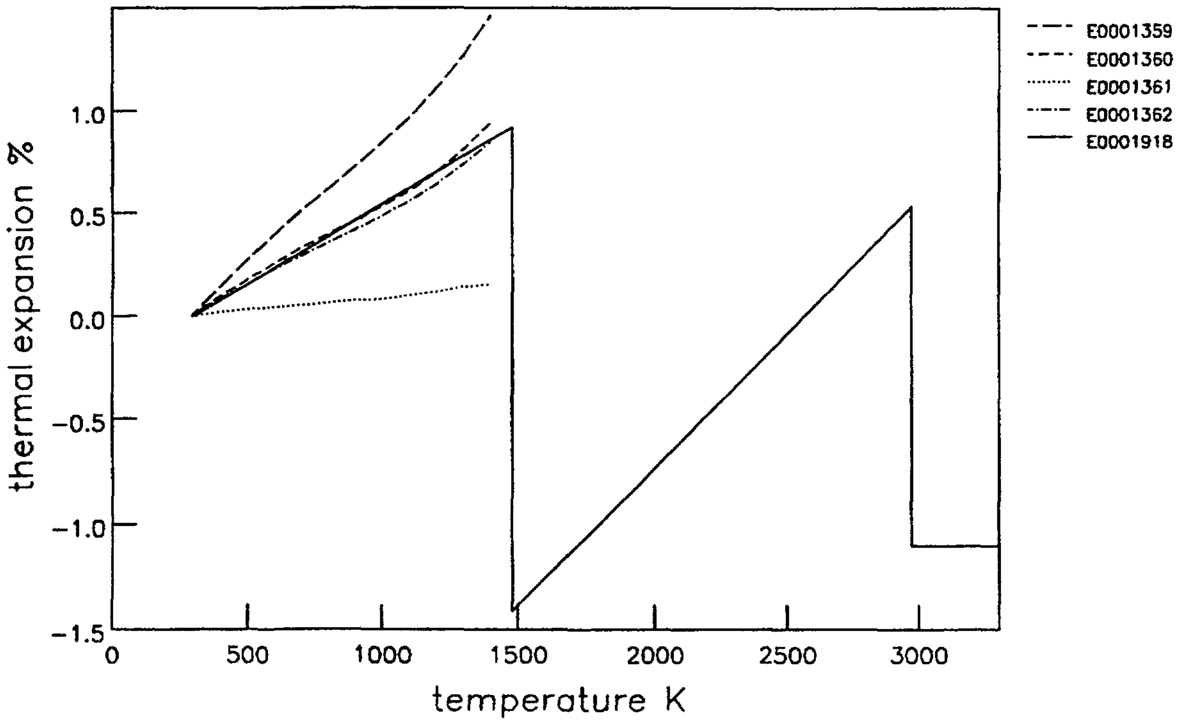

Figure 4.2.4.4 Thermal expansion of ZrO_2

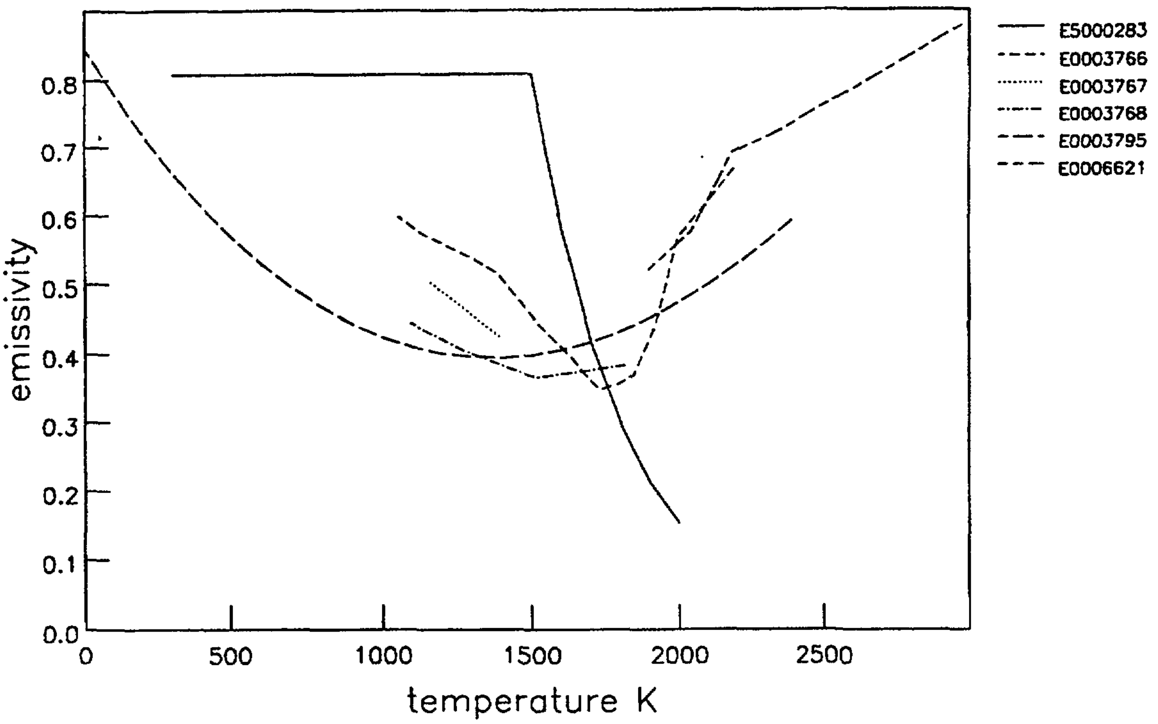

Figure 4.2.4.5 Emissivity of ZrO_2 in function of temperature

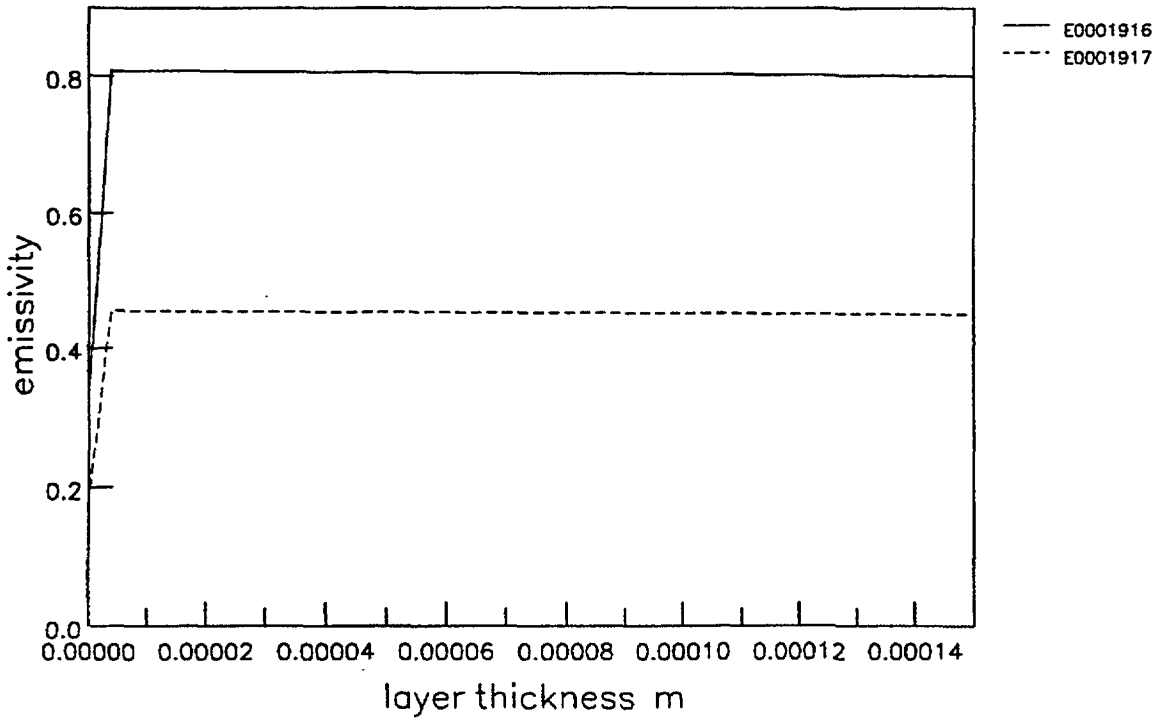

Figure 4.2.4.6 Emissivity of ZrO_2 in function of oxide layer thickness

References to Section 4.2.4

Note: literature stored in THERSYST is referenced by document number, e.g. J0000926, etc.

J0000926 GILCHRIST K. E., "Thermal property measurements on Zircaloy-2 and associated oxide layers up to 1200°C", J. Nucl. Mat. 62 (1976), 257-264

J0001160 KIRILLIN V. A., SHEINDLIN A. E., CHEKHOVSKOI V.Ya., ZHUKOVA I. A., TARASOV V. D., Tepl. Vys. Temp. 4, 878 [English Trans. High Temp. 4, 813] (1966)

J0001458 CABANNES F., "Thermal conductivity and emissivity of oxide ceramics at high temperatures", High Temp. -High Pressures 8 (1976), 155-166

J0001722 ZHOROV G. A., ZAKHAROV B. M., "Emissivity of sprayed layers of yttrium oxide and a solid solution of zirconium dioxide", High Temp. 18 (1980), 578-582

J0002988 DUA A. K., et al., "Thermal conductivity of oxide coating on Zircaloy-2", Thin Solid Films 69 (1980), L1-L3

J0003026 FAUCHER M., et al., "Arc-imaging technique for measuring high-temperature thermal conductivity and diffusivity of refractory oxides", J. Am. Ceram. Soc. 58 (1975), 368-371

J0003027 VISHNEVSKII I. I., SKRIPAK V. N., "Thermal conductivity of some oxygen compounds of zirconium and hafnium", Refractories 35 (1970), 693-694

J0003084 GILCHRIST K. E., "Thermal conductivity of oxide deposited on Zircaloy fuel tube material - a continuation of previous work", J. Nucl. Mater. 82 (1979), 193-194

R0000043 PEARS C. D., OSMENT D., Report ASD-TDR 62-765 (1963)

J0003247 CHEKHOVSKOI V.Ya., ZHUKOVA I. A., TARASOV V. D., Tepl. Vys. Temp. 17, 754 [English Trans. High Temp. 17, 637] (1979)

J0003248 ARTHUR J. S., J. Appl. Phys. 21, 732 (1950)

R0000144 WHITSON Jr. M. E., "Handbook of the infrared optical properties of Al_2O_3, carbon, MgO, and ZrO_2. Volume 1", SAMSO-TR-75-131, Vol. I

RT000063 HOHORST, J. K. (Ed.), "SCDAP/RELAP5/MOD2 Code Manual, Vol. 4: MATPRO - a library of materials' properties for light water reactor accident analysis", NUREG/CR-5273 (1990)

TPM13000 TOULOUKIAN Y. S., KIRBY R. K., TAYLOR R. E, LEE T. Y. R., "Thermophysical Properties of Matter. Vol. 13: Thermal Expansion - Nonmetallic Solids", IFI/Plenum, New York-Washington (1977)

RT0000250 CORDFUNKE E. H. P., KONINGS R. J. M., "Thermophysical data for reactor materials and fission products," North-Holland, Elsevier Science Publishers B. V., Amsterdam, The Netherlands (1990)

Literature used for evaluation by HEMATIC

[1] KIRILLIN V. A. et al., "Enthalpy and specific heat of zirconium dioxide in the temperature range of 1100 K to 2500 K", Teplofizika vysokykh temperatur (1968), v. 4, N 6, p. 878-879 (in Russian)

[2] TCHEKHOVSKOY V. Ja. et al., "Enthalpy and specific heat of zirconium dioxide in the temperature range 1100 to 2500 K", Teplofizika vysokykh temperatur (1979), t. 17, N 4, p. 754-758 (in Russian)

[3] TCHIRKIN V. S., "Thermophysical properties of materials for nuclear technology", Reference book, Atomizdat (1968), 484 p

[4] "Super refractory elements and compounds", Reference book, Metallurgia (1969), 376 p. (in Russian)

[5] "Physical-chemical properties of oxides", Reference book. Ed. G. V. SAMSONOV. M., Metallurgia (1968) (in Russian)

[6] TKATCHENKO I. G., FEN E. K., "Electrodynamic properties of transient metal oxides", Neorganitcheskie materiali (1982), v.18, N 6, p. 979-982 (in Russian)

[7] WICKS K. E., BLOCK F. E., "Thermodynamical properties of 65 elements, their oxides, halides, carbides and nitrides", Transl. from Engl., Metallurgia, 1965, 240 p.

[8] KULIKOV I. S., "Thermodynamics of oxides", Reference book, M. Metallurgia (1986), 3 44 p. (in Russian)

[9] HARGMAN D. L., "Material property models for severe core damage analysis", EGG-CD D-5801. Idaho National Engineering Laboratory (1982)

[10] GOROV G. A., "Emittancy of metals when heated in air", Teplofisika visokich temperatur, (1967), t. 5, N 3, p. 450-456

[11] COFFINBERRY A. S., MINER W. N., "The metallic plutonium", Chicago. Univ. Press. (1961), p. 387

[12] MAYER W. Z., Electrochem (1944), Bd. 50, s. 274

[13] "Physical-chemical fundamentals of ceramics", Collected articles. Ed. Budnikov P. P. Gosstrojizdat, 1956 (in Russian)

[14] SCHEIBE H., Interceram. (1965), v. 1, p. 34

[15] DOSANJH S. S., "Melt propagation in dry core debris beds", Nuclear Technology (1989), N 10, p. 30-40

[16] CURTIS C., et al., Journal of American Ceram. Soc. (1954), v.37, p. 458

[17] BELOV A. N., SEMENOV G. A., "Mass-spectrometric determination of temperature dependence of gas oxides pressures over zirconium and thorium dioxides", Journal fizitcheskoi khimii (1970), v. 53, N 12, p. 3050-3054 (in Russian)

[18] "Thermodynamical properties of individual substances", Publ. House of USSR Acad. of Sciences (1962), t. 1 (in Russian)

4.3. ABSORBER MATERIALS

4.3.1. Boron carbide

Boron carbide is used in the form of sintered ceramic pellets which are difficult to machine.

The melting point of B_4C is 2625 K - [1,2], 2740 K - [3,4], 2440 K - [5,6], 2723 K - [7,10], 2743 ± 20 K [15].

The boiling point of B_4C is 4275 K - [3,9] or 3773 K - [7,10].

Enthalpy

Data on the enthalpy of B_4C are presented in Figure 4.3.1.1 and Table 4.3.1.1 lists the melting temperature and data sources.

MATPRO recommend the integral of the specific heat capacity given in equation (4.3.1.2).

The HEMATIC Institute in Obninsk recommended the relation proposed by Sheindlin [J0003082] over the temperature range 298 K to 2700 K:

$$\begin{aligned} H_u &= -838.892 + 1.71544T + 1.95768\times10^{-4}T^2 + \frac{9.70688\times10^4}{T} \\ &\quad + 1.481136\times10^8 \exp(-\frac{33000}{T}) \end{aligned} \qquad (4.3.1\text{-}1)$$

where $H_u = H(T) - H(298)$ Is the enthalpy (kJ/kg) and T is the temperature (K).

The RMSE is less than 2.5%.

Specific heat capacity

Experimental and recommended data for the specific heat capacity of B_4C are presented in Figure 4.3.1.2. Table 4.3.1.2 lists density, melting temperature, heat of fusion and data sources.

MATPRO recommend the following relations for the specific heat:

For 300 K < T < 2700 K,

$$C_P = 563 + T(1.54 - 2.94\times10^{-4}T) \qquad (4.3.1\text{-}2)$$

For $T \geq 2700$ K,

$$C_P = 2577.740 \qquad (4.3.1\text{-}3)$$

where C_P is the specific heat (J/kg·K) and T is the temperature (K). The standard error is near 0.10.

HEMATIC recommend the relation proposed by Sheindlin [J0003082] for the temperature range 300 K to 2700 K:

$$C_P = 1.71544 + 3.992\times10^{-4}T - \frac{9.70688\times10^4}{T^2} + \frac{4.882728\times10^{12}}{T^2}\exp\left(-\frac{33000}{T}\right) \qquad (4.3.1\text{-}4)$$

The mean specific heat over the temperature range from 400 to 1500 K is given by the relation:

$$C_P = 2.485 - \frac{1058}{T-273} \log_{10} \frac{T}{273} \qquad (4.3.1\text{-}5)$$

where C_P is the specific heat capacity (kJ/(kg·K)) and T is the temperature (K). The RMSE is less than 2.5%.

Thermal conductivity

Data on the thermal conductivity of B_4C are presented in Figure 4.3.1.3. In Figure 4.3.1.4 data for irradiated B_4C with different irradiation dose and temperature are shown. The details for the curves presented are listed in Table 4.3.1.3.

The MATPRO recommendation for thermal conductivity is as follows:

For 300 K < T < 1700 K,

$$\lambda = \frac{1}{1.79\times10^{-2} + 4.98\times10^{-5}T} \qquad (4.3.1\text{-}6)$$

For $T \geq$ 1700 K,

$$\lambda = 9.750390 \qquad (4.3.1\text{-}7)$$

where λ is the thermal conductivity (W/(m·K)) and T is the temperature (K). A standard deviation of 50% is recommended because of the significant effect of density on the thermal conductivity.

HEMATIC propose the following relation for the temperature range 293 K to 973 K:

$$\lambda = 19.84 - 0.0252T + 1.19\times10^{-5}T^2 \qquad (4.3.1\text{-}8)$$

where λ is the thermal conductivity (W/(m·K)) and T is the temperature (K). The RMSE is less than 1%.

Thermal expansion

Data on the thermal expansion of B_4C are presented in Figure 4.3.1.5. Details of the curves are listed in Table 4.3.1.4.

MATPRO recommend the following relation for the thermal expansion:

For 300 K < T < 2800 K

$$\varepsilon = -1.10\times10^{-3} + T(3.09\times10^{-6} + 1.88\times10^{-9}T) \qquad (4.3.1\text{-}9)$$

where ε is the thermal expansion strain (m/m) and T is the temperature (K). The expected standard error is ± 0.2 of the predicted value.

The HEMATIC recommendation for the thermal expansion coefficient in the temperature range 293 K to 1073 K is: $\alpha = 4.5\times10^{-6}$/K [5] for formula:

$$\Delta l = l\,(1 + \alpha\,\Delta T) \qquad (4.3.1\text{-}10)$$

The density of a sintered B_4C at 293 K and 0.1 MPa is 2510-2520 kg/m^3 [5,7,10,11].

The electrical resistivity of B_4C at 293 K is 0.9 Ω·cm.

Nomenclature to Section 4.3.1

C_p - specific heat capacity, (J/(kg·K), other units: 1 J/(g·K) = 10^3 J/(kg·K);
H_u - enthalpy, (J/kg), other units: 1 kJ/kg = 10^3 J/kg,
1 J/g = 10^3 J/kg;
T - temperature (K);
α - thermal expansion coefficient, (1/K);
ε - thermal strain, (m/m), other unit: %;
λ - thermal conductivity, (W/(m·K)).

Table 4.3.1.1 B_4C ENTHALPY

EKEY	MELTT	MELTH	DEN	DONO	AU
E0006260	2713	-	2.50	J0003082	Sheindlin
E0006265	-	-	-	R0000147	Gibby
E0006266	-	-	-	R0000147	Gibby
E0006471	2743	274	2.50	RT000063	MATPRO

Descriptors, unit			
MELTT melting temperature	(K)	DEN density	(g/cm^3)
MELTH enthalpy of fusion	(J/g)		

Table 4.3.1.2 B_4C SPECIFIC HEAT CAPACITY

EKEY	MELTT	MELTH	DEN	DONO	AU
E0001906	2743	274	2.50	RT000063	MATPRO
E0003098	-	-	2.44	J0000093	Wood
E0003099	-	-	2.38	J0000093	Wood
E0003100	-	-	2.48	J0000093	Wood
E0003101	-	-	2.43	J0000093	Wood
E0006261	2713	-	-	J0003082	Sheindlin
E0006267	-	-	-	R0000147	Gibby
E0006268	-	-	-	R0000147	Gibby
E0006408	-	-	-	J0003086	Gilchrist
E0006427	-	-	-	P0000050	Tuerkes

Descriptors, unit			
MELTT melting temperature	(K)	DEN density	(g/cm^3)
MELTH heat of fusion	(J/g)		

Table 4.3.1.3 B_4C THERMAL CONDUCTIVITY

EKEY	DEN	POR	TREATI	TRIDOS	TRITEM	DONO	AU
E0001907	2.50	-		-	-	RT000063	MATPRO
E0006386	2.40	-		-	-	J0003088	Bairamashvili
E0006394	1.85	26.6	UNTR	-	-	J0003086	Gilchrist
E0006395	2.24	11.0	UNTR	-	-	J0003086	Gilchrist
E0006396	2.44	11.0	UNTR	-	-	J0003086	"
E0006397	-	-	NEUT	0.4E21	873.2	J0003086	"
E0006398	-	-	NEUT	0.4E21	1043	J0003086	"
E0006399	-	-	NEUT	0.7E21	1053	J0003086	"
E0006400	-	-	NEUT	0.7E21	1053	J0003086	"
E0006401	-	-	NEUT	0.7E21	893.2	J0003086	"
E0006402	-	-	NEUT	0.7E21	893.2	J0003086	"
E0006403	-	-	NEUT	0.218E22	873.2	J0003086	"
E0006404	-	-	NEUT	0.128E22	873.2	J0003086	"
E0006405	-	-	NEUT	0.212E22	873.2	J0003086	"
E0006406	-	-	NEUT	0.390E22	823.2	J0003086	"
E0006407	2.20	-		-	-	J0003086	"
E0006417	1.66	34.0		-	-	P0000051	Moss
E000418	2.03	18.0		-	-	P0000051	Moss
E0006419	2.52	0.0		-	-	P0000051	Moss
E0006428	-	-		-	-	P0000050	Tuerkes
E0006429	-	-		-	-	P0000050	Tuerkes
E0006430	-	-		-	-	P0000050	Tuerkes

Descriptors, units		Codes	
DEN	density (g/cm^3)	UNTR	untreated
POR	porosity (%)	NEUT	neutron irradiation
TRIDOS	irradiation dose (Bq)		
TRITEM	irradiation temperature (K)		

Table 4.3.1.4 B_4C THERMAL EXPANSION

EKEY	DIR	VAL	DONO	AU
E0001538	polycrystalline	TPRC	TPM13000	Touloukian
E0001908	polycrystalline	RECO	RT000063	MATPRO
E0006262	polycrystalline		J0003083	Preston
E0006416	parallel to deposition		B0000025	Neshpor
E0006424	perpendicular to c-axis		J0003085	Tsagareish
E0006425	parallel to c-axis		J0003085	Tsagareish

	Codes	
	TPRC	TPRC recommended data
	RECO	recommended data
	DIR	measuring direction
	VAL	valuation of data

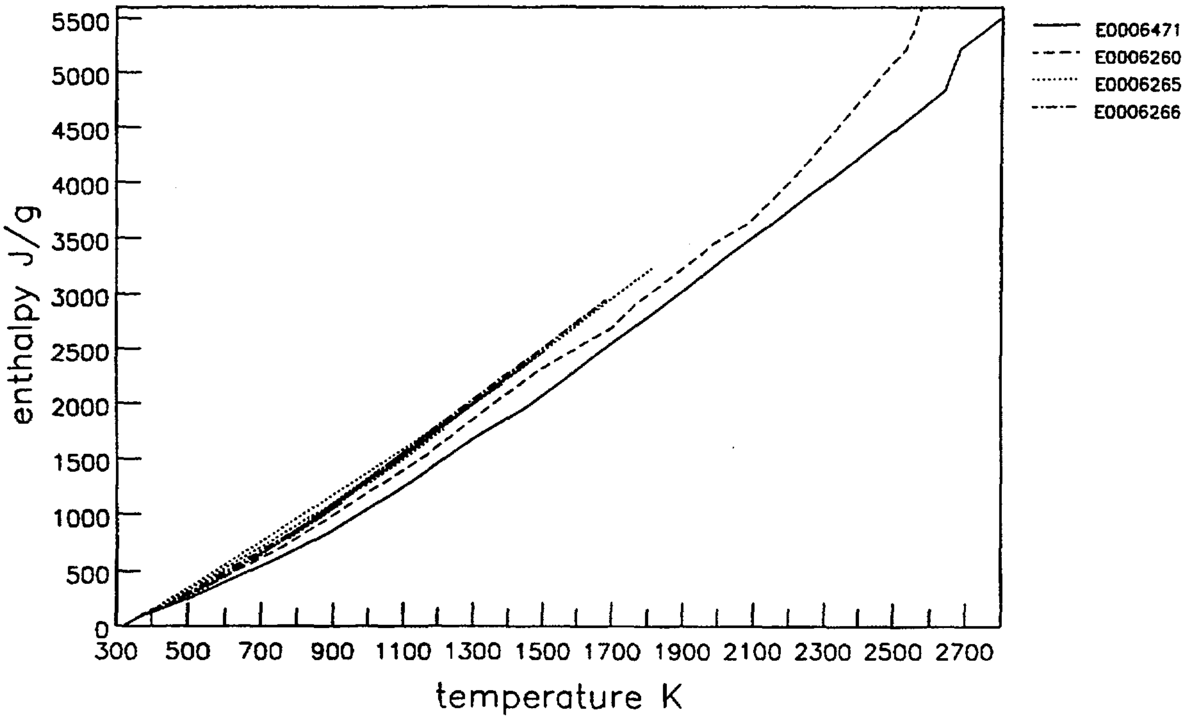

Figure 4.3.1.1 Enthalpy of B_4C

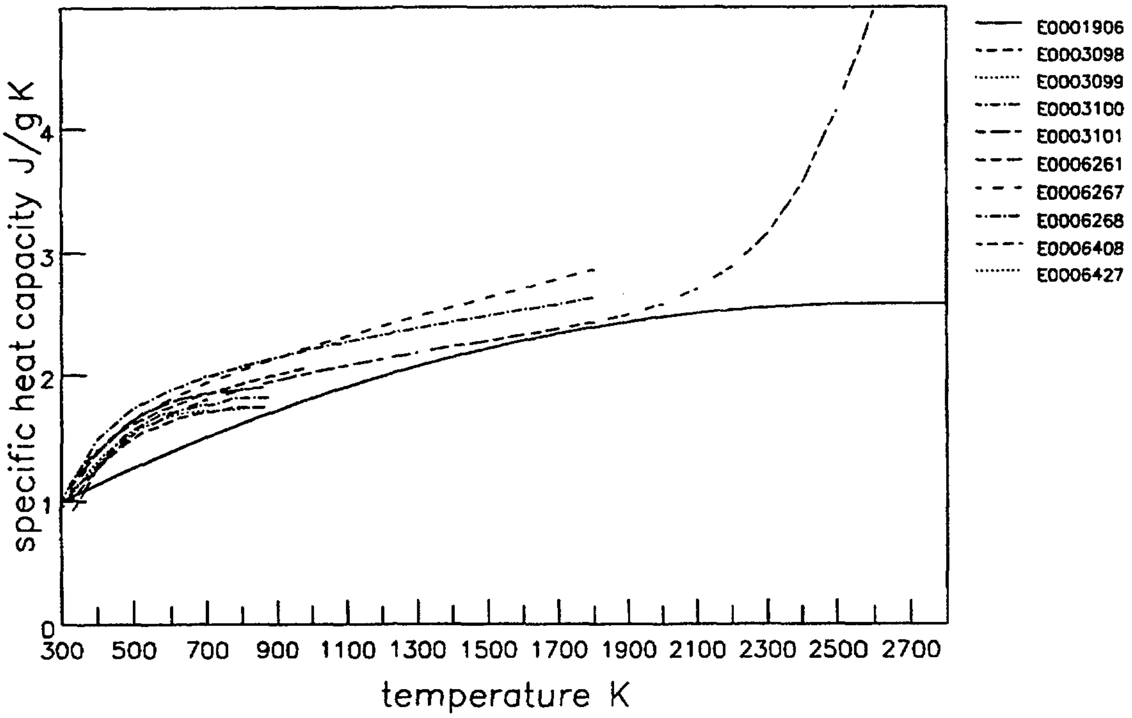

Figure 4.3.1.2 Specific heat capacity of B_4C

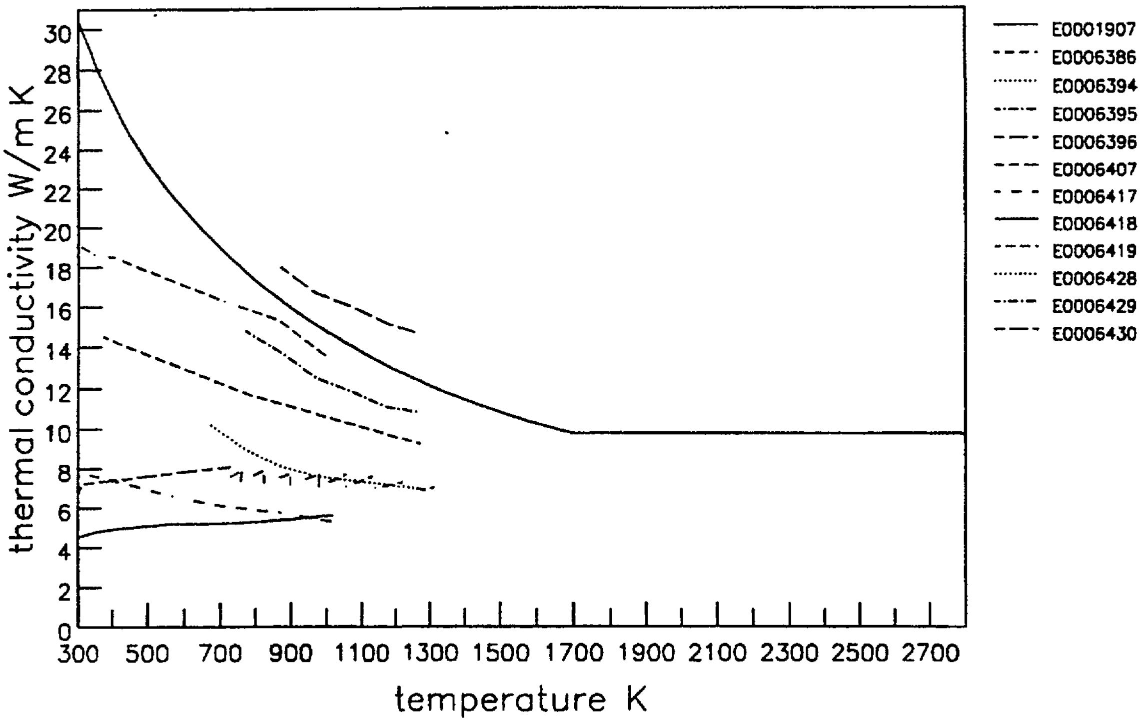

Figure 4.3.1.3 Thermal conductivity of B_4C

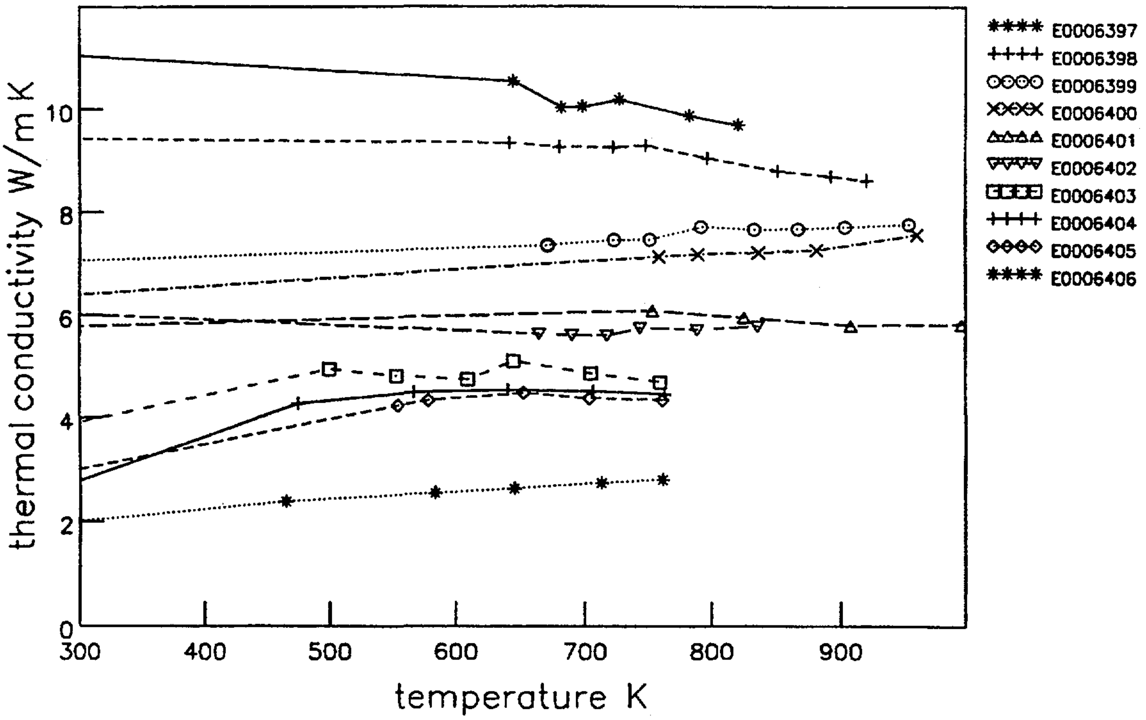

Figure 4.3.1.4 Thermal conductivity of irradiated B_4C

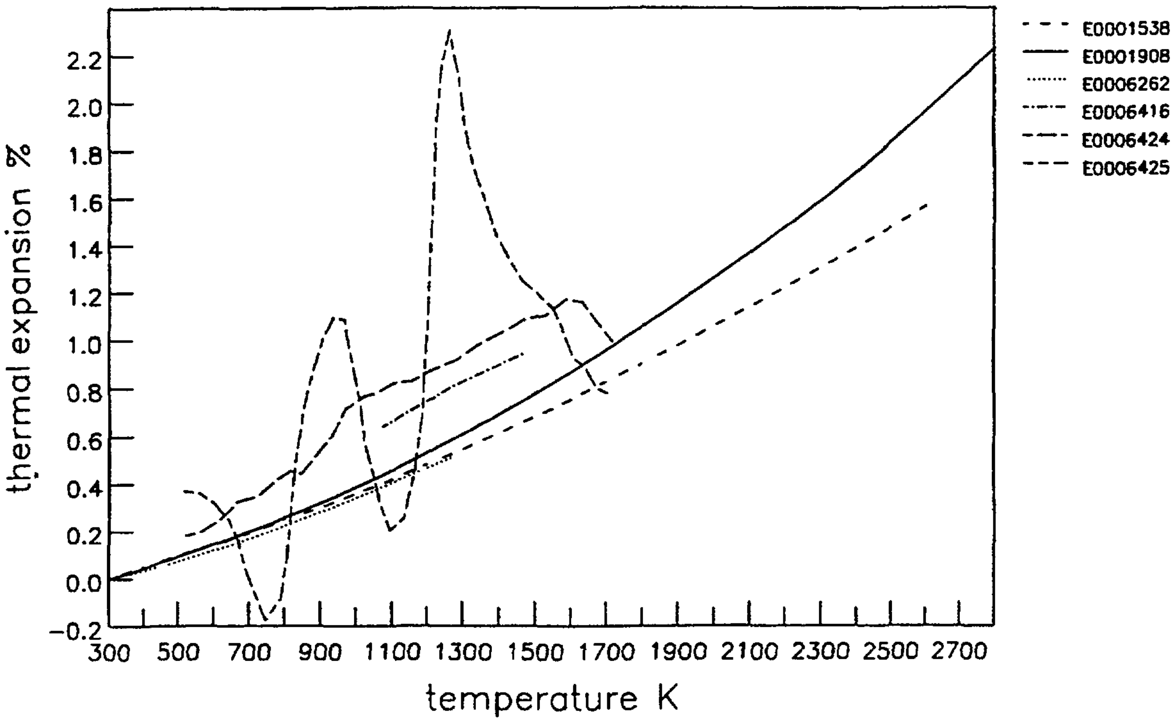

Figure 4.3.1.5 Thermal expansion of B_4C

References to Section 4.3.1

Note: literature stored in THERSYST is referenced by document number, e.g. B0000025, etc.

B0000025 NESHPOR V. S., et al., "Some physical properties of pyrolytic boron carbide", Refractory carbides; Ed. Samson, New York (1974) p. 221-229

J0000093 WOOD C., EMIN D., GRAY P. E., "Thermal conductivity of boron carbide", Phys. Rev. B 31 (1985), 6811-6814

J0003082 SHEINDLIN A. E., et al., "Enthalpy and heat capacity of boron carbide in the temperature range 273-2600 K", High Temp. 10 (1972), 369-371

J0003083 PRESTON S. D., "Thermal expansion measurements on boron carbide and europium sesquioxide by laser interferometry", High Temp. -High Pressures 12 (1980), p. 441-446

J0003085 TSAGAREISHVILI G. V., et al., "Thermal expansion of boron and boron carbide", J. Less-Common Metals 117 (1986)

J0003086 GILCHRIST K. E., "The thermal conductivity of boron carbide after fast neutron irradiation", High Temp. -High Pressures 17 (1985), p. 671-681

J0003088 BAIRAMASHVILI I. A., KALANDADZE, CHOTULIDI V. V., "An investigation of the physicomechanical properties of B_6O and SiB_4", J. Less-Common Metals 67 (1979)

P0000050 TUERKES P. R. H., et al., "Thermal properties of boron and boron carbides", Proc. Int. Conf. Phys. & Chem. of Boron Carbides Albuquerque (1985); AIP Conf. Proc.

P0000051 MOSS M., "Thermal conductivity of boron carbides", Proc. Symp. Mat. Res. Soc. vol. 97 (1987), p. 77-82

R0000147 GIBBY R. L., "Thermal properties of B_4C and Eu_2O_3", HEDL-TME 75-104 (1975), p. 1-21

RT000063 HOHORST J. K. (Editor), "SCDAP/RELAP5/MOD2 Code Manual, vol. 4: MATPRO-a library of materials properties for light-water-reactor accident analysis", NUREG/CR-5273 (1990)

TPM13000 TOULOUKIAN Y. S., KIRBY R. K., TAYLOR R. E, LEE T. Y. R, "Thermophysical Properties of Matter. Vol. 13: Thermal Expansion - Nonmetallic Solids", IFI/Plenum, New York-Washington.

Additional literature evaluated at HEMATIC

[1] WICKS C. E., BLOCK F. E., "Thermodynamic properties of 65 elements - their oxides, halides, carbides and nitrides", US Dep. of the Interior. Translation into Russian, Metallurgy (1965)

[2] BREWER L., BROMLEY L. A., GILLES P. W., LOFGREN N. L., "Thermodynamic and physical properties of nitrides, carbides, sulphides, silicates and phosphide", Paper 4 in National Nuclear Energy Series IV, Vol. 19B, Chemistry and Metallurgy of Miscellaneous Materials: Thermodynamics, by L. L. Quill. McGraw-Hill Book Co., Inc., New York (1950)

[3] KULIKOV I. S., "Thermodynamics of carbides and nitrides", Reference book, Tcheljabinsk, Metallurgy (1988) (in Russian)

[4] "Janaf Thermochemical Tables", Washington, C. -ov. Print off (1951), VIX, N24/US National Bur. Stand., Ed. Stull D. R

[5] SAMSONOV G. V., SEREBRJAKOVA T. I., HERONOV V. A., "Borids", Atomizdat (1975) (in Russian)

[6] SCHEINDLIN A. E., BELEVITCH I. S., KOZEVNIKOV I. G., "Enthalpy and specific heat of boron carbide in temperature interval from 273 to 2600 K", Teplofizika vysokikh temperatur (1972), vol. 10, #2, pp. 421-423 (in Russian)

[7] "Neutron absorber materials for reactor control", Ed. by W. Kermit Anderson and J. S. Theilacker, Naval Reactor Div. of reactor Development US Atomic Energy Commission, 1962, - cited in Russian translation, Atomizdat (1965)

[8] "Thermodynamic properties of individual substances", Vol. 3, Book 2, Nauka (1981) (in Russian)

[9] "Periodic Table of elements", USA, NSRDS, Sargent-Welch Scientific Company, Illinois (1980)

[10] "A handbook on boron carbide, elemental boron and other stable boron rich materials", Worcester, Mass., North. (1955)

[11] JERMEN J., "Heterogeneous catalysis", (translated to Russian), Inostrannaja literatura (1961)

[12] ELLIOTT B. P., "Constitution of binary alloys", (first supplement), McGraw Hill, NY Translated to Russian, Metallurgy (1970)

[13] SAMSONOV G. V., MARKOVSKI L. JA., JIGATCH A. F., VALJASCHKO M. G., "Boron, its compounds and alloys", Kiev, Publ. House of Ukrainian Academy of Sc. (1960) (in Russian)

[14] SAMSONOV G. V., PODTCHERNJAEVA I. A., FOMENKO V. S, "Emissivity coefficient of refractory compounds", Poroschkovaja metallurgija (1969), 5, p. 43-50 (in Russian)

[15] CHASE M., et al., Third edition of the JANAF Thermochemical Tables, Journal of Physical and Chemical Reference Data Volume 14, Supplement 1 (1985), American Chemical Society and the American Institute of Physics (1986)

4.3.2. Silver-indium-cadmium alloy

No experimental data exist on silver-indium-cadmium alloy, which is used as a control rod neutron absorber. Its chemical composition is: Ag-80, In-15, Cd-5 wt.%. MATPRO has prepared a set of properties for this alloy which allows the modelling of its flow and freezing during a severe core disruption. The melting range of the alloy is 1073 to 1123 K. Density at 300 K is assumed to be 10.17 g·cm^{-3}.

The expressions used for the **specific heat capacity** of Ag-In-Cd are atomic fraction weighted averages of the specific heat capacities of silver, indium, and cadmium

$$C_P = \frac{0.808\,C_{Pm_{Ag}} + 0.143\,C_{Pm_{In}} + 0.0049\,C_{Pm_{Cd}}}{0.109\,kg/mole\ alloy} \tag{4.3.2-1}$$

where C_P is the specific heat capacity of the alloy (J/(kg·K)),
C_{PmAg} is the molar heat capacity of silver (J/(mol·K)),
C_{PmIn} is the molar heat capacity of indium (J/(mol·K)),
C_{PmCd} is the molar heat capacity of cadmium (J/(mol·K))

The molar specific heat capacity of each element can be calculated up to 1073 K using the relation:

$$C_{Pm} = a + b{\times}10^{-3}T + d{\times}10^{5}T^{-2} \tag{4.3.2-2}$$

where C_{Pm} is the molar heat capacity (J/(mol·K)), and T is the temperature (K) and the constants a, b, and d are listed in Table 4.3.2.1. Above 1073 K, C_P is assumed to remain constant. A standard error of 10% of the calculated value is predicted.

Table 4.3.2.1 MOLAR HEAT CAPACITY CONSTANTS FOR EQUATION (4.3.2-2)

Metal	a J/(mol·K)	b J/(mol·K^2)	d J·K/mol
Silver	21.3	4.27	1.51
Indium	24.3	10.5	0
Cadmium	22.2	12.3	0

The following expressions are recommended for the **thermal conductivity**.

For 300 K ≤ T < 1073 K

$$\lambda = 2.805{\times}10^{1} + T(1.101{\times}10^{-1} - 4.436{\times}10^{-5}T) \tag{4.3.2-3}$$

For 1073 K ≤ T < 1123 K

$$\lambda = 1.119736{\times}10^{3} - 0.954592\,T \tag{4.3.2-4}$$

For T ≥ 1123 K

$$\lambda = 47.730 \tag{4.3.2-5}$$

where λ is the thermal conductivity (W/(m·K)) and T is the temperature (K). An expected standard error of 0.20 is recommended.

The **thermal expansion** of the Ag-In-Cd alloy can be calculated using following expressions:

For 300 K $\leq T <$ 1073 K

$$\varepsilon = 2.25\times10^{-5}(T - 300) \qquad (4.3.2\text{-}6)$$

For 1079 K $\leq T <$ 1123 K

$$\varepsilon = 0.25875 + 2.625\times10^{-4}T \qquad (4.3.2\text{-}7)$$

For $T \geq$ 1123 K

$$\varepsilon = 3.0\times10^{-2} \qquad (4.3.2\text{-}8)$$

where ε is the thermal expansion strain (m/m) and T is the temperature (K). The expected standard error of equations (4.3.2.6) to (4.3.2.8) is ± 0.10.

The recommended curves are presented at Figure 4.3.2.1 to Figure 4.3.2.3.

Nomenclature to Section 4.3.2

C_P - specific heat capacity, (J/(kg·K), other units: 1 J/(g·K) = 10^3 J/(kg·K);
T - temperature (K);
ε - thermal strain, (m/m), other unit: %
λ - thermal conductivity, (W/(m·K)).

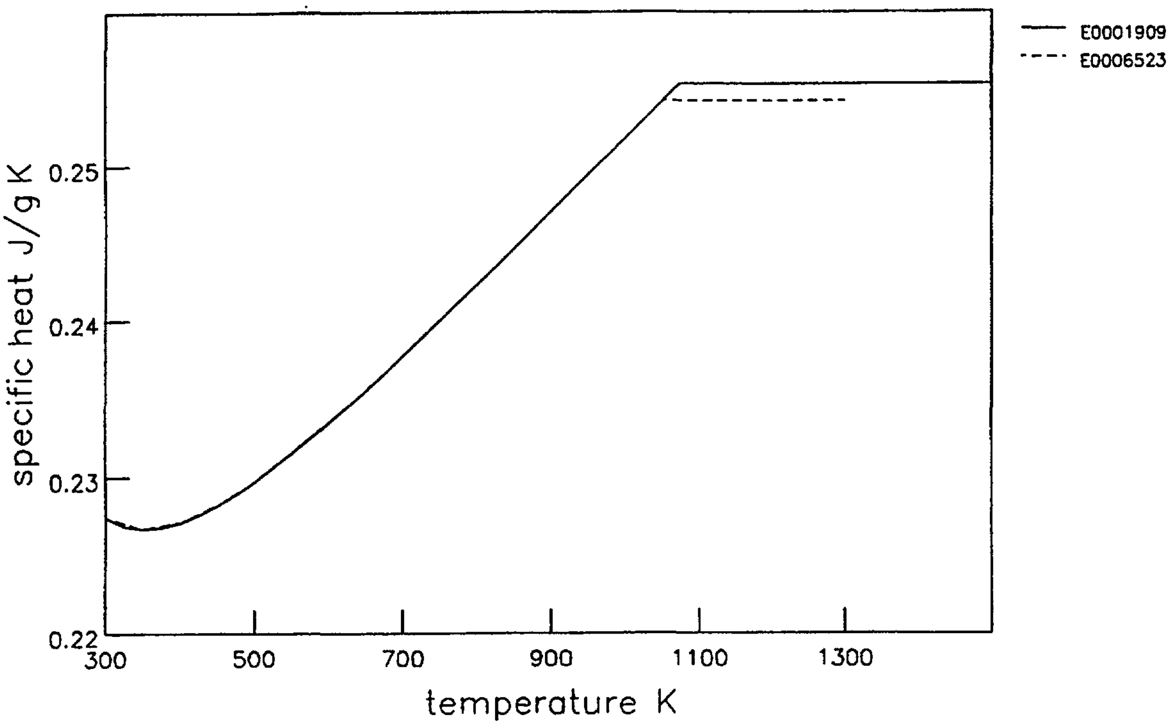

Figure 4.3.2.1 Specific heat of Ag-In-Cd alloy

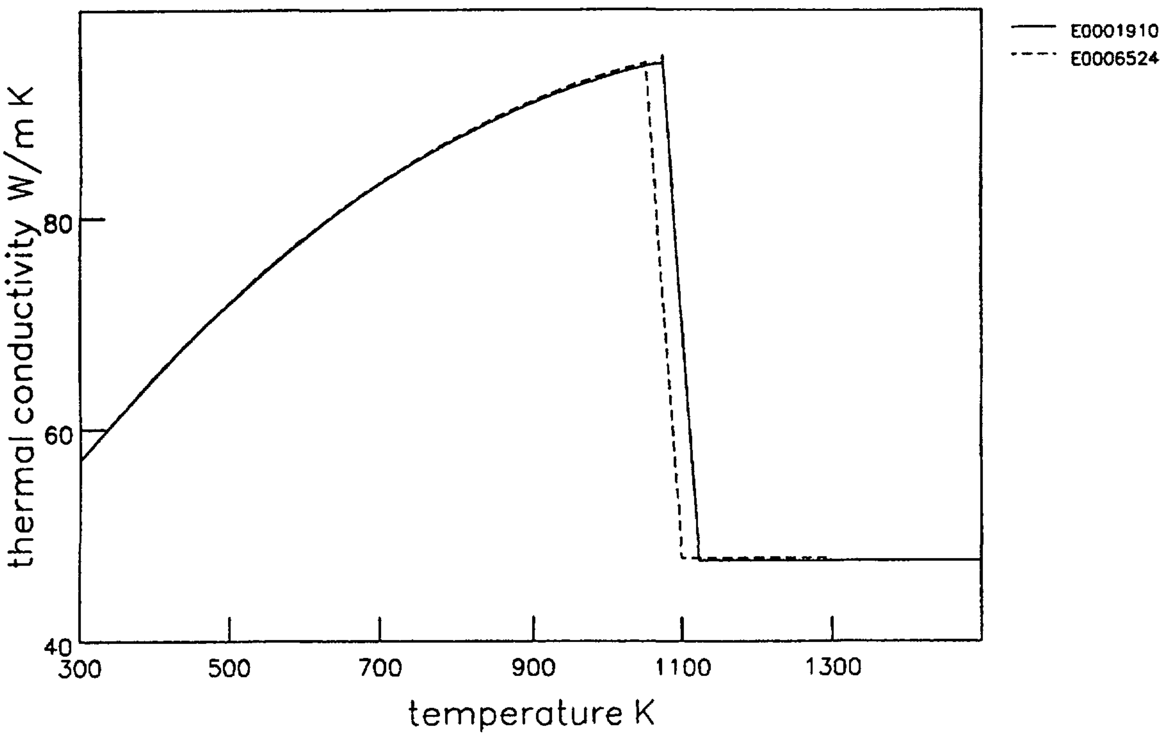

Figure 4.3.2.2 Thermal conductivity of Ag-In-Cd alloy

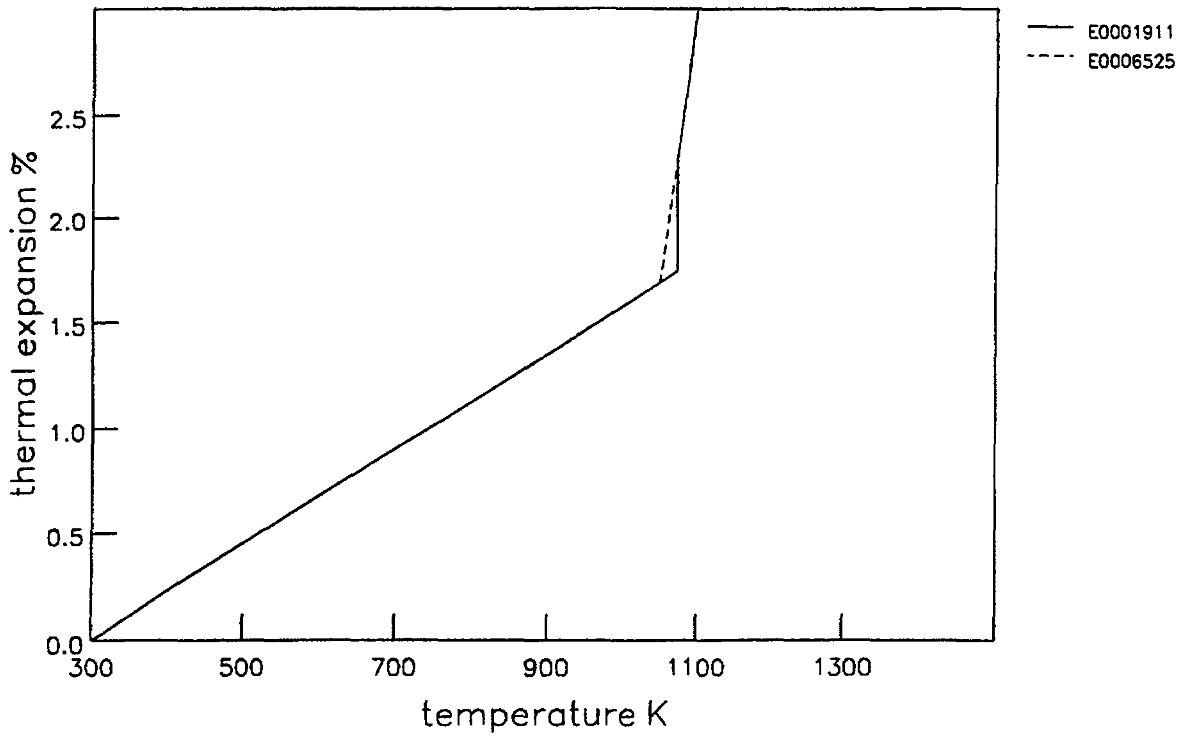

Figure 4.3.2.3 Thermal expansion of Ag-In-Cd alloy

References to Section 4.3.2

RT000063 HOHORST J. K. (Editor), "SCDAP/RELAP5/MOD2 Code Manual, vol. 4: MATPRO-a library of materials properties for light-water-reactor accident analysis", NUREG/CR-5273 (1990)

4.4. STRUCTURAL MATERIALS

4.4.1. Austenitic stainless steel

The following austenitic stainless steels are used in the nuclear power industry:

AISI 304	(1.4301)
AISI 316	(1.4401/1.4436)
AISI 347	(1.4550)
X 10 NiCrMoTiB 15 15	(1.4970)

Numbers in parenthesis are the German standard No. (Source: C.W. Wegst "Stahlschlüssel" Hersg. Verlag Stahlschlüssel Wegst GmbH, Marbaer, 1986).

Steel AISI 304

In MATPRO the recommendations for the thermophysical properties of AISI 304 steel are given as follows:

Enthalpy, H_u (J/kg) reference temperature 300 K:

for $300\ \text{K} < T \leq 1558\ \text{K}$

$$H_u = 326T + 0.149T^2 - 3.187\times10^{-5}T^3 \tag{4.4.1-1}$$

for $1558\ \text{K} < T < 1671\ \text{K}$

$$H_u = -1.206610\times10^5 + 558.228T \tag{4.4.1-2}$$

for $1671\ \text{K} \leq T \leq 1727\ \text{K}$

$$H_u = -8.475661\times10^6 + 558.228T \tag{4.4.1-3}$$

for $T > 1727\ \text{K}$

$$H_u = 1.593390\times10^5 + 558.228T \tag{4.4.1-4}$$

Specific heat capacity, C_P (J/(kg·K))

for $300 \leq T < 1558\ \text{K}$

$$C_P = 326 + 0.298T - 9.56\times10^{-5}T^2 \tag{4.4.1-5}$$

for $T \geq 1558\ \text{K}$

$$C_P = 558.228 \tag{4.4.1-6}$$

Thermal conductivity, λ (W/(m·K))

for $300\ \text{K} \leq T < 1671\ \text{K}$

$$\lambda = 7.58 + 0.0189T \tag{4.4.1-7}$$

for 1671 K $\le T <$ 1727 K

$$\lambda = 610.9393 - 0.3421767T \tag{4.4.1-8}$$

for $T \ge$ 1727 K

$$\lambda = 20 \tag{4.4.1-9}$$

Thermal expansion, given by thermal strain ε (m/m):

for 300 K $\le T <$ 1671 K

$$\varepsilon = 1.57\times10^{-5}T + 1.69\times10^{-9}T^2 \tag{4.4.1-10}$$

for 1671 K $\le T <$ 1727 K

$$\varepsilon = -2.986634\times10^{-1} + 1.972573\times10^{-4}T \tag{4.4.1-11}$$

for $T \ge$ 1727 K

$$\varepsilon = 4.2\times10^{-2} \tag{4.4.1-12}$$

Steel AISI 316

Harding worked out the recommendations for AISI 316 steel [RT000062].

Enthalpy, H_u (J/kg) reference temperature 298.15 K:

for 300 K $< T \le$ 1683 K

$$H_u = -1.285\times10^5 + 407.8T + 0.1055T^2 \tag{4.4.1-13}$$

Specific heat, C_P (J/(g·K))

for 300 K $< T \le$ 1683 K

$$C_P = 0.4078 + 0.2111\times10^{-3}T \tag{4.4.1-14}$$

for $T >$ 1683 K

$$C_P = 0.76 \tag{4.4.1-15}$$

Thermal conductivity, λ (W/(m·K)):

for 300 K $< T \le$ 1683 K

$$\lambda = 9.735 + 0.01434T \tag{4.4.1-16}$$

for 1683 K $< T <$ 2073 K (liquid)

$$\lambda = 10.981 + 0.003214T \tag{4.4.1-17}$$

The upper limit of λ in the liquid state is given by:

$$\lambda = 9.567 + 0.008891\,T \qquad (4.4.1\text{-}18)$$

the lower limit of λ in the liquid state is given by:

$$\lambda = 11.362 + 0.000355\,T \qquad (4.4.1\text{-}19)$$

Thermal expansion, given by the mean linear expansion coefficient α (1/K):

for $293\ \mathrm{K} < T \leq 1683\ \mathrm{K}$

$$\alpha = 1.417\times10^{-5} + 4.381\times10^{-9}\,T \qquad (4.4.1\text{-}20)$$

The data on austenitic steels collected in THERSYST are represented in Figures 4.4.1.1 to 4.4.1.5. The data sources and the densities are given in Tables 4.4.1.1 to 4.4.1.5.

Nomenclature to Section 4.4.1

C_p - specific heat capacity, (J/(kg·K), other units: 1 J/(g·K) = 10^3 J/(kg·K);
H_u - enthalpy, (J/kg), other units: 1 J/g = 10^3 J/kg;
T - temperature (K);
α - thermal expansion coefficient, (1/K);
ε - thermal strain, (m/m), other unit: %
λ - thermal conductivity, (W/(m·K)).

Table 4.4.1.1 ENTHALPY OF AUSTENITIC STEELS

EKEY	MNAM	TRATXT	TRAT	DONO	AU
E0007364	AISI 316	solidus	1683	RT000062	Harding
		liquidus	1708		
E0007336	AISI 304	solidus	1671	RT000063	MATPRO
		liquidus	1727		

Descriptors, Units	
TRATXT Phase transition	
TRAT transition temperature (K)	

Table 4.4.1.2 SPECIFIC HEAT OF AUSTENITIC STEELS

EKEY	MNAM	DEN	MELTH	DONO	AU
E0007363	AISI 316	7.96	-	RT000062	Harding
E0004744	AISI 304	7.90	-	TPSAM002	Touloukian
E0007335	AISI 304	7.90	280	RT000063	MATPRO
E9000721	X10NiCrMoTiB	7.90	-	AK000012	Binkele

Descriptors, units	
DEN Density (g/cm^3)	MELTH enthalpy of fusion (J/g)

Table 4.4.1.3 THERMAL CONDUCTIVITY OF AUSTENITIC STEELS

EKEY	MNAM	VAL	DONO	AU
E0000109	AISI 347	TPRC	TPM01000	Touloukian
E0004650	AISI 347	RECO	R0000100	Bogaard
E0005218	AISI 347	RECO	R0000019	Fieldhouse
E0005269	AISI 347		R0000068	Powers
E0005282	AISI 347		R0000075	Vianey
E0005217	AISI 347		R0000019	Fieldhouse
E0005220	AISI 347		R0000126	Matolich
E0005843	AISI 316		J0001778	Filoni
E0007365	AISI 316	RECO	RT000062	Harding
E0007366	AISI 316	RECO	RT000062	Harding
E0007367	AISI 316	RECO	RT000062	Harding
E0007368	AISI 316	RECO	RT000062	Harding
E0004419	AISI 304		J00001425	Tye
E0004670	AISI 304	RECO	R0000100	Bogaard
E0004743	AISI 304	RECO	TPSAM002	Touloukiaan
E0005222	AISI 304		R0000127	Smith
E0005270	AISI 304		R0000068	Powers
E0005306	AISI 304		J0002832	Ewing
E0005842	AISI 304		J0001778	Filoni
E0005909	X 5 CrNi 18		J0002963	Kohlhaas
E0006081	AISI 304		R0000073	Deverall
E0006082	AISI 304		R0000073	Deverall
E0006233	X 5 CrNi 18		J0002826	Brauner
E0007337	AISI 304	RECO	RT000063	MATPRO
E9000720	X10NiCrMoTiB	RECO	AK000012	Binkele

Codes			
TPRC	TPRC recommended data	RECO	recommended data

Table 4.4.1.4 THERMAL EXPANSION OF AUSTENITIC STEELS

EKEY	MNAM	DEN	VAL	DONO	AU
E0000940	AISI 347,316	-	TPRP	TPM12000	Touloukian
E0007358	AISI 316	7.96	RECO	RT000062	Harding
E0004745	AISI 304	7.90	RECO	TPSAM002	Touloukian
E0007338	AISI 304	7.90	RECO	RT000063	MATPRO

Descriptors, units		Codes	
DEN Density	(g/cm^3)	TPRP	TPRC provisional data
		RECO	Recommended data

Table 4.4.1.5 TOTAL EMISSIVITY OF AUSTENITIC STEELS

EKEY	MNAM	DONO	AU
E0006303	AISI 316	P0000021	Morris

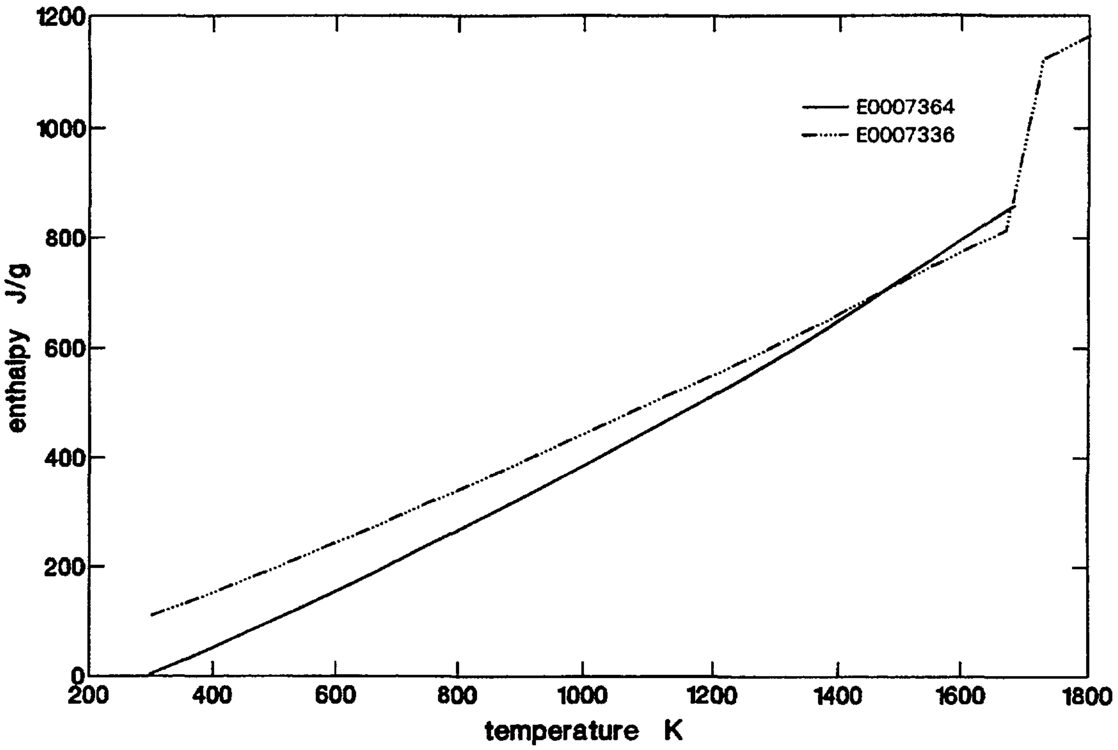

Figure 4.4.1.1 Enthalpy of austenitic steels

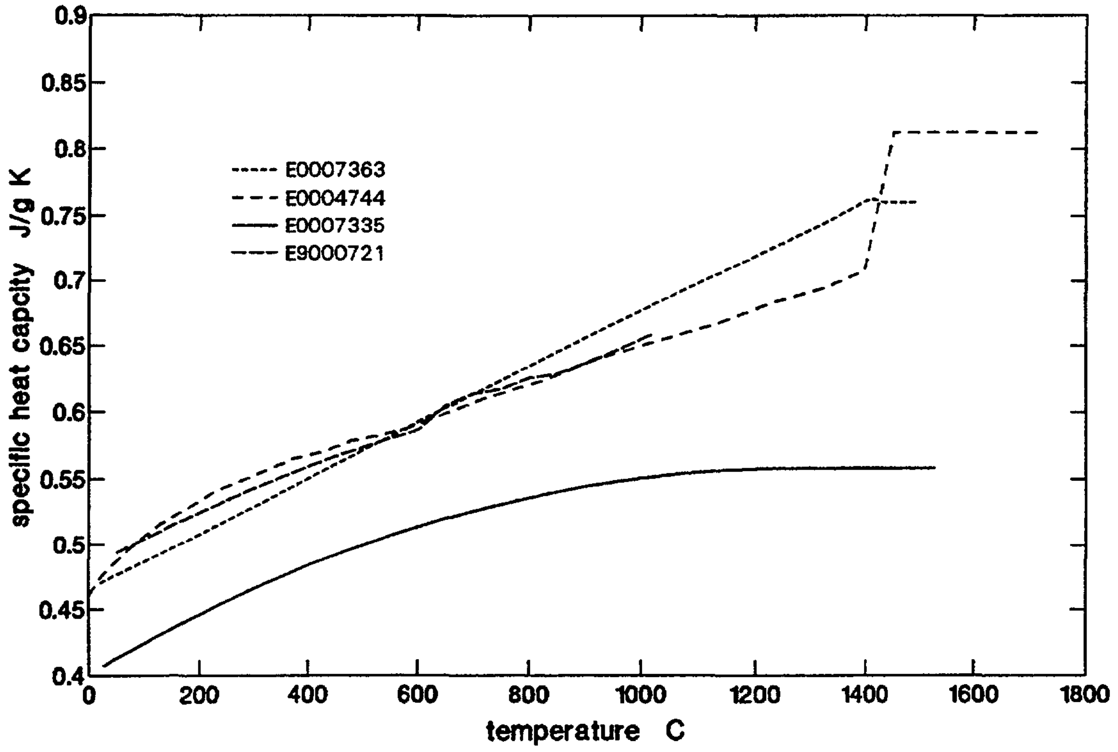

Figure 4.4.1.2 Specific heat capacity of austenitic steels

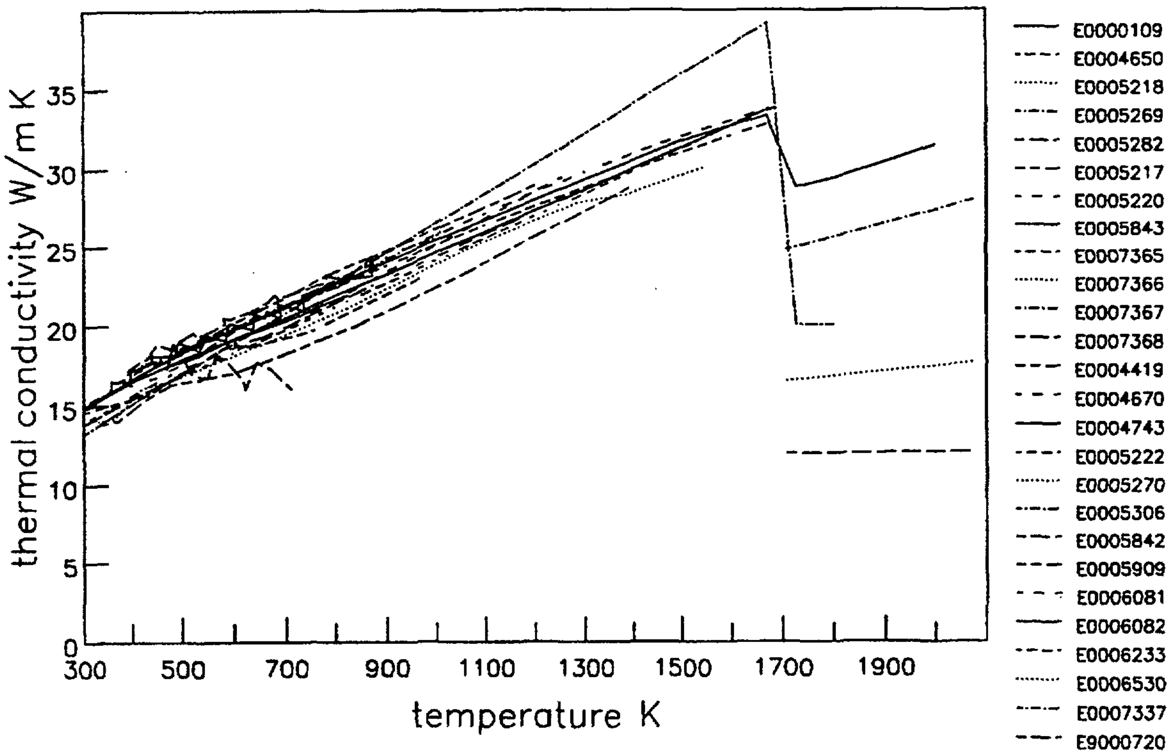

Figure 4.4.1.3 Thermal conductivity of austenitic steels

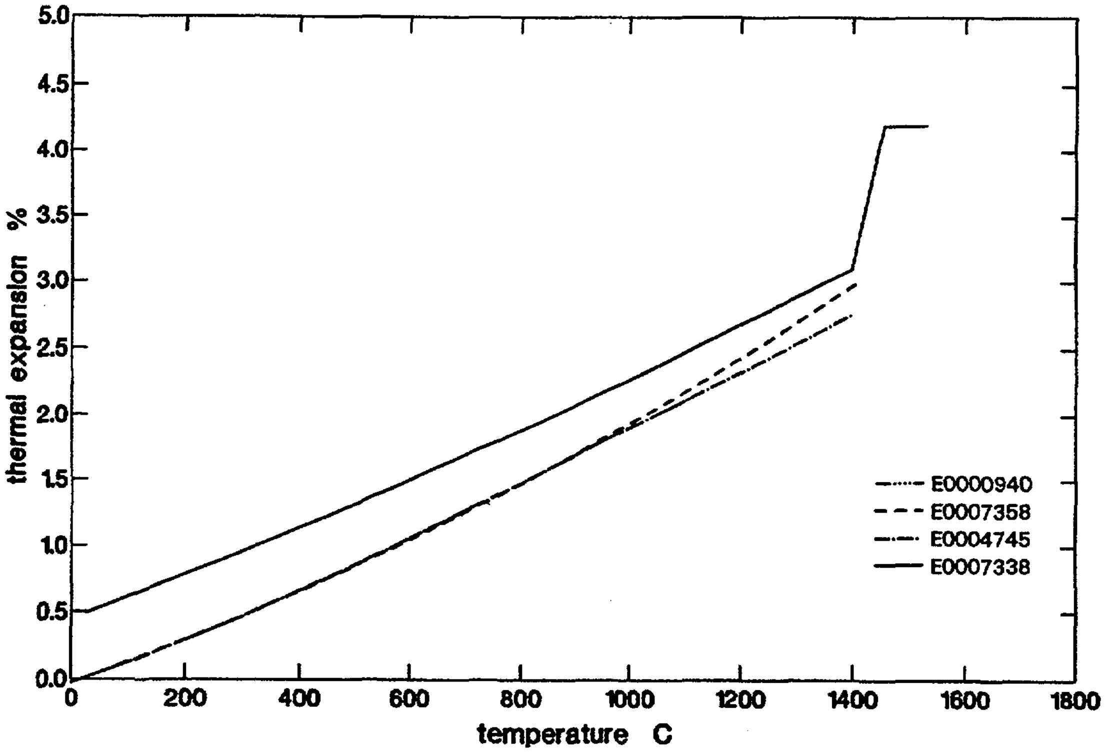

Figure 4.4.1.4 Thermal expansion of austenitic steels

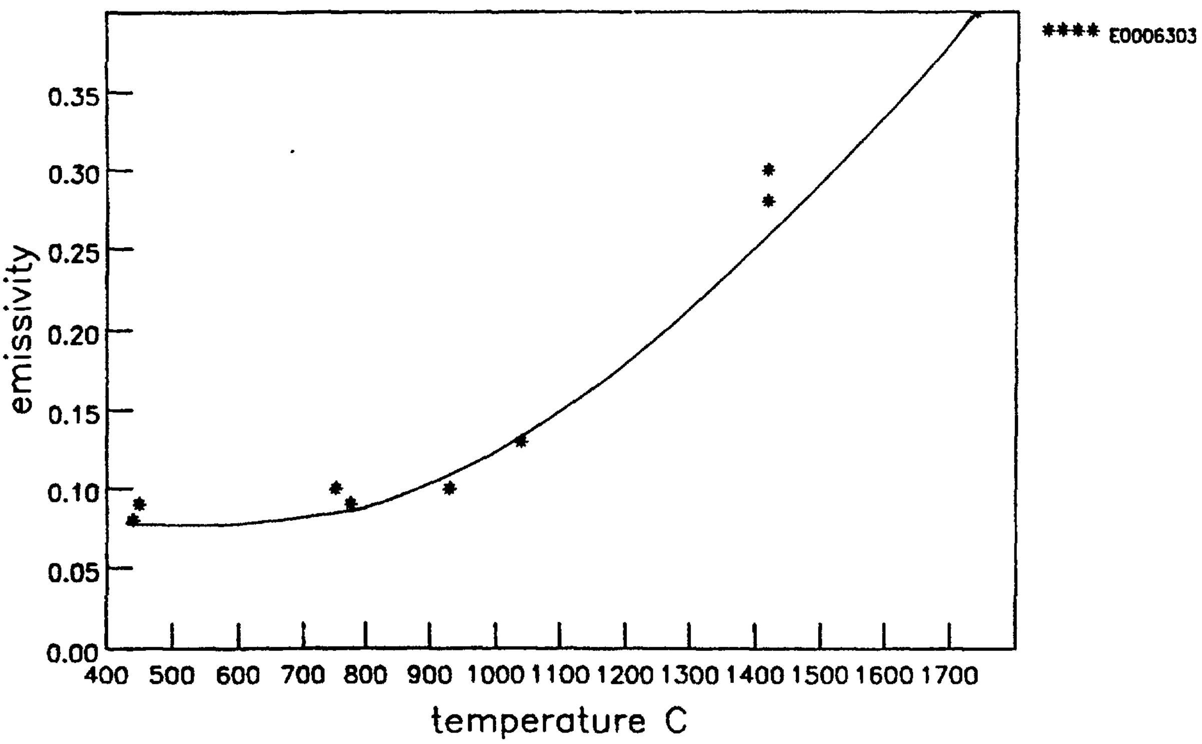

Figure 4.4.1.5 Emissivity of austenitic steels

References to Section 4.4.1

Note: literature stored in THERSYST is referenced by document number e.g. AK000012, etc.

AK000012	Arbeitskreis Thermophysik, "Austenitischer Chromnickelstahl als Standardreferenzmaterial bei Messung der Waerme- und Temperaturleitfaehigkeit", DKG, Fachausschussbericht Nr. 28, "Thermophysik"; Erstatted von Binkele
J0001425	TYE R. P., HAYDEN R. W., SPINNEY S., "The thermal conductivity of a number of alloys at elevated temperatures", High Temp. -High Pressures 4 (1972), 503-511
J0001778	FILONI L., ROCCHINI G., "Thermal conductivity of iron, plain carbon and stainless steels, and Inconel 718 from 360 K to 900 K", High Temp. -High Pressures 19 (1987) 381-387
J0002826	BRAUNER J., FRIEDHOFF P., "Einfaches Verfahren zur Bestimmung der Waermeleitfaehigkeit von Staehlen", Materialpruef. 13 (1971), 230-23
J0002832	EWING C. T., et al., "Thermal conductivity of mercury and two sodium-potassium alloys", J. Phys. Chem. 59 (1955), 524-528
J0002963	KOHLHAAS R., KIERSPE W., "Waermeleitfaehigket von reinem Eisen und einigen ferritischen und austenitischen Staehlen zwischen der Temperatur der fluessigen Luft und Raumtemperatur", Arch.Eisenhuettenw. 36 (1965), 301-309
P0000021	MORRIS J. C., SHURIN B., OLSON O., "The total emissivity of aircraft construction materials", Proc. Symp. on Thermal Properties, New York, McGraw-Hill Book Comp
R0000019	FIELDHOUSE I. B., et al., "Measurements of thermal properties", WADC-TR-58-274, 1-79 (1958)
R0000068	POWERS R. W., et al., "The thermal conductivity of metals and alloys at low temperatures -II- Data on iron and several steels between 25 and 300 K. Influence of alloying constituents", USAF-TR-264-6, 1-14 (1951)
R0000073	DEVERALL J. E., "The thermal conductivity of a molten Pu-Fe eutectic (9.5 A/O Fe)", USAEC Rept. LA-2269, 1-62 (1959)
R0000075	VIANEY L. R., "Thermal conductivity of 347 stainless steel and zirconium", USAEC Rept. NP-1989, PB 123-175
R0000100	BOGAARD R. H., "Thermal conductivity of British, French, and West German stainless steels", TEPIAC/CINDAS Report 68 (1983)
R0000126	MATOLICH J. JR., "Thermal conductivity and electrical resistivity of type 316 stainless steel from 0 to 1800 F", NASA-CR-54151, 1-25 (1965)
R0000127	SMITH C. F., "Apparatus for determining low temperature thermal conductivity", NASA-TMX-50852, 1-31 (1963)
RT000062	HARDING J. H., et al., "Thermophysical and thermochemical properties of fast reactor materials", EUR 12402EN (1989), 1-90
RT000063	HOHORST J. K. (Editor), "SCDAP/RELAP5/MOD2 Code Manual, vol. 4: MATPRO-a library of materials properties for light-water-reactor accident analysis", NUREG/CR-5273 (1990)
TPM01000	TOULOUKIAN Y. S., et al., "Thermophysical Properties of Matter. Vol. 1: Thermal Conductivity - Metallic Elements and Alloys", IFI/Plenum, New York-Washington (1977)
TPM12000	TOULOUKIAN Y. S., et al., "Thermophysical Properties of Matter. Vol. 12: Thermal Expansion - Metallic Elements and Alloys", IFI/Plenum, New York-Washington (1977)
TPSAM002	TOULOUKIAN Y. S., HO C. Y., "Thermophysical properties of selected aerospace materials. Part II: Thermophysical properties of seven materials", Thermophysical properties, Part II. (1977)

4.4.2. Martensitic stainless steel

Thermophysical property data for the following martensitic stainless steels were found in the literature:

X 7 Cr 13	(1.4000)
X 20 Cr 13	(1.4021)
X 40 Cr 13	(1.4034)
X 8 Cr 17	(1.4016)
X 12 CrMoS 17	(1.4104)
2 Kh 13	(1.4021)

Numbers in parenthesis are the German standard No. (Source: C.W. Wegst "Stahlschlüssel" Hersg. Verlag Stahlschlüssel Wegst GmbH, Marbaer, 1986).

Thermal conductivity, thermal expansion and emissivity are presented in Figure 4.4.2.1 to 4.4.2.3, respectively. The source of the data and the densities of the steels are given in Tables 4.4.2.1 to 4.4.2.3.

There are also data for the AISI 403 stainless used in CANDU reactors. Thermal conductivity and thermal expansion for the steel are give in Tables 4.4.2.4 and 4.4.2.5 respectively, the specific heat capacity as a function of temperature is shown in Figure 4.2.4.4. (Note that the specific heat capacity is actually for AISI 410 stainless, a material so close in composition to AISI 403 stainless that the thermophysical properties are interchangeable between the two steels.) The sources of the data are given in the reference list.

Nomenclature to Section 4.4.2

T - temperature (K)
ε - thermal strain (m/m), other unit: %
λ - thermal conductivity (W/(m·K))
α - thermal expansion (1/K)

Table 4.4.2.1 THERMAL CONDUCTIVITY OF MARTENSITIC STEELS

EKEY	MNAM	DEN	DONO	AU
E0004651	AISI 420 (G)	-	R0000100	Bogaard
E0004652	AISI 420 (G)	-	R0000100	Bogaard
E0005197	AISI 420	7.71	R0000107	Fieldhouse
E0004687	AISI 430	-	R0000100	Bogaard
E0005212	AISI 430	-	R0000050	Francis
E0005213	AISI 430	-	R0000050	Francis
E0006093	AISI 430	-	J0002895	Silverman
E0005235	AISI 403	-	R0000129	Evans

Descriptor, unit	DEN Density	(g/cm^3)

Table 4.4.2.2 THERMAL EXPANSION OF MARTENSITIC STEELS

EKEY	MNAM	TREATT	TRTEM	TRTIM	DONO	AU
E0000962	AISI 420, 420C	ANNE	---	---	TPM12000	Touloukian
E0002858	20 Kh 13		---	---	J0001033	Belayev
E0002860	1Kh12N2WMF	ANNE	650	2 hs	J0001033	Belayev
E0002861	14Kh17N2		---	---	J0001033	Belayev
E0002863	Kh15N5D2T	ANNE	650	2 hs	J0001033	Belayev

Descriptor, unit	TRTEM	(°C)
Signification of Codes	ANNE	annealed

Table 4.4.2.3 TOTAL NORMAL EMISSIVITY OF MARTENSITIC STEEL 2Kh13

EKEY	RZ (roughness)	DONO	AU
E0003412	-	J0000457	Komarek
E0003414	5.92	J0000457	Komarek
E0003415	12.40	J0000457	Komarek
E0003416	11.10	J0000457	Komarek
E0003417	6.53	J0000457	Komarek
E0003418	6.25	J0000457	Komarek

Table 4.4.2.4 THERMAL CONDUCTIVITY FOR AISI 403 STAINLESS

From [1]		From [2]	
T (K)	K (W/(m·K))	T (K)	K (W/(m·K))
426	27.3	293	25.3
477.6	27.0	323	25.5
533.2	26.8	348	25.7
588.7	26.7	373	25.8
644.3	26.2	398	25.9
699.8	25.9	423	26.1
755.4	25.6	448	26.3
810.9	25.2	473	26.4
842.6	24.9	498	26.6
		523	26.7
		548	26.9
		573	27.1

Table 4.4.2.5 THERMAL EXPANSION DATA FOR AISI 403 STAINLESS [2]

T (K)	α for Extrusion ($\times 10^{-6}$/K)	α for Forging ($\times 10^{-6}$/K)
323	8.4	7.4
348	9.1	8.1
373	9.7	8.7
398	10.2	9.3
373	10.5	9.8
448	10.7	10.1
473	10.9	10.4
498	11.1	10.7
523	11.3	10.9
548	11.5	11.1
573	11.7	11.3
598	11.8	11.5
623	11.9	11.7

The expansion α is listed as the mean value from 294 K to the indicated temperature

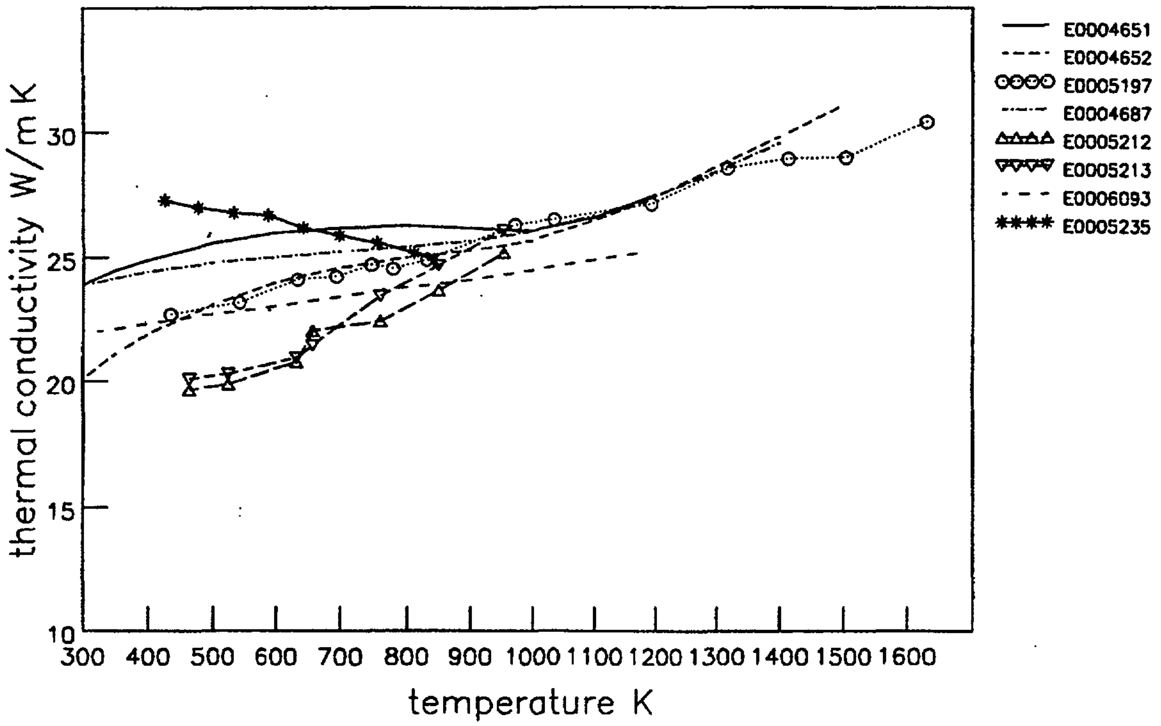

Figure 4.4.2.1 Thermal conductivity of martensitic steels

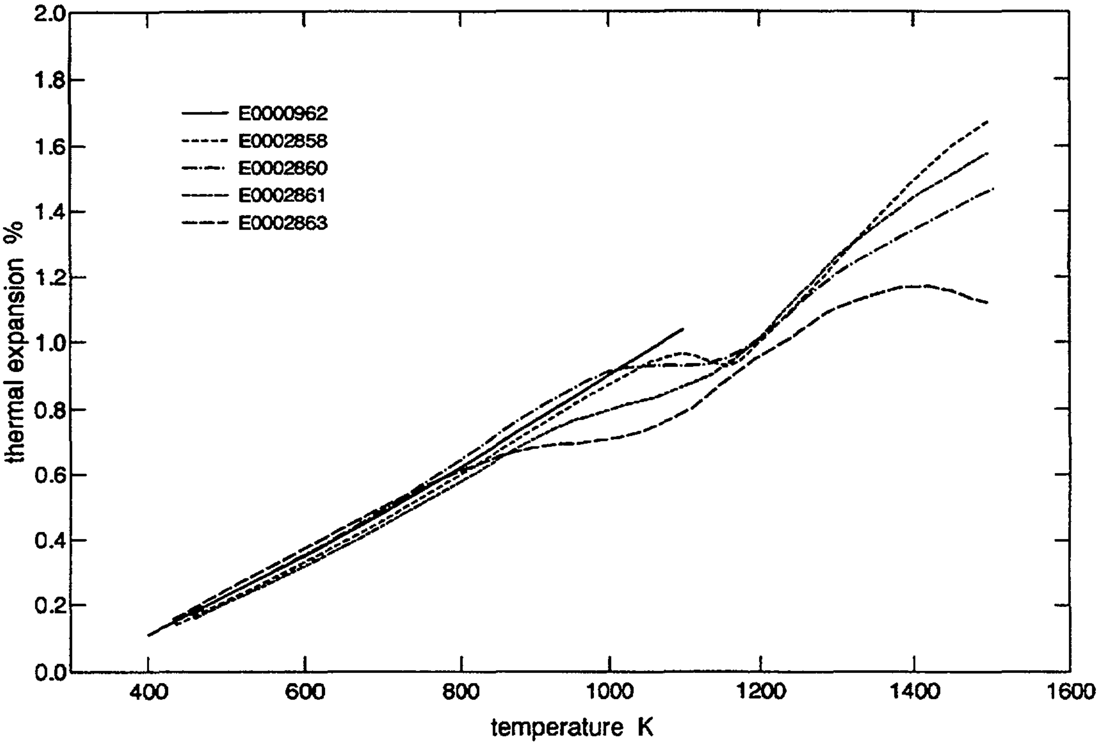

Figure 4.4.2.2 Thermal expansion of martensitic steels

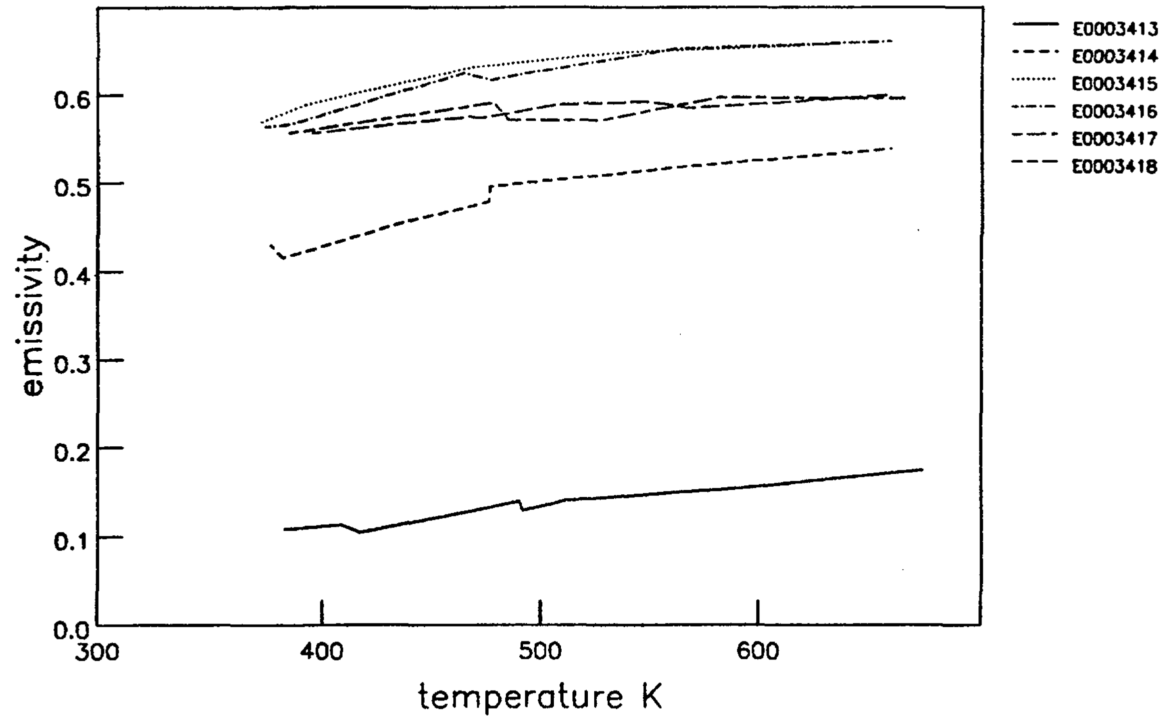

Figure 4.4.2.3 Total emissivity of martensitic steels 20Kh13

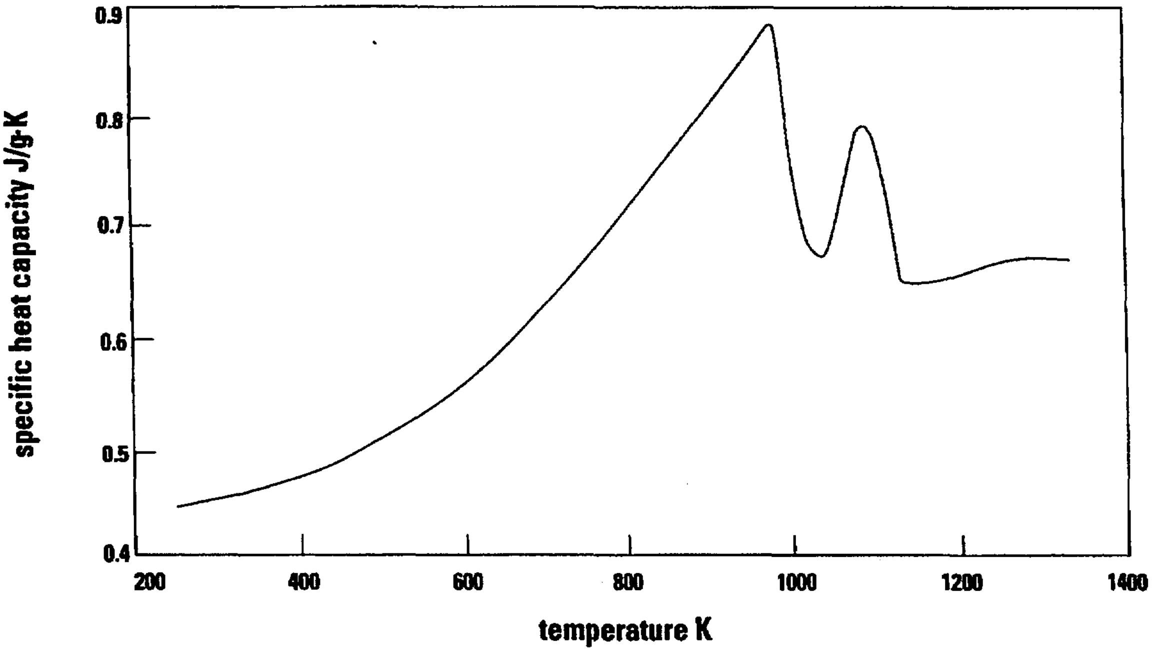

Figure 4.4.2.4 Specific heat capacity of AISI 410 stainless [3]

References to Section 4.4.2

Note: literature stored in THERSYST is referenced by document number, e.g. J0000457, etc.

J0000457 KOMAREK A., STRIGIN B. K., "Determination of the emissivity of stainless steel after various surface treatments as a function of temperature", High Temp. 1 (1963), 24-26

J0001033 BELYAEV R. A., et al., "Linear expansion of high-alloy steels and alloys", Teplofiz. Vys. Temp. 17 (1979), 74

J0002895 SILVERMAN L., "Thermal conductivity data presented for various metals and alloys up to 900°C", J. Met. 5 (1953), 631-632

R0000050 FRANCIS R. K., et al., "Metal-ceramic laminates", WADC-TR-58-600, 1-69 (1958)

R0000100 BOGAARD R. H., "Thermal conductivity of British, French, and West German stainless steels", TEPIAC/CINDAS Report 68 (1983)

R0000107 FIELDHOUSE I. B., LANG J. I., "Measurements of thermal properties", WADD-TR-60-904, 1-119 (1961)

R0000129 EVANS J. E. Jr., "Thermal conductivity of 14 metals and alloys up to 1100 F", NACA-RM-E50L07, 1-15 (1951)

TPM12000 TOULOUKIAN Y. S., et al., "Thermophysical properties of matter. Vol. 12: Thermal expansion - metallic elements and alloys", IFI/Plenum, New York-Washington (1977)

Additional references for Section 4.4.2

[1] Touloukain Y. S., Powell R. W., Ho C. Y., Klemens P. G., "Thermophysical properties of matter Vol. 1, Thermal conductivity of metallic elements and alloys", IFI/Plenum, New York-Washington, USA, p. 1151 (1970)

[2] Canadian Standards Association, "Martensitic stainless steel for fuel channel end fittings", National Standards of Canada, Toronto, Canada, CAN/CSA-N285.6.8-88, Section 3.2.2, p. 81 (1988)

[3] Ho C. Y., Mindlin H. Holt J. M., "Structural Alloys Handbook Volume 2, 1992 Edition", CINDAS/Purdue University, Indiana, USA, 410 Stainless Physical Properties, p. 3 (1992)

4.5. CONCRETES, INCLUDING EROSION IN CONCRETE-CORE MELT INTERACTION

4.5.1. Introduction

In the most severe accident scenario for a light water reactor, the core melts its way through the bottom of the pressure vessel and into a reactor pit [1, 2]. At a temperature of 2700 K the melt would erode ordinary concrete at a rate of 1.5 to 3.0 meters per day. To prevent this erosion, special "catchers" have been designed which restrict further movement of the melt until it has solidified. The design and reliability of these catchers depend on the properties of the construction materials used. The materials need to be capable of withstanding temperatures in the region of 2200 to 2700 K in an oxidizing environment. The refractory oxides of zirconia and alumina are suitable for the application, having melting points of 3000 and 2300 K respectively, as well as being comparatively inexpensive and non-toxic. They can be used to make hydration hardening refractory concrete, the properties of which have been studied at the HEDRC for some time. Experimental results are presented for the thermal properties of these concretes as well as thermodynamic data relevant to the melt-concrete interaction. Silicate concretes are widely used in nuclear power plant construction, so data on the thermal properties of these have been included.

4.5.2. Refractory concrete properties

Two types of refractory concretes were investigated: alumina concrete (AC), filled with electric-melted corundum (Al_2O_3), and zirconium dioxide concrete (ZDC) filled with electric-melted zirconium dioxide, stabilized by 6-7 mol.% Y_2O_3. Both concretes hydration harden. The operating temperature of AC is about 2000 K, and is 2500-2600 K for ZD concrete. AC and ZDC are more refractory than conventional concretes, which decompose and melt between 1600 and 1800 K. AC and ZDC also contain less water than conventional concretes resulting in reduced gas release at high temperatures. Compositions and properties of AC and ZDC are given in Table 4.5.1.

The experimental data presented below was obtained for ZDC composition 2, Table 4.5.1. The ZDC composition 1 and 3 give the similar results as ZDC composition 2.

Properties of zirconium dioxide concrete

ZDC thermal conductivity

The thermal conductivity of a ZDC sample was measured in a one-dimensional stationary regime [3]. The sample had a cylindrical shape with a diameter of 15 mm and a height of 20 mm. To heat the sample, radiation from a xenon lamp with a power up to 10 kW was focused on the upper end of the sample. The lower end was cemented to the copper surface of a flowing water calorimeter. The sides of the sample were insulated to ensure one-dimensional axial heat flow. The temperature distribution along the sample was measured by four platinum-rhodium thermocouples located inside the sample.

The uniformity of the surface heating was tested with a pyrometer, which viewed the upper end of the sample through an adjustable modulator to eliminate direct radiation from the lamp. One-dimensionality of the heat flow was checked with radial chromel-alumel thermocouples. The surface temperature was varied smoothly by decreasing the lamp power and by defocusing the optics. The experimental error on thermal conductivity measurement was ±15 to 20%.

The experimental results are presented in Table 4.5.2. It is typical for the thermal conductivity of concrete to be smaller in the lower temperature range, and independent of temperature in the upper temperature range. After reheating, $\lambda(T)$ was reduced by a factor of 1.2. Such behaviour is due to the cement dehydrating during heating, especially if $T < 600$ K.

ZDC thermal expansion

The thermal expansion of ZDC was investigated using an optical comparative procedure in a high temperature dilatometer [3]. A vacuum electric furnace with a graphite heater was used to heat the concrete samples. The heater looks like a cage rotor. The samples were suspended vertically inside the heater and had an initial length of 0.15 m. A microscope with a moving telescope viewed the ends of the sample through slots in the heater. At low temperatures, the sample was illuminated and at high temperatures the hot sample was visible against the cold part of the furnace. The error in the elongation measurements was up to ±5%. The sample elongation results recorded during heating and cooling are given in Table 4.5.3. The initial sample length was measured at 293 K.

During heating, the expansion of the sample deviated from a straight line over the temperature ranges 570-770 K and 1470-1670 K. The first deviation may be due to concrete dehydrating, which comes to an end at 1270 K.

The cooling curve is strictly a straight line, returning to zero. Thus, ZDC would not shrink (at least, during heating up to 2100 K).

Cooling over the temperature range 2070-290 K, the average coefficient of linear thermal expansion was 11.1×10^{-6} 1/K, which is similar to the value for a coarse-grained sintered zirconium dioxide with stabilizer [4]. The thermal expansion data was used to calculate the density of ZDC over the temperature range 400-2000 K (Table 4.5.3).

The ZDC density was calculated for a previously heated sample. The initial density of the ZDC sample was 4500 kg/m^3 at 293 K.

Radiation characteristics of ZDC

The normal spectral emissivity $\varepsilon_{n\lambda}$ and the normal total emissivity ε_{nt} of ZDC were investigated by a radiative technique. A hollow cylindrical graphite heater with a diametrical partition in the middle was placed vertically inside an induction furnace. Both the upper and lower parts of the heater produce black body radiation. The inductor frequency was 60 kHz. The sample was suspended inside the upper part of the heater close to the partition. After heating the sample, the heater was dropped and the radiation of the suspended sample was recorded by a fast apparatus [5]. The error on the measurements was 5%.

The $\varepsilon_{n\lambda}$ measurements were carried out in the argon atmosphere at a pressure of 0.1 MPa, the spectral region covered being $(1.0\text{-}5.5) \times 10^{-6}$ m. Two samples were measured over the temperature range 900 to 1600 K, with thicknesses of 4.0 and 5.1 mm. The experimental data are shown in Figure 4.5.1, with point 3 taken from reference [6]. The point 3 corresponds to the $\varepsilon_{n\lambda}$ emissivity of zirconium dioxide ceramics stabilized by yttrium oxide at a wavelength of 5×10^{-6} m over the temperature range 1500 to 1800 K.

It is typical for the $\varepsilon_{n\lambda}$ of ZDC to increase from 0.24 to 0.675 as the wavelength increases from 1×10^{-6} m to 5.5×10^{-6} m, $\varepsilon_{n\lambda}$ does not depend on temperature in the range of 600-1800 K.

It should be noted, that at room temperature the difference in $\varepsilon_{n\lambda}$ between curves 1 and 2 in Figure 4.5.2 may be due to the increase in accessible porosity (from 32% to 38%) and the change in structure which occurred during heating.

The normal total emissivity of ZDC was measured in vacuum over the temperature range 600 to 1700 K with an uncertainty of 5% (curve 1 in Figure 4.5.3). The thickness of the samples used was 4.0 and 5.1 mm. Over the temperature range 600 to 1600 K and for wavelengths greater than 6 mm, the normal total ZDC emissivity was calculated using the emissivity data given in reference [5], and data taken from the reference [6].

As would be expected for oxide ceramics, in accordance with [5], the $\varepsilon_{n\lambda}(T)$ function consistently decreases with rising temperature. The experimental data are listed in Table 4.5.4.

Alumina concrete properties

AC thermal conductivity

The thermal conductivity of AC was investigated by a one-dimensional radial heat flow technique over the temperature range 500 to 1800 K [8]. The sample consisted of several hollow concrete cylinders of height 20-40 mm, inside diameter 6 mm and outside diameter 60 mm. The total height of the sample was 320 mm. To generate a radial heat flow, a molybdenum rod-type heater with a diameter of 6 mm was placed through the sample. To measure the temperature distribution, four platinum/platinum-rhodium thermocouples were fixed along the radius of the central portion of the sample. Both unfired and partly fired (1500 K) samples have been investigated. The experimental results are presented in Table 4.5.5.

The conductivity of the unfired sample is lower than that of the fired sample over the temperature range 500 to 1000 K due to the presence of calcium hydroaluminate in the unfired sample. At higher temperatures the water of crystallization is removed and the curves for the two samples come together. At temperatures above 1100 K there is a 4% uncertainty on the experimental thermal conductivity data.

AC thermal expansion

The thermal expansion of AC was investigated by the optical comparative procedure [9]. A square cross section sample of length of 120 mm, 7 mm wide, was situated in a furnace and the elongation measured using a microscope to a precision of 1.5 mm. The samples were dried out at 400 K and fired at 1100 K before the investigations. Experimental data and calculated AC density data are shown in Table 4.5.6. The initial sample length was measured at 293 K. The initial density of AC was 2800 kg/m^3 at 293 K. The average calculated thermal expansion coefficient was 8.47×10^{-6} 1/K over the temperature range 293 to 1800 K.

AC radiation characteristics

The normal spectral emissivity, $\varepsilon_{n\lambda}$, of AC has been investigated at $\lambda = 0.546\times10^{-6}$ m (visible range) and $\lambda = 5\times10^{-6}$ m (infrared range). In the visible range, the reflection technique was used, with diffuse reflection from the concrete surface taken into account [7]. The incident light was produced by a high pressure mercury vapor lamp and the reflected radiation recorded by a photomultiplier fitted with a monochromator. In the infrared region both brightness and true temperatures were measured simultaneously and independently by two different techniques.

The samples were in the form of a plain disk with a diameter of 15 mm, 2-3 mm thick. One side of the sample disk was heated by an acetylene torch, and the other side was used for the measurements. The sample temperature was controlled by varying the distance between the sample and the torch. The experimental curves obtained are shown in Figure 4.5.2. As temperature rises, $\varepsilon_{n\lambda}(T)$ decreases, but, it starts to increase at 1750 K. Such behaviour is most noticeable in the infra red region (curve 2 in Figure 4.5.4). Table 4.5.7 lists the $\varepsilon_{n\lambda}$ experimental data in the visible and infrared regions.

AC heat capacity, enthalpy, and thermal diffusivity

The AC heat capacity, enthalpy, and thermal conductivity have been calculated in the temperature range 1100 to 2200 K. At these temperatures the concrete becomes completely dry and consists of sintered refractory oxides. The calculations have been performed using the additivity principle, the concrete composition being 95 wt.% of Al_2O_3 and 5 wt.% of CaO. The data have been taken from [11]. The calculated data are shown in Table 4.5.8. The initial enthalpy $H = 0$ was taken at 0 K.

Thermal properties of silicate concretes

SC thermal conductivity

The thermal conductivity of silicate concrete (SC) depends upon parameters such as the chemical composition, the aggregate grain size, porosity, moisture, hardening time, and temperature. Variation of these parameters significantly effects the concrete properties. For example, the thermal conductivity depends on the type of concrete and varies from 0.0 W/(m·K) to 2.5 W/(m·K) at room temperature [12].

The thermal conductivity of a heavy silicate concrete is greater than that of a conventional one, with the $\lambda(T)$ function showing a typical decreasing behaviour. The greater the concrete density and moisture content, the greater its thermal conductivity.

With experiments performed over a wide range of temperatures, the heat of chemical reaction can not be taken into account, thus, only an average thermal conductivity is measured, and the estimated experimental error is around 15-20%. Including different types of concrete and differing operating conditions, this error increases to 15-20%. Table 4.5.9 lists the thermal conductivity of hard concrete with granite aggregate [12].

SC heat capacity

The specific heat capacity per unit volume and weight of SC depends only slightly on temperature, with the exception of two peaks at about 400 K and 700-800 K. The first peak is due to an endothermic reaction and the second peak is due to the $Ca(OH)_2$ dehydrating. In general, only an average heat capacity can be measured. Thus, the experimental data do not correspond to the actual $C_p(T)$ function. The SC average heat capacity is shown in Table 4.5.10.

SC thermal expansion

The thermal expansion of SC depends considerably upon the concrete structure. It also depends upon temperature, operation condition, rate of heating and even the sample size. On the one hand the components of a concrete expand as the material is heated, on the other hand, the concrete shrinks due to densification and dehydration. If the heating rate is high enough, steam pressure inside the material influences the expansion. These effects produce considerable variation in the available experimental data. The data taken from [12] are shown in Table 4.5.11. Hollow concrete cylinders have been used in the experiments.

SC enthalpy, density, and thermal diffusivity

The enthalpy, density, and thermal diffusivity coefficient of SC have been calculated using the previously mentioned data for the heat capacity, thermal expansion, density at 300 K and the thermal conductivity. The calculated values are listed in Table 4.5.12.

The initial enthalpy $H = 0$ had been taken at $T = 300$ K. The density and thermal diffusivity coefficient have been calculated for hard SC with granite aggregate.

4.5.3. Investigation of melt-concrete interaction thermophysics

Determination of the concrete resistance to the high temperatures melt was the main aim of the experiments. Thus, in order to reduce oxidation of the liquid melt, an argon atmosphere was used inside the chamber. Oxidation of the metal results mainly from concrete dehydration and gas release from the concrete.

Various AC and ZDC samples have been investigated. The experimental conditions and results are shown in Table 4.5.13. Compositions and properties of AC and ZDC are shown in Table 4.5.1.

The cross section of an alumina concrete sample is shown in Figure 4.5.5. One can see three layers in the sample. The first layer with the great amount of pores lies directly under the set melt; the layer thickness is 1.5 mm. The second layer with a thickness of 4.0 mm looks like a sintered uniform mass. The third layer is that of the initial concrete. Gas was released at the melt-concrete boundary (see Figure 4.5.5), that resulted in bubble generation inside the melt. Molten metals melted through the concrete with molten oxides forming on the melt surface. The axial erosion velocity was 0.5 mm/min.

The cross section of an ZDC sample is shown in Figure 4.5.6, the sample composition corresponds to the composition 1 (Table 4.5.1). One can see three layers: a glassy layer at the melt-concrete boundary, a layer of sintered material, and a layer of the initial concrete. The axial erosion velocity of the ZDC sample was 0.013 mm/min. The gas samples in the experiment 1 (Table 4.5.13) had the following composition: 96.7 vol.% of O_2 + Ar_2 + N_2, 0.3 vol.% of CO_2, 0.5 vol.% of CO, 2.5 vol.% of H_2. Hydrogen was a product of the Zr + Fe + H_2O reaction.

The erosion rates of concrete sample 3 (Table 4.5.13) was close to zero, for a melt temperature of 1900 K. The axial and radial erosion rates of sample 2 are different, the axial rate, which depended on the melt-concrete interaction, was close to zero. The radial rate, which depended on the oxide-concrete interaction in the upper part of the crucible, was 0.05 mm/min.

Analysis points to the following processes as being important during the melt-ZDC interaction: (i) metal penetration into the ZDC, (ii) exothermic oxidation of the metal with hydrogen release, (iii) oxides-concrete interaction.

4.5.4. Conclusions

The refractory concretes investigated are worth considering when designing catchers for molten reactor materials. The erosion rate of AC is a few times and of ZDC about a hundreds times smaller than conventional structural concretes (erosion rate 3.6-60 mm/min) at similar melt temperatures (1800-2200 K) [13].

The ZDC concrete is the suitable material for a core catcher. It will be necessary to conduct investigations of high temperature interactions of ZDC with metal melts including interaction with Zr and oxides including UO_2.

The experimental data on the thermophysical properties of concretes will be useful in designing light and heavy water reactors.

Nomenclature to Section 4.5

C_P - specific heat capacity, (kJ/(kg·K),
$\lambda(T)$ - thermal conductivity, (W/(m·K)),
a - thermal diffusivity, (m^2/s)
$\varepsilon_{n\lambda}$ - normal spectral emissivity,
ε_{nt} - normal total emissivity,
λ - light wavelength, (m),
H - enthalpy, (kJ/kg).

Table 4.5.1 COMPOSITIONS AND PROPERTIES OF REFRACTORY CONCRETES

Concrete type	ZDC (Zirconium-dioxide concrete with hydration hardening)			AC (alumina concrete)
	Comp. 1	**Comp. 2**	**Comp. 3**	
Filler	80 wt.% ZrO_2 (grain size 2.0-0.05 mm)			80 wt.% Al_2O_3
Cement compos., (wt.%)	ZrO_2 70 BaO Al_2O_3 30	BaO ZrO_2 70 BaO Al_2O_3 30	CaO $2Al_2O_3$ 80 CaO Al_2O_3 20	CaO $2Al_2O_3$ 80 CaO Al_2O_3 20
Density (kg/m^3)	4500-4700	4400-4600	3800	2700-2900
Porosity (%)	15-17	14-20	12-14	18-20
Max. compress. strength (MPa)	30-39	30-40	27	60

Table 4.5.2 THERMAL CONDUCTIVITY OF ZDC

Temperature (K)	**400**	**600**	**800**	**1000**	**1200**	**1400**	**1500**
	Thermal conductivity (W/(m·K))						
The first heating	2.44	1.68	1.54	1.57	1.61	1.66	1.69
Reheating	2.44	1.34	1.27	1.27	1.27	1.29	1.30

Table 4.5.3 ELONGATION AND THE DENSITY OF ZDC

T (K)	**400**	**500**	**600**	**700**	**800**	**900**	**1000**	**1100**	**1200**	**1300**	**1400**	**1500**	**1600**	**1700**	**1800**	**1900**	**2000**
	Elongation (%)																
Heating	0.214	0.41	0.49	0.56	0.64	0.76	0.88	0.92	0.98	1.14	1.36	1.44	1.50	1.57	1.65	1.73	1.85
Cooling	0.107	0.26	0.40	0.46	0.53	0.68	0.85	0.91	0.95	1.12	1.23	1.36	1.43	1.54	1.65	1.73	1.85
	Density (kg/m^3)																
	4480	4460	4440	4430	4420	4410	4390	4380	4370	4350	4330	4320	4310	4300	4280	4270	4260

Table 4.5.4 ZDC NORMAL TOTAL EMISSIVITY

T (K)	**700**	**800**	**900**	**1000**	**1100**	**1200**	**1300**	**1400**	**1500**	**1600**
ϵ_{nt}	0.7	0.68	0.64	0.60	0.57	0.54	0.51	0.49	0.48	0.47

Table 4.5.5 AC THERMAL CONDUCTIVITY

T (K)	473	573	673	773	873	973	1073	1173
	Thermal conductivity (W/(m·K))							
Fired sample	3.06	2.72	2.45	2.26	2.14	2.06	2.04	2.04
Unfired sample	2.06	2.03	2.02	2.01	2.01	2.02	2.04	2.07

T (K)	1273	1373	1473	1573	1673	1773
	Thermal conductivity (W/(m·K))					
Fired sample	2.07	2.13	2.20	2.28	2.33	2.49
Unfired sample	2.07	2.11	2.16	-	-	-

Table 4.5.6 AC THERMAL EXPANSION AND DENSITY

Temperature (K)	1073	1173	1273	1373	1473	1573	1673	1873
Elongation (%)	0.71	0.80	0.89	0.99	1.08	1.17	1.22	1.25
Density (kg/m^3)	2740	2730	2720	2710	2707	2705	2701	2689

Table 4.5.7 AC NORMAL SPECTRAL EMISSIVITY

Temperature (K)	1600	1700	1800	1900	2000
	Normal spectral emissivity				
$\lambda = 0.546\times10^{-6}$ (m)	0.17	0.15	0.25	0.34	-
$\lambda = 5.0\times10^{-6}$ (m)	0.76	0.69	0.69	0.75	0.90

Table 4.5.8 AC SPECIFIC HEAT CAPACITY, ENTHALPY, AND THERMAL DIFFUSIVITY

Temperature (K)	Heat capacity (kJ/(kg·K))	Enthalpy (kJ/kg)	Thermal diffusivity (10^{-7} m^2/s)
1100	1.222	979	6.349
1200	1.234	1102	6.309
1300	1.251	1226	6.045
1400	1.267	1353	6.172
1500	1.282	1479	6.207
1600	1.298	1608	6.488
1700	1.314	1739	6.572
1800	1.329	1872	6.954
1900	1.345	2006	-
2000	1.361	2141	-
2100	1.377	2278	-
2200	1.392	2416	-

Table 4.5.9 THERMAL CONDUCTIVITY OF HARD SILICATE CONCRETE WITH GRANITE AGGREGATE

Temperature (K)	300	400	500	600	700	800	900
Thermal conductivity (W/(m·K))	1.30	1.26	1.23	1.19	1.16	1.12	1.09

Table 4.5.10 SC MEAN SPECIFIC HEAT CAPACITY

Temperature (K)	300	400	500	600	700	800	900	1000	1100
Mean spec. heat capacity (J/(kg·K))	481	565	649	733	817	901	985	1069	1153

Table 4.5.11 THERMAL EXPANSION OF HARD SILICATE CONCRETE WITH GRANITE AGGREGATE

Temperature (K)	373	573	773	973
Elongation (%)	0.25	0.375	1.125	0.125

Table 4.5.12 DENSITY, THERMAL DIFFUSIVITY, AND ENTHALPY OF SILICATE CONCRETE

Temperature (K)	300	500	700	900	1100
Density (kg/m^3)	2330	2286	2252	2211	2164
Thermal diff. $a \times 10^6$ (m^2/s)	1.16	0.829	0.630	0.501	0.408
Enthalpy (kJ/kg)	0.0	112.8	259.2	439.8	653.6

Table 4.5.13 THE EXPERIMENTAL RESULTS OF MELT-CONCRETE INTERACTION

Concrete type	Melt mass (kg)	Liquid melt composition, (wt.%)	Melt temp. (K)	Time of interac. (hrs)	Erosion rate (mm/min) **/*
ZDC/Comp. 1 (zirconium dioxide concrete)	0.1	67% - low alloyed steel 21% - stainless steel 12% - Zr	2000	2.5	0.013/0
ZDC/Comp. 2	0.2	100% - low alloyed steel	2500	1.0	0/0.05
ZDC/Comp. 3	0.25	57% - low alloyed steel 17% - stainless steel 26% - Zr	1900	3.0	0/0
AC (alumina concrete)	0.1	57% - low alloyed steel 17% - stainless steel 26% - Zr	2130	0.5	0.5/-

Note: ** - axial, * - radial

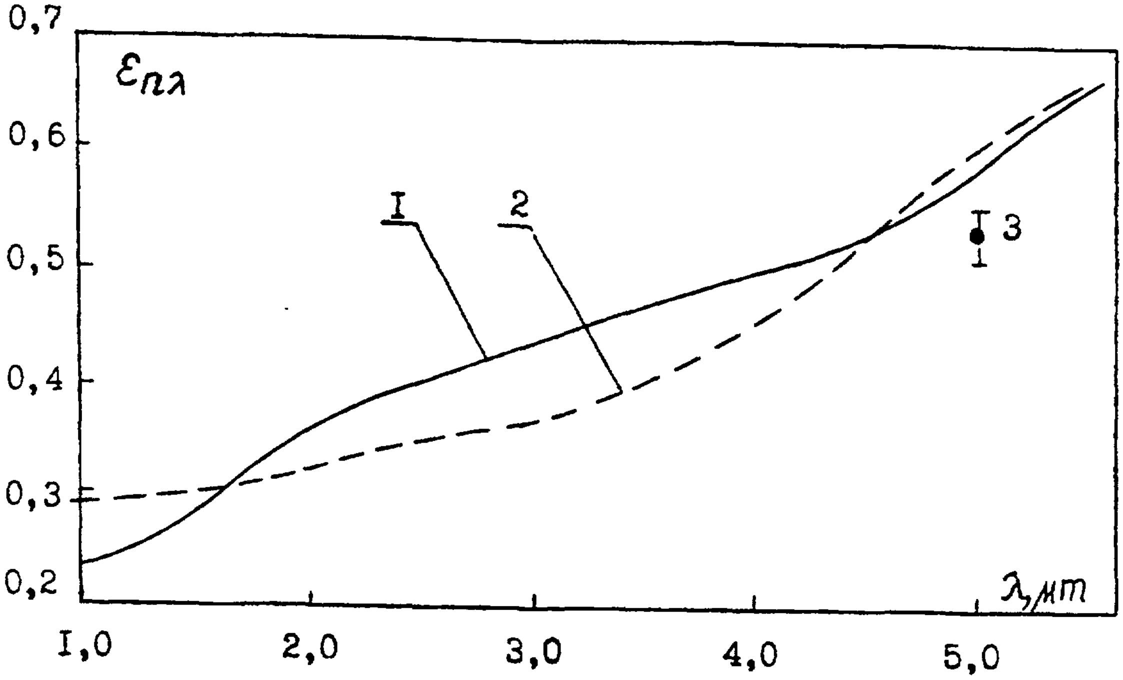

Figure 4.5.1 The ZDC normal spectral emissivity 1 - [5]; 2 - [6]; 3 - [7]

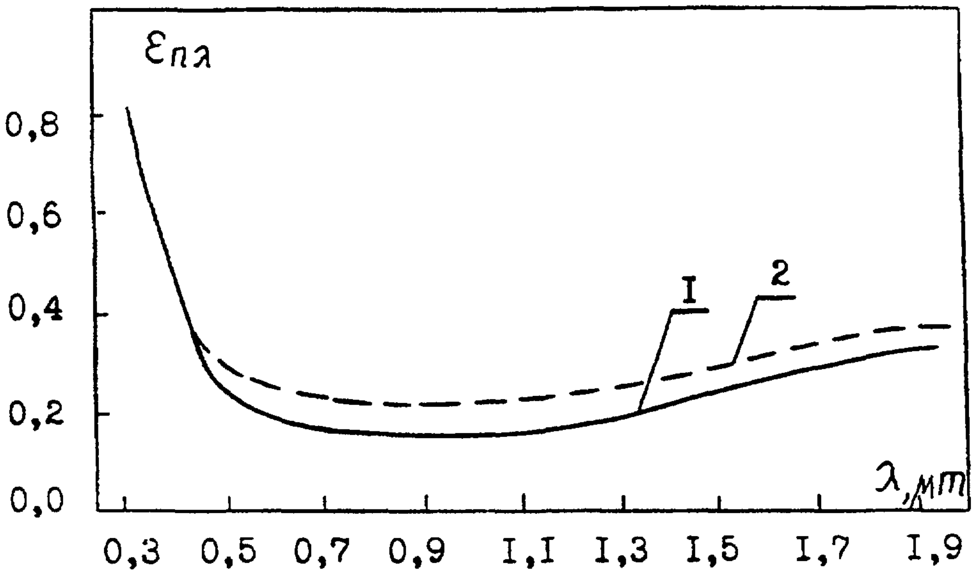

Figure 4.5.2 The ZDC normal spectral emissivity at room temperature
1 - before heating; 2 - after heating

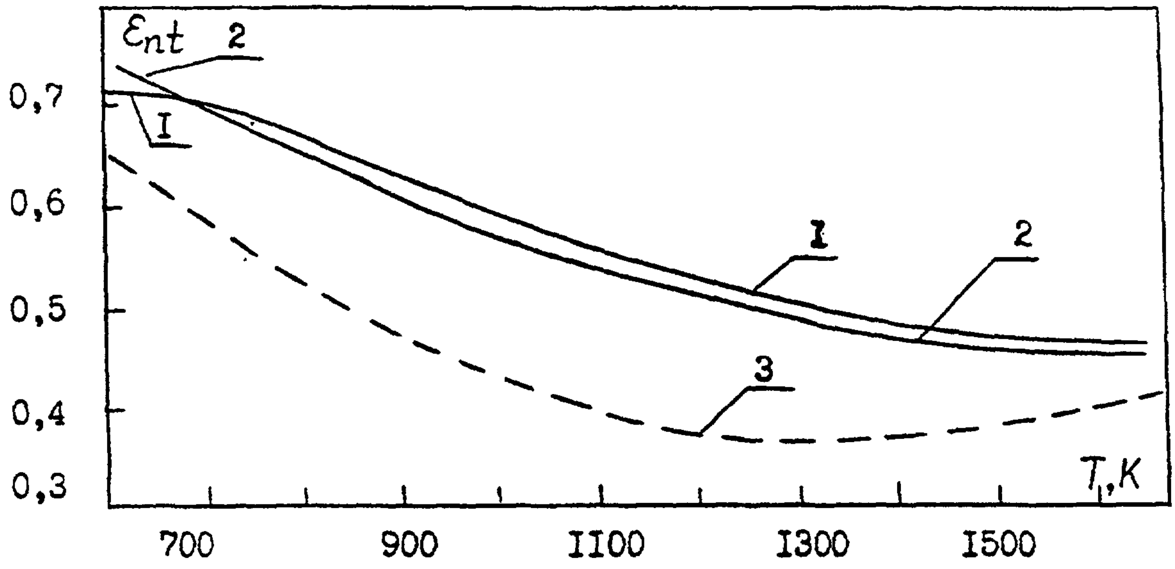

Figure 4.5.3 The ZDC normal total emissivity
1 - experimental data; 2 - calculated data; 3 - [7]

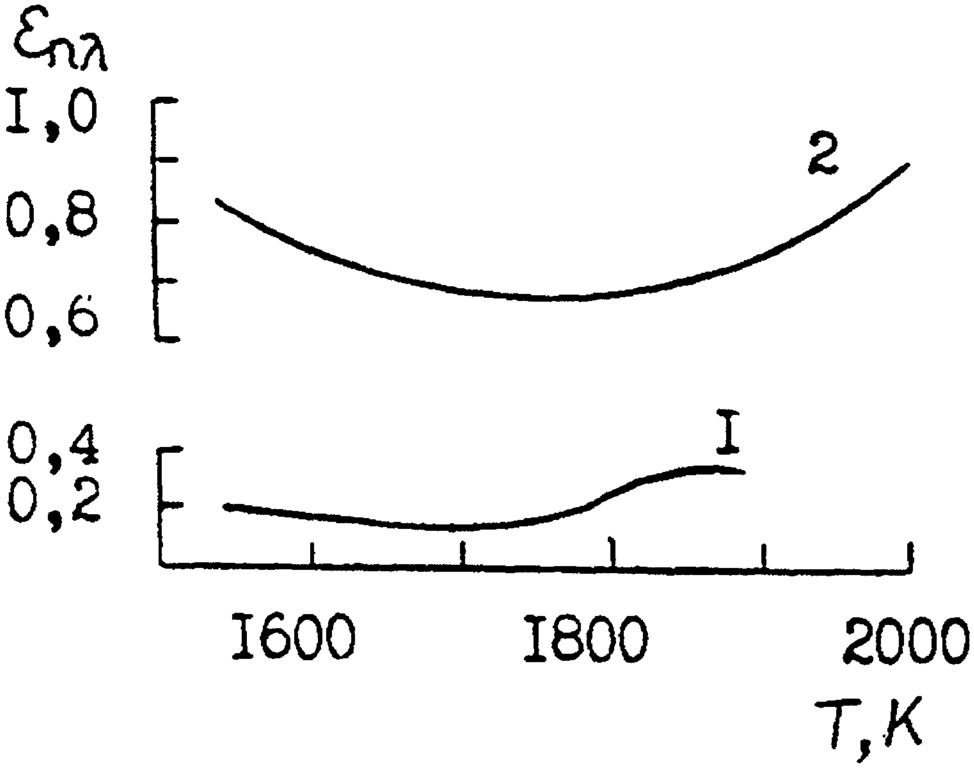

Figure 4.5.4 The AC normal spectral emissivity, 1 - λ = 0.546 μ m; 2 - λ = 5.0 μm

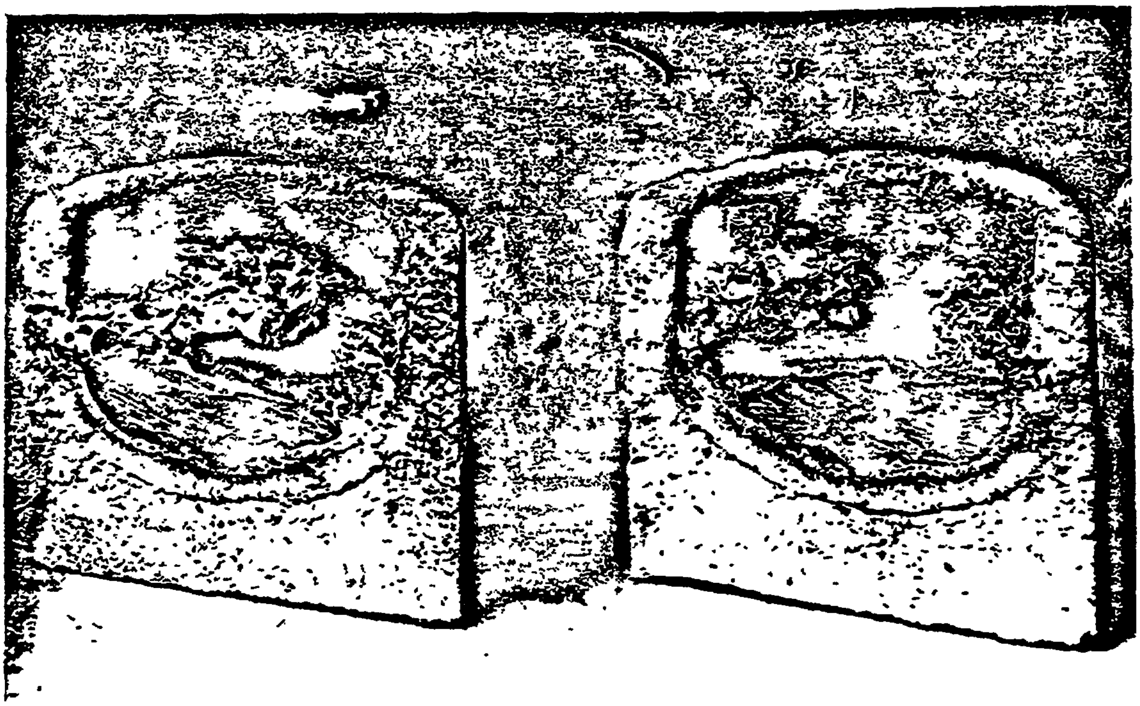

Figure 4 5 5 Cross-section of AC crucible after the experiment

Figure 4 5.6 Cross-section of ZDC crucible after the experiment

References to Section 4.5

[1] HOSEMAN J. P., HENNIES H. H., HASSMANN K., "German results on consequences of LWR severe accidents", Transactions of the American Nuclear Society, 48 (1984) 41-59

[2] WILSON R., et al., "Report to the American Physical Society of the study group on radionuclide release from severe accidents at nuclear power plants", Reviews of Modern Physics, Vol. 57 3 (1985) 1-154

[3] AKOP'AN A. A., BARYKIN B. M., BOROVKOVA L. B., and PAKHOMOV E. P., "Thermophysical characteristics of refractory concrete based on zirconium dioxide", Teplofizika Vysokikh Temperatur (in Russian), No. 4 (1990) 811

[4] KRZHIZHANOVSKII R. E., and SHTERN Z. YU., "Thermophysical Properties of Nonmetallic Matter", Energiya (in Russian), Leningrad (1973)

[5] ANDRIANOVA V. G., PETROV V. A., REZNIK V.YU., et al., "Investigation of radiation characteristics of some refractory materials used in MGD designing", preprint No. 1-111 (in Russian), IVTAN, Moscow (1983)

[6] TOULOUKIAN Y. S., et al., "Thermophysical Properties of Matter", Vol. 8, New York (1972)

[7] ABRAMOV A. S., BARYKIN B. M., ROMANOV A. I., et al., "Materials for a MGD-Generator Channel", Nauka (in Russian), Moscow (1969) 129-134

[8] CHEKHOVSKOI V. YA., ROMANOV A. I., KAULENAS A. A., and STAVROVSKII G. I., "The thermal conductivity of refractory alumina concrete in the temperature range 200-1500°C", Teplofizika Vysokikh Temperatur (in Russian), Vol. 5, No. 5 (1967) 789

[9] DROZDOV R. YA., ROMANOV A. I., and SMIRNOVA A. G., "Materials for a MGD-Generator Channel", Nauka (in Russian), Moscow (1969) 140-142

[10] ABRAMOV A. S., BARYKIN B. M., ROMANOV A.I., et al., "Materials for a MGD-Generator Channel", (in Russian) Nauka, Moscow (1969) 119-128

[11] GURVICH L. V., VEITS I. V., MEDVEDEV V. A., et al., "Thermodynamical Properties of materials" (in Russian)., Vol. 3 (1981)

[12] YAKOVLEV A. I., "Calculations for concrete buildings", Stroyisdat (in Russian), Moscow (1988)

[13] ALSMEYER H., "Beta experiments in verification of the WECHSL code: experimental results on the melt-concrete interaction", Nuclear Engineering and Design, 103 No. 1 (1987) 115-125

5. THERMOPHYSICAL PROPERTIES OF LIGHT AND HEAVY WATER

5.1. INTRODUCTION

As part of the IAEA's CRP, the thermophysical properties of light and heavy water have been reviewed in the Reactor Safety Division of the Bhabha Atomic Research Center (BARC), Mumbai, India. A number of relevant publications were identified and studied and the most suitable formulations for the thermophysical properties of light and heavy water were identified. Details of the literature survey are given in Section 5.2 of this report. Details regarding the evolution of International Association for the Properties of Steam (IAPS) formulations are given in Section 5.3. Sections 5.2 and 5.3 deal with both light and heavy water. The details regarding the mathematical formulations adopted and the computer codes developed for calculating the thermophysical properties of heavy water are given in Sections 5.4 to 5.8.

India has adopted the IAPS formulations, wherein the relevant equation covers the entire range of temperature and pressure (typically up to 1000°C and 1000 MPa) for the property concerned. Such equations are very useful in many applications, particularly in the complex safety analysis codes, where, apart from the property values, their derivatives are also required. However, these equations are quite complex and there are many engineering applications where simpler equations could be gainfully used over a limited range. Such equations have been submitted by Russia for light water and steam. The property values predicted by these equations have been compared with those of IAPS formulations and the differences are insignificant from the point of view of engineering applications. Details of the Russian work are given in Supplement S8. The mathematical formulations (IAPS Formulations) adopted by BARC, India and the details of the computer codes developed for calculating the thermophysical properties of light water and steam are given in Supplement S9.

5.2. LITERATURE SURVEY

In all nearly 75 publications were studied as part of the Indian work. The literature survey revealed that over the last few decades substantial advances have been made in the areas of measurement of thermophysical properties of both light and heavy water and in the representation of these properties using wide ranging algebraic formulations. A large volume of highly accurate data has been reported on density, specific heat, thermal conductivity, viscosity etc. Critical parameter values of light and heavy water have been assessed using experimental data obtained in the critical region. With the improved understanding of the critical point singularity, the saturation states of light water have been redetermined. Results are presented in the form of equations for vapor pressure, densities, enthalpies and entropies of the equilibrium saturated liquid and vapor. These equations are continuous between the triple point and critical point temperatures.

Although limited range equations have been shown to be very useful, the major emphasis in the recent past on thermodynamic property formulations has been on canonical equations that cover the entire range between triple point pressure and temperature to about 1000 MPa and 1000°C. IAPS has made a major contribution to the on going process of evaluating the accuracy of reported data as well as developing formulations on the thermophysical properties of light and heavy water. A brief discussion on the evolution of IAPS formulations is given in the next section.

5.3. EVOLUTION OF IAPS FORMULATIONS

The need for reliable information on the thermodynamic properties of water and steam resulted in a series of International Conferences on the properties of steam [1-3], the first of which was held in 1929. However, the first real results were obtained when the Third International conference on the properties of steam, held in 1934, adopted a set of skeleton tables for the specific volume and enthalpy of water [4-6]. These tables covered temperatures up to 500°C and pressures up to 400 bar. The work on international standardization was interrupted by World War II and resumed again at the Fourth International Conference on the properties of steam, held in 1954. Subsequent activities led to the adoption of a new set of International skeleton tables for the thermodynamic properties of water substance by the Sixth International Conference on the properties of steam, held in 1963 [7]. These tables covered temperatures up to 800°C and pressures up to 1000 bar.

At the Sixth International Conference on the properties of steam held in 1963 a panel was elected, which completed the first international formulation for the transport properties of water in 1964. This conference also constituted an International Formulation Committee (IFC), which completed a formulation for the thermodynamic properties of water for industrial use in 1967 [8] (IFC-67 Formulation) and a formulation for the thermodynamic properties of water for scientific and general use in 1968 [9] (IFC-68 Formulation). The IFC, having completed its tasks, was dissolved at the Seventh International Conference on the properties of steam held in 1968. To provide continuity, the seventh conference formed the International Association for the Properties of Steam (IAPS). In subsequent years the IAPS set up a number of working groups for the study of various properties of light and heavy water substances.

Work to further improve the IFC Formulations was carried out for the following reasons:

(i) Since the IFC formulations consist of separate equations applicable for different subregions, these formulations do not yield a smooth representation of the derivatives of the thermodynamic functions at the boundaries of the subregions [10,11]. This necessitated the development of a single algebraic equation over the entire region covered by the IFC Formulations.

(ii) Geophysical and other technical applications generated a demand for a formulation that would be valid over wider ranges of temperatures and pressures.

(iii) A significant quantity of new accurate experimental data had become available making it possible to develop more accurate formulations for both light and heavy water.

Consequently the IAPS adopted, in 1982, a Provisional IAPS Formulation 1982 for the Thermodynamic properties of ordinary water for scientific and general use and a Provisional IAPS Formulation 1982 for the thermodynamic properties of heavy water [12]. Subsequently the Tenth International Conference on the properties of steam, held in 1984, adopted the IAPS Formulation 1984 for the thermodynamic properties of ordinary water for scientific and general use and the IAPS formulation 1984 for the thermodynamic properties of heavy water [13]. The formulations adopted in 1984 for the thermodynamic properties of light and heavy water are identical with the provisional formulations adopted, earlier, in 1982, except that the equations were given in dimensionless form.

The formulations for the transport properties adopted in 1964 were based on the information available at that time. Since then a considerable quantity of new experimental data for the transport properties of water had become available. This new information made it possible to reduce the deficiencies in the earlier formulations and extended them over a wide range of pressures and temperatures. In view of these considerations the Eighth International Conference on the properties of steam declared the 1964 Formulations for the transport properties obsolete and created a special committee for establishing new formulations for the viscosity and the thermal conductivity of water. Based on the recommendations of the special committee, IAPS issued a document entitled "Release on dynamic viscosity of water substance" in 1975 and a document entitled "Release on conductivity of water substance" in 1977. Tables and equations for the transport properties given in these releases, issued in 1975 and 1977, are to be used in conjunction with the IFC-67 and IFC-68 Formulations for thermodynamic properties.

In 1982 the IAPS amended the release on the viscosity of light water issued in 1975 and the release on thermal conductivity of light water issued in 1977, so as to make these releases consistent with the provisional IAPS formulation 1982 for the thermodynamic properties of ordinary water for scientific and general use [14-15]. Also in 1982, the IAPS adopted formulations for the viscosity and thermal conductivity of heavy water [16]. Subsequently, in 1985, the IAPS issued a release on the

IAPS formulation 1985 for the viscosity of ordinary water and a release on the IAPS Formulation 1985 for the thermal conductivity of ordinary water which superseded the earlier releases on the transport properties issued in 1975 and 1977 and amended in 1982 [14, 15, 17]. These new releases, issued in 1985, were necessitated by the need to make the formulations for transport properties of ordinary water valid over a wider range of temperature and pressure, and to enable better agreement with the experimental data with fewer terms and to account for the singular behaviour of viscosity near the critical point.

The IAPS Formulations have the advantage of not only avoiding the combination of piecewise equations for different regions, but also ensure consistency of all thermodynamic properties over the entire range of validity of the fundamental equations. In view of this the IAPS formulations have been adopted for developing computer programs for the prediction of thermodynamic and transport properties of light and heavy water. The language used is FORTRAN 77. Details of the IAPS formulations for heavy water are given in the following sections. The IAPS formulations for light water, adopted by India, are given in Supplement S9.

5.4. THERMODYNAMIC PROPERTIES OF HEAVY WATER

A computer program was developed for calculating the different thermodynamic properties of heavy water using the IAPS-84 formulation for the thermodynamic properties of heavy water [18]. The different thermodynamic properties that can be calculated using the program are density, specific internal energy, specific entropy, specific enthalpy, C_p, C_V, isothermal compressibility, etc. The formulation is based on the fundamental equation for the Helmholtz function in terms of temperature and density as given below:

$$\bar{A}(\bar{T},\bar{\rho}) = \bar{A}_0(\bar{T},\bar{\rho}) + \bar{A}_1(\bar{T},\bar{\rho}) \tag{5.4-1}$$

where

$$\bar{A}_0(\bar{T},\bar{\rho}) = (A_{00}+A_{01}\bar{T})\ln\bar{T} + \sum_{j=2}^{7} A_{0j}\,\bar{T}^{j-2} + A_{08}\bar{T}\ln\bar{\rho} \tag{5.4-2}$$

$$\bar{A}_1(\bar{T},\bar{\rho}) = \bar{T}\bar{\rho}\left(\frac{1}{\bar{\bar{T}}}-\frac{1}{\bar{\bar{T}}_1}\right)\sum_{i=1}^{7}\left(\frac{1}{\bar{\bar{T}}}-\frac{1}{\bar{\bar{T}}_i}\right)^{i-2}\left[\sum_{j=1}^{8} A_{ij}(\bar{\rho}-\bar{\rho}_i)^{j-1} + \exp(-1.5394\bar{\rho})\left(\sum_{j=9}^{10} A_{ij}\,\bar{\rho}^{j-9}\right)\right] \tag{5.4-3}$$

The values of the parameters A_{OJ}, $\bar{A}_{ij}$, $\bar{T}_i$ and $\bar{\rho}_i$ are listed in the Tables 5.4.1 to 5.4.3.

All thermodynamic properties are expressed in terms of $\bar{A}$ ($\bar{T}$, $\bar{\rho}$) and its first and second derivatives with respect to $\bar{T}$ and $\bar{\rho}$ are as follows

$$\bar{V} = \bar{\rho}^{-1} \tag{5.4-4}$$

$$\bar{P} = \bar{\rho}^2\left(\frac{\partial\bar{A}}{\partial\bar{\rho}}\right)_{\bar{T}} \tag{5.4-5}$$

$$\left(\frac{\partial\bar{P}}{\partial\bar{\rho}}\right)_{\bar{T}} = \frac{2\bar{P}}{\bar{\rho}} + \bar{\rho}^2\left(\frac{\partial^2\bar{A}}{\partial\bar{\rho}^2}\right)_{\bar{T}} \tag{5.4-6}$$

$$(\bar{K}_T)^{-1} = \bar{\rho}\left(\frac{\partial\bar{P}}{\partial\bar{\rho}}\right)_{\bar{T}} \tag{5.4-7}$$

$$\left(\frac{\partial \bar{P}}{\partial \bar{T}}\right)_{\bar{\rho}} = \bar{\rho}^2 \frac{\partial^2 \bar{A}}{\partial \bar{\rho}\, \partial \bar{T}} \tag{5.4-8}$$

$$\bar{s} = -\left(\frac{\partial \bar{A}}{\partial \bar{T}}\right)_{\bar{\rho}} \tag{5.4-9}$$

$$\bar{U} = \bar{A} + \bar{T}\bar{s} \tag{5.4-10}$$

$$\bar{h} = \bar{U} + \frac{\bar{P}}{\bar{\rho}} \tag{5.4-11}$$

$$\bar{G} = \bar{A} + \frac{\bar{P}}{\bar{\rho}} \tag{5.4-12}$$

$$\bar{C}_V = -\bar{T}\left(\frac{\partial^2 \bar{A}}{\partial \bar{T}^2}\right)_{\bar{\rho}} \tag{5.4-13}$$

$$\bar{C}_P = \bar{C}_V + \left(\frac{\bar{T}}{\bar{\rho}^2}\right) \frac{(\partial \bar{P}/\partial \bar{T})^2_{\bar{\rho}}}{(\partial \bar{P}/\partial \bar{\rho})_{\bar{T}}} \tag{5.4-14}$$

$$\bar{w} = \left[\frac{\bar{C}_P}{\bar{C}_V}\left(\frac{\partial \bar{P}}{\partial \bar{\rho}}\right)_{\bar{T}}\right]^{1/2} \tag{5.4-15}$$

$\bar{T} = T/T^*$ $\qquad$ $\bar{P} = P/P^*$

$\bar{A} = A/A^{**}$ $\qquad$ $\bar{V} = V\rho^*$

$\bar{h} = h/A^{**}$ $\qquad$ $\bar{U} = U/A^{**}$

$\bar{s} = s/s^{**}$ $\qquad$ $\bar{G} = G/A^{**}$

$\bar{C}_P = C_P/s^{**}$ $\qquad$ $\bar{C}_V = C_V/s^{**}$

$\bar{w} = w/w^{**}$ $\qquad$ $\bar{K}_T = K_T P^*$

$\bar{\rho} = \rho/\rho^*$

where

T^* = 643.89 K, $\qquad$ ρ^* = 358.0 kg/m^3,

P^* = 21.671 MPa, $\qquad$ A^{**} = 605.3352 • 10^2 J/kg,

s^{**} = 94.01221 J/kg-K, $\qquad$ w^{**} = 246.036 m/s.

Range of validity: 276.95 K $\leq T \leq$ 800 K and 0 $\leq P \leq$ 100 MPa

For calculating density, an initial value is required for iterative calculations. Up to 373 K, an initial guess density of 1100 kg/m^3 is suitable. For temperatures between 373 K and 623.15 K, the program calculates the vapor pressure of heavy water and then by comparing it with the given pressure, determines whether the heavy water is in the liquid or gaseous phase at the given temperature and pressure. If it is in the liquid phase, an initial density of 1100 kg/m^3 is used and if it is in gaseous phase an initial density corresponding to the gaseous phase density, calculated by ideal gas law works satisfactorily. For temperatures between 623.15 K and 723.15 K, an initial density of either 1100 kg/m^3 or some fraction/multiple of the gas phase density is arbitrarily chosen, depending on the pressure, for rapid convergence. Above 723.15 K, the gas phase density calculated by the ideal gas law is used as an initial value.

5.5. THERMAL CONDUCTIVITY OF HEAVY WATER

A computer program was developed for calculating the thermal conductivity of heavy water according to IAPS-1982 release [16]. The formulation is as follows:

$$\lambda = 0.742128\times10^{-3}(\lambda_0+\Delta\lambda+\Delta\lambda_c+\Delta\lambda_L) \qquad (5.5\text{-}1)$$

$$\lambda_0 = \sum_{i=0}^{5} A_i T_r^i \qquad (5.5\text{-}2)$$

$$\Delta\lambda = B_0\left[1-\exp(B_e\rho_r)\right]+\sum_{j=1}^{4} B_j\rho_r^j \qquad (5.5\text{-}3)$$

$$\Delta\lambda_c = C_1 f_1(T_r) f_2(\rho_r)\left[1+[f_2(\rho_r)]^2\left\{\frac{C_2[f_1(T_r)]^4}{f_3(T_r)}+\frac{3.5 f_2(\rho_r)}{f_4(T_r)}\right\}\right] \qquad (5.5\text{-}4)$$

$$\Delta\lambda_L = D_1\left[f_1(T_r)\right]^{1.2}\left\{1-\exp\left[-(\rho_r/2.5)^{10}\right]\right\} \qquad (5.5\text{-}5)$$

$$f_1(T_r) = \exp\left(C_{T1}T_r+C_{T2}T_r^2\right) \qquad (5.5\text{-}6)$$

$$f_2(\rho_r) = \exp\left[C_{R1}(\rho_r-1)^2\right]+C_{R2}\exp\left[C_{R3}(\rho_r-\rho_{r1})^2\right] \qquad (5.5\text{-}7)$$

$$f_3(T_r) = 1+\exp[60(\tau-1)+20] \qquad (5.5\text{-}8)$$

$$f_4(T_r) = 1+\exp[100(\tau-1)+15] \qquad (5.5\text{-}9)$$

$$\tau = \frac{T_r}{|T_r-1.1|+1.1} \qquad (5.5\text{-}10)$$

$$T_r = T/T^* \qquad (5.5\text{-}11)$$

$$\rho_r = \rho/\rho^* \qquad (5.5\text{-}12)$$

The constants appearing in the above equations are listed below:

T^* = 643.89 K
A_0 = 1.0000
A_1 = 37.3223
A_2 = 22.5485
A_3 = 13.0465
A_4 = 0.0
A_5 = -2.60735

ρ^* = 358.0 kg/m^3
B_e = -2.50600
B_0 = -167.310
B_1 = 483.656
B_2 = -191.039
B_3 = 73.0358
B_4 = -7.57467

C_1 = 0.354296×10^5
C_2 = 0.5×10^{10}
C_{T1} = 0.144847
C_{T2} = -5.64493
C_{R1} = -2.8
C_{R2} = -0.080738543

D_1 = -741.112 ρ_{r1} = 0.125698 C_{R3} = -17.9430

For calculating the thermal conductivity values at different temperatures and pressures, the corresponding density values can be calculated using the IAPS-84 formulation.

Range of validity: 277 K $\leq T \leq$ 825 K and 0 MPa $< P \leq$ 100 MPa.

5.6. VISCOSITY OF HEAVY WATER

A computer program has been developed to calculate the viscosity of heavy water using the IAPS-82 release [16]. The recommended equation is:

$$\eta = \eta_0(T_r)\exp\left[\rho_r\left\{\sum_{i=0}^{5}\sum_{j=0}^{6} A_{ij}\left(T_r^{-1}-1\right)^i(\rho_r-1)^j\right\}\right] \qquad (5.6\text{-}1)$$

where

$$\eta_0(T_r) = HT_r^{1/2}\left(\sum_{k=0}^{3} B_k T_r^{-k}\right)^{-1} \qquad (5.6\text{-}2)$$

The reduced variables are:

$T_r = T/T^*$ and $\rho_r = \rho/\rho^*$

where

T^* = 643.89 K and ρ^* = 358 kg/m^3.

Values for the coefficients are given in Table 5.6.1 and Table 5.6.2.
Range of validity: 277 K $\leq T \leq$ 775 K and 0 MPa $< P \leq$ 100 MPa.

5.7. SATURATION PROPERTIES OF HEAVY WATER

A computer program has been developed to calculate the vapor pressure of heavy water for a given value of temperature. The equation [19] adopted for programming into the computer code is as follows:

$$\ln[P/P_C] = T_C/T\left[n_1\tau + n_2\tau^{1.9} + n_4\tau^2 + n_{11}\tau^{5.5} + n_{20}\tau^{10}\right] \qquad (5.7\text{-}1)$$

where

τ = [1 - T/T_C]
T_C = 643.89 K
P_C = 21.66 MPa
n_1 = -7.81583
n_2 = 17.6012
n_4 = -18.1747
n_{11} = -3.92488
n_{20} = 4.19174

5.8. RESULTS AND DISCUSSIONS

The thermophysical properties of heavy water have been calculated using the computer programme described earlier. The results are in excellent agreement with the values given in the corresponding references. The ranges of validity of the formulations adopted for calculating the various thermophysical properties of heavy water are different for different properties, as indicated in the relevant sections. In all cases the range is below 800°C. As per the matrix drawn up in the earlier phase of CRP, the database is to include properties up to 800°C. Since published information on the properties of heavy water beyond the temperature ranges given in the earlier sections for the IAPS formulations is not available, it is suggested that the same IAPS formulations be used for generating heavy water property data up to 800°C. Judging from the trends of the data so generated over the extended range, using IAPS formulations, it seems reasonable to assume that the same IAPS formulations could be used to calculate various thermophysical properties of heavy water up to 800°C.

The uncertainties/errors involved are not expected to be significant. However, this should be checked as and when the measured data over the extended range becomes available. Future activities should include a review of literature data to examine the accuracy of extrapolation of the IAPS formulation.

Nomenclature to Chapter 5

A - Helmholtz function, dimensionless
C_P - specific heat at constant pressure, J/(kg·K)
C_V - specific heat at constant volume, J/(kg·K)
G - specific Gibbs function, dimensionless
h - enthalpy, J/kg
η - viscosity of heavy water, Pa·s
P - pressure, MPa
s - specific entropy, J/(kg-K)
T - temperature, K
U - internal energy, J/kg
V - specific volume, m^3/kg
w - speed of sound, m/s
ρ - density, kg/m^3
λ - thermal conductivity, W/(m·K)
K_T - isothermal compressibility

Subscripts

c - critical point

Superscripts

$-$ - dimensionless
$*$ - reference value
$**$ - derived reference value

Table 5.4.1 COEFFICIENTS A_{0j} FOR A_0 ($\bar{T}$, $\bar{\rho}$)

j	A_{0j}
0	0.5399322597 E-2
1	-0.1288399716 E 2
2	0.3087284587 E 2
3	-0.3827563059 E 2
4	0.4424799189
5	-0.1256336874 E 1
6	0.2843343470 E 0
7	-0.2401555088 E-1
8	0.4415884023 E 1
Remark:	The notation E± stands for decimal exponent, for example 0.539E-5 = 0.539×10^{-5}

Table 5.4.2 COEFFICIENTS A_{ij} FOR A_1 ($\bar{T}$, $\bar{\rho}$)

i	j	A_{ij}
1	1	0.115623643567 E 3
1	2	-0.161413392951 E 3
1	3	0.108543003981 E 3
1	4	-0.471342021238 E 2
1	5	0.149218685173 E 2
1	6	-0.360628259650 E 1
1	7	0.686743026455
1	8	-0.951913721401 E-1
1	9	-0.157513472656 E 4
1	10	-0.433677787466 E 3
2	1	0.607446060304 E 2
2	2	-0.927952190464 E 2
2	3	0.632086750422 E 2
2	4	-0.264943219184 E 2
2	5	0.905675051855 E 1
2	6	-0.578949005123
2	7	0.665590447621
2	8	-0.525687146109 E-1
2	9	-0.341048601697 E 4
2	10	-0.146971631028 E 4
3	1	0.444139703648 E 2
3	2	-0.580410482641 E 2
3	3	0.354090438940 E 2
3	4	-0.144432210128 E 2
3	9	-0.102135518748 E 4
3	10	-0.136324396122 E 4
4	1	0.157859762687 E 2
4	2	-0.194973173813 E 2
4	3	0.114841391216 E 2
4	4	-0.196956103010 E 1
4	9	-0.277379051954 E 3
4	10	-0.481991835255 E 3
5	1	-0.619344658242 E 2
5	2	0.791406411518 E 2
5	3	-0.484238027539 E 2
5	4	0.191546335463 E 2
5	9	0.128039793871 E 4
5	10	0.186367898973 E 4
6	1	-0.749615505949 E 2
6	2	0.947388734799 E 2
6	3	-0.575266970986 E 2
6	4	0.173229892427 E 2
6	9	0.137572687525 E 4
6	10	0.231749018693 E 4
7	1	-0.260841561347 E 2
7	2	0.328640711440 E 2
7	3	-0.186464444026 E 2
7	4	0.484262639275 E 1
7	9	0.430179479063 E 3
7	10	0.822507844138 E 3

Coefficients not given in this table are zero

Table 5.4.3 PARAMETERS $\bar{T}_i$ AND $\bar{\rho}_i$

	$\bar{T}_i$	$\bar{\rho}_i$
1	0.1000038832 E 1	0.1955307263 E 1
2	0.6138578282	0.3072625698 E 1
3	0.6138578282	0.3072625698 E 1
4	0.6138578282	0.3072625698 E 1
5	0.6138578282	0.3072625698 E 1
6	0.6138578282	0.3072625698 E 1
7	0.6138578282	0.3072625698 E 1

Table 5.6.1 THE COEFFICIENTS A_{ij}

i j	0	1	2	3	4	5
0	0.4864192	-0.2448372	-0.8702035	0.8716056	-1.051126	0.3458395
1	0.3509007	1.315436	1.297752	1.353448	0.0	0.0
2	-0.2847572	-1.037026	-1.287846	0.0	0.0	-0.02148229
3	0.07013759	0.4660127	0.2292075	-0.4857462	0.0	0.0
4	0.01641220	-0.02884911	0.0	0.1607171	0.0	-0.009603846
5	-0.01163815	-0.008239587	0.0	0.0	0.0	0.004559914
6	0.0	0.0	0.0	-0.003886659	0.0	0.0

Table 5.6.2 THE COEFFICIENTS H AND B_k

H = 55.2651×10^{-6} Pa·s
B_0 = 1.0000
B_1 = 0.940695
B_2 = 0.578377
B_3 = -0.202044

References to Chapter 5

[1] BEITLER, S.R., in Proceedings of the 8th International Conference on the Properties of Steam, edited by P. Bury, H. Perdon, and B. Vodar (Editions Europeennes Thermiques et Industries, Paris (1975), p. 9

[2] HAUSEN, H., in Proceedings of the 9th International Conference on the Properties of Steam, edited by J. Straub and K. Schefiler (Pergamon, New York, 1980), p. 11

[3] WHITE, H. J., in Proceedings of the 9th International Conference on the Properties of Steam, edited by J. Straub and K. Schefiler, Pergamon, New York (1980), p. 18

[4] KEENAN, J. H. and KEYES, F. G., Thermodynamic Properties of Steam, Wiley, New York (1936)

[5] KOCH, W., VDI-Wasserdampftafeln, Springer, Berlin (1937)

[6] CALLENDAR, G. S. and EGERTON, A. C., The 1939 Calendar Steam Tables, Arnold, London (1939)

[7] MEYER, C. A., McCLINTOCK, R. B., SILVESTRI, G. J., and SPENCER, R. C., ASME Steam Tables, 5th Ed., American Society of Mechanical Engineers New York) (1983) pp. 4

[8] MEYER, C. A., McCLINTOCK, R. B., SILVESTRI, G. J., and SPENCER, R. C., ASME Steam Tables, 5th Ed., American Society of Mechanical Engineers New York (1983), pp. 1

[9] The 1968 IFC Formulation for scientific and general use, American Society of Mechanical Engineers, New York (1968)

[10] BASU, R. S., SENGERS, J. V. and KESTIN, J., in Proceedings of the 9th International Conference on the Properties of Steam, edited by J. Straub and K. Schefiler, Pergamon, New York (1980), p. 445

[11] SENGERS, J. V., BASU, R. S., KAMGAR-PARSI, B. and KESTIN, J., Mech. Eng. 104 (5), 60 (1982)

[12] KESTIN, J., SENGERS, J.V. and SPENCER, R.C., Mech. Eng. 105 (3), 72 (1983)

[13] KESTIN, J., SENGERS, J. V., Mech. Eng. 107 (6), 89 (1985)

[14] SENGERS, J. V., and KAMGAR-PARSI, B., J. Phys. Chem. Ref. Data 13, 185 (1984)

[15] SENGERS, J. V., WATSON, J. T. R., BASU, R. S., KAMGAR-PARSI, B. and HENDRICKS, R. C., J. Phys. Chem. Ref. Data 13, 893 (1984) 21

[16] MATSUNAGA, N., and NAGASHIMA, A., J. Phys. Chem Ref. Data 12, 933 (1983)

[17] WATSON, J. T. R., BASU, R. S. and SENGERS, J. V., J. Phys. Chem. Ref. Data 9, 1255 (1980)

[18] KESTIN, J. and SENGERS, J. V., J. Phys. Chem. Ref. Data 15, 1, 305 (1986)

[19] HILL, P. G. and MacMILLAN, R. D., J. Phys, Chem. Ref. Data, 9, 3, 735 (1980)

6. THERMOPHYSICAL PROPERTIES OF GASES

This chapter has been prepared by Messrs V. Bobkov, L. Fokin, V. Popov, V. Ljusternic of the Institute of Physics and Power Engineering, Obninsk, Russia. Interpreter is Mr. V. Vinogradov.

6.1. THE PROPERTIES OF HYDROGEN

The thermophysical properties of hydrogen are presented here covering the ranges 300 to 2000 K and from 0.1 to 1.2 MPa. These ranges correspond to the gaseous state of hydrogen.

Normal hydrogen n-H_2 (below H_2) is a mixture of ortho-hydrogen (75%) and para-hydrogen (25%) which corresponds to the high-temperature equilibrium concentration. The recommendations presented here are for non-dissociated hydrogen.

The molecular weight $M(H_2)=2.0159 \pm 0.0003$ kg/kmol [1]. Natural hydrogen is the mixture of isotopes: 99.985% of hydrogen and 0.015% of deuterium. The value of the specific gas constant now accepted is $R=4124.5 \pm 0.1$ J/(kg·K) [2,3].

The main experimental data had been obtained from Refs [4-10] and the data analysis is outlined in [11].

Here and below the errors are the doubled root mean squares $\Delta_{0.9} \cong 2\sigma$ corresponding to the 90% probability level.

The specific volume V can be calculated using the real gas equation taking into account the second virial coefficient, m^3/kg, [13]:

$$V = \frac{RT}{P} + B(T) \qquad (6.1\text{-}1a)$$

where

$$B(T) = b_0 \cdot B^*,$$

$$B^* = \sum_{i=1}^{5} a_i (\ln T^*)^{-(i-1)} \qquad (6.1\text{-}1b)$$

where

P is in Pa, T in K, $b_0 = 18.603\times10^{-3}$ m^3/kg, $T^* = T/\varepsilon$, $\varepsilon = 25.7$ K, the values of a_i are presented in Table 6.1.1. The errors are less than 6%.

Specific heat capacity at constant pressure, J/(kg·K), [2,7]:

$$C_P = C_{P0} - \frac{B_2 P}{T} \qquad (6.1\text{-}2a)$$

where

$$\frac{C_{P0}}{R} = \sum_{i=-2}^{4} f_i (T\ 10^{-4})^i; \qquad B_2 = b_o\ T^{*2} \frac{d^2 B^*}{d(T^*)^2} \qquad (6.1\text{-}2b)$$

values for f_i are presented in Table 6.1.1. The errors are less than 0.1% in the ranges of T and P: from 200 to 2000 K and from 0.1 to 1.2 MPa.

Specific heat capacity at constant volume, J/(kg·K), [2,7]:

$$C_V = C_{V0} - \frac{(2B_1 + B_2)P}{T} \qquad (6.1\text{-}3)$$

where

$$C_{V0} = C_{P0} - R,, B_1 = T\frac{dB}{dT} = b_o T^* \frac{dB^*}{dT^*} \qquad B_2 \text{ is above.}$$

The errors are less than 0.1% in the ranges of T and P: from 200 to 2000 K and from 0.1 to 1.2 MPa.

Sound velocity, m/s, [13]:

$$\omega = \sqrt{\frac{C_{P0}}{C_{V0}} V^2 \left(\frac{dP}{dV}\right)_T} \tag{6.1-4}$$

Specific enthalpy, J/kg, [7]:

$$h = \left(H^o_{300} - H^o_0\right) M^{-1} + 10^4 \int_{0.03}^{\tau} C_{P0} d\tau + \left(B - B_1\right) P \tag{6.1-5a}$$

$$H^o_{300} - H^o_0 = 8.521 \cdot 10^6 \quad J/kmol. \tag{6.1-5b}$$

The initial point is the gaseous state at $T = 0$ K, $\tau = (10^{-4} \cdot T)$ K, and where B, B_1 and C_{P0} have been given above. The errors are less than 0.2% in the T ranges 300 to 2000 K and for $P < 1.2$ MPa.

Specific entropy, J/(kg·K), [8]:

$$s = S^o_{300} \; M^{-1} + \int_{0.03}^{\tau} C_{P0} d\left(\ln \tau\right) - R \ln \frac{P}{P_0} - \frac{B_1 P}{T} \tag{6.1-6a}$$

$$S^o_{300} = 130.747 \times 10^3 \quad J/(kmol \cdot K) \tag{6.1-6b}$$

where M is the molecular weight, and the last term is the entropy at standard temperature and pressure ($T = 300$ K, $P_0 = 0.101325 \times 10^6$ Pa), C_{P0}, τ and B are presented above. The errors are less than 0.1% in the ranges of T and P from 300 to 2000 K and 0.1 to 1.2 MPa, respectively.

Dynamic viscosity, Pa·s, [13]:

$$\mu = \frac{2.669 \times 10^{-6} \sqrt{M\,T}}{d^2 K} \tag{6.1-7a}$$

$$K = \sum_{i=1}^{5} c_i \left(\ln T^*\right)^{-(i-1)} \tag{6.1-7b}$$

where d = 3.1 Å (Angstrom), the values of c_i are presented in Table 6.1.1. The errors are 1% for $300 < T < 1000$ K and 1.5% for $1000 < T < 2000$ K.

Thermal conductivity, W/(m·K) [14]:

$$\lambda = \mu \, C_{V0} f_E \tag{6.1.8a}$$

$$f_E = 3.75 \frac{R}{C_{V0}} + E \frac{C_{in}}{C_{V0}} \tag{6.1.8b}$$

$$C_{in} = C_{P0} - \frac{5}{2} R \tag{6.1.8c}$$

$$E = 1.2 \sum_{i=1}^{3} e_i \left(\ln T^*\right)^{-(i-1)} \tag{6.1-8d}$$

where μ(Pa·s) and C_{V0}(J/kg·K) are presented above, values of c_i are given in Table 6.1.1. The errors are 2% for 300 K < T < 1000 K and 3% for 1000 K < T < 2500 K.

The additional properties can be calculated using the well known equations:
thermal diffusivity, $a = \lambda/(\rho \cdot C_P)$, m^2/s; kinematic viscosity, $\nu = \mu/\rho$, m^2/s; Prandtl number, $Pr = \nu/a$.

The error on all the equations presented can be estimated using the method of error propagation. The recommendations lie within the error limits for the recent data on hydrogen [14-17].

6.2. THE PROPERTIES OF HELIUM

Presented here are the thermophysical properties of gaseous helium (He) in the ranges 300 K < T < 2500 K and 0.1 < P < 6 MPa.

Natural helium consists of ^{4}He (99.999863 ± 6×10^{-6}%) and ^{3}He. The atomic weight is M = 4.002602 ± 4×10^{-6} kg/kmol [1,2]. The specific gas constant is R = 2077.27 ± 0.04 J/(kg·K) [3]. Here and below the errors are the doubled root mean squares $\Delta_{0.9} \cong 2\sigma$ corresponding to the 90% probability level.

The boiling temperature of He at normal pressure, (P_0 = 0.101325 MPa), is T_b = 4.22 K, the critical point parameters are: temperature T_{cr} = 5.19 K, pressure P_{cr} = 0.227 MPa, density ρ_{cr} = 70.2 kg/m^3 [3]. The range of parameters considered, correspond to the ratios: $\rho/\rho_{cr} < 0.17$ and $T/T_{cr} > 60$, i.e. to the gaseous helium. In this state the thermophysical properties are described by the ideal gas equation $PV = RT$ with a very small correction to volume due to the second virial coefficient. At the same time binary interactions determine the dynamic viscosity and thermal conductivity, small corrections due to triple interactions.

Within the last ten years two calculational methods have been reported for the thermophysical properties of gaseous He which cover the high temperatures region. The first is the semi-empirical method which consider all inert gases in terms of binary interactions [18]. The second is the description of the various properties of He in terms of interaction potentials obtained from multiproperty analysis [19]. In the last case the authors have used both the experimental data on differential and integral He-He cross-sections and the experimental thermophysical data on the second virial coefficient at temperature up to 1473 K [20], on viscosity - up to 1600 K [21] and 2150 K [22] and on thermal conductivity - up to 1200 K [23] and 2100 K [24]. On this basis [19] the reference data tables for viscosity and thermal conductivity at temperature from 5 to 5000 K [25] were obtained. These tables were accepted in Russia as the standard reference data [26] and are within the estimated errors of the experimental data [18,19,25].

Specific volume can be calculated using the real gas equation taking the second virial coefficient, m^3/kg into account [18,27]:

$$V = \rho^{-1} = \frac{RT}{P} + B(T) \tag{6.2-1a}$$

$$B(T) = a_1 T^{*-\frac{1}{2}} + a_2 T^{*-\frac{1}{3}} + a_3 T^{*-\frac{1}{4}} \tag{6.2-1b}$$

where $T^* = T/10.4$, T is in K, the values of a_i are given in Table 6.2.1. The errors associated with $B(T)$ are: 2% for 300 K < T < 1300 K and 5% for 1300 K < T < 2500 K.

Specific heat capacity at constant pressure, *J/(kg·K) [27]:*

$$C_P(T,P) = C_{P0} - \left(RT^2 \frac{d^2B}{dT^2} \right) \frac{P}{RT} \tag{6.2-2}$$

where $C_{P0} = 5R/2 = 5193.17$ J/(kg·K), T is in K, P is in Pa. The errors are less than 0.1%.

Specific heat capacity at constant volume, *J/(kg·K) [27]:*

$$C_V = C_{V0} - R \left(2T\frac{dB}{dT} + T^2 \frac{d^2B}{dT^2} \right) \frac{P}{RT} \tag{6.2-3}$$

where $C_{V0} = 3R/2 = 3115.91$ J/kg·K. The errors are less than 0.1%.

Isoentropic coefficient, *[27]:*

$$k = -\frac{C_P}{C_V} \left(\frac{d \ln P}{d \ln V} \right)_T \tag{6.2-4}$$

where at $P \Rightarrow 0$ there is the limit: $k^0 = 5/3$.

Thermodynamic sound velocity, *m/s, [27]:*

$$w = \sqrt{k \left(1 + B \frac{P}{RT} \right) RT} \tag{6.2-5}$$

where P is in Pa, T is in K.

Specific enthalpy, *J/kg, [27]:*

$$h = \Delta h_0 + \left(B - T\frac{dB}{dT} \right) P \tag{6.2-6}$$

where $\Delta h_0 = C_{P0}T = 5193.17\ T$. The initial point is the ideal gas state (0 K). The errors are less than 0.1% for 300 K < T < 2500 K and 0.1 < P < 6 MPa.

Specific entropy, *J/(kg·K), [27,28]:*

$$s = s_0(T) - R \ln\frac{P}{P_0} - \frac{1}{T} \left(T\frac{dB}{dT} \right) P \tag{6.2-7a}$$

where

$$s_0(T) = 31522 + 5193.17 \ln(T/300) \tag{6.2-7b}$$

Here T is in K, P is in Pa, $P_0 = 0.101325 \times 10^6$ Pa. The errors are less than 0.1% for 300 K < T < 2500 K and 0.1 < P < 6 MPa.

***Dynamic viscosity**, Pa·s, [27]:*

$$\mu = \mu_0(T)\left\{1 + 10^{-3}\left[k_1(T^*)\right]^{3/2}\frac{P}{RT}\right\} \tag{6.2-8a}$$

where

$$\mu_0(T) = \frac{0.7884\times10^{-6}\sqrt{T}}{k_1(T^*)} \tag{6.2-8b}$$

$$k_1(T^*) = \exp\left[\sum_{i=1}^{5} b_i\,(\ln T^*)^{i-1}\right] \tag{6.2-8c}$$

Here $T^* = T/10.4$, T is in K, P is in Pa and the values of b_i are given in Table 6.2.1. The errors are 1.5% for T from 300 to 1200 K and 2.5% at T from 1200 to 2000 K and 3% above $300 < T < 1200$ K, 2.5% for $1200 < T < 2000$ K and 3% above 2000 K.

***Thermal conductivity**, W/(m·K), [18,25,27]:*

$$\lambda = \lambda_0(T)\left\{1 + 3.2\times10^{-3}\left[k_1(T^*)\right]^{3/2}\frac{P}{RT}\right\} \tag{6.2-9a}$$

where

$$\lambda_0(T) = \frac{6.161\times10^{-3}\sqrt{T}}{k_1(T^*)} \tag{6.2-9b}$$

k_1 is given above. The errors are 1.5% for $300 < T < 1200$ K, 2.5% for $1200 < T < 2000$ K and 3% above 2000 K.

Additional properties can be calculated using the known equations: $\nu = \mu/\rho$; $a = \lambda/(C_P\cdot\rho)$; $Pr = \nu/a$.

6.3. THE PROPERTIES OF KRYPTON

The thermophysical properties of gaseous krypton (Kr) are given here for the temperature range 300 to 2500 K and the pressure range 0.1 to 6 MPa.

Natural Kr is a mixture of isotopes from ^{78}Kr to ^{86}Kr with a prepanderance (57%) of ^{84}Kr. The atomic weight of Kr is $M = 83.80 \pm 0.02$ kg/kmol [1,2,11]. The specific gas constant is $R = 99.218 \pm 0.02$ J/(kg·K) [2].

The boiling temperature of Kr is $T_b = 119.93$ K at normal pressure ($P_0 = 0.101325$ MPa), the critical point parameters are: $T_{cr} = 209.41$ K, $P_{cr} = 5.50$ MPa, $\rho_{cr} = 1090$ kg/m^3 [2]. The range of T and P_1 considered corresponds to the gaseous state of krypton with the ratios: $\rho/\rho_{cr} \leq 0.2$ and $T/T_{cr} \geq 1.5$. The thermophysical properties described here have been derived from the ideal gas state equation $P = \rho RT$ with the binary atomic interactions and triple atomic collisions adding a small correction to this equation. At the same time the dependencies of kinetic coefficients such as viscosity and thermal conductivity on temperature are defined by binary interactions and triple collisions which generate small corrections in terms of density.

In the last ten years several new methods [18,19,25,29] have been used to describe the thermophysical properties of gaseous Kr in the high temperature regions.

The kinetic coefficients derived by the various methods agree with each other at temperatures from 300 to 2000 K and are inside the limits of errors of most precise experimental data. The corresponding reference data [16] overpredict the experimental values [18,19,25,29] by 4% at 500 K, but this decreases with increasing temperature.

The recommendations presented here are based on results of [18,19,25]. The errors are doubled root mean squares that corresponding to the 90% probability level.

Specific volume can be calculated with the use of the real gas equation taking into account the second virial coefficient, m^3/kg, [27]:

$$V = \rho^{-1} = \frac{RT}{P} + B(T) \tag{6.3-1a}$$

where

$$B(T) = \sum_{i=1}^{7} a_i/(T^*)^{\frac{3}{4}(i-1)} \tag{6.3-1b}$$

$T^* = T/197.8$, T is in K, and the values of a_i are given in Table 6.3.1. The errors are less than 0.05% for 300 K < T < 1000 K and 0.1% for 1000 K < T < 2500 K.

Specific heat capacity at constant pressure, J/(kg·K), [27]:

$$C_P = 248.05 - RT^2 \frac{d^2B}{dT^2} \frac{P}{RT} \tag{6.3-2}$$

where B is given above. The errors are less than 0.1% for 300 K < T < 2500 K.

Specific heat capacity at constant volume, J/(kg·K), [27]:

$$C_V = 198.83 - R\left(2T\frac{dB}{dT} + T^2\frac{d^2B}{dT^2}\right)\frac{P}{RT} \tag{6.3-3}$$

The errors are less than 0.1% for < 2000 K.

Isoentropic coefficient, [13]:

$$k = -\frac{C_P}{C_V}\left(\frac{d\ln P}{d\ln V}\right)_T \tag{6.3-4}$$

Sound velocity, m/s, [27]:

$$w = \sqrt{k\left(1 + B\frac{P}{RT}\right)RT} \tag{6.3-5}$$

The errors are less than 0.1% over the entire temperature range.

Specific enthalpy, J/kg, [27]:

$$h = 248.05T + \left(B - T\frac{dB}{dT}\right)P \tag{6.3-6}$$

Here the initial point corresponds to $T = 0$ K. The errors are less than 0.1% for 300 < T < 2500 K.

Specific entropy, J/(kg·K), [27,28]:

$$s = 1958.3 + 248.05\,\ln\frac{T}{300} - R\,\ln\frac{P}{P_0} - \frac{1}{T}\left(T\,\frac{dB}{dT}\right)P \qquad (6.3\text{-}7)$$

where T is in K, P is in Pa, $P_o = 0.10132\times10^6$ Pa, B is the same as above. The errors are less than 0.1%.

Dynamic viscosity, Pa·s, [27,29]:

$$\mu = \frac{1.921\times10^{-6}\,\sqrt{T}}{k_1}\left(1 + B_\mu\frac{P}{RT}\right) \qquad (6.3\text{-}8a)$$

where

$$k_1 = \exp\left[\sum_{i=1}^{5} b_i\,(\,\ln T^*\,)^{(i-1)}\right] \qquad (6.3\text{-}8b)$$

Values for b_i are given in Table 6.3.1. The density correction to μ is

$$B_\mu\,\frac{P}{RT} = \alpha\,b_0\frac{P}{RT} \qquad (6.3\text{-}8c)$$

given by where $b_0 = 0.00069$ m^3/kg,

$$\alpha = \sum_{i=1}^{6} d_i\,(T^*)^{-(i-1)} \qquad (6.3\text{-}8d)$$

$T^* = T/197.8$, and the values of d_i are given in Table 6.3.1. The errors are less than 1.5% for 300 K < T < 1500 K and 2.5% for 1500 K < T < 2500 K.

Thermal conductivity, W/(m·K), [27]:

$$\lambda = \frac{0.716\times10^{-3}\,\sqrt{T}}{k_1}\left(1 + b_0\beta\frac{P}{RT}\right) \qquad (6.3\text{-}9a)$$

$$\log_{10}\beta = \sum_{i=1}^{4} e_i\left(\log_{10}T^*\right)^{i-1} \qquad (6.3\text{-}9b)$$

Here K_1, b_0 and T^* are the same as above and the values of e_i are given in Table 6.3.1. The errors are less than 1.5% for 300 K < T < 1000 K and 2.5% for 1000 K < T < 2500 K.

Additional properties can be calculated using the equations: $\nu = \mu/\rho$; $a = \lambda/(\rho\cdot C_P)$; $Pr = \nu/a$.

6.4. THE PROPERTIES OF XENON

The thermophysical properties of gaseous xenon (Xe) are given here for the temperature range 300 to 2500 K and the pressure range 0.1 to 6 MPa.

Natural Xe is a mixture of isotopes ranging from ^{124}Xe to ^{136}Xe with significant portions of ^{129}Xe (26.4%), ^{131}Xe (21.1%) and ^{132}Xe (26.9%). The atomic weight of Xe is = 131.29 ± 0.04 kg/kmol [1,2] and the specific gas constant is = 63.329 ± 0.02 J/(kg·K) [2,3].

The boiling temperature of Xe is T_b = 165.11 at normal pressure (P_0 = 0.101325 MPa), and the critical point parameters are: T_{cr} = 289.73 K, P_{cr} = 5.84 MPa, $\rho_{cr} = 1.11\times10^3$ kg/m^3 [2]. The range of T and P considered corresponds to the gaseous state of Xenon with the ratios: $\rho/\rho_{cr} \leq 0.3$ and $T/T_{cr} \geq 1$. The thermophysical properties are described here or a first approximation by the ideal gas equation = ρRT.

In the last ten years there have been three investigations of the thermophysical properties of gaseous Xe at high temperature. The authors of [18] used the conception of corresponding states to obtain the properties of all the inert gases. The authors of [19] used the six-parametric potential of interatomic interaction. The experimental data on viscosity and thermal conductivity for gaseous xenon and its second virial coefficient cover temperatures up to 2000 K. Using the results of [19] the authors of [25] calculated tables of reference data on μ and λ up to 5000 K. These last data have been accepted in Russia as the standard data [29]. The reference book [16] includes tables of thermodynamic transport properties of gaseous Xe from 500 ($P \leq 16$ MPa) to 3000 K ($P \leq 120$ MPa).

The recommendations presented here are based on results of [19,25]. The reference data has been validated by comparison with other sets of experimental data and by the use of physical models. The coefficients for the following equations are given in Table 6.4.1. The errors are doubled root mean squares defining the 90% probability level.

Specific volume can be calculated from the real gas equation taking into account the second virial coefficient, m^3/kg, [27]:

$$V = \frac{1}{\rho} = \frac{RT}{P} + B(T) \qquad (6.4\text{-}1a)$$

where

$$B(T) = \sum_{i=1}^{7} b_i \left(T^{*\frac{3}{4}} \right)^{-(i-1)} \qquad (6.4\text{-}1b)$$

T^*= T/274, T is in K, P is in Pa, and the values of a_i are given in Table 6.4.1. The errors are less than 0.2% in the full region of T.

Specific heat capacity at constant pressure, *J/(kg·K), [27]:*

$$C_P = \frac{5}{2} R - \left(T^2 \frac{d^2B}{dT} \right) \frac{P}{T} \qquad (6.4\text{-}2)$$

where B is given above. The errors are less than 0.1%.

Specific heat capacity at constant volume, *J/(kg·K), [27]:*

$$C_V = \frac{3}{2} R - \left(T^2 \frac{d^2B}{dT^2} + 2T \frac{dB}{dT} \right) \frac{P}{T} \qquad (6.4\text{-}3)$$

The errors are less than 0.1%.

Isoentropic coefficient, *[13]:*

$$k = -\frac{C_P}{C_V} \left(\frac{d \ln P}{d \ln V} \right)_T \qquad (6.4\text{-}4)$$

Sound velocity, m/s, [27]:

$$w = \sqrt{k\,(1 + B\rho)\,RT} \tag{6.4-5}$$

where k is given above. The errors over the entire temperature range are less than 0.1%.

Specific enthalpy, J/kg, [27]:

$$h = 158.322\ T + \left(B - T\frac{dB}{dT} \right) P \tag{6.4-6}$$

The errors are less than 0.1%.

Specific entropy, J/(kg·K), [27]:

$$s = 1292.58 + 158.322\ \ln\left(\frac{T}{300}\right) - R\ln\frac{P}{P_0} - \frac{dB}{dT}P \tag{6.4-7}$$

where T is in K, P is in Pa, B is given above and $P_0 = 0.101325$ MPa. The errors are less than 0.1%.

Dynamic viscosity, Pa·s, [27]:

$$\mu = \frac{2.030\times10^{-6}\sqrt{T}}{k_1}\left(1 + B_\mu\frac{P}{RT}\right) \tag{6.4-8a}$$

where

$$k_1 = \exp\sum_{i=1}^{5} d_i\,(\ln T^*)^{(i-1)} \tag{6.4-8b}$$

$$B_\mu = 0.55\times10^{-3}\sum_{i=1}^{6}\frac{b_i}{T^{*(i-1)}} \tag{6.4-8c}$$

where $T^* = T/274$, the values of b_i and d_i are given in Table 6.4.1. The errors are less than 1.5% for 300 K < T < 1500 K and 2.5% for 1500 K < T < 2500 K.

Thermal conductivity, W/(m·K), [27]:

$$\lambda = \frac{0.4826\times10^{-3}\sqrt{T}}{k_1}\left(1 + 0.55\times10^{-3}\,B_\lambda\frac{P}{RT}\right) \tag{6.4-9a}$$

where

$$\log_{10} B_\lambda = \sum_{i=1}^{4} q_i\,(\log_{10} T^*)^{(i-1)} \tag{6.4-9b}$$

Here $T^* = T/274$, T is in K, P is in Pa and the values of q_i are given in Table 6.4.1. The errors are less than 1.5% for 300 K < T < 1500 K and 2.5% for 1500 K < T < 2500 K.

Additional properties can be calculated using the known equations: $\nu = \mu/\rho$; $a = \lambda/(\rho\cdot C_p)$; $Pr = \nu/a$.

6.5. THE PROPERTIES OF MIXTURES OF INERT GASES

The equations for calculating the thermophysical properties of He, Kr and Xe are valid for 300 K < T < 2500 K and $P \leq 6$ MPa. Analysis shows that in this region the thermophysical properties of these gases are described to a first approximation by the ideal gas equation $PV = RT$ with small corrections to binary atomic interactions. In this region the transport properties (dynamic viscosity, thermal conductivity etc.) can be calculated using the results of modern kinetic theory of binary atomic interactions. At the same time triple collisions generate first order corrections to the kinetic coefficients in terms of density. This concept is also valid for mixtures of these gases.

In last ten years two approaches have been used to describe the thermophysical properties of mixtures of rarefied inert gases. In the first case the generalization of data on the second virial coefficient and on kinetic coefficients was done for all pure inert gases and their mixtures simultaneously on the base of conception of corresponding states [18]. In the second case multiproperty experimental data were used to recover 6-parametric potentials of pairing atomic interactions [19]. Both approaches give good agreement with each other and with the experimental data.

The correlations presented here use the kinetic theory of gases and their mixtures [13]. The results of [26] modified for use at high temperatures were accepted for the description of second virial coefficients and the collision integral.

Specific volume (Volume of mixture for unit mass), m^3/kg, [13,31]:

$$V = \rho^{-1} = \frac{RT}{P} + B(T,x) \tag{6.5-1a}$$

where $R = R^*/M$ is the specific gas constant, $R^* = 8314.51 \pm 0.14$ J/(kmol·K) is universal gas constant, $M(x)$ is the molecular weight of mixture, x_i is the mole fraction of i-th component, M_i is the molecular weight of this component (Table 6.5.1),

$$M = \sum_{i=1}^{k} x_i \, M_i \, , \quad kg/kmol \tag{6.5-1b}$$

second virial coefficient

$$B\,(\,T, x\,) = \bar{B}\,/\,M\,, \quad m^3/kg \tag{6.5-1c}$$

$$\bar{B} = \sum_{i=1}^{k} \sum_{j=1}^{k} x_i \, x_j \, \bar{B}_{ij}\,(\,T\,) \tag{6.5-1d}$$

$$\bar{B}_{ij}(T) = b_{ij}^{o} B^*\left(T_{ij}^*\right) \tag{6.5-1e}$$

$$b_{ij}^{o} = 1.2613 \times 10^{-3} \, d_{ij}^{3} \quad , \, m^3/kmol \tag{6.5-1f}$$

$$B^*\left(T_{ij}^*\right) = T^{*\frac{1}{2}} \exp\left(\frac{1}{T^*}\right) \sum_{i=1}^{6} a_i \,(\ln T^*)^{i-1} \tag{6.5-1g}$$

$$T_{ij}^* = \frac{T}{e_{ij}} \tag{6.5-1h}$$

The values of d_{ij}, e_{ij} and a_i are given in Tables 6.5.2 and 6.5.3.

Specific heat capacity at constant pressure, J/(kg·K), [13]:

$$C_P(T,P,x\ ) = \frac{5}{2}\ R\ -\ T\ \frac{d^2B}{dT^2}\ P \tag{6.5-2}$$

where P is in Pa, T is in K and R and B are given above. The errors in C_P is determined by the error in R and B given above.

Specific heat capacity at constant volume, J/(kg·K), [13]:

$$C_V = \frac{3}{2}\ R\ -\ \frac{1}{T}\left(2T\frac{dB}{dT}\ +\ T^2\ \frac{d^2B}{dT}\right)P \tag{6.5-3}$$

See remarks for preceding item.

Isoentropic coefficient, [13]:

$$k\ =\ -\ \frac{C_P}{C_V}\left(\frac{d\ \ln P}{d\ \ln V}\right)_T \tag{6.5-4}$$

where P is in Pa, V is in m^3/kg.

Thermodynamic sound velocity, m/s, [13]:

$$\omega\ =\ \sqrt{k\left(1\ +\ \frac{BP}{RT}\right)RT} \tag{6.5-5}$$

Specific enthalpy, J/kg, [13]:

$$h\ (T,P,x)\ =\ 2.5RT\ +\ \left(B - T\ \frac{dB}{dT}\right)P \tag{6.5-6}$$

where P is in Pa, T is in K and R and B are given above. The error are less than 0.5% if the composition of the mixture is known.

Specific entropy, J/(kg·K), [13,28]:

$$s(T,P,x) = \frac{1}{M}\sum_{i=1}^{3}\ s_i^0 + \frac{5}{2}\ R\ln\frac{T}{300} - R\ln\frac{P}{P_0} - R\sum_{i=1}^{k} x_i \ln x_i - \frac{dB}{dT}\ P \tag{6.5-7}$$

See remarks above, the values of s_i^0 are given in Table 6.5.1. The errors are the same as above.

Dynamic viscosity, Pa·s, [13,16]:

$$\mu(T,P,x)\ =\ \mu_0(T,x)\left(\ 1\ +\ B_\mu(T,x)\ \frac{P}{RT}\ \right) \tag{6.5-8a}$$

A precise equation for the viscosity of gases $\mu_0(T,x)$ but it contains determinants. We recommend a simpler relation which is suitable for industrial use, [32]:

$$\mu_0(T,X) = \sum_{i=1}^{k} \frac{\mu_{0i}}{\frac{1}{X_i} \sum_{j=1}^{k} X_j \, \Phi_{ij}} \tag{6.5-8b}$$

where

$$\Phi_{ij} = \frac{\left[1 + (\mu_{0i}/\mu_{0j})^{0.5} (M_j/M_i)^{0.25} \right]^2}{\left[8 \left(1 + M_i/M_j \right) \right]^{0.5}} \tag{6.5-8c}$$

$$\mu_{0i} = \frac{2.6696\times10^{-6} \sqrt{M_i T}}{d_i^2 \exp \sum_{j=1}^{5} C_j \, (\ln T^*)^{j-1}} \tag{6.5-8d}$$

The density correction to the viscosity is

$$B_\mu(T,x) \frac{P}{RT} = \frac{1}{M} \frac{P}{RT} \sum_{i=1}^{k} x_i b_i^0 \alpha_i \tag{6.5-8e}$$

where $T^*_i = T/e_i$, see (6.5-1e) and (6.5-1f) for values of b_i and e_i. The errors are less than 2.5% for 300 K $< T <$ 1500 K and 4% for 1500 K $< T <$ 2500 K.

$$\alpha_i = 0.175 + 2.54/T_i^* - 2.5/T_i^{*2} \;, \quad \textit{see } b_i^0 \textit{ in } (6.5\text{-}1f) \tag{6.5-8f}$$

Thermal conductivity, W/(m·K).

Here we recommend the use of the simple relations from [32]:

$$\lambda(T,P,x) = \lambda_0(T,x) \left(1 + B_\lambda \frac{P}{RT} \right) \tag{6.5-9a}$$

where

$$\lambda_0(T,x) = \sum_{i=1}^{k} \frac{\lambda_{0i}}{\frac{1}{x_i} \sum_{j=1}^{k} x_j \, \Phi_{ij}} \tag{6.5-9b}$$

ϕ_{ij} are the same as in (6.5.8.2).

$$\lambda_{0i} = \frac{83.236\times10^{-3} \sqrt{T/M_i}}{d_i^2 \, \exp \sum_{j=1}^{6} C_j \, (\ln T^*)^{j-1}} \tag{6.5-9c}$$

The density correction to thermal conductivity is

$$B_\lambda \frac{P}{RT} = \frac{1}{M} \frac{P}{RT} \left(\sum_{i=1}^{k} x_i \, b_i^0 \, \beta_i^* \right) \tag{6.5-9d}$$

where

$$\log_{10} \beta^*_i = 0.47 - 1.59 \left(\log_{10} T_i^* \right) + 1.26 \left(\log_{10} T_i^* \right)^2 - 0.37 \left(\log_{10} T_i^* \right)^3 \tag{6.5-9e}$$

See the values of b_i in (6.5-1f) and c_i given in Table 6.5.3. The errors are less than 5% for 300 K < T < 1500 K and 7% for 1500 K < T < 2500 K.

The additional properties can be calculated using the known equations: $\nu = \mu/\rho$, $a = \lambda/(\rho \cdot C_P)$, $Pr = \nu/a$.

Nomenclature to Chapter 6

R - gas constant, J/(kg·K), V - specific volume, m^3/kg,
ρ - specific density, kg/m^3, P - pressure, Pa,
C_P - specific heat capacity at constant pressure, J/(kg·K),
C_V - specific heat capacity at constant volume, J/(kg·K),
ω - sound velocity, m/s, h - specific enthalpy, J/kg,
s - specific entropy, J/(kg·K), M - molecular weight,
μ - dynamic viscosity, Pa·s, υ - kinematic viscosity, m^2/s,
λ - thermal conductivity, (W/(m·K)),
Pr - Prandtl number, k - isoentropic coefficient.

Table 6.1.1 THE VALUES OF COEFFICIENTS IN EQUATIONS FOR HYDROGEN PROPERTIES

i	a_i	f_i	c_i	e_i
-2	-	-1.81996 E-4	-	-
-1	-	0.0	-	-
0	-	4.00126	-	-
1	-7.19805 E-1	-1.56159 E 1	-3.71991 E-1	1.19903
2	9.93238	1.78060 E 2	6.88310	-2.11897 E-1
3	-2.84411 E 1	-6.50552 E 2	-1.69271 E 1	1.26810 E-1
4	3.17303 E 1	8.32583 E 2	2.10628 E 1	-
5	-1.35541 E 1	-	-1.01934 E 1	-
Remark: here and below the notation E±n stands for decimal exponent: 0.12345 E-5 = 0.12345×10^{-5}				

Table 6.2.1 REGRESSIONS COEFFICIENTS FOR HELIUM

i	a_i	b_i
1	-0.00436074	0.46041
2	0.00591117	-0.56991
3	-0.00190460	0.19591
4	-	-0.03879
5	-	0.00259

Table 6.3.1 REGRESSION COEFFICIENTS FOR KRYPTON

i	a_i	b_i	d_i	q_i
1	4.69713 E 1	4.6841 E-1	-0.15159	0.47
2	-3.16783 E 2	-5.6991 E-1	2.54126	-1.59
3	2.21790 E 3	1.9591 E-1	-3.10830	1.26
4	-8.25525 E 3	-3.8790 E-2	0.52764	-0.37
5	1.43958 E 4	2.59000 E-3	0.50741	-
6	-1.22682 E 4	-	-0.23042	-
7	4.08835 E 3	-	-	-

Table 6.4.1 REGRESSION COEFFICIENTS FOR XENON

i	a_i	b_i	d_i	q_i
1	2.66243 E-4	4.6641 E-1	-0.1595 E-1	0.47
2	2.19567 E-4	-5.6991 E-1	2.5412	-1.59
3	-2.17915 E-4	1.9591 E-1	-3.1083	1.26
4	-0.91279 E-2	-3.8790 E-2	0.52764 E-1	-0.37
5	1.77392 E-2	2.5900 E-3	0.50741 E-1	-
6	-1.38045 E-2	-	-2.3042 E-1	-
7	3.77490 E-3	-	-	-

Table 6.5.1 ATOMIC WEIGHTS OF ELEMENTS [1]. THE VALUE OF ENTROPY s^0 OF THE ELEMENTS IN THE STANDARD GASEOUS STATE (300 K) ARE TAKEN FROM [9]

Gas	He	Kr	Xe
M kg/kmol	4.002602±0.000004	83.80±0.02	131.29±0.04
s^0 J/(mol·K)	126170	164103	169703

Table 6.5.2 SCALE PARAMETERS FOR ELEMENTS

Gas	He	Kr	Xe
He	$d = 2.61$ Å	$d = 3.267$ Å	$d = 3.533$ Å
	$e = 10.40$ K	$e = 31.05$ K	$e = 29.77$ K
Kr	$d = 3.267$ Å	$d = 3.571$ Å	$d = 3.753$ Å
	$e = 31.05$ K	$e = 197.8$ K	$e = 225.4$ K
Xe	$d = 3.533$ Å	$d = 3.753$ Å	$d = 3.85$ Å
	$e = 29.77$ K	$e = 225.4$ K	$e = 274.0$ K

Table 6.5.3 REGRESSIONS COEFFICIENTS FOR GAS MIXTURES

i	a_i	b_i
1	-0.775684	0.46641
2	1.243430	-0.56991
3	-0.628821	0.19591
4	0.148384	-0.03879
5	-0.017106	0.00259
6	7.801350 E-4	-

References to Chapter 6

[1] Atomic Weights of the Elements 1991, Commission of Atomic Weights and Isotopic Abundances, Pure Appl. Chem. (1992), v. 64, pp. 1519-1534

[2] CRC Handbook of Chemistry and Physics, 74 ed., ed. by D. R. Lide, Roca Raton, CRC Press, 1993

[3] Fundamental Physical Constants. Tables of Standard Reference Data, GSSSD 1-87, Moscow, Publishing House of Standards (1989) (in Russian)

[4] MICHELS A. et al., "Compressibility isotherms of hydrogen and deuterium at temperatures between -175 and +150°C". Physica (1959), v. 25, p. 25

[5] MICHELS A., SCHIPPER A. S., RINTOUL W. H., "The viscosity of hydrogen and deuterium at pressure up to 2000 atm", Physica, 1953, v. 19, pp. 1011-1019

[6] KOMPANEETZ V. Ya., "The experimental investigation of viscosity of gases and gaseous mixtures at high temperature", The collection of reports of Leningrad Agriculture Engineering Institute, Moscow-Leningrad, Publishing House of Agriculture Literature (1953), p. 113

[7] Thermodynamic properties of individual substances. 4th edition. Ed. by Gurvich L., Veyts I., Alcock C. N.-Y., Hemisphere (1989)

[8] CLIFFORD A. A., DICKINSON E., GRAY P., SCOTT A. C., "Testing intermolecular potential function using transport property data", J. Chem. Soc. Faraday Trans. (1975), v. 71, pp. 1953-1961

[9] TIMROT D. L., UMANSKY A. S., "Investigation of thermal conductivity of hydrogen and argon", Theplofizika Vysokikh Temperatur (1966), v. 4, pp. 289-291 (in Russian)

[10] SAXENA S. C., "Thermal conductivity of gases and gaseous mixtures at high temperatures", High Temp. Sci. (1971), v. 3, p. 168

[11] FOKIN L. R., LUSTERNIK V. E., "Mercury. Coefficients of viscosity, thermal conductivity, self-diffusion and second virial coefficient at temperatures 400-2000 K and low pressures at in the gaseous state", The Tables of Standard Data, GSSSD 57-83, Moscow, Publishing House of Standards (1985), p. 16 (in Russian)

[12] Tables of collision integrals and second virial coefficients for the intermolecular function / Klein. M et al - Wash., Gov. Print off (1974) (US Dep. of Commerce, NBS-NSRDS, #47)

[13] HIRSCHFELDER J., CURTIS C., BIRD R., "The molecular theory of gases and fluids", NY., Wiley (1954)

[14] ASSAEL M. J., MIXAFENDI S., WAKCHAM W. A., "The Viscosity and Thermal Conductivity of Normal Hydrogen in the Limit of Zero Density", J. Phys. Chem. Ref. Data (1986), v. 15, pp. 1315-1322

[15] Normal Hydrogen, The coefficients of dynamic viscosity and thermal conductivity at temperatures from 14 to 1500 K and pressure up to 100 MPa (Kozlov A. D., Kuznetsov V. M., Mamonov Yu. V.) The Tables of Reference Data, R-233-81, Moscow, Publishing House of Standards (1987) (in Russian)

[16] ZUBAREV V. N., et al., "Thermophysical properties of gases of industrial use at high temperature and pressure", Moscow, Energoatomizdat (1989), p. 232

[17] ARTYM R. I., KLEIN M., "Berechnung des Zweiten Virialcoeffizienten für gasfoermigen molecularen Wasserstoff im Temperatur Intervall von 1 K bis 3000 K", Ber. Bunsenges Phys. Chem. (1991), Bd. 95, s. 1274-1279

[18] KESTIN J., KNIERIM K., MASON E. A., "Equilibrium and transport properties of the noble gases and their mixtures at low densities", J. Phys. Chem. Ref. Data (1984), v. 13, pp. 229-303

[19] AZIZ R., MCCOURT F., WONG C., "A new determination of the ground state interatomic potential for He_2", Mol. Phys. (1987), v. 61, pp. 1487-1511

[20] YNTEMA J. L., SCHNEIDER W. G. "Compressibility of gases at high temperatures. Iii. The second virial coefficient of he in the temperature range 600 to 1200°C", J. Chem. Phys., 1950, v. 18, pp. 641-650

[21] DAWE R., SMITH E., "Viscosity of inert gases at high temperatures", J. Chem. Phys. (1970), v. 52, pp. 693-703

[22] GUIVARA F., MCINTEER B., WAGEMAN W., "High-temperature viscosity ratios for gases", Phys. Fluids (1969), v. 12, p. 2493

[23] VARGAFTIK N. B., ZIMINA N. H., "Thermal conductivity of helium at temperature 0-1000°C and Pressure 1-200 atm", Atomnaya Energiya (1965), v. 19, pp. 300-303 (in Russian)

[24] FAUBERT F., SPRINGER G. S., "Measurement of the thermal conductivity of helium up to 2100 K by the column method", J. Chem. Phys. (1973), v. 58, pp. 4080-4083

[25] BICH E., MILLAT J., VOGEL E., "The viscosity and thermal conductivity of pure monoatomic gases from their normal boiling point up to 5000 K in the limit of zero density and at 0.101325 MPa", J. Phys. Chem. Ref. Data (1990), v. 19, pp. 1289-1305

[26] He, Ne, Ar, Kr, Xe. Dynamic viscosity and thermal conductivity at atmospheric pressure (0.101325 MPa) in the temperature range from normal boiling point up to 5000 K, The Tables of Standard Reference Data, GSSSD 138-89. Moscow, The Publishing House of Standards (1992), p. 24 (in Russian)

[27] HIRCHFELDER J. O., CURTISS C. F., BIRD R., "Molecular theory of gases and liquids", NY., Wiley (1954)

[28] Thermodynamic properties of individual substances, 4th edition. Eds, Gurvich L. V., et al., NY., Hemisphere (1989)

[29] KAMENETSKY V. R., "Calculation of the coefficient of dense gases viscosity and their mixtures using the modified enskog equation", Journal Phiz. Chim. (1978), v. 52, pp. 1496-1497 (in Russian)

[30] The 1986 Adjustment of the fundamental physical constants. CODATA Bull. # 63 (1986)

[31] MASON E., SPURLING T., "The virial equation of state", The International Encyclopedia of Physical Chemistry. v. 10/2. NY., Pergamon Press (1969)

[32] REID R., PRAUSNITZ J., SHERWOOD TH., "The properties of gases and liquids", 3rd ed., NY., McGraw Hill (1977)

7. CONCLUSIONS

Thermophysical properties of reactor and construction materials have been collected and systematized for normal, transient and accident conditions.

1. This report presents the main thermophysical properties - thermal conductivity, thermal diffusivity, specific heat capacity, enthalpy, thermal expansion, emissivity for:

- Fuel materials
- Cladding materials
- Absorber material
- Structural material
- Concretes.

2. During this programme, property measurements were made on U-Al alloys, UO_2, Zr-Nb alloys, Zircaloy-2, and Hastelloy. Other data presented here on thermophysical properties of reactor materials have been collected from the literature.

3. High temperature oxidation properties of zirconium-based alloys have been measured, analyzed, and reported in a semi-empirical form suitable for computer simulation codes.

4. For light water, heavy water and steam, the thermodynamical properties (equation of state, density, entropy, enthalpy, energy, specific heat) and saturation properties, thermal conductivity, viscosity, surface tension are presented as formulae.

5. The thermodynamic and transport properties of hydrogen, helium, xenon, krypton gases and their mixtures are presented at temperatures up to 2500 K and pressure up to 6 MPa.

6. Thermophysical properties of zirconium dioxide, alumina and silicate concrete, and the thermophysics of high temperature concrete-core melt interaction are presented.

7. Selected experimental information on mechanical properties of construction materials are discussed.

8. The report supplements describe some of the experimental methods and equipment used to determine the material properties.

9. The thermophysical properties of solid reactor materials are collected in the THERSYST computer data base.

10. The PC based supplementary data base management system (TPSYS) has been developed to provide an interface to THERSYST through interchangeable data files.

Supplement S1

OXIDATION KINETICS OF ZIRCONIUM BASED ALLOYS

S1.1. INTRODUCTION

During asevere accident in a LWR, high temperature steam will oxidize zirconium alloy cladding with a corresponding increase in clad temperature due to the heat of reaction and the degradation of its mechanical strength. Special interest has been paid to the oxidation behaviour of Zircaloy at very high temperatures since the accident at Three Mile Island, for the following reasons:

- heat generated during fuel cladding oxidation can play a substantial role in increasing the reactor core temperature;
- in high enough concentration, H_2 can be explosive.

S1.2. OXIDATION KINETICS

Steam reacts with zirconium alloys at temperatures above the $(\alpha+)\beta/\beta$ transformation temperature. Two additional oxygen-rich layers are formed: a superficial zirconium oxide layer from the exothermic reaction

$$Zr + 2H_2O = 2H_2 + (Zr + 2O) + heat \qquad \text{(S1-1)}$$

and an intermediate layer of oxygen-stabilized α-Zr phase. Heat and hydrogen evolved in the reaction (S1-1) plays an important role in severe fuel damage and severe accident analysis. Mechanisms and elementary physical processes of zirconium oxidation are depicted in Figure S1.1. It is generally accepted and proved by numerous experiments that the mechanism which governs the oxidation reaction is the diffusion of oxygen anions through the anion-deficient ZrO_2 lattice. Therefore, at constant temperature, for thick samples and under unlimited steam supply, the reaction rate can be described by a parabolic expression of form

$$\delta^2 = K_\delta t \qquad \text{(S1-2)}$$

where δ is a measure of the extent of reaction, t is the reaction time, and K_δ is the parabolic reaction rate constant. The extent of reaction (per unit area) can be expressed as a mass of reacting element:

- zirconium reacted in reaction (S1-1);
- or oxygen absorbed in all oxidation processes (oxygen uptake);

or as the thicknesses of layers, etc. Oxidation kinetics obey the parabolic law at temperatures above ~1000°C; below this temperatures a tendency to a cubic law was observed.

So that reaction rate constants can be adopted as basic quantities for characterizing oxidation properties the rate constant is related to temperature by an Arrhenius form of expression

$$K_\delta(T) = A\exp\left(-\frac{Q}{RT}\right) \qquad \text{(S1-3)}$$

where A and Q are constants, R is the gas constant and T is the temperature in Kelvin. According to equation (S1-3) the K_δ dependence on temperature in an Arrhenius plot ($\log K_\delta$ versus $1/T$) is linear (see Figure S1.2).

S1.3. FACTORS AND PHENOMENA AFFECTING OXIDATION

Several factors and phenomena affect the oxidation kinetics which as a result, lead to deviations from "ideal" time-temperature dependencies (S1-2), (S1-3). The most important of them are discussed here.

The presence of temperature gradients across the oxide and metal layers of the specimen affects the diffusion of oxygen in the material and conflict with the assumption of "isothermal oxidation". The observable difference in experimentally determined reaction rates for different specimen heating methods can, in part, be attributed to a temperature gradient effect (see Figure S1.2).

During a severe LWR accident a large amount of hydrogen is generated in the reactor vessel. It is expected, that at least the upper part of the fuel rods will be exposed to a hydrogen rich steam-hydrogen mixture. The influence of this "steam starvation" effect was only observed below very low concentrations of steam in the steam/gas mixture. An example is illustrated in Figure S1.3a. The critical concentration limit is about 5 mol% of steam in the mixture. This limit was confirmed for various composition of steam/argon [20,22], steam/helium [23] and steam/hydrogen [22,23] mixtures. A similar effect occurs for a very limited steam supply to the reacting surface [19] - see Figure S1.3b.

A discontinuity in the reaction rate constant temperature dependence was observed around 1500°C [8,13,14,23]. Above this temperature the reaction rate is accelerated. This phenomenon is illustrated in Figure S1.2 and is associated with the development of a high-temperature cubic oxide phase (phases of Zircaloy and zirconium are schematically depicted in Figure S1.4). In this phase the diffusion ability of oxygen is greater than in the tetragonal phase and the oxygen concentration gradient in the cubic layer is higher.

Dependence of oxidation kinetics on steam pressure, if any is observed, is very weak for commercially used zirconium alloys. Alloy Zr-1%Nb is an exception - in the temperature range up to 1200°C this dependence is significant [32] and must be taken into account.

S1.4. MATHEMATICAL MODELLING OF OXIDATION

A useful tool for evaluating experimental data is a computerized mathematical model of the oxidation process. This approach gives a well-founded insight into the role of various phenomena and factors affecting the oxidation kinetics and enables temperature ranges to be covered where there is a lack of experimental data.

Computer code FRAOXI-1 [33], that was developed in NRI, is even more useful as it can predict the formation,. growth and disappearance of various reaction layers formed as a result of chemical interactions of the solid zirconium cladding material, not only with steam or oxygen, but also with uranium dioxide fuel. The present version of this code has been incorporated into a more complex code for simulating fuel element behaviour under accident conditions.

With respect to zirconium oxidation this code allows the solution of the following problems:

- prediction of the formation, growth and disappearance of reaction layers in the fuel element cladding and the determination of the mechanical state of the cladding (embrittlement);
- calculation of the oxygen concentration profile in the clad wall;
- the microstructure during temperature variations (α to β transformations in Zr);
- treatment of the steam starvation effect;
- oxidation of the molten metallic reaction layers.

The model is based on the solution of the Fick and Stefan equations in cylindrical geometry and as input data, the temperature profiles varying or constant in time, are requested.

The mathematical model of oxidation used in FRAOXI is based on the oxygen balance in an infinitesimally small volume. The differential form of the balance is (in cylindrical r-geometry)

$$\frac{\delta C}{\delta t} = \frac{1}{r}\frac{\delta}{\delta}r(rJ_r) \qquad \text{(S1-4)}$$

where $C = C(r,t)$ is the oxygen concentration, and J_r is the oxygen flux.

Flux is approximated by a simplified Fick's law

$$J_r = -D\frac{\delta C}{\delta r} \qquad \text{(S1-5)}$$

where D is the oxygen diffusion coefficient.

Equations (S1-4), (S1-5) are completed by a set of initial and boundary conditions and solved by standard finite-difference techniques. Layers interface motion is respected.

Computer code FRAOXI has been widely tested on a great variety of oxidation experiments. Typical examples of code verification on isothermal and simple non-isothermal experiments are illustrated in Figures S1.5-S1.7.

For isothermal oxidation experiments the following conclusions can be formulated:

- Typical parabolic oxidation kinetics under isothermal conditions is simulated with very good experimental agreement (Figure S1.5b).
- Agreement with experiments is satisfactory for the entire temperature range above 1000°C (Figures S1.5a, S1.6a, S1.6b).
- FRAOXI is able to simulate with a great degree of reliability phenomena such as accelerated oxidation at temperatures above the threshold of cubic ZrO_2 formation (see Figures S1.5a-S1.6b for temperatures above 1550°C) and the effect of finite specimen dimensions on oxidation kinetics (Figure S1.7a), etc.

It must be emphasized that this agreement was achieved without any artificial modification of the diffusion coefficients (they have been selected as the "most reliable set" from the evaluation of published data).

The wide applicability of the FRAOXI code is illustrated in Figure S1.7b. Oxidation experiments with simple temperature transients (linear increase followed by linear decrease) were simulated. First calculations using the oxygen boundary concentrations, strictly following the temperature, over estimated the layer thickness at the end of the transient. After limiting the rate of change of the boundary concentrations with temperature, a much better agreement with experiment was achieved (see Figure S1.7b).

The results of the FRAOXI verifications are very promising for its use in the reliable evaluation of collected data and for extrapolation to temperatures above 1500°C, where a lack of data exists (Section 4.2.2. mentions the lack of data on weight gain at temperatures above ~1500°C).

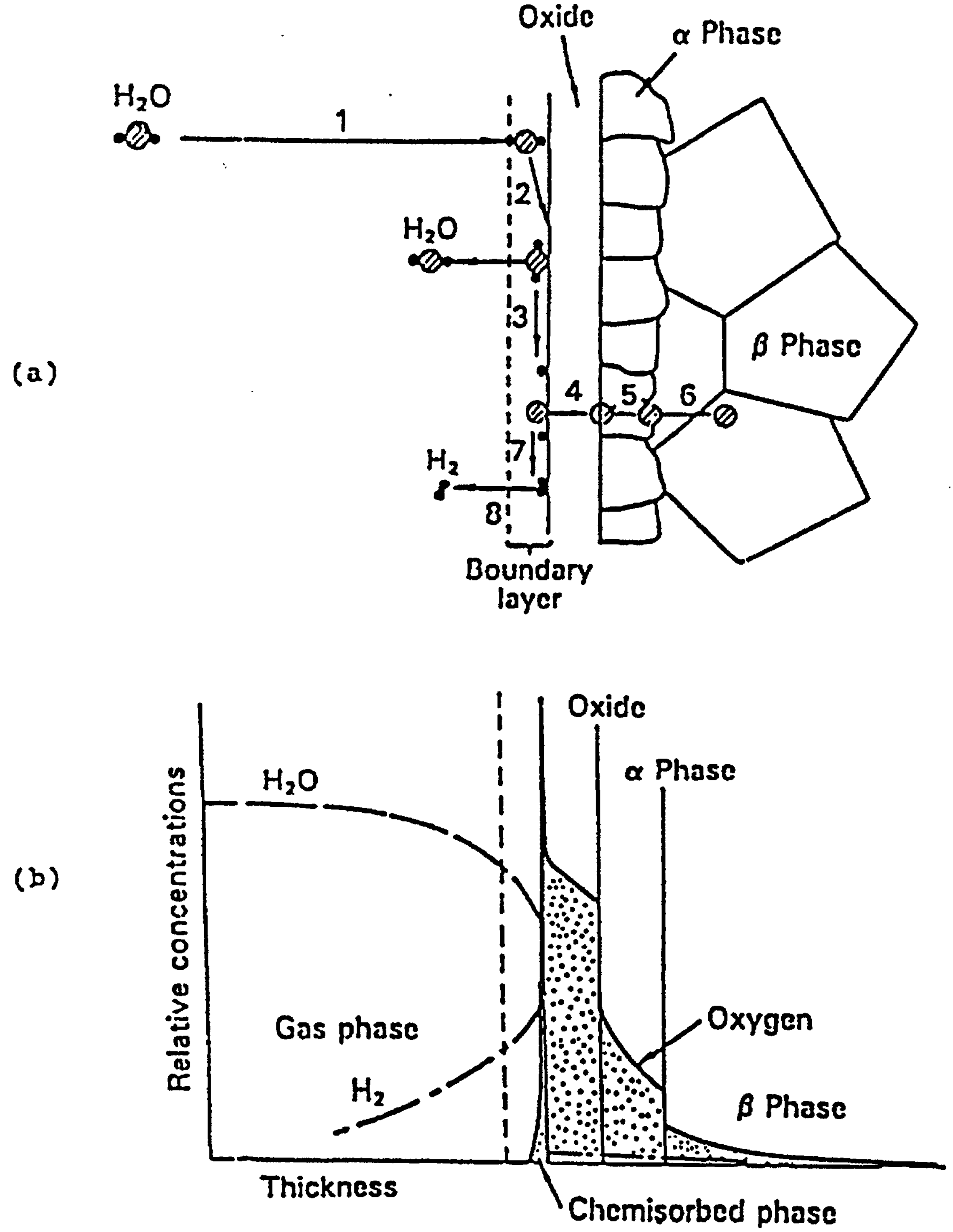

(a) the processes playing the major roles in zirconium oxidation in steam. Elementary steps in the oxidation are: gaseous diffusion of steam (1), chemisorption of steam (2), dissociation of water molecule into oxygen and hydrogen atoms (3), diffusion of oxygen in the zirconium dioxide layer (4), diffusion of oxygen in the alpha (5) and beta (6) layers, recombination of hydrogen (7) and desorption of gaseous hydrogen (8)

(b) oxygen concentration profiles in different layers (schematically)

Figure S1.1 *Schematic representation of the zirconium oxidation in high temperature steam; oxidized layers (ZrO_2 oxide and oxygen stabilized α phase α-Zr(O)); oxygen concentration in phases.*

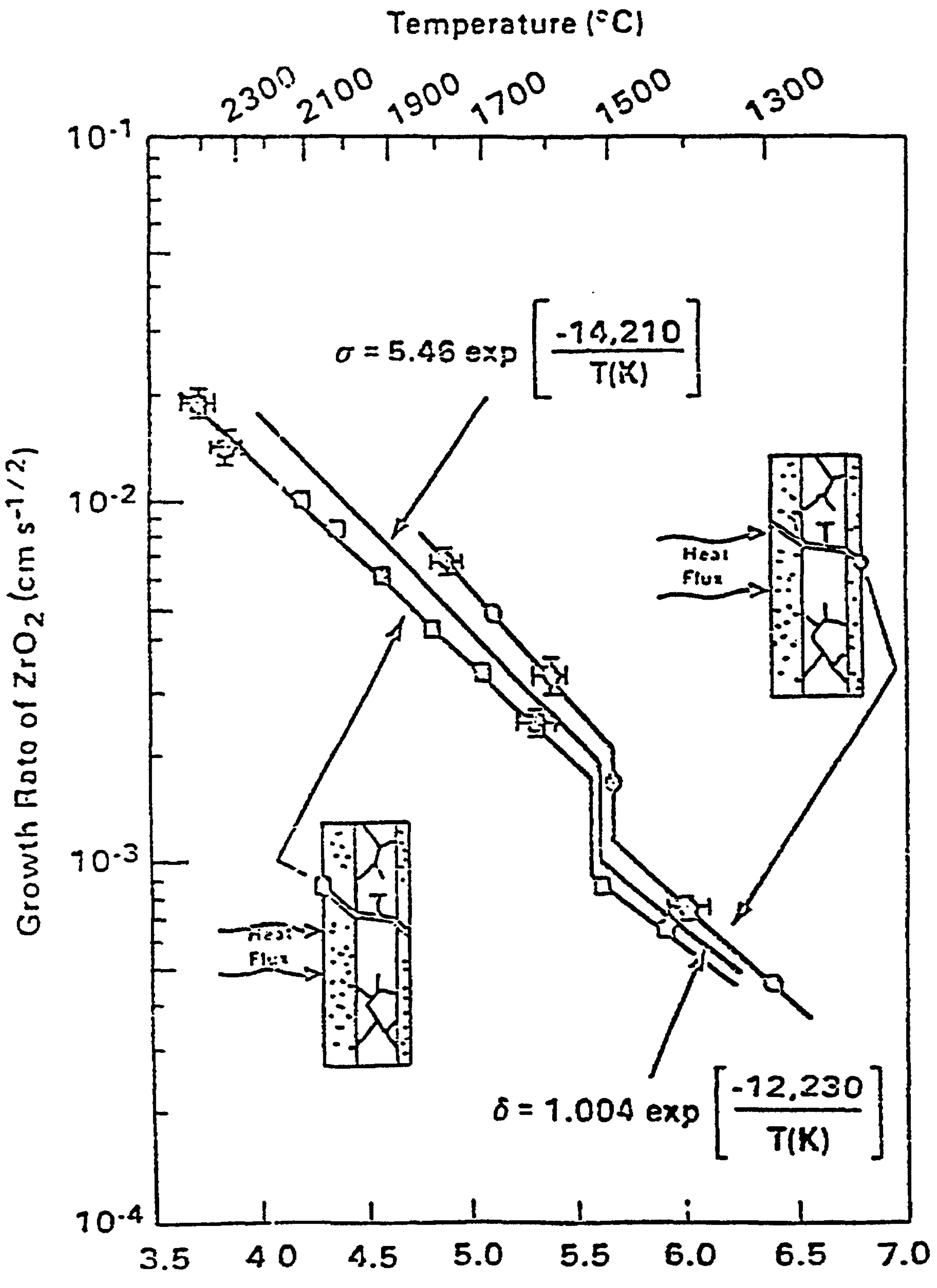

Figure S1.2 *Parabolic rate constant for ZrO_2-layer growth at temperatures from 1300 to 2400°C. Reproduced from [23]. Discontinuity in temperature dependence is at 1510°C and above this temperature the oxidation is accelerated.*

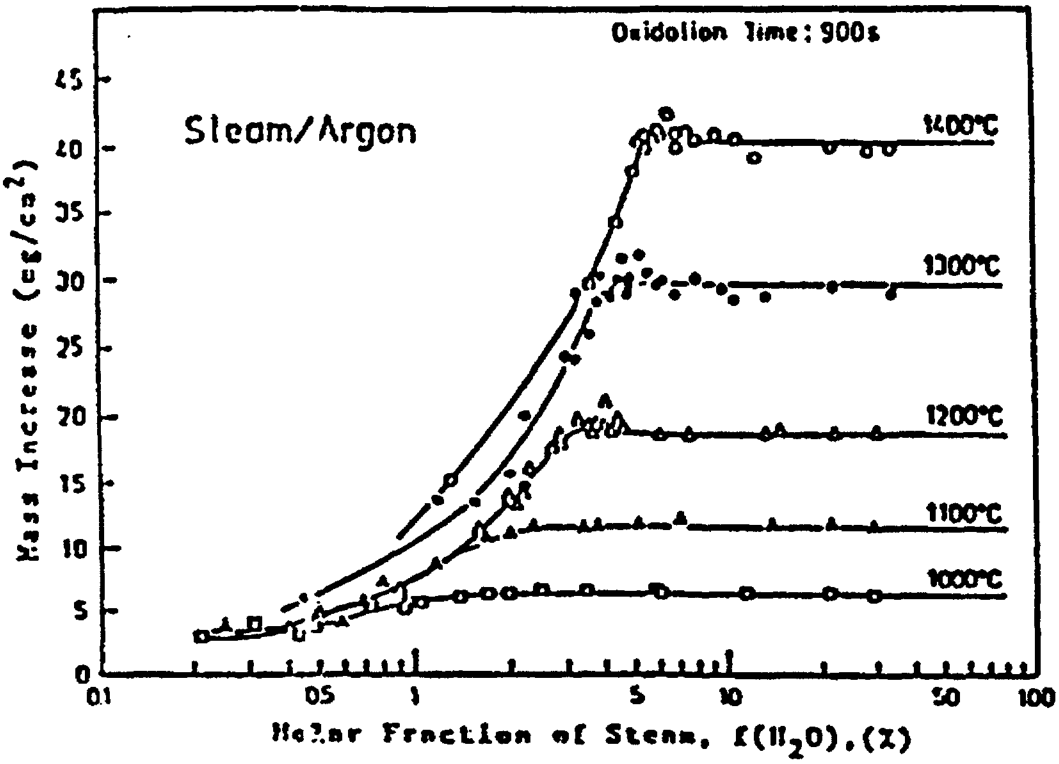

Figure S1.3a Steam starvation effect. Mass increase of Zircaloy-4 oxidized in steam/argon mixture. After [20].

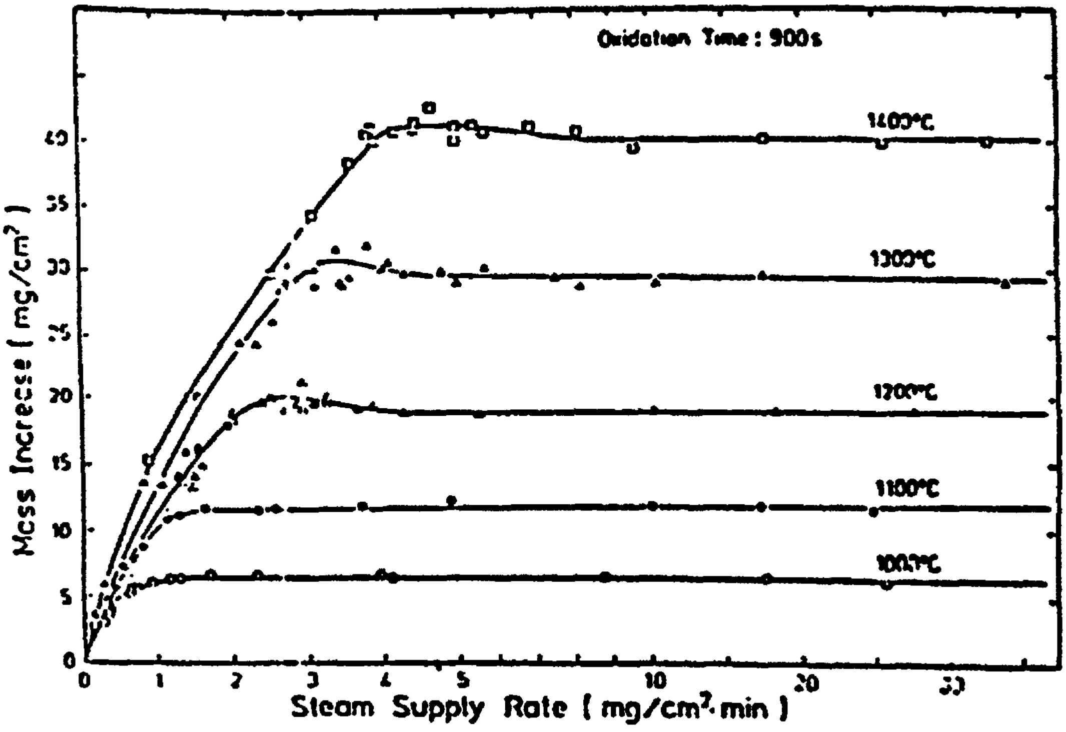

Figure S1.3b Steam starvation effect. Mass increase of Zircaloy-4 oxidized under limited steam supply. After [19].

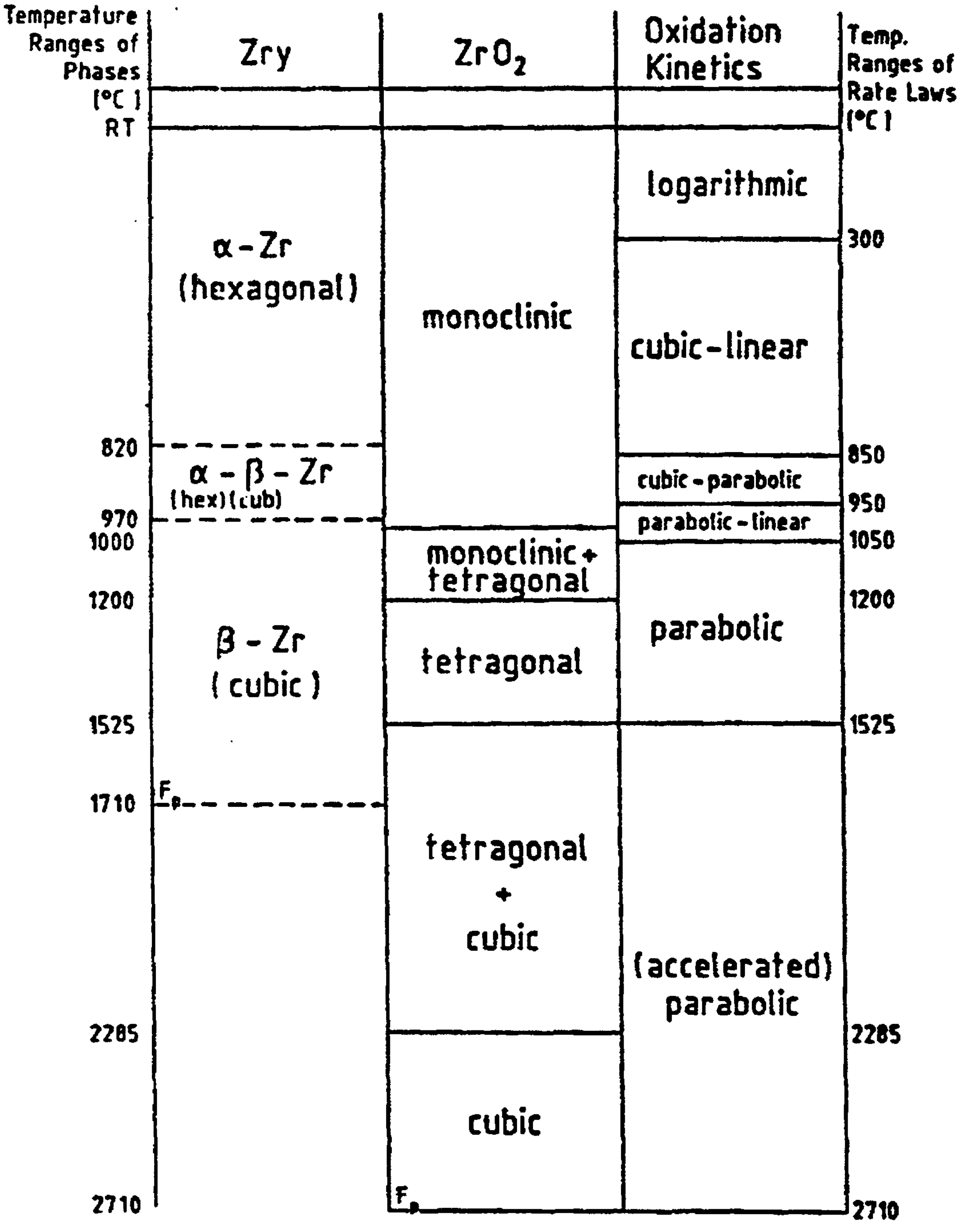

Figure S1.4 *Phases, transformations and melting regions of Zr and ZrO_2; approximate ranges of validity of the oxidation kinetics laws versus exposure temperature. Reproduced from [12]. Melting points: 1710°C (β-Zr), 1978°C (saturated α-Zr(O)), 2710°C (ZrO_2).*

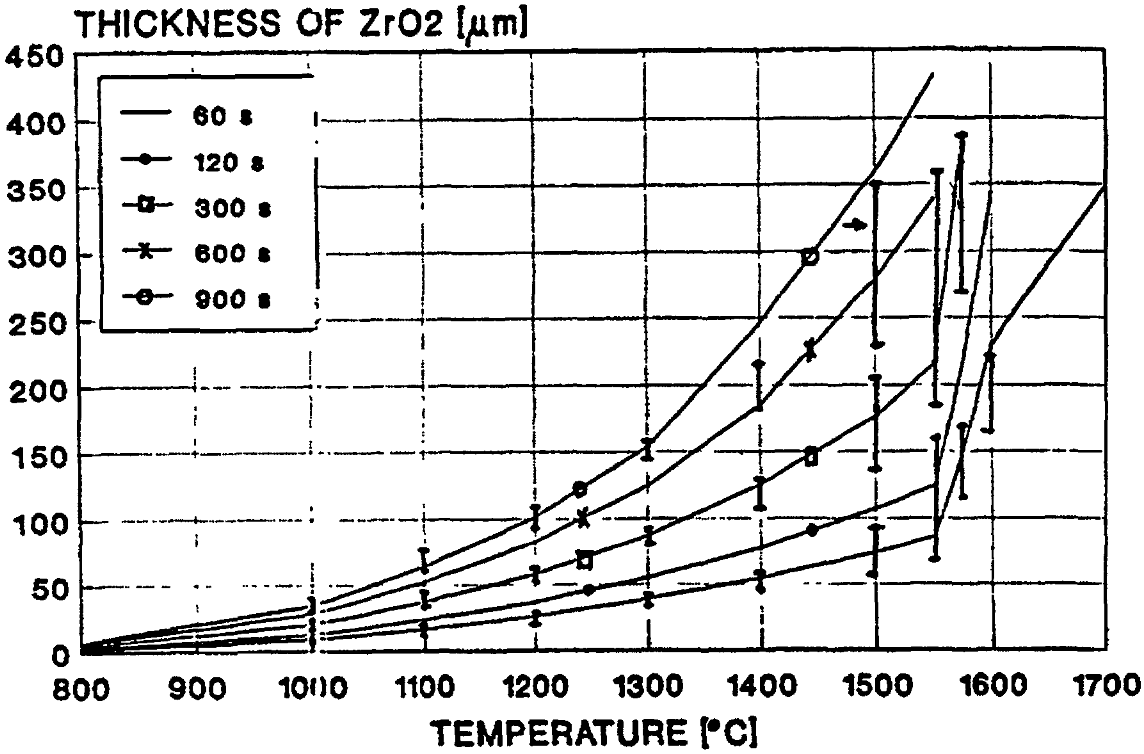

Figure S1.5a *ZrO_2 layer thickness for various exposition periods and temperatures*

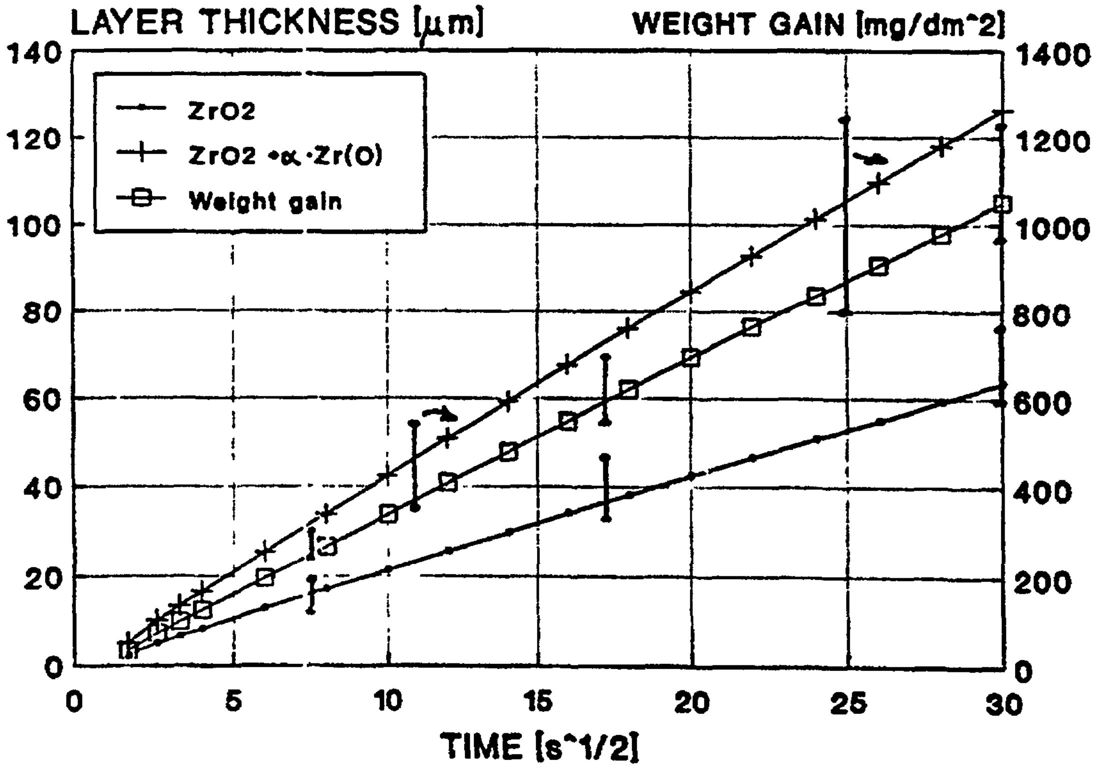

Figure S1.5b *Oxidation kinetics ("parabolic" time dependence). Weight gain and layers growth during oxidation at 1100°C*

Figure S1.5 *FRAOXI code validation - Zircaloy-4 isothermal experiments (their range is represented by vertical abscissae).*

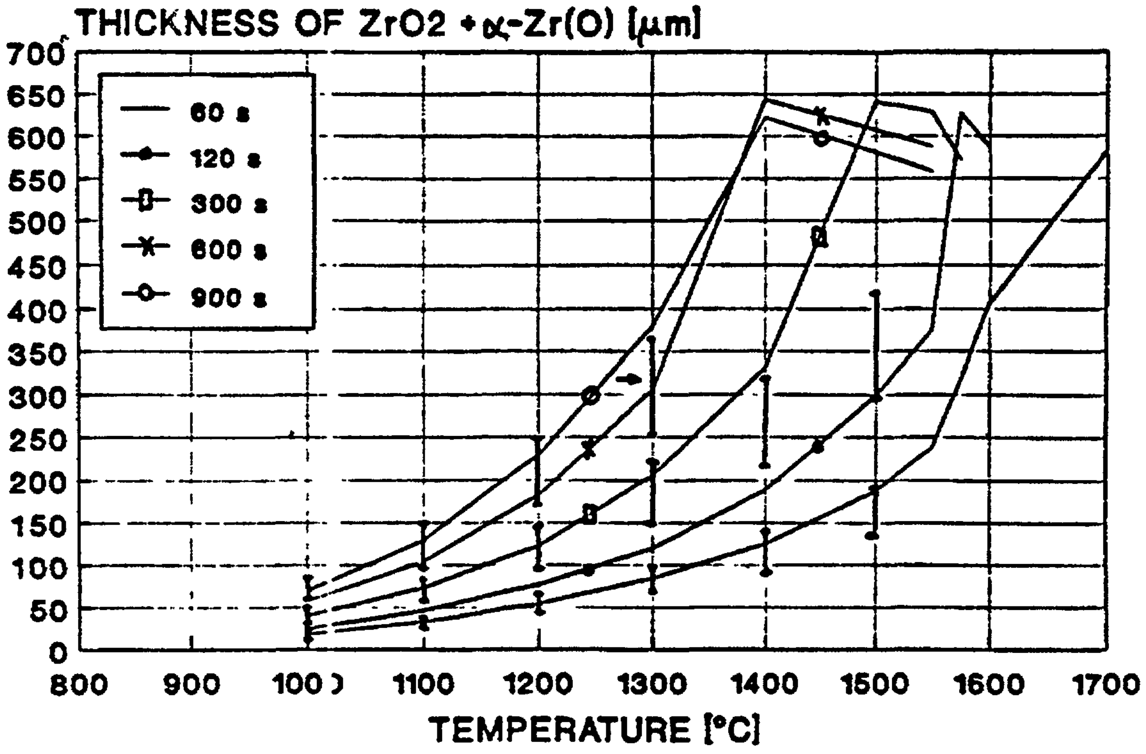

Figure S1.6a double ZrO_2 + α-Zr(O) layer thickness for various exposition periods and temperatures

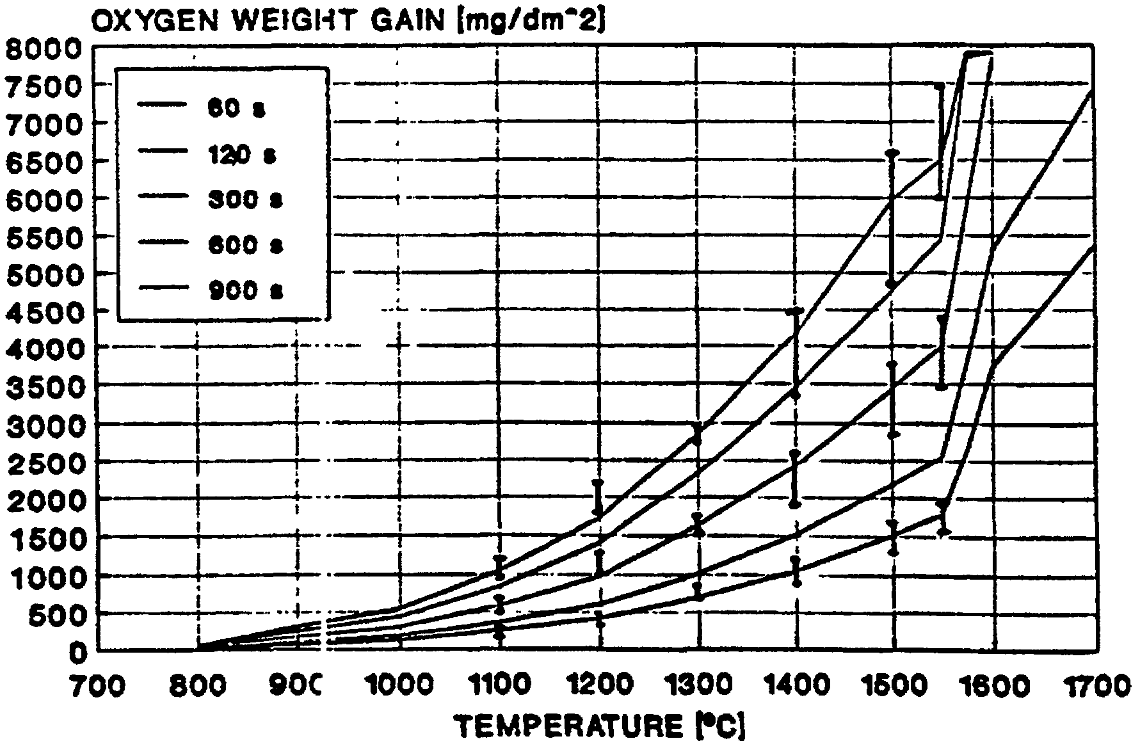

Figure S1.6b Specimen weight gain for various exposition periods and temperatures.

Figure S1.6 FRAOXI code validation - Zircaloy-4 isothermal experiments (their range is represented by vertical abscissae).

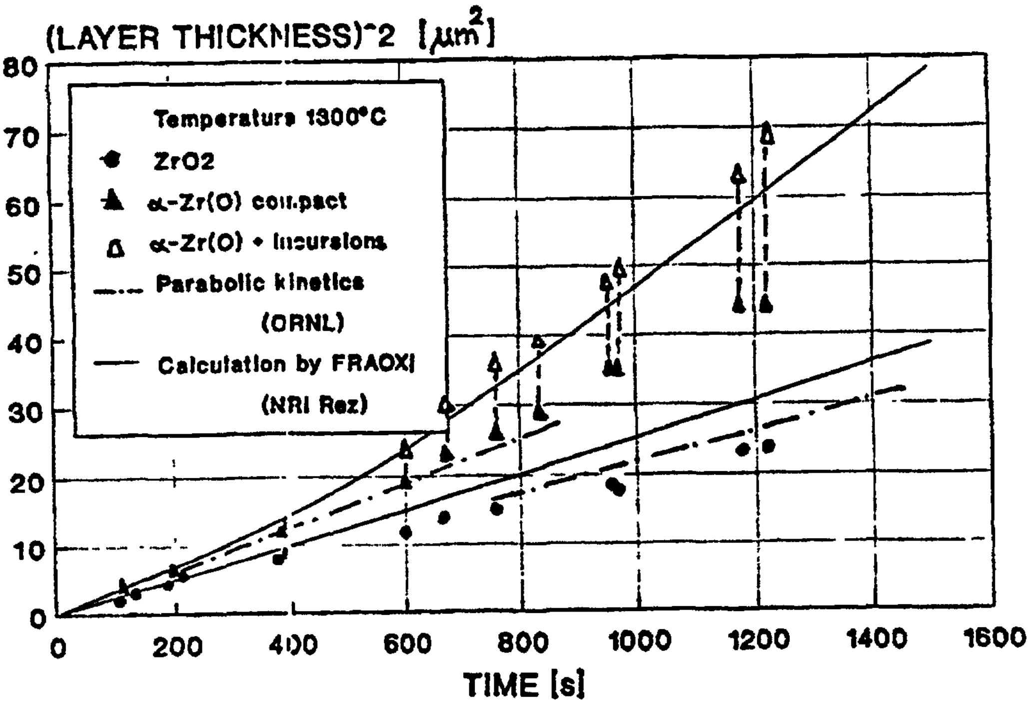

Figure S1.7a *Isothermal oxidation of Zircaloy-4 at 1300°C (experimental data from [34]). Effect of finite specimen geometry on oxidation kinetics*

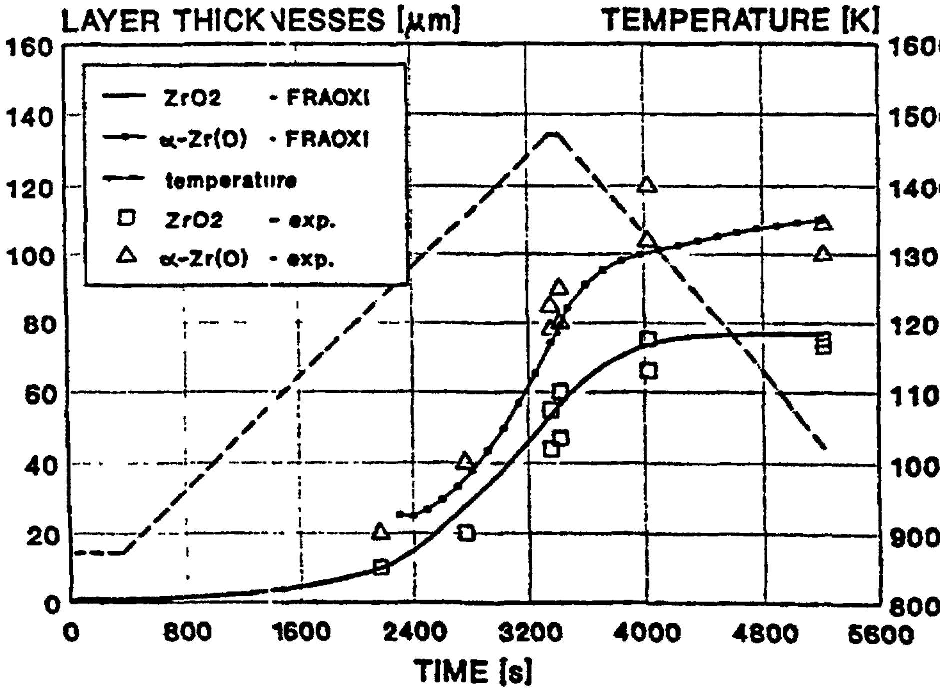

Figure S1.7b *Oxidation of Zr-1%Nb under temperature transient. Experimental data from [35]*

Figure S1.7FRAOXI code validation - zirconium alloys experiments.

References to Supplement S1

See references for Section 4.2.2.

Supplement S2

CONCRETE-CORE MELT INTERACTION INVESTIGATION: EQUIPMENT AND EXPERIMENTAL PROCEDURES

S2.1. INSTALLATION

To investigate the melt-concrete interaction, an experimental installation has been designed and operated at the High Energy Density Research Centre of the Russian Academy of Science. A schematic diagram of the installation is shown in Figure S2.1. The installation consists of a high temperature chamber 1, heating source 5, inert gas input and outputs 7, 8, and 9, temperature measurement device 10, and gas analyzers 11, 12, 13, 14, 15. A high frequency induction furnace with a power of 25 kW and a frequency of 0.44 MHz was used to melt the metals. A diagram of the high temperature chamber with the concrete crucible is shown in Figure S2.2. The chamber volume is 22 liters and the stainless steel chamber walls were water cooled. The chamber windows were used to measure the temperatures of the melt and the crucible. Shields protected the windows from the products of concrete decomposition and melt oxidation.

S2.2. MELT-CONCRETE TEMPERATURE MEASUREMENTS

Temperature measurement of the melt is a problem, because the aggressive medium and high temperatures make it difficult to use thermocouples. Optical techniques are difficult to apply due to instability of the melt surface radiation caused by oxides flowing over the liquid metal surface, melt intermixing and gas release. To eliminate these effects the crucible is made into a black body radiator by placing a zirconium dioxide concrete lid on the crucible with a small hole in the centre. To measure the melt temperature, an optical pyrometer was sighted at the hole. The lid and the crucible walls were thick enough (10-20 mm) to reduce temperature non-uniformity and generate black body radiation. Correction of the measured temperature was made, due to radiation reduction by the chamber window and reflection from a mirror. To measure the crucible temperature, both a thermocouple and the optical technique can be used. In the first case, chrome-alumel thermocouples are placed in the concrete at different distances from the bottom. The thermocouples operate up to 1300 K. They can also be used to determine the concrete erosion velocity. To measure temperature above 1300 K, the optical pyrometer was used.

S2.3. GAS COMPOSITION AND GAS YIELD DETERMINATION

The gas analyzer (Figure S2.1) consists of a gas supply, a heated chamber, a hygrometer, a sampler pipette, a chromatograph and a gas meter. To measure moisture, a conventional hygrometer was used, which operates on the piezo-sorption technique. To prevent water condensation, the temperature of the inductor and the chamber were kept at 340 K and the gas supply was specially heated up to 340 K.

The moisture level of the input gas was measured continuously during heating. The gas was sampled periodically. The total gas amount was determined by a drum type gas meter. Concentrations of H_2, O_2, N_2, CO_2, CO were measured by the chromatograph.

S2.4. CONCRETE EROSION VELOCITY DETERMINATION

The boundary between the liquid melt and the concrete moved during an experiment due to erosion. To determine the erosion velocity, the boundary displacement was measured on a cross section of the concrete sample after the experiment. The displacement of the lower boundary was also recorded by a pulsed X-ray apparatus. If the melt temperature was below 2000 K, the velocity was measured by thermocouples which were placed in the concrete at different depths.

S2.5. THE EXPERIMENTS WITH REFRACTORY CONCRETES

Two types of refractory concretes were investigated: alumina concrete (AC), filled with electric-melted corundum (Al_2O_3), and zirconium dioxide concrete (ZDC), filled with electric-melted zirconium dioxide stabilized by 6-7 mol.% of Y_2O_3. Both concretes hydration harden. The AC operates up to about 2000 K, and ZD concrete up to 2500-2600 K. AC and ZDC are more refractory than conventional concretes, which decompose at 1600-1800 K. AC and ZDC also contain less water than conventional concretes, resulting in less gas being released at high temperatures. Compositions and properties of AC and ZDC are shown in Table 4.5.1.

The concrete crucibles are cylindrical in shape with a height of 80-120 mm, a diameter of 50-60 mm and a wall thickness of 11-8.5 mm. The inside of the crucible may be either truncated cones with heights of 22 and 45 mm, upper and lower diameters of 50 and 48 mm, 32 and 28 mm, respectively, or a hemisphere with a radius of 22 mm.

The composition of the melt was estimated from a computer model. The model simulates a damaged water-water reactor WWER-1000 with a crushed and melted core, and with the lower part of the pressure vessel melted. A typical melt composition is estimated as: 6.33 m^3 of low-alloyed steel, 1.92 m^3 stainless steel, and 3.51 m^3 of zirconium with 1% niobium. To prepare a melt of this composition, a metal charge or a steel ampule containing zirconium and stainless steel was melted in the crucible.

Before heating, the chamber was evacuated and filled with argon up to atmospheric pressure. During the experiment, a great amount of steam was generated due to dehydration and concrete decomposition. The pressure inside the chamber was kept at atmospheric pressure by periodically pumping out the steam and refilling with argon. During the gas analysis the argon flow was kept at 2 l/min.

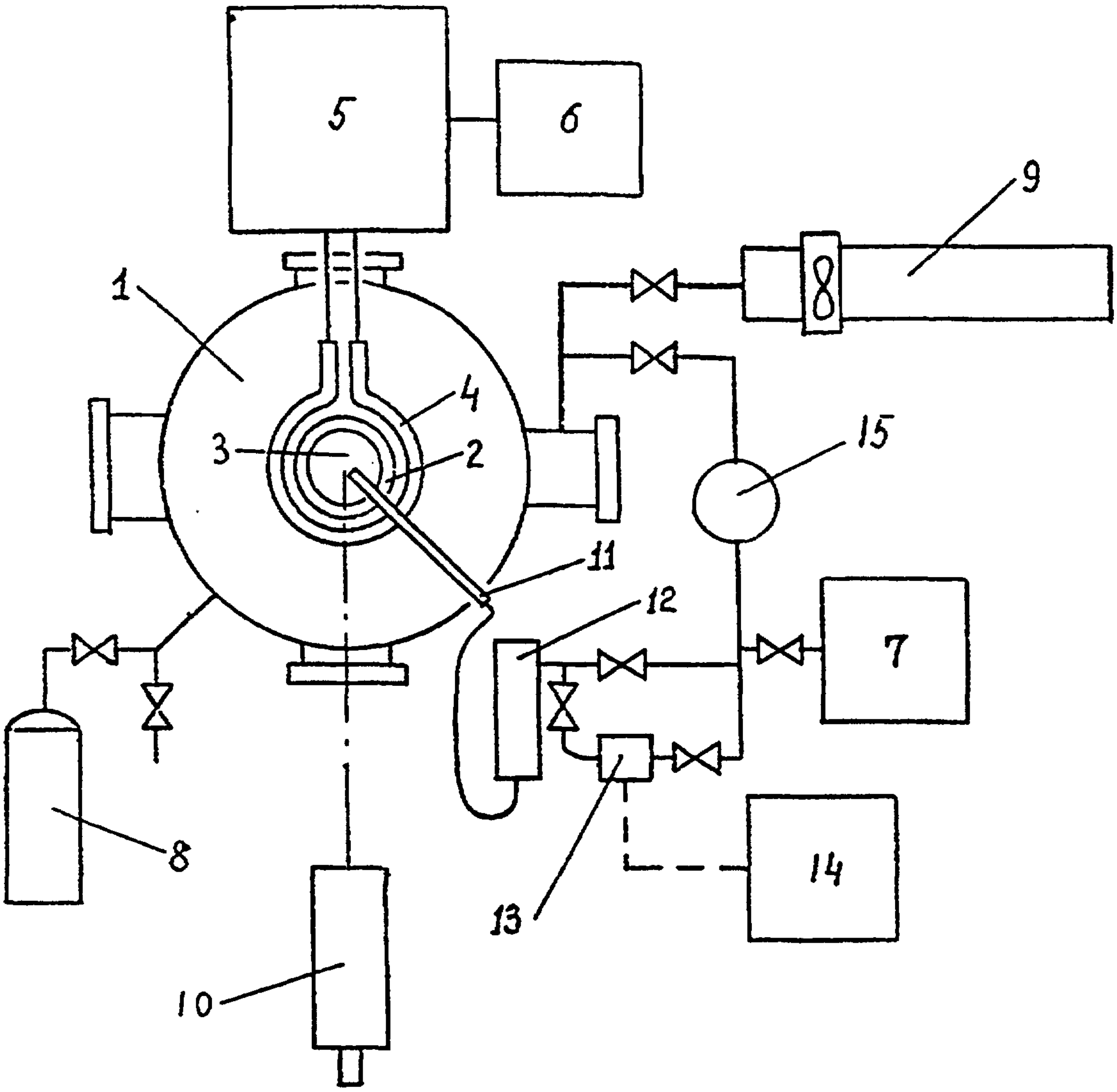

1 - the high temperature chamber;
2 - the concrete crucible;
3 - the metal melt;
4 - the inductor;
5 - the high frequency generator;
6 - the stabilizer;
7 - the vacuum pump;
8 - the gas cylinder;
9 - the ventilating pipe;
10 - the pyrometer;
11 - the sampler;
12 - hygrometer;
13 - the sample pipette;
14 - chromatograph;
15 - gas clock

Figure S2.1 The schematic diagram of the experimental installation

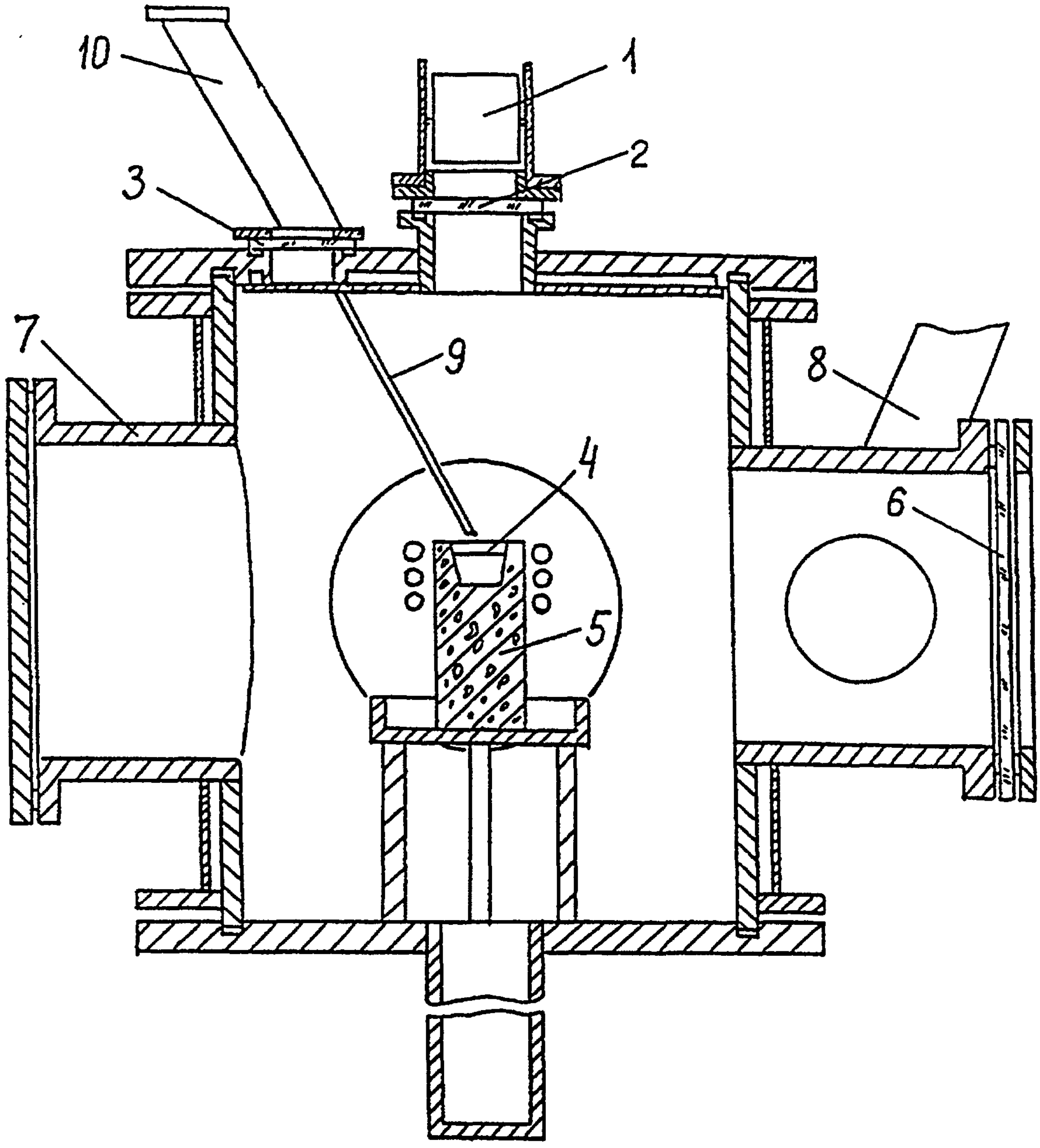

1 - the turning mirror;
2 - the window for measuring temperature;
3 - the access window;
4 - the metal melt;
5 - the concrete crucible;
6, 7 - the X-ray input and the X-ray film holder;
8 - the output gas pipe;
9 - the sampler;
10 - the sampler gearing.

Figure S2.2 The high temperature chamber

Supplement S3

THERMAL CONDUCTIVITY OF U-Al ALLOY AND UO_2

S3.1. THE THERMAL CONDUCTIVITY OF U-Al ALLOY

S3.1.1. Introduction

U-Al alloy has been used as a fuel material in most Engineering Test Reactors (ETR) and High Flux Material Test Reactors (HMTR). This alloy of U-Al_4 particles is dispersed in a low absorbing cross section Al matrix. Because of its good thermal conductivity, strength, resistance to corrosion, radiation stability, ease of manufacture and low cost, this alloy is very attractive for test reactors and research reactors.

In 1943, research on U-Al alloy was included as part of the Manhattan project. After P. Gordon and A. R. Kaufman determined the phase diagram of U-Al alloy [1], H. A. Saller [2] of American BMI and B. S. Borie [3] of ORNL further studied the relationship between the constitution and properties of the alloy. ORNL first used this alloy as fuel elements in an MTR [4,5]. ANL collaborating with NMD manufactured the fuel elements used in CP-5 in 1960 [6]. Generally, the uranium content of the U-Al alloy does not exceed 30 wt.% for use in test and research reactor.

Thermal conductivity is an important design parameter for fuel elements and reactor safety analysis, but there is little early data published. Thermal conductivity depends on material composition and processing conditions, because of this the thermophysical properties of U-Al alloy were measured in the 1960's when it was planned to build a high flux reactor in China [7,8].

S3.1.2. The measurement of the thermal conductivity of U-Al alloy

Sample

The U-Al was provided by the China National Nuclear Industry Corporation. The method of vacuum-induction melting and centrifugal casting in air was employed. The uranium content of the alloy is 25.4 wt.%. Metallographic examination has shown that the structure of this alloy is a eutectic between α-Al and UAl_4 and there is UAl_3 which is about 4% in volume existing in the alloy at room temperature. The sample used in this experiment is an extruded rod 220 mm long and 2.965 mm in diameter. There is a textural tendency during extrusion and then the rod was annealed for 1 hour at 893 K.

Experiment - principle, method and execution of measurement

The method of steady state longitudinal thermal flux with direct electric heating of the sample was employed to measure the thermal conductivity. This is a method of stable heat conduction with inner heat source. The differential equation for this method is more complex than with external heating. With a simplified mathematical model and different boundary conditions, there are more than ten solutions. The measurement method we used is based on B.K. Miklokov and the instrument was made by the Beijing Metallurgy Meter Factory. The structure of the instrument is shown in Figure S3.1.

When the sample rod was heated by direct current, the Joule heat produced by the sample resistance was conducted from the middle of the sample to both of the extreme points along the sample longitudinally while the heat exchange with its surroundings exits in the radial direction. The heat equilibrium equation is:

$$\gamma\left(\frac{dV}{dx}\right)^2 + K\frac{d^2t}{dx^2} + \alpha P\frac{t_0 - t}{S} = 0 \qquad \text{(S3-1)}$$

Here, γ and K are electrical conductivity and thermal conductivity respectively, α is the heat exchange coefficient, t_0 is the average temperature of the periphery medium, P is the girth of the sample, S is the cross-sectional area. The solution of equation (S3-1) is

$$K = \frac{-\gamma \Delta V^2}{2(\Delta t_s - \varepsilon N)} \qquad \text{(S3-2)}$$

$$\gamma = \frac{LI}{S \Delta V} \qquad \text{(S3-3)}$$

where ΔV is the average electric potential difference between the measured points of the rod; I is the current through the sample. Δt_s is the temperature difference between the measured points.

$$\Delta t_s = t_5 - \frac{t_4 + t_6}{2} \qquad \text{(S3-4)}$$

ε, N is a correction factor for

$$N = \left(t_2 - \frac{\Delta t_l}{6}\right) - \left(t_5 - \frac{\Delta t_s}{6}\right), \quad \varepsilon = \frac{\Delta t_s}{N_0}, \quad \Delta t_l = t_2 - \frac{t_1 + t_3}{2} \qquad \text{(S3-5)}$$

"N_0" is the corresponding value when the power is switched off. At equilibrium there is a parabolic temperature distribution along the rod. The average temperature of the sample is

$$t = t_5 - \frac{\Delta t_s}{3} \qquad \text{(S3-6)}$$

The experiment was performed with the furnace and sample situated in a vacuum chamber at a pressure of $3 \cdot 10^{-3}$ Pa.

Measurement results

The instrument was calibrated using American NBS SRM-1464 and Chinese GB200-75 DT-7 electrolytic pure iron. The measured results agree with the reference data to within 5%. The thermal conductivity of the U-Al sample was measured over the temperature range 356 to 617 K. The results are shown in Table S3.1, and fitted by the least square method to get the following expression:

$$K = 180.26 - 2.29 \times 10^{-2}\, T \qquad \text{(S3-7)}$$

The standard deviation of above expression is ± 2.04%.

The sample was then annealed at 893 K for 24 hours and measured again. The conductivity data were reported in the reference [10]. The uncertainty of the measurement is ±5%. The data measured above and the thermal conductivity of an U-Al alloy (Al 77.3 wt.%, U 22.7 wt.%) measured by H.A Saller are shown in Figure S3.2. From this figure it can be seen that the thermal conductivity of the U-Al alloy falls slowly and linearly with rising temperature.

S3.1.3. Discussion

In 1955, H. A. Saller [2] measured the thermal conductivity of several forged U-Al rods (uranium content 12.5, 22.7, 30.5 wt.% respectively) in the temperature range 373-673 K by the comparative method (using lead as a reference material). The sample was annealed at 643 K for half an hour. The results, together with the values for pure aluminum and the 25.4 wt% U-Al alloy are shown in Figure S3.3. All the conductivity values tend to decrease with increasing uranium content (see Figure S3.4) as might be predicted.

From the data obtained, the average values given in Table S3.1 are suggested.

The thermal conductivity data for the U-Al alloy (Al 77.3 wt.%, U 22.7 wt.%) measured by Saller has also been fitted by the least square method and the following expression obtained:

$$K = 187.39 - 4.18\times10^{-2}\ T \quad (W/(m\cdot K)) \tag{S3-8}$$

Allowing for the different aluminium content, our expression is about 3.5% higher than Saller. This may be due to the processing of the material or the impurity level. In any event, the temperature dependance of the thermal conductivity is small.

The thermal conductivity of the annealed sample is about 5% higher than that of the unannealed sample because the texture produced by extrusion has been removed and a stable microstructure has been achieved.

Annealing does not affect the thermal conductivity of a pure metal, but for alloys quenching and cold working forms a textured microstructure. For example, annealing the U-Al alloy converts the elongated particles of UAl_4 into spherical particles. Elongation of these particles affects both the lattice conductivity and electronic contribution to the thermal conductivity.

T. I. Jones et al [9] measured the thermal conductivity (at 338 K) of several U-Al alloy samples of different uranium and aluminium weight percent, before and after annealing at 893 K for 5 days, by means of a comparative method using Cu as the reference sample. The results showed that annealing had an affect on the thermal conductivity and the size of the extent was related to the uranium and aluminium weight percentage (see the Figure S3.5.). For example, the thermal conductivity of the 21.43 wt.% U-Al alloy after the annealing was 21% higher than that before annealing. When the uranium content decreases to 12.91 wt.%, the increase was 3.7% less. However when the uranium content is higher than 30 wt.%, the thermal conductivity decreases. So the preparation technology, microstructure and composition are all factors which affect the thermal conductivity.

It can be seen from the phase diagram [1] that a eutectic between α-Al and UAl_4 is produced at 13 wt.% and 913 K. When the uranium content is higher than 18 wt.%, UAl_3 is formed. The higher the uranium content, the more UAl_3 is produced. In the process of solidifying, the UAl_3 reacts with the Al to produce UAl_4. At room temperature, the uranium exists as a α-U and UAl_4 eutectic. Because there are no phase transformation below 873 K (the DTA curve is stable), the result can be extrapolated to obtain the thermal conductivity up to 873 K.

It is well known that the thermal conductivity of aluminum rises slowly with increasing temperature. Because the UAl_4 dispersed in the Al-matrix will affect the lattice thermal conduction, the thermal conductivity of a U-Al alloy will be lower than that of pure Al. In general, the thermal conductivity of an alloy can be divided into two parts; the crystal lattice thermal conductivity and the electronic thermal conductivity. At low temperatures, the crystal lattice conductivity decreases with rising temperature while at high temperature electronic conduction contributes to the thermal conductivity. According to the above consideration, the thermal conductivity data extrapolated to 873 K might be conservative. Therefore the extrapolated data can be used in the design and safety analyses of fuel elements having an uncertainty of ± 5%.

S3.2. THE THERMAL CONDUCTIVITY OF UO_2

S3.2.1. General review

The thermal conductivity of UO_2 is an important parameter in the design and safety analysis of nuclear fuel elements. A lot of data about the thermal conductivity of UO_2 has been published and evaluated by many researchers [11-14]. Several recommended expressions have been based on the data recommended by the IAEA in 1965 [15] and those obtained by the USAEC Round Robin Measurement project [16] in 1970 in which high density, stoichiometric UO_2 was measured. Further expressions based on measured data have been derived in [12,17,18,19]. Both out of pile and in pile measurement on UO_2 have been performed since the 70's in China, and expressions obtained based on [20-25]. Some of them have been reported in the 2nd RCM.

Data on the thermal conductivity of UO_2 from 3023 K to the melting point has not been published except J.C. Weilbacher's data [19] above 2773 K that include 8 data points measured by the laser flash technique.

The data measured by different researchers below 1773 K are more consistent (± 10%) than those at high temperatures (± 20-30%). The results measured in-pile are more variable.

The data on thermal diffusivity and thermal conductivity of molten UO_2 are very important in reactor safety analysis for an hypothetic core melt accident. Few of the data on this aspect have been reported [26, 27, 30, 38]. Due to different view on the heat transfer mechanism with UO_2, the estimated values of thermal conductivity by different authors differ significantly. Based on a reassessment of existing data, J.K. Fink et al.,recommended a new value of 5.6 W/(m·K) for the thermal conductivity of UO_2 [35].

This appendix will mainly introduce the measured data and suggested results on solid UO_2 obtained in China.

S3.2.2. Evaluation of the suggested expressions for UO_2 thermal conductivity

The thermal conductivity of UO_2 is a function of temperature, density and stoichiometric composition. The thermal conductivity decreases with rising temperature from room temperature to 2000 K, and after reaching a minimum at 2000 K rises until the melting point. Thermal conductivity is generally considered to be the sum of contributions due to lattice vibrations, electron-hole pairs and radiant heat transfer.

The experimental results of most researchers show that the thermal resistance of UO_2 is linear with temperature from the Debye temperature to 1500 K, eg.

$$R = \frac{1}{K_L} = A+BT \tag{S3-9}$$

where A is the thermal resistance due to phonon-impurities and grain-boundary collisions, BT is the thermal resistance induced by phonon-phonon scattering. Since the average phonon path cannot be less than the distance between atoms, some researchers consider equation (S3-9) valid until T_l = 2050 K [17] or 2323 K [28] where K_L becomes constant, equal to the value of the expression at temperature T_l. Others [29] consider that the equation (S3-9) is invalid at high temperature because the atoms are far from harmonic vibrators and a lot of defects exist, so parameter A should depend on temperature. A suitable expression for high temperature phonon conduction has not yet been reported. The average phonon free path calculated in reference [18] is always longer than that between atoms. The average phonon free path length given in reference [23] for measurement up to 2773 K has a value of 4.4 Å (2500 K), and an extrapolated value of 3.7 Å (3000 K), which is close to the actual distance between atoms. So most researchers consider the phonon thermal conductivity to be given by equation (S3-9) from room temperature to the melting point, for example, Brandt and Neuer [12] and J. H. Harding et al [18] used equation (S3-9) to calculate the phonon thermal conductivity. J.K. Fink et al [13] fitted (existing) experimental data using the following expression for the phonon contribution.

$$K_L = \frac{1}{A+BT+CT^2} \tag{S3-10}$$

This incorporates a third term for contributions from phonon-phonon collisions by four-phonon processes. This contribution is in the CT^2 term. This term improves the fitting precision of thermal conductivity in the range of 1300-2100 K.

The thermal resistance deviates from linear above 1500 K because other mechanisms begin to contribute to the thermal conductivity. In the early 60's, the increase in the thermal conductivity above 2000 K was attributed to electronic conduction, and in 1972, quantitative research on this was reported by Weilbacher [19].

Electrical conductivity measurements [31] have shown that UO_2 becomes semiconducting above 1400 K and the electron-hole pairs formed, diffuse to the cold region in the form of a heat current under the effect of the temperature gradient. This is the dynamic small polaron heat transportation theory reported in recent years. As the electron-hole pairs are the most important contributor to the heat transfer process, the thermal conductivity rises at high temperature.

According to the energy band theory of a semiconductor, the electron-hole pair contribution could be expressed as follows:

$$K_e = 2\left[\frac{K_B}{e}\right]^2 T \left[\sigma + \frac{2\sigma_e\sigma_h}{\sigma}\left[\frac{E_g}{2K_BT}+2\right]^2\right] \tag{S3-11}$$

where:		
	K_e	electron thermal conductivity;
	$\sigma = \sigma_e + \sigma_h$	the electrical-conductivity of UO_2;
	K_B	Boltzmann constant;
	$E_g = 2E_a$	energy gap between the valence band and conduction band;
	e	electron charge;
	σ_e	electron conductivity;
	σ_h	hole conductivity;
	T	temperature (K).

Bates measured the electrical conductivity of UO_2:

$$\sigma = 3.57\times10^7 \exp\left(\frac{-E_g}{2K_BT}\right) \tag{S3-12}$$

that is

$$\sigma = 3.57\times10^5 \exp\left(\frac{-1.15eV}{K_BT}\right) \tag{S3-13}$$

Substituting exp. (S3-13) into exp. (S3-11)

$$K_e = 2\left[\frac{K_B}{e}\right]^2 T\times3.57\times10^7 \exp\left(\frac{-E_g}{2K_BT}\right)\left[1+\frac{2f}{(1+f)^2}\left[\frac{Eg}{2K_BT}+2\right]^2\right] \tag{S3-14}$$

where $f = \sigma_h/\sigma_e$.

The first term in expression (S3-14) is the generally known Wiedemann-Franz Law. The second term expresses the small polaron contribution. The term $2f/(1+f)^2$ varies only slightly with changing temperature, as does the term.

$$\frac{2f}{I+f^2}\left[\frac{Eg}{2K_BT}+2\right]^2$$

So, expression (S3-14) can be approximately represented by the following

$$K_e = DT\exp\left(-\frac{E_a}{K_BT}\right) \tag{S3-15}$$

where D is a constant. The measured electron thermal conductivity results have been fitted to the above form of expression and a value for E_a obtained for 98% TD UO_2 which was very close to the theoretical value. Weilbacher discovered that his experimental results were lower than predicted by $K = K_L + K_e$ above 2673 K and introduced a third contribution K_{lac} to fit his high temperature data.

This is included in the following expression

$$K = K_L+K_e-K_{lac} = \frac{1}{A+BT} + DT\exp\left(-\frac{E_a}{K_BT}\right) - F\exp\left(-\frac{E_D}{K_BT}\right) \tag{S3-16}$$

where K_{lac} come from K_{mes} - ($K_L + K_e$).

Brandt and Neuer also employed a third term which reduces the thermal conductivity due to dislocations to fit their experimental data, and put $E'_D = -3.29$. Because different experimental data were used in the fitting expression, the parameters are different, especially the impurity defects which have more of an effect on the A value, shown in the following,

	$A\times10^{-2}$	$B\times10^{-4}$	$D\times10^{-2}$	E_a	$F\times10^5$	G
Brandt & Neuer	4.39	2.16	11.20	-1.18	-4.18	-3.29
Weilbacher	5.91	2.02	9.58	-1.13	-4.18	-3.29

So, in general the thermal conductivity of UO_2 can be expressed by:

$$K = \frac{1}{A+BT+CT^2} + DT\exp\left(\frac{E_a}{K_BT}\right) + F\exp\left(\frac{G}{K_BT}\right) \tag{S3-17}$$

Recently it has been shown by both measurement and theoretical research on the specific heat, electrical-conductivity, thermoelectrical potential and thermal diffusion, that the electron is the most important contributor to the transfer properties of UO_2 above 1400 K. As the physical properties of materials are related to each other, all researchers believe that the contribution of electron-hole pairs at high temperature make the thermal conductivity increase with temperature. Fink believed that the thermal conductivity was better expressed by a linear equation above the phase transformation at 2670 K, and recommended the following expressions:

For $T < 2670$ K

$$K = \frac{1}{A+BT+CT^2} + DT\exp\left(\frac{E_a}{K_BT}\right) \tag{S3-18a}$$

for T > 2670 K

$$K = L_1 + L_2 T \tag{S3-18b}$$

where L_1 and L_2 are constants.

Six forms of expressions were compared by Fink who chose expression (S3-18) to fit all the combined data with a relative standard deviation of 6.23%, which is lower than that of the Brandt Neuer equation(7.34%). Fink believed that the inclusion of the four-phonon collision term CT^2 is more statistically important than including the dislocation term. The dislocation term appears to mainly contribute to fitting of the eight high-temperature data points. So, the dislocation term was not included in Fink's expression.

Recently, Harding and Martin [18] also recommended expression (S3-19) for the thermal conductivity of fully dense solid UO_2 between 773 and 3120 K.

$$K = \frac{1}{(0.0375+2.165\times10^{-4}T)} + \frac{4.715\times10^{9}}{T^2}\exp\left(-\frac{1.41}{K_B T}\right) \tag{S3-19}$$

The uncertainty of the above expression is about 7% up to about 1800 K and about 15% at 3120 K. The first term, due to the contribution from the phonon, will take effect up to the melting point, and the second term is due to small polaron contribution. The two mechanisms are important at high and low temperature respectively. The dislocation term was omitted.

In conclusion we believe that the thermal conductivity expressions for fully dense stoichiometric UO_2 obtained by different researchers do not differ significantly below 2670 K. Further work is needed to obtain an expression for temperatures above 2670 K owing to uncertainty on the thermal conductivity mechanisms and the lack of experimental data.

S3.2.3. Evaluation of the experimental result and recommended expressions in China

Since 1970 the thermal conductivity of UO_2 has been measured in China by means of Laser Pulse Method and Radial Heat Current Method. According to the UO_2 thermal conductivity mechanisms considered, each author obtained an expression for thermal conductivity. Wendan Li and Lili Zhang [21] measured the thermal diffusivity and calculated the corresponding thermal conductivity of sintered 96.5% TD, UO_2 pellets with an O/U ratio of 2.003 over the range 573 to 2773 K. The following expression was obtained:

$$K_{96.5} = \frac{1}{A+BT} + CT\exp\left(-\frac{E_a}{k_B T}\right) + D\exp\left(-\frac{E_a'}{k_B T}\right) \tag{S3-20}$$

where:

$A = 5.38\cdot10^{-2}$ m·K/W;	$B = 2.09\cdot10^{-4}$ m/W;
$C = 6.052\cdot10^{-2}$ W/(m·K^2);	$E_a = 1.12$ eV;
$D = 4.07\cdot10^{5}$ W/(m·K);	$E'_a = 3.72$ eV;
k_B = Boltzmann constant.	

The maximum fitting deviation is 0.4 W/(m·K).

Because $K_{mes} < K_L + K_e$ when the temperature is over 2670 K, a third term was added. Due to electron scattering by the oxygen vacancies activated at high temperature. The calculated results from expression (S3-20) are shown in Table S3.2. The integrated thermal conductivity is

$$\int_{773}^{3123} K_{96.5} dT = 6.97\ KW/m$$

with a deviation of ± 0.8 kW/m and is in good agreement with data recommended in the literature [34].

Shihao Ying [23] et al measured the thermal diffusivity of seven sintered UO_2 pellets (95.3%TD, U/O=2.003) in temperature range 291 to 2791 K and calculated the corresponding thermal conductivity. The following polynomial expression was obtained using least squares:

$$K_{95.3} = 10.4266 - 1.26014\times10^{-2}T + 7.79138\times10^{-6}T^2$$
$$- 2.48177\times10^{-9}T^3 + 3.4824\times10^{13}T^4 \quad (W/m{\cdot}K)$$

The standard deviation is ±3.2%.

At the same time, in the temperature range 500 to 3100 K, an equation for the thermal conductivity of stoichiometric UO_2 with a porosity $P < 0.1$ was recommended on the basis of consideration of the thermal conductivity mechanisms and experimental data

$$K = F\left[\frac{1}{A+BT} + DT\exp\left(-\frac{E_a}{k_BT}\right)\left[1+H\left(\frac{E_a}{k_BT}+2\right)^2\right]\right] \quad (W/(m{\cdot}K)) \qquad \text{(S3-21)}$$

where:
$F = 1-\alpha P$; $\alpha = 2.7 - 5.8{\cdot}10^{-4}\ T$;
$A = 3.68{\cdot}10^{-2}$ m·K/W; $B = 2.25{\cdot}10^{-4}$ m /W;
$D = 5.31{\cdot}10^{-3}$ W/(m·K^2); $E_a = 1.15$ eV;
$H = 0.264$; $k_B = 8.6144{\cdot}10^{-5}$ eV/K.
and P in the volume fraction of porosity.

The standard deviation of the expression (S3-21) is ± 3.6%. The integrated thermal conductivities are:

$$\int_{773}^{3123} K_{95} dT = 6.4\ KW/m \qquad \int_{773}^{3123} K_{100} dT = 7.0\ KW/m$$

which are close to the 7.3 ± 5 kW/m recommended in other literature.

This equation takes account of the porosity and the oxygen vacancy term and values for the above expression are listed in Table S3.3.

Jinnan Yu et al [22] measured the thermal conductivity of UO_2 (97% TD O/U=2.00) pellets in-pile and obtained an integrated thermal conductivity curve over the range 478 to 2836 K (see Figure S3.6) and the thermal conductivity over the range 486 to 2773 K with an error = 8%. The thermal conductivity was expressed as $K = K_L + K_e$, i.e.,

$$K = \frac{1}{A+BT} + CT\exp\left(-\frac{E_a}{K_BT}\right) \qquad \text{(S3-22)}$$

where:
$A = 7.01{\cdot}10^{-2}$ m·K/W; $B = 1.89{\cdot}10^{-4}$ m/W;
$C = 2.29{\cdot}10^{-5}$W/m; $E_a = 1.48$ eV.

The results of both the experiment and equation are given in Table S3.4.

Porosity has a great effect on the thermal conductivity of UO_2. At present, there is no theory which could describe the general relation between the thermal conductivity and the porosity. Most researchers [17] believe that the Loeb's semi-empirical formula

$$K_P = K_0(1-\alpha P) \tag{S3-23}$$

provides the best fit to the measured results of UO_2 with different porosity. Here, K_P and K_0 are the thermal conductivity when the porosity is P and zero respectively, α is the porosity coefficient. The Craeynest's [37] relation between α and temperature was recommended for $T < 1273$ K

$$\alpha = 2.74 - 0.58\times10^{-3}T \tag{S3-24}$$

The modified Maxwell-Eucken expression can also be used to correct for porosity.

$$K_p = K_0\left[\frac{1-P}{1+\beta P}\right] \tag{S3-25}$$

The above formula is theoretically based and is generally valid for porous ceramics. Both ß and α are related to the shape, distribution and the heat transfer properties of the pores. It can be seen that both α and ß decrease with increasing temperature. This phenomena can be explained as the increases of the gas heat transfer and heat radiation in pores with temperature increasing, which causes the decrease of the pore effects on thermal conductivity.

For the comparison between experimental and calculated results, the thermal conductivity of UO_2 has been modified by means of expression (S3-23) and (S3-24). The thermal conductivity in references [21,23] was corrected to that of 100% TD, and was compared with that in other references (see Figure S3.7).

S3.2.4. Conclusions

This section has evaluated the expressions recommended for the thermal conductivity of UO_2, the main experimental results and the recommended expressions for the thermal conductivity of UO_2 use in China.

It is very important for the design and operation of fuel elements in light and heavy water reactors to use a data base which not only has physical meaning but an experimental basis. From this point of view, it is appropriate to describe the thermal conductivity of UO_2 by using both the phonon and small polaron models, which fit both the direct experimental measurements and the integral values. It is also appropriate to add a defect scattering term (CT^2) for high temperatures ($T > 2670$ K). Whether a linear term should be used for the defect scattering is open to conjecture at present because of the lack of experimental data and disagreement on the conduction mechanism. At present the general formula [18] should still be used, but it should be continually reviewed, based on new thermal conductivity data and integrated thermal conductivity data as to whether a defect scattering term is necessary and as to its exact form.

Table S3.1 THE SUGGESTED VALUES OF THE THERMAL CONDUCTIVITY OF THE U-Al ALLOY WITH DIFFERENT URANIUM CONTENT (W/(m·K))

T	The content of uranium (wt.%)					
(K)	**0.0**	**12.5 [1]**	**22.7 [1]**	**25.4***	**25.4****	**30.5 [1]**
373	211	-	-	169	171.7	-
473	222	183	168	168	169.4	151
573	228	181	164	167	167.1	149
673	230	179	159	165	164.8	148
773	-	-	-	-	162.6	-

* Values recommended Z.Z. Lei et al   ** Results by current author

Table S3.2 MEASURED RESULT OF THERMAL CONDUCTIVITY OF 96.5% TD UO_2

Temperature (K)	Conductivity (W/(m·K))
573	5.76
673	5.14
773	4.64
873	4.23
973	3.89
1073	3.59
1173	3.34
1273	3.12
1373	2.93
1473	2.76
1573	2.61
1673	2.48
1773	2.42
1873	2.35
1973	2.30
2073	2.29
2173	2.30
2273	2.34
2373	2.42
2473	2.53
2573	2.69
2673	2.88
2773	3.13
-	-

Table S3.3 THE THERMAL DIFFUSIVITY (a, 10^6 m^2/s) AND CONDUCTIVITY (K, W/(m·K)) of UO_2 [23]

T (K)	a	$K_{95.3}$	K_{100}
300	2.98	7.28	9.57
400	2.41	6.48	7.87
500	2.01	5.79	6.69
600	1.72	5.18	5.81
700	1.51	4.66	5.14
800	1.35	4.20	4.60
900	1.22	3.82	4.17
1000	1.11	3.48	3.81
1100	1.01	3.20	3.51
1200	0.922	2.96	3.26
1300	0.845	2.75	3.04
1400	0.788	2.58	2.86
1500	0.723	2.44	2.70
1600	0.679	2.33	2.57
1700	0.647	2.24	2.47
1800	0.625	2.17	2.40
1900	0.609	2.12	2.35
2000	0.597	2.11	2.32
2100	0.586	2.11	2.34
2200	0.570	2.15	2.37
2300	0.550	2.21	2.43
2400	0.527	2.31	2.52
2500	0.502	2.44	2.63
2600	0.490	2.63	2.78
2700	0.509	2.86	2.95
2800	-	-	3.15
2900	-	-	3.38
3000	-	-	3.63
3100	-	-	3.91
-	-	-	-

Table S3.4 THE THERMAL CONDUCTIVITY OF UO_2 MEASURED IN-PILE [22]

T (°C)	$K_{\text{Experiment}}$ (W/(m·K))	$K_{\text{Calculation}}$ (W/(m·K))
210	6.56	6.20
300	5.30	5.60
400	4.88	5.06
500	4.51	4.63
600	4.20	4.25
700	3.92	3.94
800	3.67	3.66
900	3.44	3.43
1000	3.28	3.22
1100	3.12	3.04
1200	3.00	2.87
1300	2.80	2.73
1400	2.70	2.61
1500	2.50	2.50
1600	2.40	2.40
1700	2.30	2.33
1800	2.20	2.28
1900	2.25	2.26
2000	2.25	2.27
2100	2.37	2.32
2200	2.50	2.41
2300	2.60	2.55
2400	2.70	2.74
2500	2.90	2.98

Table S3.5 MEASURED RESULTS OF THE THERMAL CONDUCTIVITY OF U-Al ALLOY

Temperature (K)	Conductivity (W/(m·K))
356	166.1
357	165.3
360	172.0
363	167.8
370	173.2
382	165.3
392	168.2
395	170.7
403	172.8
414	167.4
431	169.0
445	166.9
447	172.4
452	166.1
468	163.6
470	169.0
479	169.0
487	166.5
492	166.9
494	170.7
509	169.5
514	169.5
519	166.5
529	171.5
527	166.1
537	167.4
539	169.5
559	169.5
593	166.9
598	166.9
606	166.1
617	166.1
700	162.6 (extrapol.)
800	158.4 (extrapol.)

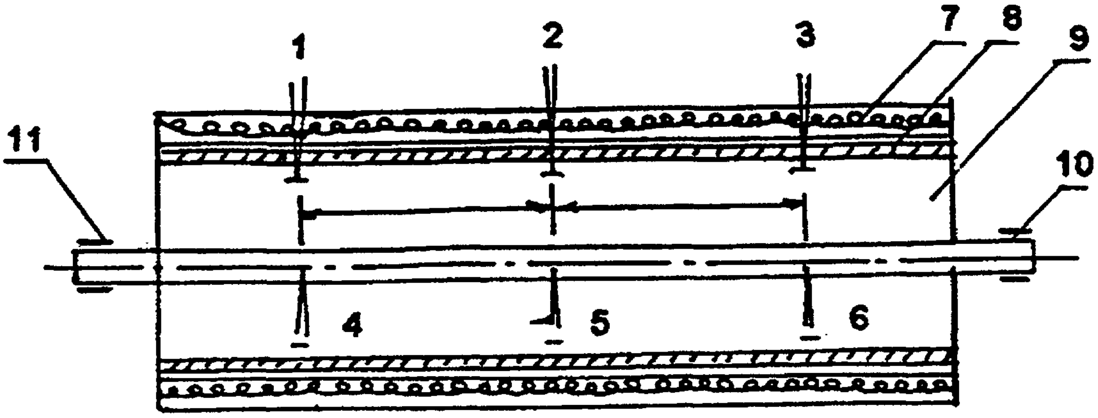

1,2,3	*Thermo-couples used to measure the temperature of environment*
4,5,6	*Thermo-couples used to measure the temperature of sample*
7	*Compensating heater*
8	*Uniform temperature tube*
9	*Heat-insulating materials (foam Al_2O_3)*
10	*Sample*
11	*Electrode*

Figure S3.1 Sketch for the principle of apparatus

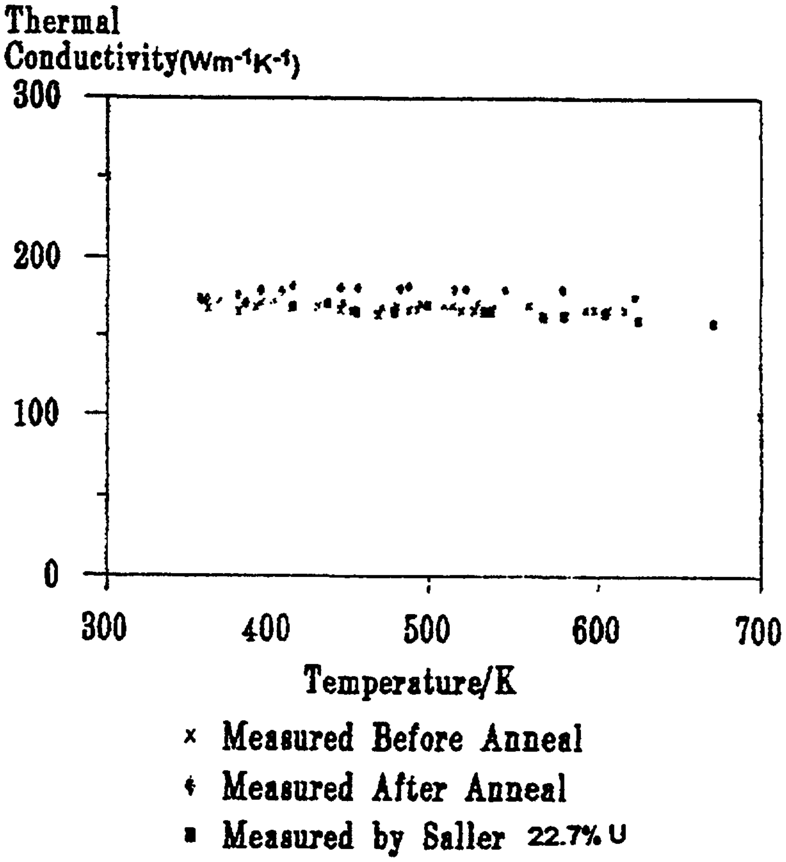

Figure S3.2 The measured results of the thermal conductivity of U-Al alloy

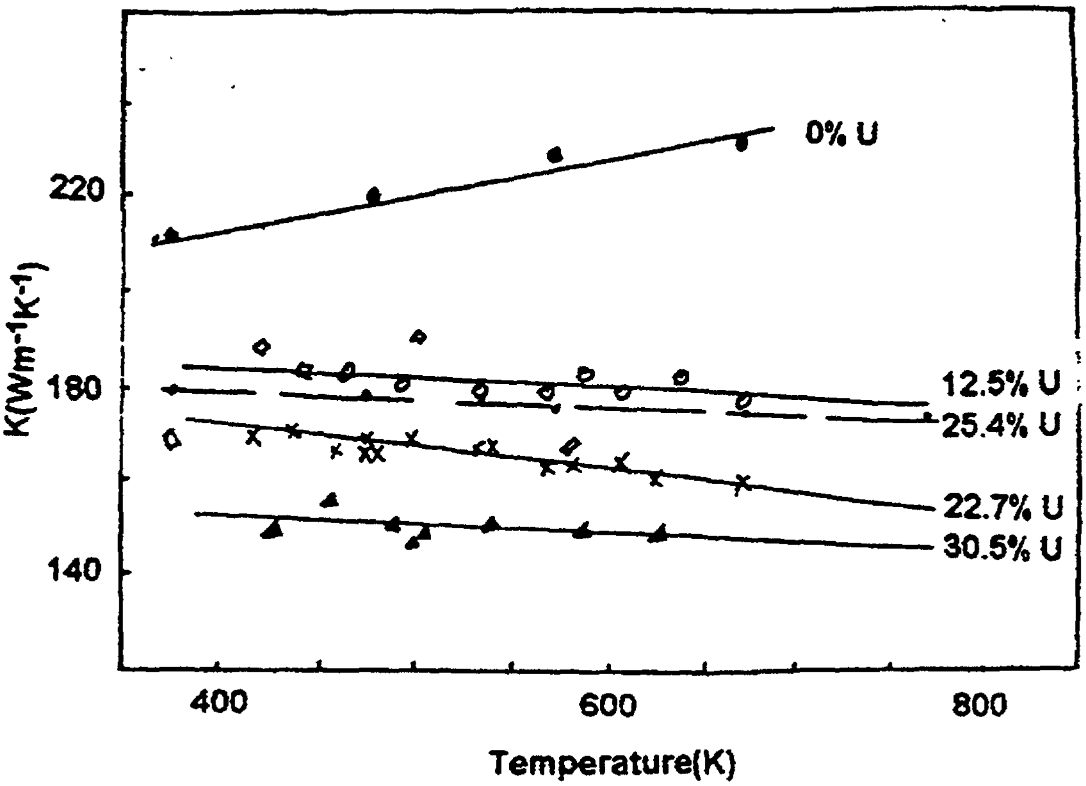

Figure S3.3 Thermal conductivity of U-Al alloys

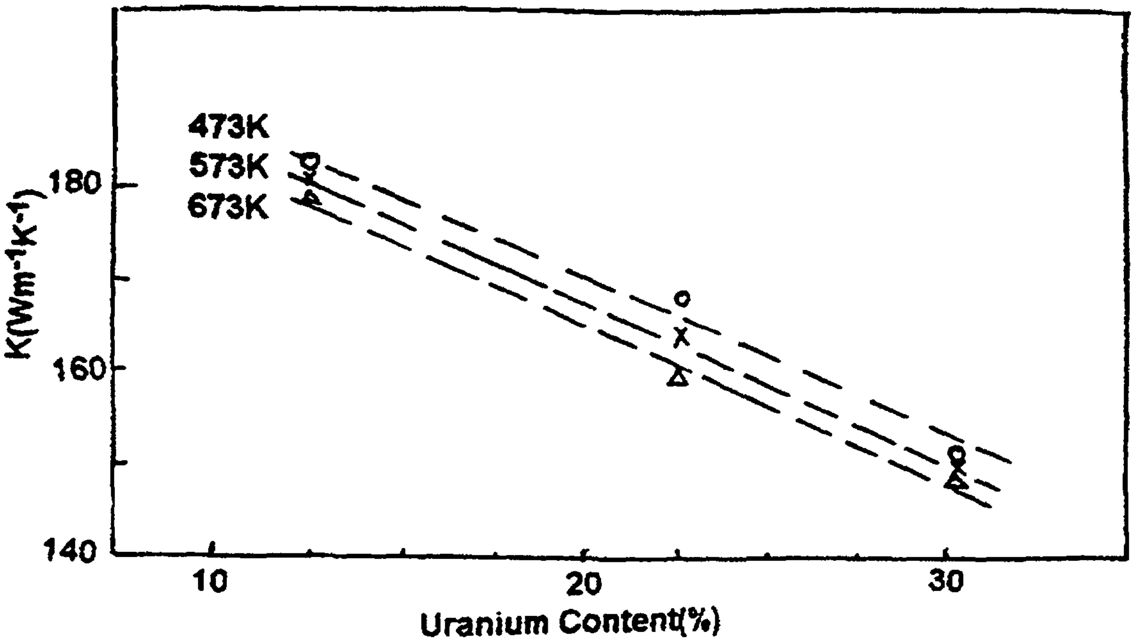

Figure S3.4 Relation between the thermal conductivity of U-Al alloy and the uranium content

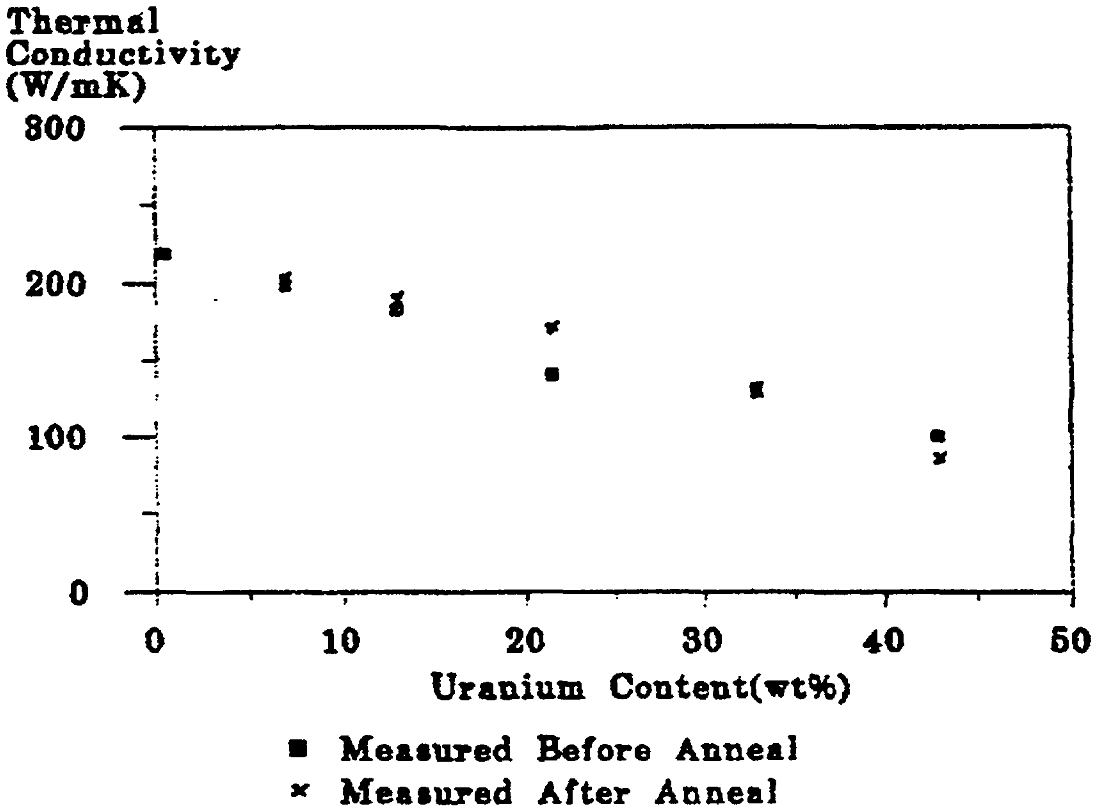

Figure S3.5 The anneal effect on the thermal conductivity of U-Al alloy

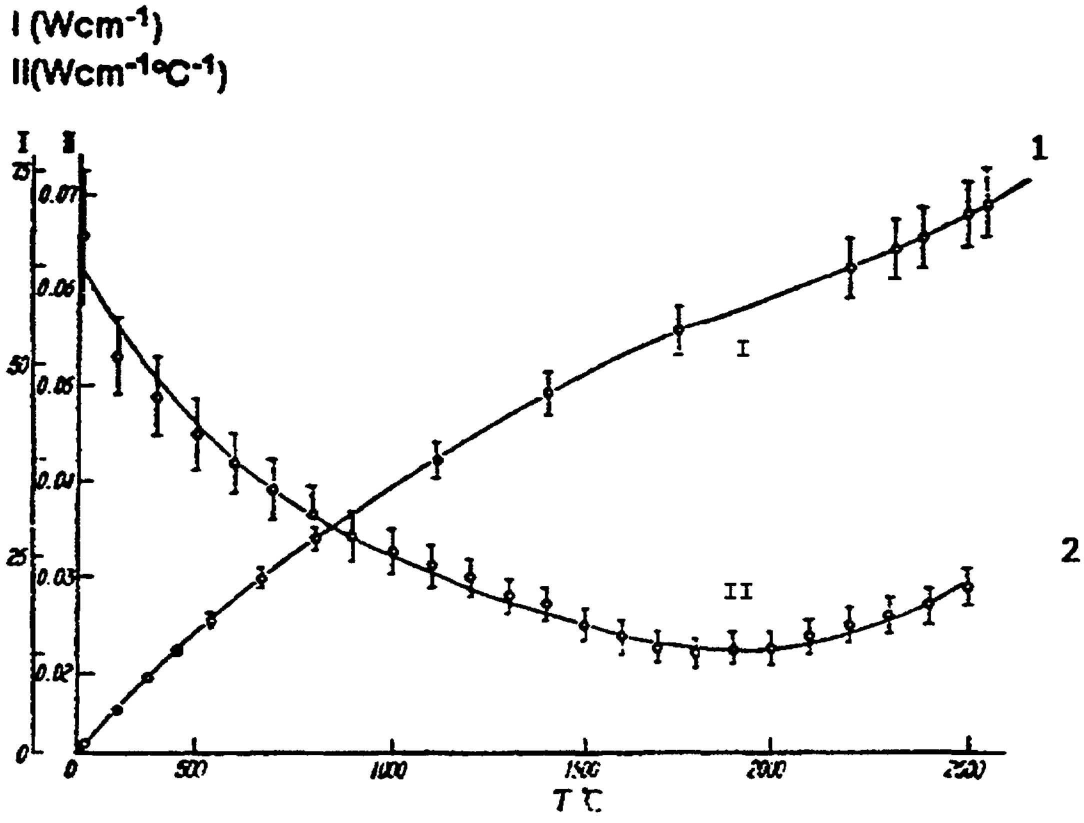

Figure S3.6
1. Integral of thermal conductivity
2. Experimental curve of thermal conductivity of UO_2

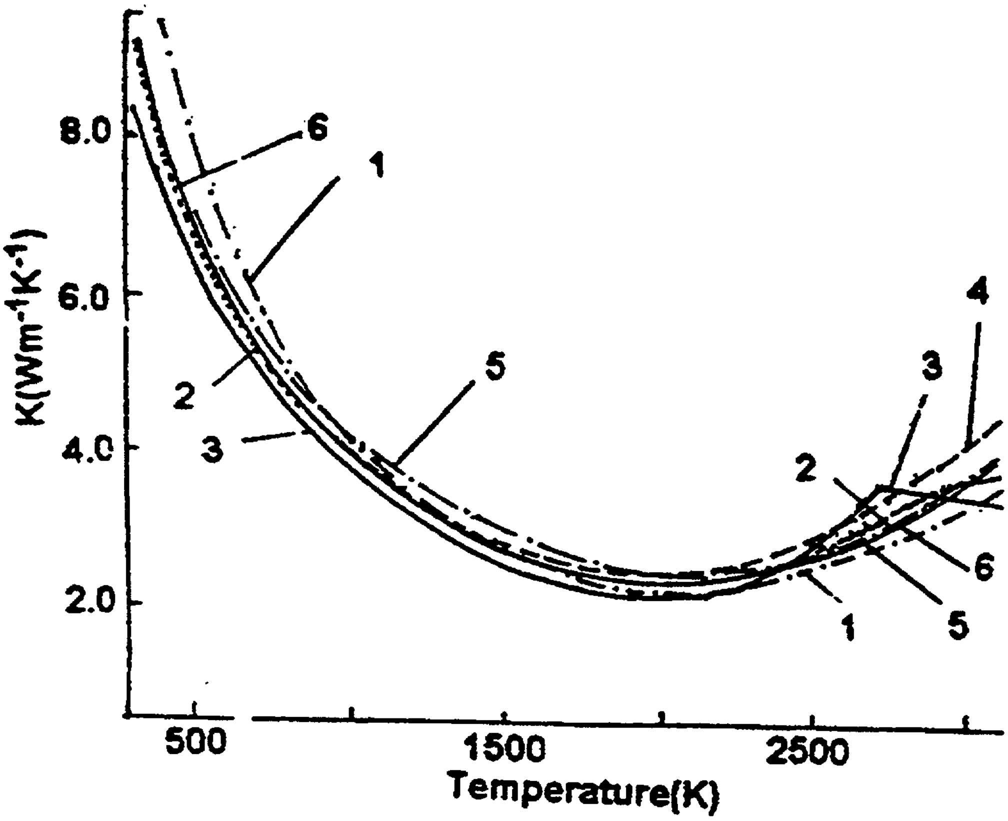

1. MATPRO-11-Rev. [17]
2. Brandt [12]
3. Fink, et al.,[13]
4. Killeen [36]
5. Weidan Li, et al.,[21]
6. S. Ying, et al.,[23]

Figure S3.7 *The comparison of the recommended expression of the thermal conductivity of 100% TD UO_2*

References to Supplement S3

[1] P. GORDON, A. R.KAUFMAN, "The alloy system U-Al and U-Fe", J. Metals 188 (No. 1) Trans. 182-94 (1950)

[2] H. A. SALLER, "Preparation and, properties of aluminum alloys cladding, Peaceful uses of Atomic Energy", Vol. 9 (1955), pp. 562--214

[3] BORIE, B. S., Jr., "Crystal structure of UAl_4", J. of metals 3: 800-802 (Sept., 1951)

[4] SMITH, C. D., et al, "Production of fuel assemblies for the materials testing reactor mock-up critical experiments", ORNL-951, (April 9, 1951), p. 63

[5] HAMNY, C. D., ORNL-911 Jan. 8 (1951),p. 14

[6] A. B. SHUCH, ANL-7708 (1970)

[7] Z. Z. LEI, et al, "The experimental report on the thermal conductivity of the U-Al alloy" (1971) Private communication

[8] H. Y. ZHOU, L. L. ZHANG, "The thermal conductivity of the U-Al alloy measured by the DEH Method" (1978) (Private Communication)

[9] T. I. JONES, et al., Canadian Met. Quarterly 2(1), p. 53-72 (1963)

[10] L. L. ZHANG, B. LU, "The measurement of thermal conductivity of nuclear fuel in China"

[11] A. B. G. Washington TRG-Rep 2236 (1973)

[12] R. BRANDT, NEUER G. Non-Equil. Thermophys. 1 (1976), 3

[13] J. K. FINK, et al, J. Nucl. Mat. 102 (1981) 17

[14] D. G. MARTIN, J. Nucl. Mat. 110 (1982) 73

[15] "Thermal conductivity of UO_2", IAEA Report of a panel held in Vienna, April (1965)

[16] J. B. CONWAY, A.D. FEICH, GEMP-715 (1969)

[17] MATPRO-V11, Revision NUREG/CR-0497, Rev. 1 (1980)

[18] J. H. HARDING, D. G. MARTIN, J. Nucl. Materials, 166 (1989) p. 223-226

[19] J. C. WEILBACHER, High Temp. -High Press, 4, 431-438; CEA-R-4572 (1974)

[20] S. YING, Z. JI, Nucl. Power Engineering, 1 (1980) 1-12

[21] W. LI, et al, Nucl. Science and Engineering, 3 (1983) 251

[22] J. YU, et al, Atomic Energy Science and Technology, 3 (1981) 298

[23] S. YING, Z. JI, Proc. of 1st Asian Thermophysical Properties Conference (1986) 658-664

[24] J. SHEN, Z. LIANG, Private Communication 1983, 9

[25] W. Li and L. L. Zhang, Atomic Energy Science and Technology, 22 (1988), 455-462

[26] C. S. KIM, R. A. BLOMQUIST, J. HALEY, R. LAND, J. FISCHER, M. G. CHASANOV and L. LEIBOWITZ, "Measurement of Thermal Diffusivity of Molten UO_2", Proceedings of the Seventh Symposium on Thermophysical Properties, pp. 338-343, ed. A. Cezairliyan ASME, N.Y. (1977)

[27] E. E. ANDERSON, Nucl. Tech. 30 (1976) 65-70

[28] H. E. SCHMIDT, J. Nucl. Mat., 39 (1971) 234

[29] G. J. HYLAND, J. Nucl. Mat., 113 (1983) 125

[30] C. OTTER and D. DAMIAN, High Temperature - High Pressures, 16 (1984), 1-6

[31] J. L. BATES, et al, J. Am. Ceram. Soc., 50, 652 (1967)

[32] J. R. GOLDSMID, Thermal conduction in semiconductors, Pergamon Press, Oxford, 1961

[33] H. J. GOLDSMID, The thermal properties of solids, Dovex Publications Inc., New York (1965)

[34] H. MARCHANDISE, Report EUR-4568 (1970)

[35] J. K. FINK, L. LEIBOWITZ, High Temp. -High Pressures, 17 (1985) 17-26

[36] J. C. KILLEEN, J. Nucl. Mat. 92 (1980) 1362.52

[37] CRAEYNEST VAN J. C., STORA J. P., J. Nucl. Mat. 37 (1970) 153-158

[38] H. A. TASMAN, D. PEL, J. RICHTER, et al., High Temp. -High Pressures 15 (1983) 419-431

Supplement S4

MECHANICAL PROPERTIES OF STEELS*

S4.1. BACKGROUND

The strength of solid structural materials is measured on extremely short time scales by the spallation which occurs when two shock waves interact in a body producing enough tension to fracture it. The tensile stresses generated inside a body are the result of two shock waves propagating in opposite directions. The best way to determine the fracturing stresses at spalling is to measure the free-surface velocity history under dynamic loading [1]. Fracture of the material under tension, leads to a fast reduction of the tensile stress to zero and as a result, a compression wave is produced in the bulk material. This wave propagates to the free rear surface and forms a so-called spall pulse in the free surface velocity profile. The spall strength σ^* is determined from the so-called "velocity pullback", the free surface velocity decrement between its peak value and immediately preceding the spall pulse.

For this approach the following linear approximation is used:

$$\sigma * = \rho c U_{fs} \tag{S4-1}$$

where U_{fs} is the "velocity pullback", ρ is the material density, and c is the bulk sound velocity.

S4.2. EXPERIMENTAL TECHNIQUE

Dynamic measurements of the spall strength are based on the relation (S4-1). Plane shock waves for the spall strength measurements are created in samples by the impact of a projectile or the detonation of an explosive plane wave generator in contact with the sample. Guns and explosive facilities are used for launching the projectiles. A typical explosive facility is shown in Figure S4.1. Capacitance gauges [1,2] and laser velocimeters VISAR [3] are used to monitor the free surface velocity profiles.

Measurement of spall strength of elastic-plastic bodies

Figure S4.2 shows examples of measurements of free surface velocity profiles for titanium alloy BT6 (Ti - 6% Al - 4% V). One can see that the free surface velocity profile is practically a repeat of the compression pulse in a sample if the load intensity is small (profile 1). The elastic-plastic compression wave and subsequent unloading are recorded. The small velocity hysteresis is explained by elastic-plastic deformation.

The tensile stresses after the reflection of the compression pulse by the free surface increase with the growth of shock intensity. When the peak tensile stress reaches the fracture stress, fracture is initiated and the tensile stresses relax to zero. As a result, a compression wave or "spall pulse" appears on the free surface velocity profile. Reverberation of the wave is then observed between the free surface and the damage zone. The period of the oscillation is a measure of the thickness of the sample, and the velocity pullback is a measure of incipient fracture strength of the material.

S4.3. EXPERIMENTAL RESULTS

Figure S4.3 shows the results of experiments on strong Fe-Cr-Ni-Mo steel 35X3HM. Free surface velocity profiles 1, 2, 3 were obtained under loading in the rolling direction; profiles 4, 5 - under loading in the lateral direction. The profiles shown display the influence of load direction on the realized dynamic strength. The resistance to dynamic fracture is 4-4.4 GPa in the case of loading

---

*contributed by HEDRC

Fracture of this steel is relatively brittle in nature and is complete by the end of the first half-period of velocity oscillations. A slow decay and a long spall fracture was observed for more viscous materials such as stainless steel (Figure S4.4). In this case the deceleration of the spall plate continued for a long time after the spall pulse appearance. Similar behaviour was also observed for other materials when the incident pulse duration was short enough.

Results of spall strength measurements for structural steels are presented in the Table S4.1. Load conditions in the Table: A is the aluminum impactor of thickness d (mm) with velocity W (m/s), B is the detonation of explosive lens in contact with samples, $h1$ is the sample thickness, $h2$ is the spall thickness, $S1$ is the amplitude of the elastic limit, $S2$ is the yield stress and σ is the spall strength.

Nomenclature to Supplement S4

ρ - specific density, kg/m^3,
c - bulk sound velocity, m/s,
U_{fs} - free surface velocity "pullback", m/s,
σ - spall strength, GPa,
W - velocity of impactor,
$h1$ - sample thickness, mm,
$h2$ - spall thickness, mm,
$S1$ - elastic limit, GPa,
$S2$ - yield stress, GPa.

Table S4.1 RESULTS OF SPALL STRENGTH MEASUREMENTS FOR STRUCTURAL ALLOYS

Metal	Loading Condition	$h1$ mm	$S1$ GPa	$S2$ GPa	$h2$ mm	σ GPa
Armco-iron,rod	A; $d = 2$, $W = 590$	10	1	0.6	1.1	1.65+0.1
Steel 35X3HM, rod loading in the rolling direction	A; $d = 2$, $W = 445$	10.1	2.3	1.3	-	-
	A; $d = 2$, $W = 600$	10.4			1.6	4.2+0.2
	A; $d = 2$, $W = 700$	10.4			1.6	4.5+0.2
	B	15.2			9.9	4.0+0.2
Steel 35X3HM, rod, loading in the lateral direction	A; $d = 2$, $W = 700$	9.8	2.3	1.3	1.5	3.85+0.1
	B	15			9.4	3.4+0.2
Stainless, steel X18H10T, rod	A; $d = 0.4$, $W = 675$	4	0.45	0.26	0.49	2.28+0.1
	A; $d = 2$, $W = 445$	10			1.78	2.0+0.1
	A; $d = 2$, $W = 700$	10			1.61	2.0+0.1
	A; $d = 5$, $W = 600$	10			3.75	1.9+0.1
	B	15			6.9	1.85+0.1
Steel 45	A; $d = 2$, $W = 720$	11.1		2.58	1.81	4.25+0.1
	B	11.1			-	-
Steel EP-836	A; $d = 0.4$ $W = 720$	3.75	-	-	-	-
	A; $d = 2$, $W = 720$	5.42			1.5	6.19+0.2
	A; $d = 0.4$, $W = 720$	1.95			0.29	5.94+0.2

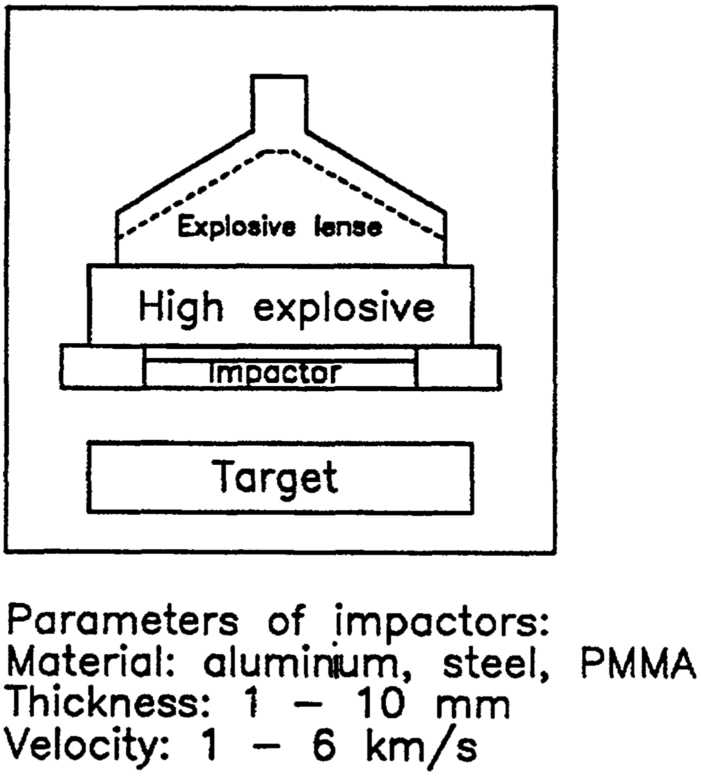

Figure S4.1 Scheme of explosive facilities for acceleration of thick impactors

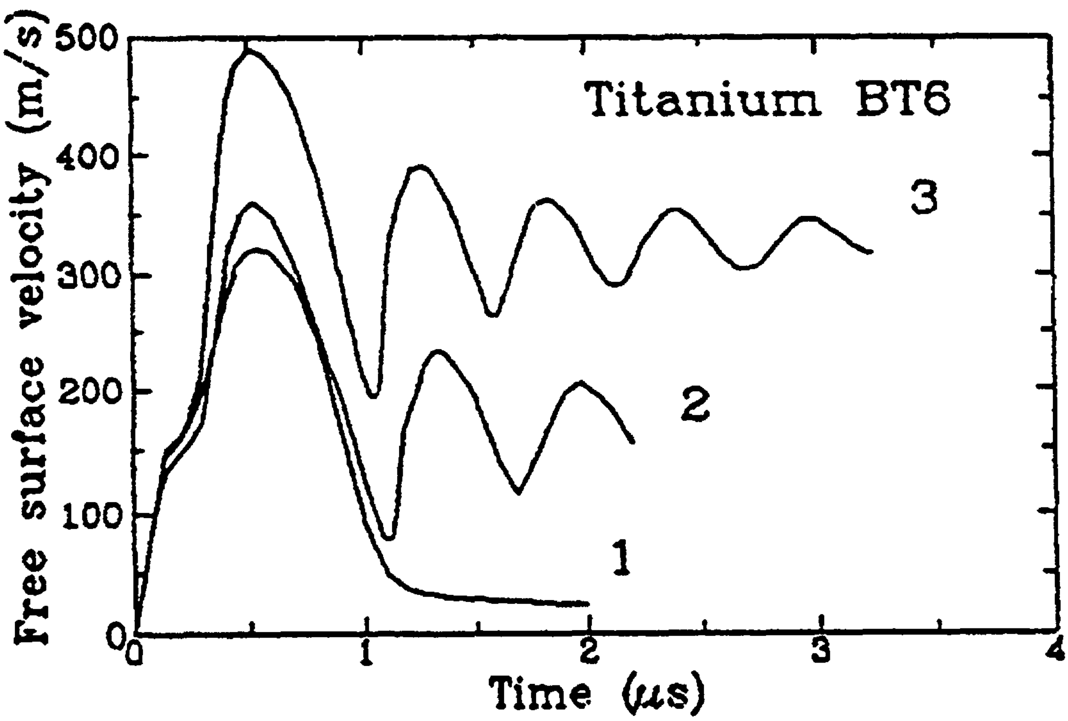

Figure S4.2 Free surface velocity profiles for samples of titanium alloy 10-12 mm thick impacted by aluminium plates 2 mm thick. Impact velocity are 445 m/s (profile 1), 600 m/s (2), and 700 m/s (3).

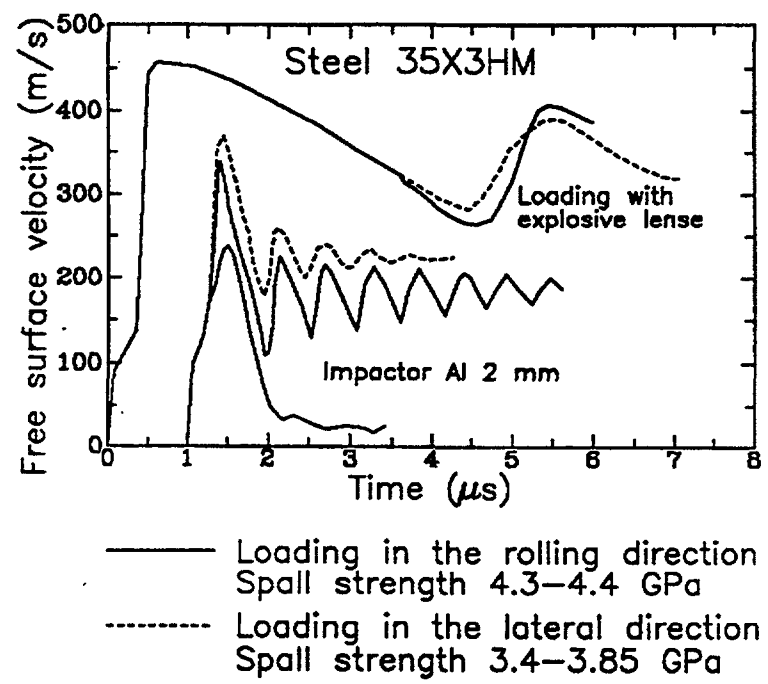

Figure S4.3 *Results of the spall strength measurements for the strong structural steel. Solid lines show free surface velocity profiles under loading in the rolling direction, dashed lines - loading in the lateral direction.*

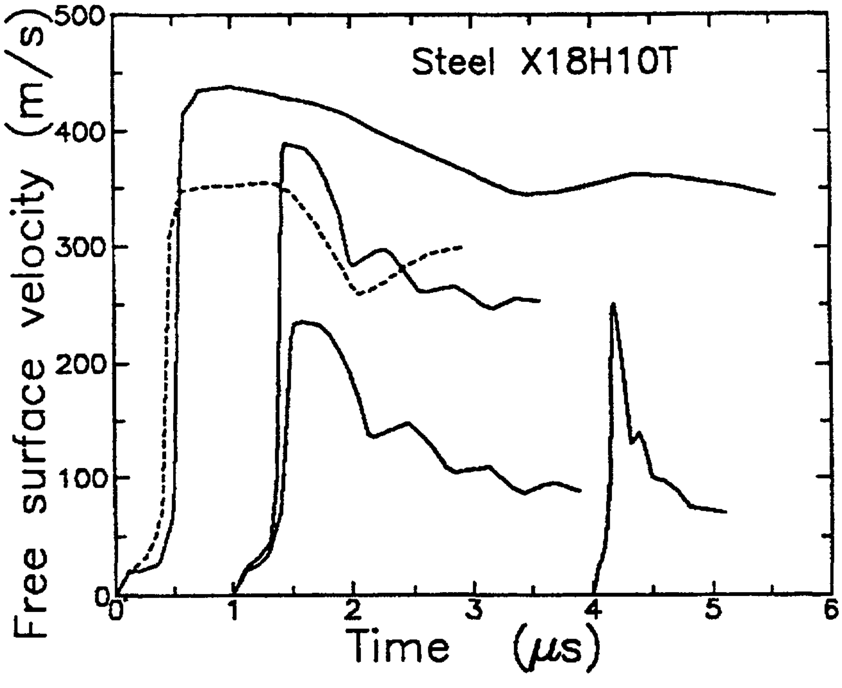

Figure S4.4 Spallations in viscous stainless steel

References to Supplement S4

[1] BUSHMAN A. V., KANEL G. I., NI A. L., FORTOV V.E., "Intense dynamic loading of condensed matter", Taylor & Francis (1993) 287

[2] IVANOV A. G., and NOVIKOV S. A. "Apparatuses and experimental technique" (in Russian)., Vol. 7, No. 1 (1963) 135

[3] ASAY J. R., and BARKER L. M., "Interferometric measurement of shock-induced internal particle velocity and spatial variations of particle velocity", J. Appl. Phys., Vol. 45, No. 6 (1974) 2540-2546

Supplement S5

THERSYST - DATA BASE

There are three data bases which deal with thermophysical properties of solid materials. The comprehensive data base system at CINDAS (West Lafayette, USA) covers all thermophysical properties for many groups of materials, such as dielectric materials, composite materials, high temperature materials, aerospace structural materials, etc [1]. But these data can only be accessed by a restricted group of users and co-operation with foreign partners is not possible. The thermal conductivity data base in Japan [2] deals with certified reference materials, candidates for reference materials, and other well-characterized materials. Other thermophysical properties (specific heat capacity, electrical resistivity, thermal expansion, and emissivity) are registered as supplemental properties only. ALUSELECT data base [3] has been developed to offer so-called harmonized values for aluminium and aluminium alloys, which can be further improved by the European Aluminium Association as the EAA official data. Data from the open literature, from handbooks and from data manufacturers sheets have been collected in the data bank but only evaluated values are accessible.

THERSYST database has been developed as a combination of a factual database for thermophysical properties of solids and a modular program system to handle the database content. The advantage of such a system is that program components can be added or deleted in a relatively easy manner to permit an optimum configuration.

As thermophysical property data are dependent on both material parameters and experimental conditions (meta-data), information on all factors of influence should be stored in the data-base and the original context between the intrinsic properties data and the meta-data should be preserved. This problem has been solved in THERSYST using the class concept [4]. The physical information is converted into a standardized form given by the THERSYST scheme of category and it is stored in the form of data-sets. The scheme is separated into five classes:

class 1, material designation,
class 2, material characterization,
class 3, experiment description,
class 4, thermophysical property data, and
class 5, bibliography.

Classes 1 to 4 are hierarchically structured, the class bibliography is linked to the corresponding data-set by a document number (Figure S5.1).The information belonging to the data-set is stored in the form of descriptors, which can be numerical, coded or in text form. In Table S5.1 some important material and experimental parameters are listed which are used in THERSYST as descriptors. It is also indicated, which thermophysical property it is related to.

The THERSYST modular program system enables:

- data selection corresponding to criteria defined by the user,
- data manipulation, e.g. conversion of units, variable transformation, regression of data, calculation of a new property from stored data on other properties, and
- representation of data in the form of tables and graphs.

A detailed description of these modula is given in [5].

Table S5.1 FACTORS INFLUENCING THERMOPHYSICAL PROPERTIES

	THC	CP	ELC	LEX	RAD	OPT
· chemical composition	+	+	+	+	+	+
· electrical resistivity	+	+	+	+	+	+
· physical state	+	+	+	+	+	+
· particular form of material (e.g. fibre, powder, etc.)	+		+	+	+	
· structure						
- microstructure	+		+	+	+	
- crystal structure	+	+	+	+	+	
- lattice parameter	+	+	+	+	+	+
- anisotropy	+		+	+	+	+
- porosity	+	+	+	+	+	
- lattice impurity	+		+	+	+	+
- grain size	+		+	+	+	+
- phases at grain boundary	+		+	+	+	+
- geometrical arrangement of phases	+	+	+	+	+	+
· surface characterization					+	
- roughness					+	
- layer composition,					+	
- thickness						
· phase transitions	+	+	+	+		+
· sample preparation	+	+	+	+	+	+
· sample treatment:						
- mechanical					+	
- chemical					+	
- thermal	+	+	+	+	+	+
- irradiation	+	+	+	+	+	+
· measurement technique	+	+	+	+	+	
· ambient atmosphere (composition, pressure, ..)	+	+	+		+	
· measuring temperature	+	+	+	+	+	+
· measuring frequency			+			
· spectral range			+		+	+

THC	thermal conductivity, thermal diffusivity
CP	specific heat capacity, enthalpy
ELC	electrical conductivity
LEX	thermal expansion (linear, volumetric)
RAD	emittance, transmittance, reflectance, absorbance
OPT	absorption coefficient, refractive index, extinction coefficient

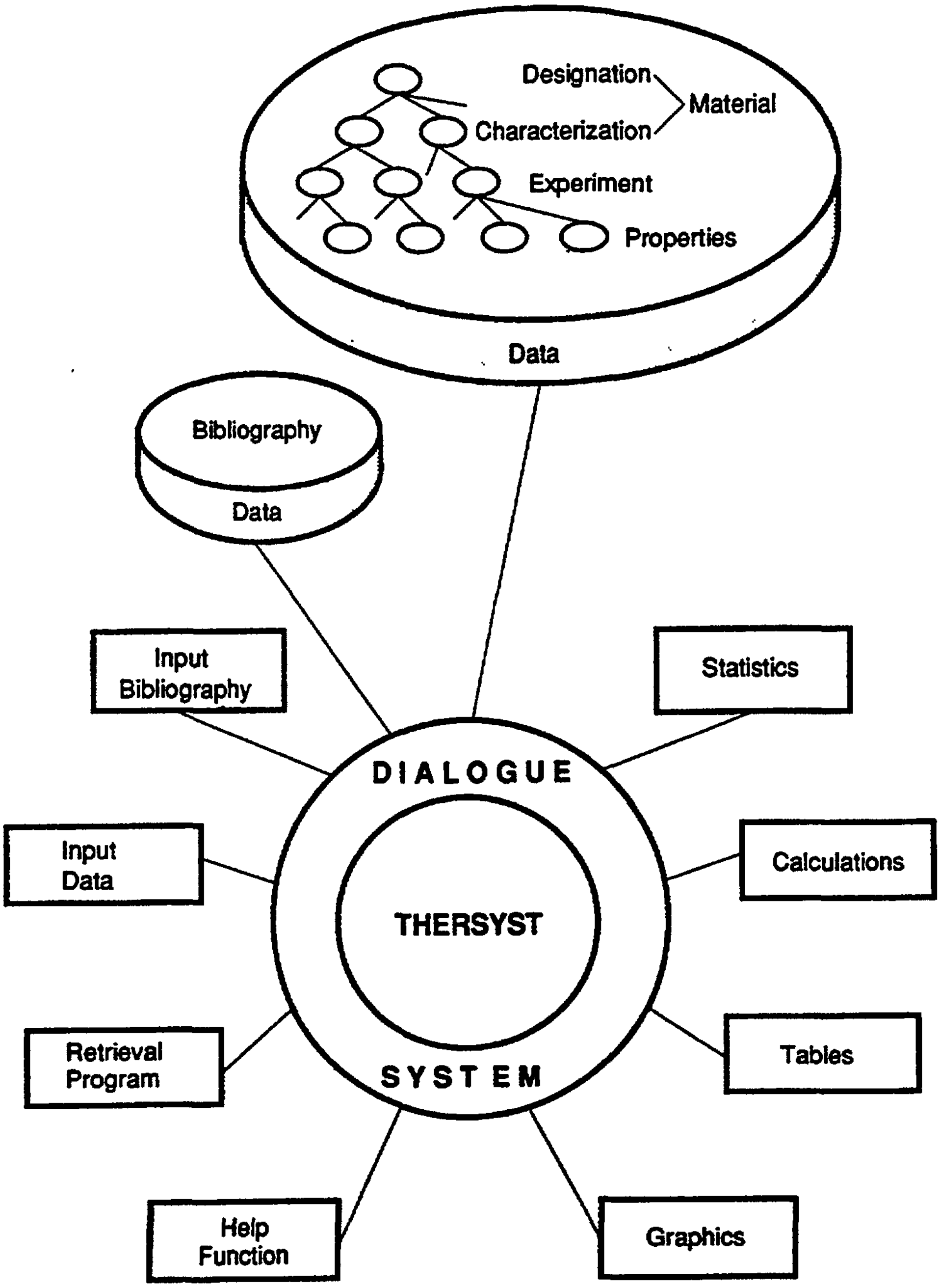

Figure S5.1 *Elements of modular system THERSYST for storage, handling and representation of thermophysical property data.*

References to Supplement S5

[1] HO C. Y., Director of CINDAS, Purdue University, West Laffayette, Indiana; private communication (1992)

[2] ARAI T., BABA T., ONO A., High Temp.- High Pressures 21 (1989), 61-68

[3] SCHÖNHOLZER P., SANDSTRÖM R., Swiss Materials 3a (1990), 25-28

[4] BRANDT R., LÖFFLER K., JAROMA-WEILAND G., NEUER G., PFLUGFELDER G. IKE-5-299-87 (Institut für Kernenergetik und Energiesysteme, Universität Stuttgart, 1987)

[5] THERSYST: User's Handbook; IKE-STB-899-87 (Institut für Kernenergetik und Energiesysteme, Universität Stuttgart, 1987)

Supplement S6

TPSYS - THERMOPHYSICAL PROPERTIES DATA BASE FOR REACTOR MATERIALS

S6.1. INTRODUCTION

As a part of IAEA's Co-ordinated Research Programme to establish a thermophysical programme on properties data base for light and heavy water reactor materials, the data base management system TPSYS has been developed by CIAE (Beijing, China*). It is designed to store information on the thermophysical properties of reactor materials. To provide a relatively high degree of data independence and less data redundancy the relational data model is employed in TPSYS [1]. Programmed in modules, the management software is primarily written in dBASE-III Plus command code [2] with a plotting and graphics user interface written in C and for computations and data conversion, FORTRAN-77 [4] is used. With the routine function of data base maintenance, the TPSYS, in addition to normal database function, has many specific features of interfacing with computing programs and other data base management system, data processing and curve fitting etc. Operating on IBM-PC (386, 486) compatible computer, TPSYS is popular and user-friendly.

S6.2. TPSYS MANAGEMENT SYSTEM

The thermophysical properties data base

At present, a lot of thermophysical properties data for reactor materials has been published in literatures and handbooks, some calculating models are also recommended by IAEA and other researchers. Based on the thermophysical properties data measured and calculated at CIAE a data base has been created for the thermophysical properties of nuclear fuels, coolant materials, moderator materials,structural materials and control materials. Figure S6.1 gives the organizational scheme for establishing a data base. The thermophysical data base is divided into 5 major data banks according to the material categories. To give rapid retrieval of materials, another 5 supplementary data banks are built to store the information on material identification and characterization. Because the property data has different correlation with temperature and pressure, especially for the coolants, a complex data base structure has been specifically designed for the purpose.

Programme modules of TPSYS

A data base system is a shared collection of interrelated data with management software. The software should provide the following capabilities for both application programmers and non-technical users:query, data manipulation, data definition, data control facilities and efficient file structures [5]. A program system of TPSYS for data representation and processing consists of the 4 major modules stated below. Figure S6.2 illustrated the main control modules of TPSYS.

EDIT module

This module is used for data base maintenance. The information on thermophysical properties and materials can be appended, modified, inserted and deleted using this module. While running this

---

* Correspondence on TPSYS development is sent to:

Jianguo Zhong
China Institute of Atomic Energy
P.O. Box 275(33)
Beijing, 102413
P. R. China

module, the user is given 8 options to locate the records in data base, i.e. 8 keywords by which the search can be conducted. They are: record number, material+ (pressure), temperature+ (pressure), material+temperature+(pressure) and (pressure). To ensure data safety, a prompt is given for confirmation before deleting each data record once the DELETE module is selected.

VIEW module

The VIEW module is designed to allow users to browse through the data base. Using this module, the thermophysical properties data of any given material over a specified temperature and pressure range, can be listed and plotted. The above query information can be printed out if necessary. Figure S6.3 shows a screen format of list. Figure S6.4 presents a plot of the thermal conductivity of UO_2 [6], the recommended MATPRO curve [7] for UO_2 is also illustrated.

Interface with MATPRO

MATPRO is a computer library of 45 subcodes dealing with the properties of uranium dioxide, uranium-plutonium dioxide, Zircaloy cladding and various gas mixture. Eleven subroutines have been extracted and linked into TPSYS. These subcodes include: FCP, FTHCON, FEMISS, FTHEXP, FENTHL, CCP, CTHCON, CTHEXP, ZOTCON and GTHCON. Reference [7] gives detailed descriptions of these codes. All these subcodes are accessed through this module, allowing data calculated by MATPRO to be accessed and plotted. Figure S6.5 is a sample graph produced by this module.

Interface with THERSYST

THERSYST [8] is a thermophysical properties data base system developed at University of Stuttgart. Due to its advantages for handling thermophysical properties data, it has been chosen as the working system for preparing a light and heavy water reactor material thermophysical property data base. The development of software to allow thermal property data to be transferred between data bases is a vital part of the CRP programme. Through the interface with the THERSYST module, TPSYS can produce a data file in a suitable format for the THERSYST data base. Table S6.1 shows an example of a data file produced by TPSYS. The first line of the file contains details of the file contents using the following rules:

A. The first 2 digits represents the properties, where:
   01--CP 02--THD 03--THC 04--ENT
   05--LEX 06--EMI 07--DEN
B. The third digit represents the materials, where:
   1---Fuels 2--Coolants 3--Moderators 4---Structures 5--Controls

The TPSYS data base is still being developed and will be revised at any time according to user's needs.

In the next development phase, our interests are:

- Extension of data base.
- Evaluation of existing data to give a recommended value.
- Upgrading the user graphics interface and data processing.
- Favorable service to more users.
- Receiving data from THERSYST and converting into TPSYS.

Table S6.1 A DATA FILE PRODUCED BY TPSYS

```
THERMAL DIFFUSIVITY OF, Zr-2.5Nb

024002,CN002,2,10,0,51,-6,
324.,8.7800,380.,8.9600,400.,8.9600,425.,9.2400,
473.,8.8900,537.,8.9400,550.,8.9300,573.,8.9100,
676.,8.6500,729.,8.6500,773.,8.6700,823.,8.7500,
881.,8.8100,923.,8.9100,973.,9.2900,1023.,9.8900,
1076.,10.2000,1096.,10.6700,1116.,10.2700,1123.,11.3200,
1155.,11.2100,1173.,11.0300,1190.,10.8700,1217.,11.4900,
1253.,12.0600,1273.,12.7300,1327.,12.1100,1373.,12.7500,
1422.,12.9700,1481.,12.8400,

683.,8.3500,722.,8.5900,781.,8.5400,824.,8.9500,
881.,9.2500,923.,8.8700,973.,9.1800,1023.,9.4200,
1052.,9.9000,1076.,1.0600,1096.,9.8900,1118.,9.5900,
1153.,10.7700,1174.,10.8900,1195.,10.7700,1210.,11.6900,
1232.,11.2700,1253.,11.8000,1273.,12.5400,1330.,11.7100,
1374.,12.3600,1422.,12.6500,1481.,13.0000,
END

REMARKS:
Zr-2.5Nb rod,29%c.w. diameter:2.081mm,thickness:10mm( 2 cycles)
```

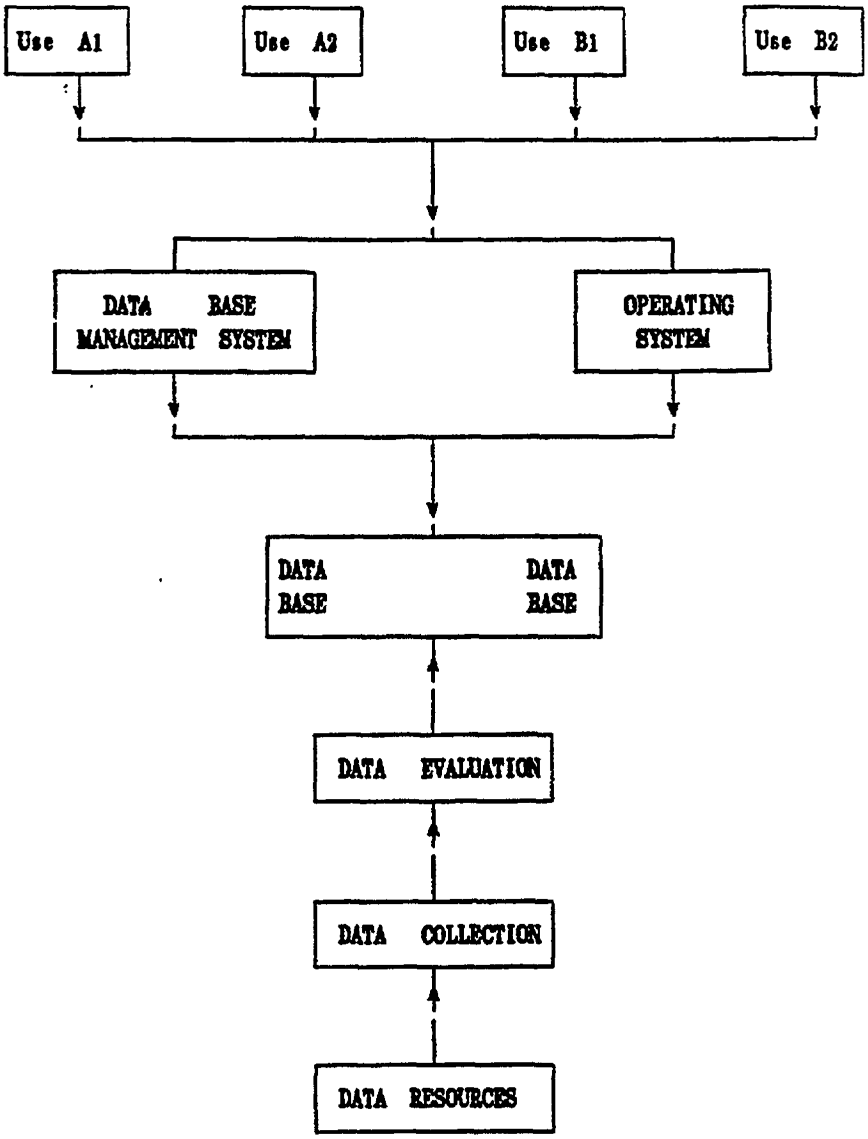

Figure S6.1 *The organizational scheme for establishing a data base*

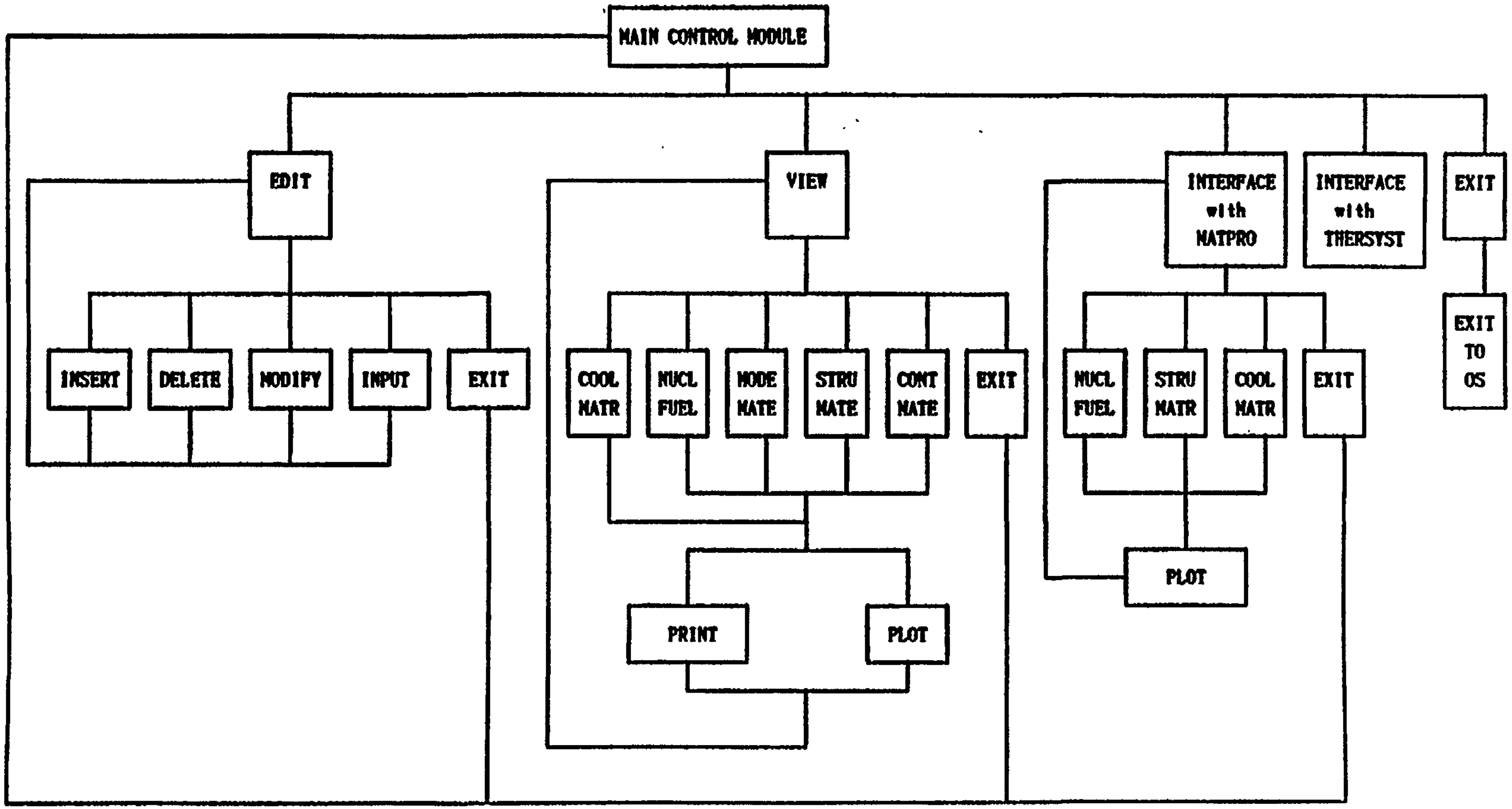

Figure S6.2 The main control module of TPSYS management system

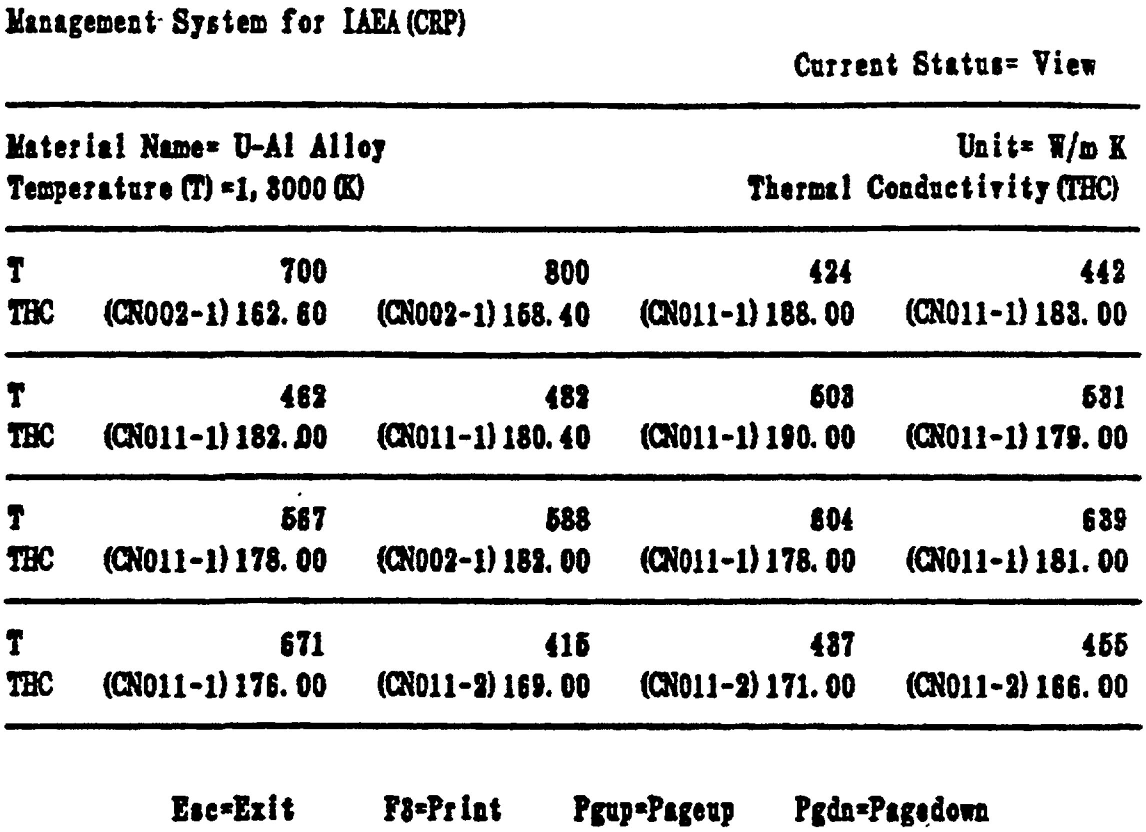

```
Management System for IAEA (CRP)
                                                    Current Status= View
--------------------------------------------------------------------------------
Material Name= U-Al Alloy                                       Unit= W/m K
Temperature (T) =1, 3000 (K)                     Thermal Conductivity (THC)
--------------------------------------------------------------------------------
T                    700                800                424                442
THC   (CN002-1) 162.60   (CN002-1) 168.40   (CN011-1) 188.00   (CN011-1) 183.00
--------------------------------------------------------------------------------
T                    462                482                503                531
THC   (CN011-1) 182.00   (CN011-1) 180.40   (CN011-1) 190.00   (CN011-1) 179.00
--------------------------------------------------------------------------------
T                    567                588                604                639
THC   (CN011-1) 178.00   (CN002-1) 182.00   (CN011-1) 178.00   (CN011-1) 181.00
--------------------------------------------------------------------------------
T                    671                415                437                455
THC   (CN011-1) 176.00   (CN011-2) 169.00   (CN011-2) 171.00   (CN011-2) 166.00
--------------------------------------------------------------------------------

        Esc=Exit        F8=Print        Pgup=Pageup        Pgdn=Pagedown
```

Figure S6.3 The screen format of LIST

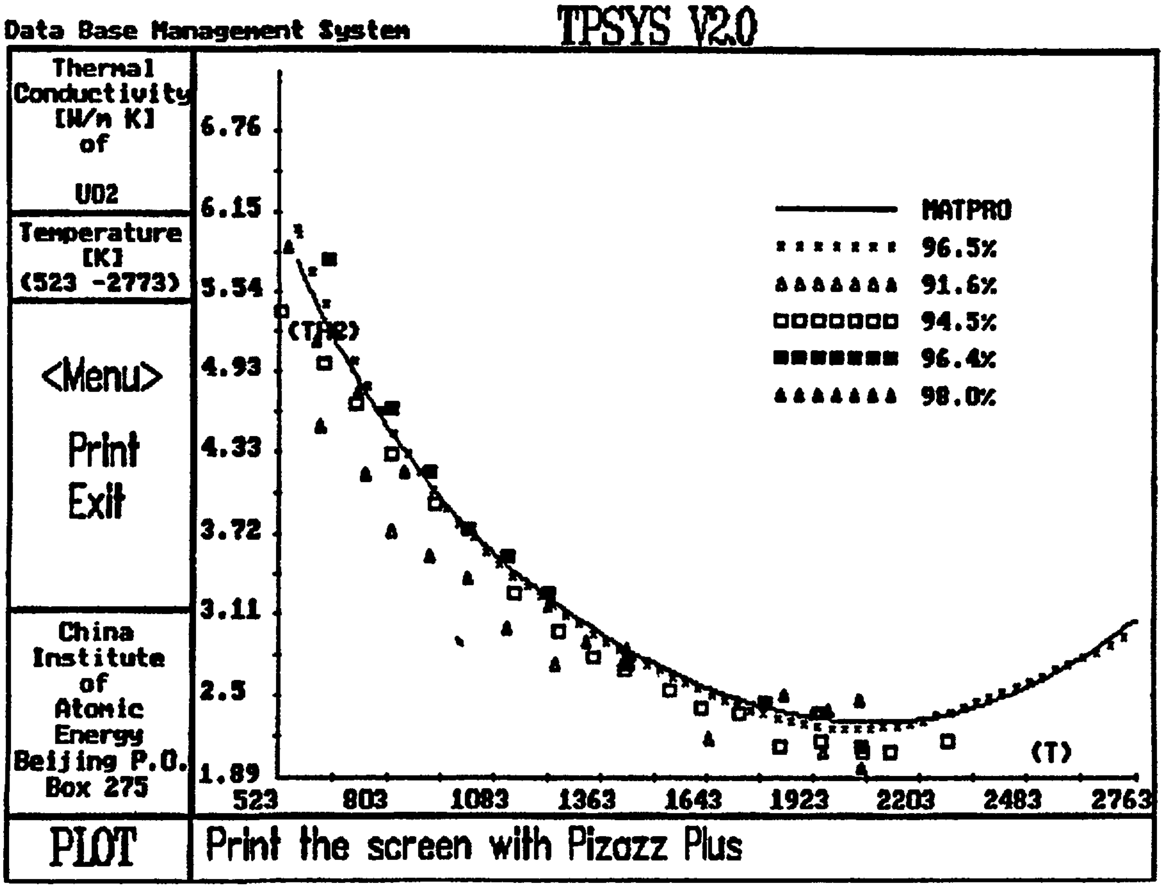

Figure S6.4 A format of PLOT by TPSYS

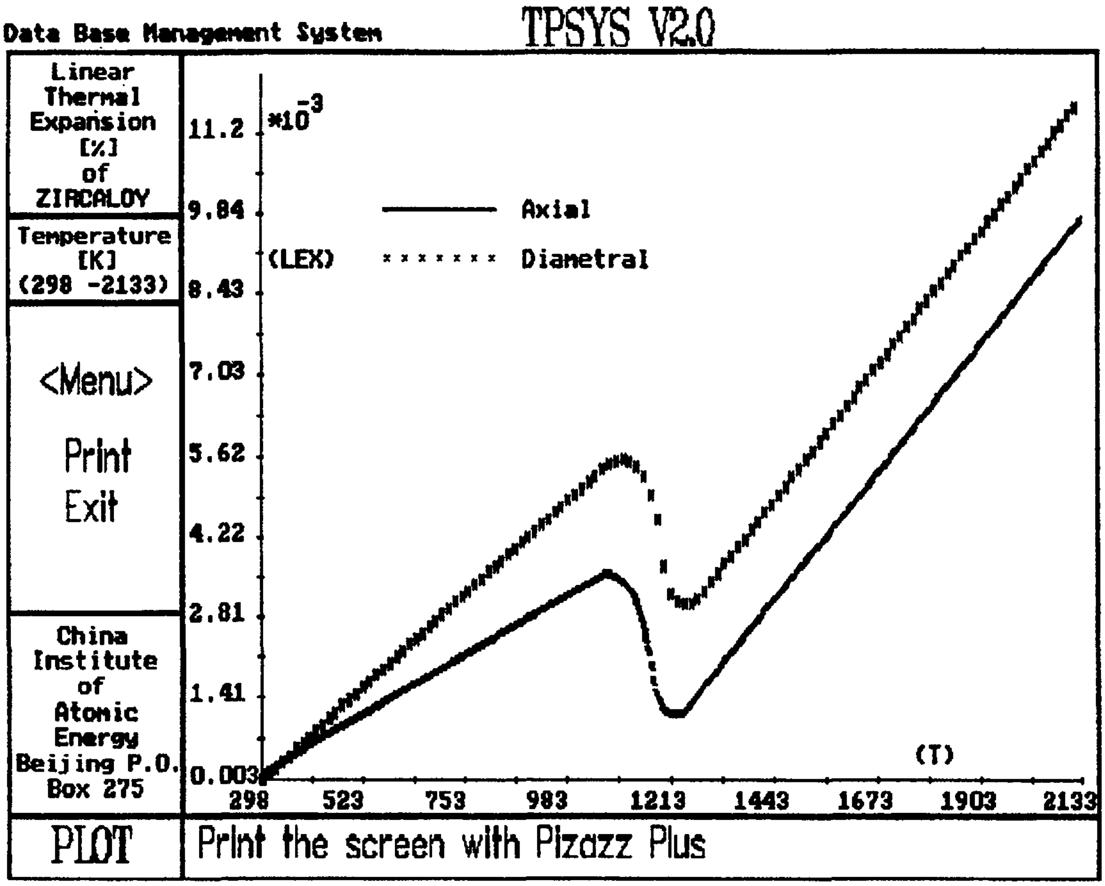

Figure S6.5 An example of TPSYS by calling MATPRO

References to Supplement S6

[1] ASTRE S., "Data base: structured techniques for design, performance and management", Wily, New York (1980)

[2] WANG YUNYI, "Principles and applications of dBASE-III PLUS". Beijing, China (1990)

[3] HERBERT SCHILDT, "Turbo C-the complete reference". USA (1989)

[4] TAN HAOQIANG, "Structured design of FORTRAN 77". QingHua University, Beijing (1991)

[5] FRED R. MCFADDEN, et al., "Data base management". The Benjamin/ Cummings, USA (1985)

[6] LI WENDAN, ZHANG LILI, et al., "Thermal diffusivity and conductivity of uranium dioxide at high temperature", Chinese Journal of Nuclear Sci. and Tech., Beijing, 3 (1983) 251-257

[7] DONALD L. HAGRMAN, et al., "MATPRO-11 (Rev. 1), A handbook of materials properties for use in the analysis of light water reactor fuel rod behaviour", NUREG/CR-0497, TREE-1280 (Rev. 1), USA, EG&G Idaho, Inc. (1980)

[8] WEILAND JAROMA, "Format of the data file", University of Stuttgart, Germany (1991)

Supplement S7

THERMOPHYSICAL PROPERTIES OF URANIUM
Experimental Data

This supplement presents the results of a literature survey on the properties of metallic uranium, and includes the experimental data given in the literature. The experimental data are presented in table form. Tables of the most reliable data are presented. The literature survey only covered material available in Russia and it is possible that other data exist that has not been covered. There is some discrepancy between the data presented which may be resolved by a more complete literature survey. It should be noted that there is a general lack of information on the properties of metallic uranium in the literature, resulting in a considerable error on some of the recommendations. All correlations are presented in Section 4.1.1.

The author, Mr. V. Bobkov, thanks his colleagues at the HEMATIC - Dr. A. A. Ivashkevitch, Mrs. T. V. Mitrofanova, Mrs. L. I. Medvedeva, Dr. V. N. Vinogradov, Mrs. V. M. Scharypina, Mrs. M. I. Terentieva and Mrs. N. V. Kozina for their contribution to this work.

7.1. INTRODUCTION

A literature search for experimental data and recommended equations for the thermophysical and other properties of metallic uranium has been carried out. To verify the recommended equation and to create new ones, the data has been analysed using the least squares method. The statistics for the data fit have been determined and limits are given for the recommended correlations. Graphical comparisons between the calculated and experimental data are presented. The discrepancies between the data of different authors may be due to "latent" effects on the boundaries between the different structural phases of metallic uranium (see below). So far it has not been possible to resolve these difficulties due to the lack of experimental data, insufficient accuracy and the lack of information on the measuring techniques. These difficulties will remain until further information becomes available.

7.2. GENERAL CHARACTERISTICS OF METALLIC URANIUM

The thermophysical properties of metallic uranium have been analysed from references [1-18]. We do not guarantee to have covered all possible references. As new information appears, additional analysis should be performed. These references have been obtained from the bibliographic data base "The properties of individual elements" at the Institute of High Temperatures (Moscow). The object of this study is to provide as complete a set of recommendations for calculating the thermophysical properties of uranium as possible.

In the solid state metallic uranium exists in three allotropic modifications called "alpha", "beta" and "gamma". Beta-phase uranium is harder and considerably more brittle than the alpha-phase. Alpha-phase uranium is comparatively soft making it easier to process.

Uranium crystals are characterized by strong anisotropic properties along their symmetry axes. Uranium is electronegative, its standard electric potential is 1.6 V. The magnetic properties of uranium are weak. Metallic uranium conducts electricity and below 0.7 K it becomes a superconductor.

Phase transitions

The phase transition temperatures of uranium as given in [8,10] are: from the alpha- to beta-phase - 940 K; from the beta- to gamma-phase - 1050 K. The heat of the phase transitions as given in [8,10] are: from the alpha- to beta-phase - 0.031 kJ/kg; from the beta- to gamma-phase - 0.052 kJ/kg.

Melting point

The melting point of uranium is (1405 ± 2)K as reported in the different sources [1-5,12,17]. The heat of fusion of uranium range from 0.146 to 0.214 kJ/kg as given in [1-5,12,17].

Boiling point

The boiling point of uranium is given in [1-5,12,17] as the mean value (4108.5 ± 27) K, the heat of vaporization is given in [1-5] and [12] respectively as 4.856 kJ/kg and 5.006 kJ/kg.

Sonic velocity of uranium

The sonic velocity is given [17] as varying from 3030 m/s to 3280 m/s for the temperature 293 K.

Electrical resistance coefficient of uranium

The electrical resistance coefficient (R, in $\Omega/(\mathrm{m \cdot K})$) can be calculated using the correlation derived on the base of the different data sources [1,9,11,17] (see Table S7.7)
for $300\ \mathrm{K} < T < 1405\ \mathrm{K}$:

$$R = 10^{-8}[3.186 + 0.1283\ T - 9.0259\times10^{-5}\ T^2 + 1.5347\times10^{-8}\ T^3] \qquad \text{(S7-1)}$$

The RMSE does not exceed 7% in the temperature range from 300 K to 1405 K.

Vapor Pressure of Uranium

The vapor pressure (P_s, in Pa) of uranium can be calculated using the correlation derived from the data given in [4,15,17]:

$$\log_{10} P_s = -60.2 + 0.062\ T - 2.12\times10^{-5}\ T^2 + 2.495\times10^{-9}\ T^3 \qquad \text{(S7-2)}$$

The RMSE does not exceed 30% in the temperature range from 1300 K to 3000 K (see Table S7.8).

7.3. SOME PROPERTIES OF LIQUID URANIUM

Density, ρ (kg/m^3)	17550-17600
Specific heat, C_P (kJ/(kg·K))	0.2
Thermal conductivity coefficient, λ (W/(m·K))	18 (13.7)
Viscosity, μ (Pa·s)	0.0065
Surface tension, σ (N/m)	1.65
Electric resistance coefficient, R (Ω/(m·K))	$60\cdot10^{-8}$
Emissivity ε at 0.67 nm	0.34

Nomenclature to Supplement S7

C_p	- Specific heat,	h	- Enthalpy
R	- Electric resistance coefficient,	r_{mel}	- Heat of melting
r_{Vap}	- Heat of vaporization,	s	- Entropy
T	- Temperature,	α	- Linear expansion coefficient
ε	- Emissivity,	λ	- Thermal conductivity
μ	- Dynamic viscosity,	ρ	- Density
σ	- Surface tension,	P_s	- Vapor pressure

Table S7.1 DENSITY OF URANIUM, ρ (10^3 kg/m^3)

Temperature (K)	References: [4]	[8]	[11]	[6]
20	18.84			
100	18.80			
200	18.75			
250	18.70			
298		19.04		
300	18.68		19.06	
350	18.65			
400	18.62		18.97	
450	18.61			
473		18.88		
500	18.60		18.88	
600	18.55		18.77	
673		18.67		
700	18.50		18.65	
800	18.44		18.51	
900	18.40		18.36	
923		18.33		18.17
935		18.17		
940	18.17			
942			18.37	
942			18.18	18.15
948				18.13
973		18.13		18.11
998				
1000			18.11	18.09
1023				
1030	18.08			18.07
1045		18.07		
1049			18.07	17.94
1049			17.94	
1050	17.94			17.91
1073				
1100	17.91			17.85
1123				17.79
1173		17.79		
1200	17.75		17.74	17.73
1223				17.67
1273				
1300	17.62			17.62
1323				17.56
1373		17.56		
1400			17.55	

Table S7.2 SPECIFIC HEAT OF URANIUM, C_p (kJ/(kg·K))

Temperature (K)	References:			
	[4]	[7]	[19]	[11]
87		0.09		
99		0.09		
100	0.13			0.09
111		0.10		
123		0.10		
141		0.10		
160		0.10		
180		0.11		
198		0.11		
200	0.13			0.11
205		0.11		
225		0.11		
245		0.11		
250	0.13			
273		0.11		
280		0.12		
297.7		0.12		
300	0.13		0.07	0.12
350	0.14		0.09	
400	0.14		0.11	0.13
450	0.14		0.12	
500	0.14		0.13	0.13
600	0.15		0.15	0.15
700	0.16		0.17	0.16
800	0.17		0.18	0.17
900	0.19		0.18	0.19
940	0.19		0.18	
942			0.18	0.20
942			0.20	0.18
1000			0.21	0.18
1030	0.20			
1049			0.22	0.18
1049			0.18	0.16
1050	0.20		0.18	
1100	0.21		0.18	0.16
1200	0.23		0.18	
1300	0.25		0.18	0.16
1400			0.18	0.16
1408			0.18	0.16
1450			0.20	
1500			0.20	

Table S7.3 ENTHALPY OF URANIUM, *h* (kJ/kg)

Temperature (K)	By correlations and references:				
	(S7-3a)	(S7-3b)	(S7-3c)	[19]	[4]
300	30.71			30.08	26.40
400	41.62			39.13	38.11
500	53.94			51.18	51.68
600	67.67			65.56	65.12
700	82.81			81.72	80.70
800	99.36			99.02	96.90
900	117.33			116.84	115.40
941	125.10			124.07	135.90
941		136.00		135.13	
1000		146.60		147.54	145.60
1047		155.05		157.88	154.80
1047			175.00	175.46	
1100			184.00	184.72	184.00
1200			200.00	202.68	202.00
1300			216.00	220.74	216.00
1375			228.00		230.00
1400				238.77	
1405				239.67	
1405				269.21	
1450				278.22	
1500				288.33	

Table S7.4 ENTROPY OF URANIUM, *s* (kJ/(kg·K))

Temperature (K)	References:		
	[12]	[19]	[17]
298	0.21	0.21	0.21
400	0.25	0.25	
500	0.28	0.28	0.28
600	0.30	0.30	
700	0.32	0.33	
800	0.35	0.35	
900	0.37	0.37	
1000	0.40	0.39	0.40
1100	0.44	0.42	
1200	0.45	0.43	
1300	0.46	0.44	
1500	0.54		0.53

Table S7.5 THERMAL CONDUCTIVITY OF URANIUM, λ (W/(m·K))

Temperature (K)	References:							
	[4]	[1]	[8]	[8]	[8]	[11]	[13]	[17]
0		26.30						
20		28.03						11.7
100		29.33				23.0	20	21.2
200	17.820.0					25.0	25	
250								
273			25.5	23.9	26.4			
293	22.5	30.54						26.7
300	25.0					27.5	27	
350								
373	26.5		27.2	25.5	28.1			
400	28.8					30.1	28	
450								
473	30.0		28.9	27.2	29.3			29.1
500						32.2	29	
573	31.8		30.6	28.9	30.6			
600						34.2	31	
673	32.8		31.8	30.6				
700		37.23				36.5	34	
720								
773			33.5	32.2				
780	32.9							35.6
800						38.7	38	
873	32.4		35.2	33.5				
900	31.3					41.5	41	
940								
953			36.0					
973			36.4					
1013	28.5		36.8					
1030								
1033	27.5		37.3					
1050	25.7							
1100	22.4							
1200	19.6							
1300	13.7							
1400	13.8							
1500								

Table S7.6 LINEAR EXPANSION COEFFICIENT OF URANIUM

Temperature(K)/ References:	α (10^{-6} 1/K)	
	[4]	[2]
250	13.0	16.4
300	15.0	16.4
350	15.2	
400	15.3	
450	15.6	
500	15.8	
600	16.4	
680		22.0
700	16.9	22.0
750		22.0
800	17.5	
810		17.0
900	18.0	17.0
940	19.3	17.0
960		17.0
1030	22.1	
1050	22.6	

Table S7.7 ELECTRIC RESISTANCE COEFFICIENT OF URANIUM, *R* (Ω/(m·K))

Temperature (K)/ References:	*R* (10^{-8} Ω/m·K)				
	[4]	[1]	[9]	[11]	[17]
200	28			20.5	
250	31				
273			33.65		32.0
300	34			30.2	
350	37		38.05		
363					
400	41	55.0		37.5	
450	44				
500	47			43.2	
527			47.00		
573					50.0
600	52			47.0	
630			51.19		
700	54			50.9	
720.8			54.57		
750		58.3			
800	56			55.1	
875			57.86		
900	58	58.7		57.0	
940	57				
940.5			58.60		
942				58.0	
942				55.0	
957.1			56.31		
973					55.7
987.6			56.50		
1000				56.0	
1023.2			56.60		
1030	55				
1049.5			56.75	56.5	
1049				52.0	
1049					
1050	58				
1073			55.42		55.7
1100	55				
1125.2			56.01		
1173					
1200	50			53.0	
1231.9			57.18		
1274.1			57.84		
1300	45				
1400	40			56.0	

Table S7.8 VAPOR PRESSURE OF URANIUM, $\log_{10} P_s$ (P_s in Pa)

Temperature (K)	References:		
	[9]	[17]	[15]
1375	-8.899		
1475	-6.876		
1650	-4.575		
1775	-3.399		
1800		-2.254	
1975	-1.876		
2000		-0.959	
2150	0.0		
2175	-0.575		
2200		0.103	
2210			0.481
2224			0.510
2256			0.696
2331			-0.146
2334			-0.154
2335			0.726
2349			0.749
2350			0.751
2401			0.841
2405			0.848
2413			0.862
2420			0.340
2446			0.479
2475	0.823		
2527			1.049
2537			0.838
2546			1.078
2557			1.095
2558			1.097
2580	2.000		
2718			1.327
2719			1.295
2720			1.330
2742			1.363
2799			1.636
2833			1.754
2834			1.727
2839			1.766
2841			1.790
2846			1.772
2900	3.000		
3800	5.000		

Table S7.9 CALCULATED DATA ON URANIUM PROPERTIES

Temperature (K)	ρ (kg/m^3)	h (kJ/kg)	λ (W/(m·K))	α (10^{-6} 1/K)	R (10^{-8} Ω/(m·K))
300	18840	13.68	25.2	15.2	33.9
400	18808	25.62	27.9	16.3	41.0
500	18747	38.56	30.5	17.1	46.6
600	18660	52.70	32.7	17.6	50.9
700	18552	68.14	34.2	18.1	54.0
800	18425	84.92	34.6	18.7	55.9
900	18282	103.00	34.0	19.3	56.7
940	18222	110.70	33.4	19.6	56.7
940		134.50			
1050	18048	154.10	30.8	20.5	56.1
1050		164.30			
1100	17966	172.40	29.3	21.0	55.5
1200	17799	188.60	25.4	21.9	53.7
1300	17632	204.80	20.8	22.6	51.1
1405	17458	221.80	15.5	23.1	47.8

References to Supplement S7

[1] SIBORG H. T., KATZ G. G., "Chemistry of active elements", - transl. from Engl., Moscow: Gosatomizdat (1960)

[2] VDOVENKO V. M., "Chemistry of uranium and transuranic elements", Academy of Sciences of the USSR, 1960; "Modern Radiochemistry", Gosatomizdat (1969)

[3] FOOT F. J, in book "Reports of International Conference on Peaceful Application of Nuclear Power; Geneva, 1955", Gosgeologizdat (1968), v. 9, p. 51

[4] TCHIRKIN V. S., "Thermophysical properties of materials for nuclear power industry", Gosatomizdat (1968)

[5] EMEL'IANOV V. S., EVSTIUKHIN A. I., "Metallurgy of nuclear fuel",- Moscow: Gosatomizdat (1969)

[6] HOLDENN A. A., "Metallurgy of uranium". Metallurgizdat (1962)

[7] SCHEVTCHENKO V. B., SUDARIKOV B. N., "Technology of uranium". -Moscow: Gosatomizdat (1961)

[8] "Materials for nuclear reactors", - transl. from Engl., Ed.: SOKURSKIY JU. N., Moscow: Gosatomizdat (1963)

[9] STERLIN I. M., "Metallurgy of uranium", Moscow: Gosatomizdat (1960)

[10] SERGEEV G. IA., TITOVA V. V., BORISOV K. A., "Metallurgy of uranium and some materials of nuclear reactors", Atomizdat (1960)

[11] ZINOV'EV V. E., "Thermoph. properties". Moscow: Metallurgy (1989)

[12] WICKS K. E., BLOCK F. E., "Thermodynamical properties of 65 elements, their oxides, halides, carbides and nitrides", - transl. from Engl., Moscow: Metallurgy (1965)

[13] Nuclear Materials. Book 1. Nuclear fuel materials. Red. SKOROV D. M., Moscow: Gosatomizdat (1961)

[14] ZINOV'EV V. E., "Kinetic properties of metals at high temperatures",- Handbook, Moscow: Metallurgy (1984), 200 pp

[15] DAS D., DHARWADKAR S. R. and CHANDRASEKHARAIAH M. S., "Thermodynamics of liquid uranium vaporization", - Journal of Nuclear Materials v. 130 (1985), p. 217-224

[16] "Properties of elements", Handbook, Ed.: DRITZ M. E.; Moscow: Metallurgy (1985), 671 pp

[17] SAMSONOV G. V., "Physico-chemical properties of elements", Handbook, Kiev: Nauko Dumka

[18] KEJ D., LEBI G., "Tables of physical and chemical constants", Moscow: Fizmatgiz (1962)

[19] MARCHIDAN D. I., CIOPEC M., "Enthalpy of Uranium to 1500 K by Drop Calorimetry", Chem. Thermodynamics (1978), 8, p. 691-701

Supplement S8

THERMOPHYSICAL PROPERTIES OF LIGHT WATER AND STEAM

S8.1. INTRODUCTION

Investigations into the thermophysical properties of water and steam have been performed for many years and they are still continuing. Many industries, including the nuclear industry, need precise values for the caloric and transport properties of water and steam. In 1968 the International Association for the Properties of Water and Steam (IAPWS) produced a set of standard tables listing values for a wide variety of properties. These tables together with equations derived from the data, form the basis of several National Standards and are the basic of simpler equations used by industry. As new data becomes available it is evaluated by the IAPWS who periodically issue updated recommendations. The last revision in 1984 saw a re-evaluation of data near the critical point and the extension of the tables up to temperature of 1273 K and 1000 MPa pressure. Such revisions are unlikely to affect the values used for water reactor under normal operating conditions.

Much of the property data used by industry came from the original 1968 standard tables which are still of sufficient precision for most industrial calculations. At the last meeting of the IAPWS (Prague, 1989, [8]) it was decided to prepare a set of approximations for industrial use. Until these approximations are issued the correlation system presented in reference [9] provides a useful means of calculating calorimetric properties. This system is internally consistent and can be used to calculate a wide range of parameter for water, steam, saturation and the near critical region with sufficient accuracy for most applications. They are simple to evaluate and require little in the way of computer resources. Some of the properties have been fitted to transcendental equations which can be evaluated using iterative techniques.

The formulations described in the Supplement S8 (S8 formulations) are short and can be calculated faster than those in the Supplement S9 (S9 formulations). However, they are approximate, with error (relative to S9 formulations or experimental data) sometimes quite large, e.g., 3% for thermal conductivity of steam; 4% for surface tension, etc. The S8 formulations ranges of validity are narrower than those of the S9 formulations and they should be checked for smoothness of transition of derivatives of the state parameters at the limits of range of validity.

The transport properties of water and steam can be evaluated over a wide range of values and at saturation using the set of equations developed in [10]. Some of the equations given below have been obtained from other sources [11-18].

This supplement presents a series of relations for calculating the properties of water and steam at saturation over a wide range of parameters including underheated water and overheated steam. Equations are given for specific volume (density), enthalpy, entropy, heat capacity, dynamic viscosity and thermal conductivity. The range of application and the error associated with each equations is also given. An equation is also given for the surface tension at saturation. Additional properties may be calculated using the well known equations.

evaporation heat - $r = h'' - h'$;
density - $\rho = 1 / V$;
thermal diffusivity - $a = \lambda / (\rho \cdot C_P)$;
kinematic viscosity - $\nu = \mu / \rho$;
Prandtl number - $Pr = \nu / a$.

The correlations system [9] contains recommendations for calculating some caloric and transport properties for water-steam mixture; making this system valuable in thermal-hydraulic calculations for nuclear reactors.

All correlations presented here were tested with the use of computer codes against the data of standard tables IAPWS-84 and IAPWS-68.

S8.2. PROPERTIES AT SATURATION

According to IAPWS-84 recommendations [20] the critical parameters for water are:

$T_{cr} = 647.14$ K, $P_{cr} = 22.064$ MPa,
$V_{cr} = 0.00317$ m^3/kg, $\rho_{cr} = 322.0$ kg/m^3.

The correlations system presented here was developed by the authors of [10] for use in the Russian nuclear industry. These correlations were tested against the data of IAPWS-84 [6] and the results of these tests are presented in tables. They are easily evaluated using a computer.

Pressure MPa, [11]:

$$\frac{P_s}{P_0} = \exp \sum_{i=0}^{11} a_i M_i(u) \qquad \text{(S8-1a)}$$

where $M_i(u)$ - Chebyshev's polynomial, the values of a_i are presented in Table S8.1.

$$u = \left[\frac{(\theta^{-1} - 0.95)^{0.4} - 1.45220717}{0.84878953}\right] \qquad \text{(S8-1b)}$$

$$\theta = \frac{T}{T_0};\ T_0 = 647.3\,K;\ P_0 = 22.12\,MPa \qquad \text{(S8-1c)}$$

The error at $T < T_0$ is 0.1%.

Temperature K, [12]:

$$\frac{T_0}{T_s} = \sum_{i=0}^{11} b_i M_i(y) \qquad \text{(S8-2a)}$$

where $M_i(y)$ - Chebyshev's polynomial, the values of b_i are presented in Table S8.1.

$$y = -\left[\frac{2\left(\ln \frac{24332}{P}\right)^{0.4} - 2.9609525}{2.17988801}\right] \qquad \text{(S8-2b)}$$

Here P is in MPa, the error at $P < P_0$ is 0.02%.

Specific volume of water, m^3/kg, [13]:

$$V' = \sum_{i=0}^{8} c_i \theta^i \qquad \text{(S8-3)}$$

where $\theta = T_s/T_0$, the values of c_i are presented in Table S8.2. The error for 273 K < T < 573 K is 0.05%.

Specific volume of steam, m^3/kg, [13]:

$$\frac{1}{V''} = \sum_{i=0}^{8} d_i \theta^i \,, \tag{S8-4}$$

where $\theta = T_s/T_0$, d_i are presented in Table S8.3. The error for 273 K < T < 623 K is 0.05%.

Enthalpy of water, kJ/kg, [13]:

$$h' = \sum_{i=0}^{8} g_i \theta^i \,, \tag{S8-5}$$

where g_i are presented in Table S8.2. The error for 273 K < T < 613 K is 0.2%.

Enthalpy of steam, kJ/kg, [13]:

$$h'' = \sum_{i=0}^{8} k_i \theta^i \,, \tag{S8-6}$$

where k_i are presented in Table S8.3. The error for 273 K < T < 623 K is 0.2%.

Specific volume of water near critical point, m^3/kg, [13]:

$$V' = \sum_{i=0}^{4} l_i (1-\theta)^{0.25i} \,, \tag{S8-7}$$

where l_i are presented in Table S8.4. The error for 613 K < T < 648 K is 0.08%.

Specific volume of steam near critical point, m^3/kg, [13]:

$$V'' = \sum_{i=0}^{4} m_i (1-\theta)^{0.25i} \tag{S8-8}$$

where m_i are presented in Table S8.5. The error for 623 K < T < 647 K is 0.08%.

Enthalpy of water near critical point, kJ/kg, [13]:

$$h' = \sum_{i=0}^{4} n_i (1-\theta)^{0.25i} \tag{S8-9}$$

where n_i are presented in Table S8.4. The error for 623 K < T < 647 K is 0.3%.

Enthalpy of steam near critical point, kJ/kg, [13]:

$$h'' = \sum_{i=0}^{4} r_i (1-\theta)^{0.25i} \tag{S8-10}$$

where r_i are presented in Table S8.5. The error for 613 K < T < 647 K is 0.9%.

Specific heat capacity of water at constant pressure, kJ/(kg·K), [14]:

$$C_P^{\prime} = 0.10833 \cdot \frac{1 + \sum_{i=6}^{9} H_i y^{i-5}}{\sum_{i=1}^{5} H_i y^i} + \frac{3\times10^{-5}}{y^{2.5}} \qquad \text{(S8-11)}$$

where $y = 1 - \theta = 1 - T_s/T_0$, H_i are presented in Table S8.6. The error for 273 K < T < 623 K is 0.15% and 1.5% for 623 K < T < 647 K.

Specific heat capacity of steam at constant pressure, kJ/(kg·K), [14]:

$$C_P^{\prime\prime} = \frac{1 + \sum_{i=8}^{9} q_i y^{i-7}}{\sum_{i=0}^{7} c_i y^i} \qquad \text{(S8-12)}$$

where $y = 1 - \theta = 1 - T_s/T_0$, q_i are presented in Table S8.6. The error for 273 K < T < 623 K is 0.25% and 11% for 623 K < T < 646 K.

Dynamic viscosity of water, Pa·s, [16]:

$$\mu^{\prime} = 0.1 \exp \sum_{i=0}^{9} p_i \left[\frac{T - 273.15}{100}\right]^i \qquad \text{(S8-13)}$$

where p_i are presented in Table S8.7. The error for 273 K < T < 603 K is 0.3%, 0.8% for 603 K < T < 643 K and 6% for 643 K < T < 647 K.

Dynamic viscosity of steam, Pa·s, [16]:

$$\mu^{\prime\prime} = \sum_{i=0}^{9} D_i \left[\frac{T - 273.15}{100}\right]^i \qquad \text{(S8-14)}$$

where D_i are presented in Table S8.7. The error for 273 K < T < 573 K is 0.3%, 0.5% for 573 K < T < 623 K, 1% for 623 K < T < 643 K and 6% for 643 K < T < 647 K.

Thermal conductivity of water, W/(m·K), [17]:

$$\lambda^{\prime} = \sum_{i=0}^{8} Z_i \left[\frac{T - 273.15}{100}\right]^i \qquad \text{(S8-15)}$$

where Z_i are presented in Table S8.8. The error for 273 K < T < 643 K is 0.6%.

Thermal conductivity of steam, (T_s < 340 K), W/(m·K), [17]:

$$\lambda^{\prime\prime} = \sum_{i=0}^{8} f_i \left[\frac{T - 273.15}{100}\right]^i \qquad \text{(S8-16)}$$

where f_i are presented in Table S8.8. The error for 273 K < T < 523 K is 0.4%, 0.7% for 523 K < T < 533 K and 0.4% for 533 K < T < 613 K.

Thermal conductivity of steam ($T_s > 340$ K), W/(m·K), [17]:

$$\lambda'' = \sum_{i=0}^{3} M_i \left[\frac{T\text{-}273.15}{100}\right]^i \tag{S8-17}$$

where M_i are presented in Table S8.8. The error for 613 K < T < 643 K is 3%.

Surface tension, Pa·s, [18]:

$$\sigma = 0.2358\left[\frac{T_{cr}-T}{T_{cr}}\right]^{1.256}\left[1-0.625\left(\frac{T-T_{cr}}{T_{cr}}\right)\right] \tag{S8-18}$$

The error for 273 K < T < 533 K is 0.1% and 4% for 533 K < T < 638 K.

Specific evaporation heat,

$$r = h'' - h' \tag{S8-19}$$

S8.3. PROPERTIES IN WIDE RANGES OF PRESSURE AND TEMPERATURE

Presented here is the correlations system for calculating the properties of water and steam at saturation and over a wide range of pressures and temperature. The correlations for caloric properties are from [9] and for transport properties (dynamic viscosity and thermal conductivity) - from [16,17].

The scale coefficients are: h_0 = 1000 kJ/kg, P_0 = 10 MPa, s_0 = 1 kJ/(kg·K), t_0 = 100°C, V_0 = 1 m^3/kg.

Specific volume of underheated and saturated water, [9]:

$$\frac{V}{V_0} = b_0 + b_1\left(\frac{P}{P_0}\right) + b_2\left[\frac{1}{(P/P_0)+2} - 0.227 + 0.018\left(\frac{P}{P_0}\right)\right] \tag{S8-20}$$

where $b_n = \sum_{i=0}^{16} b_{in}\left(\frac{t}{t_o}\right)^i$, b_{in} are presented in Table S8.9 (n = 0, 1, 2). The error for P < 140 MPa and 273 K < T < 603 K is 0.07%.

Specific volume in critical region, [9]:

$$\frac{PV}{P_0V_0} = \sum_{i=0}^{2}\sum_{j=0}^{5} a_{ij}\left(\frac{h}{h_0}-2\right)^i\left(\frac{P}{P_0}\right)^j \tag{S8-21}$$

where a_{ij} are presented in Table S8.10. The error for 15 MPa < P < 35 MPa and T > 60 is 0.5%.

Specific volume of overheated and saturated steam, [9]:

$$\frac{PV}{P_0V_0} = \sum_{i=0}^{3}\sum_{j=o}^{3} e_{ij}\left(\frac{h}{h_0}-2\right)^i\left(\frac{P}{P_0}\right)^j + \left[0.000084 - 0.000071\frac{P}{P_0} + 0.0000142\left(\frac{P}{P_0}\right)^2 - \frac{0.000084}{1+4.6(P/P_0)+120(P/P_0)^3}\right]\left[-\left(\frac{1.4}{(h/h_0)-1.68}\right)^4 + \left(\frac{1.4}{(h/h_0)-1.68}\right)^8\right] \tag{S8-22}$$

where e_{ij} are presented in Table S8.11. The error for $0 < P < 35$ MPa, 273 K $< T <$ 1073 K and h $<$ 2700 kJ/kg is 0.09%.

Enthalpy of underheated and saturated water, [9]:

$$\frac{h}{h_o} = b_3 + b_4\left(\frac{P}{P_0}\right) + b_5\left[\frac{1}{(P/P_0)+2} - 0.24927 + 0.021\left(\frac{P}{P_0}\right)\right] \qquad \text{(S8-23)}$$

where $b_n = \sum_{i=0}^{16} b_{ni}\left(\frac{t}{t_o}\right)^i$, b_{ni} are presented in Table S8.9 (n = 3, 4, 5). The error for $P < 40$ MPa and $T = 603$ K is 0.07%.

Temperature in critical region, [9]:

$$\frac{t}{t_0} = \sum_{i=0}^{4}\sum_{j=0}^{5} c_{ij}\left(\frac{h}{h_0} - 2\right)^i \left(\frac{P}{P_0}\right)^j \qquad \text{(S8-24)}$$

where c_{ij} are presented in Table S8.12. The error at P = 15-35 MPa and $h <$ 2700 kJ/kg is 1.21 K.

Temperature of overheated and saturated steam, [9]:

$$\begin{aligned}\frac{t}{t_o} = {} & \sum_{i=0}^{5}\sum_{j=0}^{5} f_{ij}X^i\left(\frac{P}{P_0}\right)^j + \left[0.5214 + 0.0018X - 0.3625X^2 + 26.0892X^3 - \right.\\ & \left. - 192.1987X^4\right]\left[\frac{1}{100 + 730(P/P_0) - 1.400(P/P_0)^2 + 14500(P/P_0)^3}\right]\end{aligned} \qquad \text{(S8-25)}$$

where $X = h/h_0 - 375$, f_{ij} are presented in Table S8.13. The error for 0.1 MPa $< P <$ 35 MPa, 273 K $< T <$ 1073 K and $h <$ 2700 kJ/kg is $<$ 0.5 K.

Entropy of overheated and saturated steam, [9]:

$$\begin{aligned}\frac{s}{s_0} = {} & \sum_{i=0}^{4}\sum_{j=0}^{4} g_{ij}X^i\left(\frac{P}{P_0}\right)^j + 6.29835 + 2.92696\log_{10}y + 1.98819\left(\log_{10}y\right)^2\\ & - 1.44026\left(\log_{10}y\right)^3 + 0.43144\left(\log_{10}y\right)^4 - 1.062689\log_{10}\left(\frac{10000P}{P_0}\right)\\ & + \frac{0.13(P/P_0) - 0.12(P/P_0)^2}{1.07 + 7.2(P/P_0)^2 + 4.0(P/P_0)^3}\,(1.7 - 0.1y)^8\end{aligned} \qquad \text{(S8-26)}$$

where $X = (2.9 - 0.1y)^2 - 2.6$; $y = 10h/h_0 - 20$, g_{ij} are presented in Table S8.14. The error for $0 < P < 35$ MPa, 273 K $< T <$ 1073 K and $h <$ 2700 kJ/kg is $<$ 0.0007 kJ/(kg·K).

Entropy in critical region, [9]:

$$\frac{s}{s_0} = \sum_{i=0}^{5}\sum_{j=0}^{4} d_{ij}\left(\frac{h}{h_0} - 2\right)^i \left(\frac{P}{P_0} - 2.5\right)^j \qquad \text{(S8-27)}$$

where d_{ij} are presented in Table S8.15. The error for 15 MPa $< P <$ 35 MPa is 0.0012 kJ/(kg·K).

Temperature at saturation, [9]:

$$\left(\frac{100t_s}{t_0}\right) = \sum_{i=0}^{11} B_i \left[\ln \frac{P_s}{0.00980655\,P_0}\right] \tag{S8-28}$$

where B_i are presented in Table S8.16. The error for 273 K < T_s < 573 K is 0.01 K and at T_s > 573 K is 0.075°C.

Pressure along saturation curve, [9]:

$$\ln\left(\frac{P_s}{0.00980655\,P_0}\right) = \sum_{i=0}^{9} A_i \left(\frac{t_s}{t_0}\right)^i \tag{S8-29}$$

where A_i are presented in Table S8.16. The error for 273 K < T_s < 573 K is 0.02 MPa and 0.01 MPa for T_s > 573 K.

Specific volume of water at saturation, [9]:

$$\frac{V'}{V_0} = \sum_{i=0}^{9} C_i \left(\frac{t}{t_0}\right)^i \tag{S8-30}$$

where C_i are presented in Table S8.16. The error for 273 K < T < 573 K is 0.0004 cm^3/g and 0.0008 cm^3/g for T > 573 K.

Enthalpy of water at saturation kJ/kg, [9]:

$$\frac{h'}{h_o} = \sum_{i=0}^{9} D_i \left(\frac{t}{t_o}\right)^i \tag{S8-31}$$

where D_i are presented in Table S8.17. The error for 273 < T < 573 K is 0.08 kJ/kg and 0.3 kJ/kg for T > 573 K.

Entropy of water at saturation kJ/(kg·K), [9]:

$$\frac{s'}{s_o} = \sum_{i=0}^{9} E_i \left(\frac{t}{t_o}\right)^i \tag{S8-32}$$

where E_i are presented in Table S8.17. The error for 273 K < T < 573 K is 0.0001 kJ/(kg·K) and 0.0005 kJ/(kg·K) for T > 573 K.

Specific volume of steam at saturation, m^3/kg, [9]:

$$\frac{PV''}{P_0 V_0} = \sum_{i=0}^{8} F_i \left(\frac{t}{t_0}\right)^i \tag{S8-33}$$

where F_i are presented in Table S8.17. The error for 273 K < T < 573 K is 0.03% and 0.015% for T > 573 K.

Enthalpy of steam at saturation, kJ/kg, [9]:

$$\frac{h''}{h_0} = \sum_{i=0}^{7} G_i \left(\frac{t}{t_0} \right)^i \tag{S8-34}$$

where G_i are presented in Table S8.18. The error for 273 K < T < 573 K is 0.12 kJ/kg and 0.14 kJ/kg for T > 573 K.

Entropy of steam at saturation, kJ/(kg·K), [9]:

$$\frac{s''}{s_0} = \sum_{i=0}^{9} H_i \left(\frac{t}{t_0} \right)^i \tag{S8-35}$$

where H_i are presented in Table S8.18. The error for 273 K < T < 573 K is 0.0006 kJ/(kg·K) and 0.0006 kJ/(kg·K) for T > 573 K.

Specific heat of evaporation:

$$r = h'' - h' \tag{S8-36}$$

Specific heat capacity at constant pressure:

$$C_p = (dh/dT)_{P=const} \tag{S8-37}$$

Thermal conductivity of water and steam, W/(m·K), [17]:

$$\lambda = \lambda_0 + \bar{\lambda} + \Delta\lambda \tag{S8-38a}$$

where

$$\lambda_0 = \left(\frac{T}{T_0} \right)^{0.5} \sum_{i=0}^{3} a_i \left(\frac{T}{T_0} \right)^i \tag{S8-38b}$$

$$\bar{\lambda} = b_0 + b_1 \left(\frac{\rho}{\rho_0} \right) + b_2 \exp\left[-0.171587 \left(\frac{\rho}{\rho_0} + 2.39219 \right) \right] \tag{S8-38c}$$

$$\begin{aligned} \Delta\lambda = {} & \left[d_1 \left(\frac{T}{T_0} \right)^{10} + d_2 \right] \left(\frac{\rho}{\rho_0} \right)^{1.8} \exp\left\{ c_1 \left[1 - \left(\frac{\rho}{\rho_0} \right)^{2.8} \right] \right\} + d_3 S \left(\frac{\rho}{\rho_0} \right)^{Q} \\ & \times \exp\left\{ \frac{Q}{Q+1} \left[1 - \left(\frac{\rho}{\rho_0} \right)^{Q+1} \right] \right\} + d_1 \exp\left[c_2 \left(\frac{T}{T_0} \right)^{1.5} + c_3 \left(\frac{\rho_0}{\rho} \right)^{5} \right] \end{aligned} \tag{S8-38d}$$

$$Q = 2.0 + c_5 (\Delta T_0)^{-0.6} \tag{S8-38e}$$

$$S = (\Delta T_0)^{-1} \ for \frac{T}{T_o} \geq 1 \,; \ S = c_6 (\Delta T_0) \ for \frac{T}{T_0} < 1 \,; \ \Delta T = \left| \left(\frac{T}{T_0} \right) - 1 \right| + c_4$$

T_0 = 647.3 K; ρ_0 = 317.7 kg/m^3; a_i, b_i, c_i, d_i are presented in Table S8.19. The error for T < 643 K is 50 mW/(m·K), for 273 K < T < 573 K and 0.1 MPa < P < 30 MPa it is 15 mW/(m·K).

Dynamic viscosity of water and steam, Pa·s, [16]:

$$\mu = 10^{-3}\mu_0 \exp\left[\frac{\rho}{\rho_0}\sum_{i=0}^{5}\sum_{j=0}^{4} b_{ij}\left(\frac{T_0}{T}-1\right)^i\left(\frac{\rho}{\rho_0}-1\right)^j\right] \qquad \text{(S8-39a)}$$

where

$$\mu_0 = \left(\frac{T}{T_0}\right)^{0.5}\left[\sum_{k=1}^{3} a_k\left(\frac{T_0}{T}\right)^k\right]^{-1} \qquad \text{(S8-39b)}$$

$T_0 = 647.27$ K, $\rho_0 = 317.763$ kg/m^3, $a_0 = 0.181583$, $a_1 = 0.0177624$, $a_2 = 0.0105287$, $a_3 = -0.0036744$; b_{ij} are presented in Table S8.20.

Nomenclature to Supplement S8

P - pressure; T - temperature, K;
t - temperature,°C; V - specific volume;
ρ - density; h - enthalpy;
s - entropy (or second -unit of time);
C_P - specific heat capacity at constant pressure;
r - specific evaporation heat; μ - dynamic viscosity;
ν - kinematic viscosity; λ - thermal conductivity;
a - thermal diffusivity; Pr - Prandtl number;
R - specific gas constant; R^* - universal gas constant;
C_V - specific heat capacity at constant volume;
w - sound velocity; M - molecular weight.
σ - surface tension; Å - Angström

Indexes

$'$ - for water; $''$ - for steam;
$_{cr}$ - for critical parameters; $_0$ - for scale parameters
$_s$ - at saturation.

Table S8.1 THE VALUES OF a_i AND b_i IN CORRELATIONS (S8-1), (S8-2)

i	a_i	b_i
0	2.8549009	1.5226465
1	-5.1176607	-0.68230952
2	-1.1700839	0.16411495
3	-1.0546138 E-1	-0.20232165 E-2
4	6.6842243 E-3	-0.19239111 E-2
5	1.1424939 E-2	-0.57454942 E-3
6	7.4735992 E-3	0.68411554 E-4
7	6.1572535 E-3	0.33650007 E-4
8	4.8597469 E-3	-0.12342248 E-4
9	2.7214236 E-3	0.1482655 E-5
10	2.7751180 E-3	-0.10211646 E-5
11	1.6549262 E-3	-0.4090809 E-5
Remark:	Here and below the notation E±n stands for decimal exponent: 0.12345 E-5 = $0.12345 \cdot 10^{-5}$	

Table S8.2 THE VALUES OF c_i AND g_i IN CORRELATIONS (S8-3), (S8-5)

i	c_i	g_i
0	0.105506870	0.215918638 E 5
1	-0.13373977 E 1	-0.294899186 E 6
2	0.742997633 E 1	0.168533091 E 7
3	-0.234015993 E 2	-0.539468966 E 7
4	0.456909720 E 2	0.106814779 E 8
5	-0.566217816 E 2	-0.134040540 E 8
6	0.434983366 E 2	0.104168615 E 8
7	-0.189459451 E 2	-0.458635700 E 7
8	0.358401536 E 1	0.876636090 E 6

Table S8.3 THE VALUES OF d_i AND k_i IN CORRELATIONS (S8-4), (S8-6)

i	d_i	k_i
0	1.601984134 E 3	-0.245090850 E 5
1	-2.084412819 E 4	0.343138528 E 6
2	1.153537410 E 5	-0.19174351 E 7
3	-3.581256407 E 5	0.605373655 E 7
4	6.848150617 E 5	-0.118862165 E 8
5	-8.271991378 E 5	0.148342520 E 8
6	6.168961537 E 5	-0.115037973 E 8
7	-2.598476710 E 5	0.507143921 E 7
8	4.735523660 E 4	-0.973927619 E 6

Table S8.4 THE VALUES OF l_i AND n_i IN CORRELATIONS (S8-7), (S8-9)

i	l_i	n_i
0	3.142594958 E 3	2.095194 E 3
1	-0.968249020 E 3	-0.223121545 E 3
2	-1.665681112 E 4	-2.14938033 E 3
3	3.839603784 E 4	2.52652835 E 3
4	-2.732658861 E 4	-3.3080553 E 3

Table S8.5 THE VALUES OF m_i AND r_i IN CORRELATIONS (S8-8), (S8-10)

i	m_i	r_i
0	3.39697600 E 3	2.0331698 E 3
1	-6.06585530 E 3	1.066557873 E 3
2	7.61661930 E 4	-1.917663821 E 3
3	-2.08275718 E 5	9.843191852 E 3
4	2.96490244 E 5	-1.072799545 E 4

Table S8.6 THE VALUES OF H_i AND q_i IN CORRELATIONS (S8-11), (S8-12)

i	H_i	q_i
0	0.000	-0.775255138 E-3
1	0.2927550602	1.88981097
2	0.1454526641 E 3	-9.95555559 E 1
3	0.9146938690 E 3	1.42469204 E 3
4	-0.2333844954 E 4	-4.93266402 E 3
5	0.5930582270 E 3	1.82587178 E 4
6	0.2951648157 E 3	-3.25912370 E 4
7	0.7980531291 E 4	2.02754251 E 4
8	0.1685557641 E 5	-4.76234279 E 1
9	-0.5348378585 E 5	6.013485 E 2

Table S8.7 THE VALUES OF p_i AND D_i IN CORRELATIONS (S8-13), (S8-14)

i	p_i	D_i
0	5.189401760	9.15793873 E-3
1	-3.507520606	4.46500987 E-3
2	3.732962083	-1.42492905 E-2
3	-4.601968450	4.42144641 E-2
4	4.653922050	-6.62047713 E-2
5	-3.234942467	5.56815892 E-2
6	1.444639152	-2.7590629 E 1
7	-3.926811178	7.98470722 E-3
8	5.885674977 E-2	-1.24769529 E-3
9	-3.721365822 E-3	8.13288117 E-5

Table S8.8 THE VALUES OF z_i, f_i AND M_i IN CORRELATIONS (S8-15), (S8-16), (S8-17)

i	z_i	f_i	M_i
0	5.63730868 E 2	1.6971630 E 1	-3.308698477 E 5
1	9.31783295 E 1	9.5538456	2.87630408 E 5
2	5.90753049 E 2	-3.30967958 E 1	-8.337376896 E 4
3	-1.49213413 E 3	1.17518155 E 2	8.061259257 E 3
4	1.58215409 E 3	-1.94700672 E 2	-
5	-9.03844219 E 2	1.8142523 E 2	-
6	2.87484093 E 2	-9.895983004 E 1	-
7	-4.79573904 E 1	3.13565128 E 1	-
8	3.2714303	-5.34852932	-
9	-	0.380528886	-

Table S8.9 COEFFICIENTS FOR EQUATIONS (S8-20), (S8-23)

i	b_{i0}	b_{i1}	b_{i2}	b_{i3}	b_{i4}	b_{i5}
0	9.9942695 E-4	-4.609152 E-6	3.00 E-6	6.4300000 E-4	9.6859913 E-3	-2.880 E-3
1	-3.4631890 E-6	3.504430 E-6	7.00 E-7	4.1982594 E-1	-3.0725260 E-3	3.200 E-3
2	6.5359352 E-5	-6.688444 E-6	-	-6.5218150 E-3	1.6722356 E-3	-
3	-2.6269070 E-5	4.868174 E-6	-	6.3656960 E-3	-8.0696010 E-4	-
4	7.8565550 E-6	-1.835593 E-6	8.00 E-7	-1.8508140 E-3	1.2093020 E-4	-
5	-5.0004200 E-7	2.128960 E-7	-	4.5199700 E-4	-2.2009100 E-5	-
6	-	-	-	-	-	5.440 E-5
16	-	-	4.55 E-12	-	-	1.682 E-9

Table S8.10 COEFFICIENTS FOR EQUATION (S8-21)

i	a_{i0}	a_{i1}	a_{i2}	a_{i3}	a_{i4}	a_{i5}
0	3.66681 E-3	1.673873 E-2	1.584386 E-2	-1.491102 E-2	-1.000221 E-2	1.381305 E-2
1	7.32940 E-4	-4.006910 E-3	-1.312040 E-3	7.555850 E-3	-5.961200 E-4	-2.73716 E-3
2	9.74000 E-5	4.622300 E-4	-1.3672 E-4	-7.469500 E-4	6.214200 E-4	-2.7310 E-4

Table S8.11 COEFFICIENTS FOR EQUATION (S8-22)

i	e_{i0}	e_{i1}	e_{i2}	e_{i3}
0	-3.9999370 E-4	2.6791050 E-2	-1.7078740 E-3	-7.41270 E-6
1	3.6864396 E-3	-1.0383050 E-2	7.6498837 E-3	-1.70630 E-3
2	-6.1993860 E-4	2.0006433 E-3	-1.4677281 E-3	3.12960 E-4
3	1.9500000 E-5	-5.7200000 E-5	2.6000000 E-5	-

Table S8.12 COEFFICIENTS FOR EQUATION (S8-24)

i	c_{i0}	c_{i1}	c_{i2}	c_{i3}	c_{i4}	c_{i5}
0	3.9517281	-4.2831438	-1.7360934 E 1	2.7102834 E 1	4.7253670 E 1	-6.5775645 E 1
1	-1.0673765	4.9117969	2.4806751 E 1	-3.7861085 E 1	-7.1613017 E 1	1.0075819 E 2
2	8.1406220 E-1	-2.2296119	-1.3799105 E 1	2.1088377 E 1	4.0227975 E 1	-5.7194453 E 1
3	-2.1039730 E-1	5.1574830 E-1	3.3288459	-5.1865516	-9.7562310	1.4047099 E 1
4	1.8895300 E-2	-4.5731100 E-2	-2.933476 E-1	4.6792610 E-1	8.6394610 E-1	-1.2593970

Table S8.13 COEFFICIENTS FOR EQUATION (S8-25)

i	f_{i0}	f_{i1}	f_{i2}	f_{i3}	f_{i4}	f_{i5}
0	4.454360	4.7805160	-3.6118300 E-1	-2.0663100 E-1	1.9770260	-
1	6.328634 E-1	-1.0776543	1.5939256	-2.7602368	-3.2893640	-1.051
2	-1.050978 E-1	1.6146320 E-1	-6.2214510 E-1	3.4448816	3.3441800	2.439
3	2.672350 E-2	6.4233400 E-2	3.4262000 E-3	-2.0225651	-1.6529210	-1.186
4	-5.952300 E-3	-3.3262900 E-2	4.8770400 E-2	5.5559550 E-1	3.4401850 E-1	1.647 E-1
5	5.840000 E-4	4.1380000 E-3	-7.7940000 E-3	-5.6351000 E-2	-2.3995000 E-2	-

Table S8.14 COEFFICIENTS FOR EQUATION (S8-26)

i	g_{i0}	g_{i1}	g_{i2}	g_{i3}	g_{i4}
0	1.8243470 E-3	-6.0296100 E-4	3.4925100 E-4	3.1548600 E-4	-1.4494070 E-4
1	5.8636936 E-3	4.7405603 E-2	2.2024349 E-2	9.4231710 E-3	1.1724252 E-3
2	-7.8975000 E-3	-9.9894300 E-3	-1.0330252 E-2	-7.2432084 E-3	-3.6430370 E-4
3	9.8552590 E-4	1.6667200 E-3	2.5383324 E-3	2.0922070 E-3	7.7018100 E-5
4	-7.5029000 E-5	-1.6314950 E-4	-2.4464940 E-4	-2.0318940 E-4	-1.1556200 E-5

Table S8.15 COEFFICIENTS FOR EQUATION (S8-27)

i	d_{i0}	d_{i1}	d_{i2}	d_{i3}	d_{i4}
0	4.265774	1.526792	-4.1270 E-2	6.569900 E-2	-7.435400 E-2
1	-3.834300 E-2	-6.013600 E-2	-6.0450 E-2	1.615000 E-2	1.237900 E-2
2	8.033000 E-3	2.143700 E-2	-9.0800 E-4	-6.528000 E-3	1.050600 E-2
3	-5.180000 E-3	-3.261000 E-3	-1.3291 E-2	-9.408000 E-3	-5.215000 E-3
4	-6.660000 E-4	4.418000 E-3	1.1204 E-2	-1.496000 E-2	1.639000 E-3
5	1.770000 E-3	-4.183000 E-3	-1.2770 E-2	1.357000 E-2	9.300000 E-4

Table S8.16 COEFFICIENTS FOR EQUATIONS (S8-28), (S8-30)

i	A_i	B_i	C_i
0	-5.078709984	9.909271199 E 1	1.0001789 E-3
1	7.270489907	2.785424215 E 1	1.3905330 E-7
2	-3.033726807	2.375357647	2.0639347 E-5
3	1.256759065	2.107780463 E-1	1.4001053 E-4
4	-5.608659370 E-1	2.129682011 E-2	-2.7979589 E-4
5	2.477563380 E-1	1.328377290 E-3	2.7254276 E-4
6	-8.659024966 E-2	-3.739348425 E-4	-1.5042234 E-4
7	2.015339284 E-2	-1.741775190 E-5	4.8021276 E-5
8	-2.693452728 E-3	2.207171179 E-5	-8.267041 E-6
9	1.553179872 E-4	1.534373134 E-6	5.968357 E-7
10	-	-4.268568510 E-7	-
11	-	-4.292460291 E-8	-

Table S8.17 COEFFICIENTS FOR EQUATIONS (S8-31), (S8-33)

i	D_i	E_i	F_i
0	-4.1600000 E-5	-1.1000000 E-4	1.26 E-2
1	4.2290733 E-1	1.5446705	4.5945234 E-2
2	-2.5507948 E-2	-3.4417244 E-1	-3.1913345 E-5
3	6.2229560 E-2	2.0307179 E-1	-3.1684010 E-4
4	-8.3823420 E-2	-1.7724907 E-1	3.3979946 E-4
5	6.9214690 E-2	1.2375197 E-1	-3.4194103 E-4
6	-3.4536790 E-2	-5.6232060 E-2	1.4519652 E-4
7	1.0322371 E-2	1.5734212 E-2	-2.8638253 E-5
8	-1.6994910 E-3	-2.467064 E-3	2.0409848 E-6
9	1.1936422 E-4	1.672019 E-4	-

Table S8.18 COEFFICIENTS FOR EQUATIONS (S8-34), (S8-35)

i	G_i	H_i
0	2.5009600	9.1563856
1	1.8430540 E-1	-2.6836757
2	1.9591100 E-4	1.3274657
3	-1.2737746 E-2	-7.3158620 E-1
4	9.3849700 E-3	4.8081603 E-1
5	-8.0477568 E-3	-2.7846878 E-1
6	2.7325329 E-3	1.0649010 E-1
7	-3.4714286 E-4	-2.4050010 E-2
8	-	2.8728 E-3
9	-	-1.4 E-4

Table S8.19 COEFFICIENTS FOR EQUATIONS (S8-38a-e)

i	a_i	b_i	c_i	d_i
0	1.02811 E-2	-3.97070 E-1	-	-
1	2.99621 E-2	4.00302 E-1	6.42857 E-1	7.01309 E-2
2	1.56146 E-2	1.06000	-4.11717	1.18520 E-2
3	-4.22464 E-3	-	-6.17937	1.69937 E-3
4	-	-	3.08976 E-3	-1.02
5	-	-	8.22994 E-2	-
6	-	-	1.00932 E-1	-

Table S8.20 COEFFICIENTS b_{ij}FOR EQUATIONS (S8-39-a,b)

j i	0	1	2	3	4
0	0.501938	0.2356220	-0.274637	0.145831	-0.0270448
1	0.162888	0.7893930	-0.743539	0.263129	-0.0253093
2	-0.130356	0.6736650	-0.959456	0.347247	-0.0267758
3	-0.907919	1.2075520	-0.687343	0.213486	-0.0822904
4	-0.551119	0.0670665	-0.497089	0.100754	0.0602253
5	0.146543	-0.0843370	0.195286	-0.032932	-0.0202595

References to Supplement S8

[1] PHILIP G. HILL., "An unified fundamental equation for the thermodynamic properties of H_2O", J. of Phys. Chem. Ref. Data., Vol. 19, No 5, p. 1233 (1990)

[2] SAUL A., et al., "A fundamental equation for water covering the range from melting to 1273 K at Pressure up to 25000 MPa", J. Phys. Chem. Ref. Data, Vol. 18, p. 1537 (1989)

[3] ALEXANDROV A. A., "The international tables and equation for the thermal conductivity of water and steam", Teploenergetika, No 4, p. 70 (1980) (in Russian)

[4] RIVKIN S. L., LEVIN A. JA., IZRAILEVSKY L. B., PTITSIN V. N., "Equations for the dynamic viscosity of liquid water", Teploenergetika, No 1, p. 68 (1973) (in Russian)

[5] ALEXANDROV A. A. "Skeleton tables for specific volume and enthalpy of water and steam", Teploenergetika, No 3, p. 71 (1987) (in Russian)

[6] SATO H., et al., "New international skeleton tables for the thermodynamic properties of water", J. Phys. Chem. Ref. Data, Vol. 17, p. 1439 (1988)

[7] ALEXANDROV A. A., "New international material on thermophysical properties of water and steam", Electroenergetika, No 2, p. 127 (1990) (in Russian)

[8] MARTINOV O. I., ALEXANDROV A. A., PETROV T. I., "The International Conference on the properties of water and steam", Teploenergetika, No 3, p. 76 (1990) (in Russian)

[9] JUSA J., "Correlations for thermodynamical properties of water and steam, recommended for computer calculations", Teploenergetika, No 1, p. 80 (1967) (in Russian)

[10] TRAKHTENHERTZ M. S., ALEXANDROV A. A., "Thermophysical properties of water and steam at ranges of temperature from 0 to 700°C and of pressure from 0.1 MPa to 30 MPa", In book "The methods of calculation of the substance properties", Moscow, IVT AN USSR, p. 78 (1983) (in Russian)

[11] WUKOLOVITCH M. P., RIVKIN S. L., ALEXANDROV A. A., "Tables of the thermophysical properties of water and steam", Moscow, Izdatelstvo standartov (1969) (in Russian)

[12] GIBSON M. R., BRUGES E. A., "New equations for the thermophysical properties of saturated water in both the liquid and vapor phases", J. Mech. Eng. Sci. v. 9, No 1, p. 24 (1967)

[13] RIVKIN S. L., ALEXANDROV A. A., "The equations for calculation of thermophysical property of saturated and undercooled steam", Teploenergetika. No 8, p. 65 (1971) (in Russian)

[14] ISHIMOTO S., UEMATSU M., TANISHITA I., "New equations for thermodynamical properties of saturated water and steam", Bull. ASME, v. 15, No 86, p. 1278 (1972)

[15] ALEXANDROV A. A., IVANOV A. I., MATVEEV A. B., "The dynamic viscosity of water and steam at wide range of temperature and pressure", Teploenergetika, No 4, p. 59 (1965)

[16] ALEXANDROV A. A., "The international tables and equations for the dynamic viscosity of water and steam", Teploenergetika, No 4, p. 87 (1977) (in Russian)

[17] ALEXANDROV A. A., "The international tables and equations for the thermal conductivity of water and steam", Teploenergetika, No 4, p. 70 (1980) (in Russian)

[18] VARGAFTIK N. B., VOLKOV B. N., VOLJAK L. D., "On the international tables for the surface tension of water", Teploenergetika, No 5, p. 73 (1979) (in Russian)

[19] RIVKIN S. L., KREMNEVSKAJA A. A., "Equations of water and steam state for computer calculation of processes and equipment of power stations", Teploenergetika, No 3, p. 69 (1977) (in Russian)

[20] ALEXANDROV A. A., "The critical parameters of light and heavy water", Teploenergetika, No 1, p. 74 (1986) (in Russian)

Supplement S9

IAPS FORMULATIONS FOR THERMOPHYSICAL PROPERTIES OF LIGHT WATER AND STEAM

S9.1. INTRODUCTION

Further to the description given in Chapter 5 on light and heavy water thermophysical properties, details of the work carried out at the Bhabha Atomic Research Centre, India on the thermophysical properties of light water and steam are given in this supplement.

S9.2. THERMODYNAMIC PROPERTIES OF LIGHT WATER

To calculate the various thermodynamic properties of light water, IAPS Formulation 1984 [1] has been adopted for developing the computer program. This formulation is based on the fundamental equation for the specific Helmholtz free energy as a function of temperature and density, developed by Haar, Gallagher and Kell [2,3]. All thermodynamic properties are made dimensionless with the aid of a reference temperature, T^*, a reference density ρ^* and a reference pressure P^*. For light water these three constants are as follows:

$T^* =$ 647.27 K
$\rho^* =$ 317.763 kg/m^3
$P^* =$ 22.115 MPa

In addition, there are several other reference constants which are simple combinations of the above-mentioned reference constants. These constants are as follows:

$A^{**} = P^*/\rho^* = 69595.89$ J/kg
$S^{**} = P^*/(\rho^*\ T^*) = 107.5222$ J/(kg·K)
$w^{**} = (P^*/\rho^*)^{1/2} = 263.810$ m/s

The fundamental equation has the form:

$$\bar{A}(\bar{T},\bar{\rho}) = \sum_{j=0}^{4} \bar{A}_j \qquad \text{(S9.2-1)}$$

where the functions $\bar{A}_j$ are as follows

$$\bar{A}_0\ (\bar{T}) = (A_{00} + A_{01}\bar{T})\ \ln\bar{T} + \sum_{i=2}^{17} A_{0i}\bar{T}^{i-4} \qquad \text{(S9.2-2)}$$

$$\bar{A}_1(\bar{T},\bar{\rho}) = \bar{\rho}\ \sum_{i=0}^{4} A_{1i}\left[\frac{1}{\bar{T}}\right]^{i-1} \qquad \text{(S9.2-3)}$$

$$\bar{A}_2[\bar{T},\bar{\rho}] = A_{20}\bar{T}\left\{\ln\left(\frac{\bar{\rho}}{1-y}\right) - \frac{130}{3(1-y)} + \frac{169}{6(1-y)^2} - 14y\right\} \qquad \text{(S9.2-4)}$$

with

$$y = \bar{\rho}\left(y_0 + y_1\ \ln\ \bar{T} + \frac{y_2}{\bar{T}^3} + \frac{y_3}{\bar{T}^5}\right) \qquad \text{(S9.2-5)}$$

$$\bar{A}_3(\bar{T},\bar{\rho}) = \sum_{i=0}^{35} A_{3i} \left(\frac{1}{\bar{T}}\right)^{l(i)} Z^{k(i)} \qquad \text{(S9.2-6)}$$

with

$$Z = 1 - e^{-z_0 \bar{\rho}}$$

$$\bar{A}_4(\bar{T},\bar{\rho}) = \sum_{i=0}^{3} A_{4i} \quad \delta_i^{n(i)} \exp\left[-\alpha_i \quad \delta_i^{m(i)} - \beta_i \quad \tau_i^2\right] \qquad \text{(S9.2-7)}$$

with

$$\delta_i = \frac{\bar{\rho} - \bar{\rho}_i}{\bar{\rho}_i} \quad \textit{and} \quad \tau_i = \frac{\bar{T} - \bar{T}_i}{\bar{T}_i}$$

The coefficients in the above equations are listed in Tables S9.2.1 to S9.2.5:

Table S9.2.1 COEFFICIENTS FOR $\bar{A}_0(\bar{T})$

i	A_{oi}
0	$-0.130840393653\times10^{+2}$
1	$-0.857020420940\times10^{+2}$
2	$0.765192919131\times10^{-2}$
3	$-0.620600116069\times10^{+0}$
4	$-0.106924329402\times10^{+2}$
5	$-0.280671377296\times10^{+1}$
6	$0.119843634845\times10^{+3}$
7	$-0.823907389256\times10^{+2}$
8	$0.555864146443\times10^{+2}$
9	$-0.310698122980\times10^{+2}$
10	$0.136200239305\times10^{+2}$
11	$-0.457116129409\times10^{+1}$
12	$0.115382128188\times10^{+1}$
13	$-0.214242224683\times10^{+0}$
14	$0.282800597384\times10^{-1}$
15	$-0.250384152737\times10^{-2}$
16	$0.132952679669\times10^{-3}$
17	$-0.319277411208\times10^{-5}$

Table S9.2.2 COEFFICIENTS FOR $\bar{A}_1(\bar{T},\bar{\rho})$

i	A_{1i}
0	$0.15383053\times10^{+1}$
1	$-0.81048367\times10^{+0}$
2	$-0.68305748\times10^{+1}$
3	$0.00000000\times10^{+0}$
4	$0.86756271\times10^{+0}$

Table S9.2.3 COEFFICIENTS FOR $\bar{A}_2(\bar{T},\bar{\rho})$

$A_{20} = 4.2923415$

i	y_i
0	0.59402227×10^{-1}
1	-0.28128238×10^{-1}
2	0.56826674×10^{-3}
3	-0.27987451×10^{-3}

Table S9.2.4 COEFFICIENTS FOR $\bar{A}_3(\bar{T},\bar{\rho})$

$Z_0 = 0.317763$

i	$k(i)$	$l(i)$	A_{3i}
0	1	1	$-0.76221190138079\times10^{+1}$
1	1	2	$0.32661493707555\times10^{+2}$
2	1	4	$0.11305763156821\times10^{+2}$
3	1	6	$-0.10015404767712\times10^{+1}$
4	2	1	$0.12830064355028\times10^{+3}$
5	2	2	$-0.28371416789846\times10^{+3}$
6	2	4	$0.24256279839182\times10^{+3}$
7	2	6	$-0.99357645626725\times10^{+2}$
8	3	1	$-0.12275453013171\times10^{+4}$
9	3	2	$0.23077622506234\times10^{+4}$
10	3	4	$-0.16352219929859\times10^{+4}$
11	3	6	$0.58436648297764\times10^{+3}$
12	4	1	$0.42365441415641\times10^{+4}$
13	4	2	$-0.78027526961828\times10^{+4}$
14	4	4	$0.38855645739589\times10^{+4}$
15	4	6	$-0.91225112529381\times10^{+3}$
16	5	1	$-0.90143895703666\times10^{+4}$
17	5	2	$0.15196214817734\times10^{+5}$
18	5	4	$-0.39616651358508\times10^{+4}$
19	5	6	$-0.72027511617558\times10^{+3}$
20	6	1	$0.11147126705990\times10^{+5}$
21	6	2	$-0.17412065252210\times10^{5}$
22	6	4	$0.99918281207782\times10^{3}$
23	6	6	$0.33504807153854\times10^{4}$
24	7	1	$-0.64752644922631\times10^{4}$
25	7	2	$0.98323730907847\times10^{4}$
26	7	4	$0.83877854108422\times10^{3}$
27	7	6	$-0.27919349903103\times10^{4}$
28	9	1	$0.11112410081192\times10^{4}$
29	9	2	$-0.17287587261807\times10^{4}$
30	9	4	$-0.36233262795423\times10^{3}$
31	9	6	$0.61139429010144\times10^{3}$
32	3	0	$0.32968064728562\times10^{2}$
33	3	3	$0.10411239605066\times10^{3}$
34	1	3	$-0.38225874712590\times10^{2}$
35	5	3	$-0.20307478607599\times10^{3}$

Table S9.2.5 COEFFICIENTS FOR $\bar{A}_4(\bar{T},\bar{\rho})$

i	$m(i)$	$n(i)$	α_i	β_i	$\bar{\rho}_i$	$\bar{T}_i$	A_{4i}
0	2	0	34	20000	1.0038928	0.98876821	-0.32329494×10^{-2}
1	2	2	40	20000	1.0038928	0.98876821	-0.24139355×10^{-1}
2	2	0	30	40000	1.0038928	0.99124013	0.79027651×10^{-3}
3	4	0	1050	25	4.8778492	0.41713659	-0.13362857×10^{1}

All thermodynamic properties of interest can be derived from the fundamental equation by the use of the same thermodynamic relations as given earlier in Section 5.4 for heavy water, i.e. equations 5.4-4 to 5.4-15.

Explicit expressions for different derivatives of $\bar{A}(\bar{T},\bar{\rho})$ with respect to $\bar{T}$ and $\bar{\rho}$ are found out and incorporated in the computer programs to calculate the values of different thermodynamic properties.

Range of validity of the formulation:

IAPS has tested the formulation and endorsed its validity over the temperature range from 273.15 to 1273.15 K and in the range of pressures described by the conditions:

$P \leq 1500$ MPa for 423.15 K $\leq T \leq$ 1273.15 K

$P \leq 100\,[\,5 + (T - 273.15)/15\,]$ MPa for 273.15 K $\leq T <$ 423.15 K

The formulation is applicable all over this range except for an excluded region around the critical point bounded by:

$$|\,T - T^*\,| \leq 1\ K \quad and \quad |\,\bar{\rho} - 1| \leq 0.3$$

Density of water at different temperatures and pressures is calculated by solving the equation:

$$\bar{P} = \bar{\rho}^2 \left(\frac{\partial \bar{A}}{\partial \bar{\rho}}\right)_{\bar{T}} \tag{S9.2-8}$$

Since the required root of this equation is obtained by using Newton-Raphson method, an initial value (guess value) of density is required to initiate the calculations. This guess value is determined in the following way for the whole range of temperature and pressure.

a) If the temperature is less than or equal to critical temperature and pressure is greater than or equal to saturation pressure, guess density is equal to the density of saturated liquid.

b) If $T \leq T_c$ and $P < P_{sat}$
guess density = density of saturated vapor
where, T_c = 647.27 K

c) If $T >$ 573.15 and $P < P_{sat}$ then for that particular pressure P corresponding saturation temperature is calculated. For this saturation temperature the corresponding saturation density of vapor (DSATV1) is calculated. Also for the temperature T, the corresponding density of saturated vapor (DSATV) is calculated. Then the guess density is taken as D = DSATV1 + (DSATV - DSATV1)/3

d) If $T > T_c$
guess density = $0.4145 \cdot e^{2.45} \cdot P^{0.25}$

This equation is chosen arbitrarily depending on the value of density for the wide range of pressures and temperatures.

S9.3. THERMAL CONDUCTIVITY OF LIGHT WATER

For calculating the thermal conductivity of light water, IAPS Formulation 1985 [4] for the thermal conductivity of ordinary water substance was adopted for programming into the computer code.

This formulation contains two recommended interpolating equations for the thermal conductivity of water.

(i) A Recommended Interpolating equation for scientific use.
(ii) A Recommended Interpolating equation for industrial use.

The two interpolating equations differ in the way they represent the thermal conductivity of steam in the critical region. In the thermal conductivity equation for scientific use, the thermal conductivity diverges towards an infinite value at the critical point as predicted by the modern theory of dynamic critical phenomena and supported by experimental evidence. The thermal conductivity equation for Industrial use yields a finite value of the thermal conductivity at the critical point by assuming certain simplified approximations of the enhancement effect.

S9.3.1. Recommended Interpolating Equation for Scientific Use:

$$\bar{\lambda} = \bar{\lambda}_0(\bar{T}) * \bar{\lambda}_1(\bar{T},\bar{\rho}) + \bar{\lambda}_2(\bar{T},\bar{\rho}) \qquad \text{(S9.3-1)}$$

where, $\bar{\lambda}_0(\bar{T})$ represents the thermal conductivity of steam in the ideal gas limit and has the form:

$$\bar{\lambda}_o(\bar{T}) = \frac{\sqrt{\bar{T}}}{\sum_{i=0}^{3}\left(\frac{L_i}{\bar{T}^i}\right)} \qquad \text{(S9.3-2)}$$

with $L_0 = 1.000000$
$L_1 = 6.978267$
$L_2 = 2.599096$
$L_3 = -0.998254$

$$\bar{\lambda}_1(\bar{T},\bar{\rho}) = \exp\left[\bar{\rho}\sum_{i=0}^{4}\sum_{j=0}^{5} L_{ij}\left(\frac{1}{\bar{T}} - 1\right)^i (\bar{\rho} - 1)^j\right] \qquad \text{(S9.3-3)}$$

with coefficients L_{ij} as given in Table S9.3.1

Table S9.3.1 COEFFICIENTS L_{ij} FOR $\bar{\lambda}_1(\bar{T},\bar{\rho})$

$j \backslash i$	0	1	2	3	4
0	1.3293046	1.7018363	5.2246158	8.7127675	-1.8525999
1	-0.40452437	-2.2156845	-10.124111	-9.5000611	0.9340469
2	0.24409490	1.6511057	4.9874687	4.3786606	0.0
3	0.018660751	-0.76736002	-0.27297694	-0.91783782	0.0
4	-0.12961068	0.37283344	-0.43083393	0.0	0.0
5	0.044809953	-0.11203160	0.13333849	0.0	0.0

$\bar{\lambda}_1(\bar{T},\bar{\rho})$ is an enhancement factor which accounts for the normal density and temperature dependence of the thermal conductivity at elevated temperatures.

$\bar{\lambda}_2(\bar{T},\bar{\rho})$ which accounts for an enhancement of the thermal conductivity in the critical region is defined as,

$$\bar{\lambda}_2(\bar{T},\bar{\rho}) = \frac{0.0013848}{\bar{\mu}_0(\bar{T})\bar{\mu}_1(\bar{T},\bar{\rho})}\left(\frac{\bar{T}}{\bar{\rho}}\right)^2\left(\frac{\partial\bar{P}}{\partial\bar{T}}\right)^2_{\bar{\rho}}\bar{\chi}_T^{0.4678}\,\bar{\rho}^{0.5}\cdot\exp\left[-18.66(\bar{T}-1)^2-(\bar{\rho}-1)^4\right] \qquad \text{(S9.3-4)}$$

where the functions $\bar{\mu}_0(\bar{T})$, $\bar{\mu}_1(\bar{T}.\bar{\rho})$ and $\bar{\chi}_T$ are same as discussed under Section S9.4 of this report on IAPS Formulation 1985 for the viscosity of ordinary water substance. The density, the isothermal compressibility, as well as the partial derivatives $(\partial\bar{P}/\partial\bar{T})_{\bar{\rho}}$ are calculated with the aid of the IAPS Formulation 1984 for the thermodynamic properties of ordinary water substance for Scientific and General use.

The reference constants are:

$T^* =$	647.27 K;	$P^* =$	22.115 MPa
$\rho^* =$	317.763 kg/m^3;	$\lambda^* =$	0.4945 W/(m·K)

Range of validity of equation:

$P \leq 400$ MPa	for 0°C $\leq t \leq$ 125°C
$P \leq 200$ MPa	for 125°C $< t \leq$ 250°C
$P \leq 150$ MPa	for 250°C $< t \leq$ 400°C
$P \leq 100$ MPa	for 400°C $< t \leq$ 800°C

S9.3.2. Recommended Interpolating Equation for Industrial Use:

$$\bar{\lambda} = \bar{\lambda}_0(\bar{T}) + \bar{\lambda}_1(\bar{\rho}) + \bar{\lambda}_2(\bar{T},\bar{\rho}) \qquad \text{(S9.3-5)}$$

The function $\bar{\lambda}_0(\bar{T})$ represents the thermal conductivity of steam in the ideal gas limit and has the form:

$$\bar{\lambda}_0(\bar{T}) = \sqrt{\bar{T}}\sum_{k=0}^{3} a_k\bar{T}^k \qquad \text{(S9.3-6)}$$

with

$a_0 = 0.0102811$; $a_2 = 0.0156146$,
$a_1 = 0.0299621$; $a_3 = -0.00422464$

$$\bar{\lambda}_1(\bar{\rho}) = b_0 + b_1\bar{\rho} + b_2\exp\left\{B_1\left(\bar{\rho} + B_2\right)^2\right\} \tag{S9.3-7}$$

with

$b_0 = -0.397070$; $B_1 = -0.171587$
$b_1 = 0.400302$; $B_2 = 2.392190$
$b_2 = 1.060000$

$$\bar{\lambda}_2(\bar{T},\bar{\rho}) = \left(\frac{d_1}{\bar{T}^{10}} + d_2\right)\bar{\rho}^{9/5}\ \exp\left[C_1\left\{1-(\bar{\rho})^{14/5}\right\}\right] + d_3 S\bar{\rho}^{\phi}\exp\left[\left\{\frac{\phi}{1+\phi}\right\}\left(1-\bar{\rho}^{1+\phi}\right)\right] + d_4\exp\left(C_2\bar{T}^{3/2} + C_3/\bar{\rho}^5\right) \tag{S9.3-8}$$

with

$$\Delta\bar{T} = |\bar{T} - 1| + C_4\ ;\quad \phi = 2 + \frac{C_5}{\Delta\bar{T}^{3/5}}$$

$$S = \begin{cases} 1/\Delta\bar{T} & \textit{for } \bar{T} \geq 1 \\ C_6/\Delta\bar{T}^{3/5} & \textit{for } \bar{T} < 1 \end{cases}$$

with coefficients d_i and C_i as given in Table S9.3.2

Table S9.3.2 COEFFICIENTS d_i AND C_i

$d_1 = 0.0701309$	$C_1 = 0.642857$
$d_2 = 0.0118520$	$C_2 = -4.11717$
$d_3 = 0.00169937$	$C_3 = -6.17937$
$d_4 = -1.0200$	$C_4 = 0.00308976$
	$C_5 = 0.0822994$
	$C_6 = 10.0932$

The reference constants are:

$T^* = 647.3$ K
$\rho^* = 317.7\ \mathrm{kg/m^3}$
$\lambda^* = 1\ \mathrm{W/(m{\cdot}K)}$

Range of validity of equation:

$P \leq 100$ MPa	for $0°\mathrm{C} \leq t \leq 500°\mathrm{C}$
$P \leq 70$ MPa	for $500°\mathrm{C} < t \leq 650°\mathrm{C}$
$P \leq 40$ MPa	for $650°\mathrm{C} < t \leq 800°\mathrm{C}$

The density values, required for this equation, are to be calculated using IFC 67 formulation for industrial use. Computer programs have been developed to calculate thermal conductivity of water using this formulation.

S9.4 VISCOSITY OF LIGHT WATER

For calculating the viscosity of light water, IAPS-85 formulation for viscosity of ordinary water substance [4] has been programmed into the computer code. According to this formulation, the viscosity is represented by the equation:

$$\bar{\mu} = \bar{\mu}_0(\bar{T}) * \bar{\mu}_1(\bar{T},\bar{\rho}) * \bar{\mu}_2(\bar{T},\bar{\rho}) \tag{S9.4-1}$$

where

$$\bar{\mu}_0(\bar{T}) = \sqrt{\bar{T}} \div \sum_{i=0}^{3}\left(\frac{H_i}{\bar{T}^i}\right) \qquad \text{(S9.4-2)}$$

This term gives the viscosity of steam in the ideal gas limit. Coefficients H_i are given in Table S9.4.1

Table S9.4.1

$H_0 = 1.000000$
$H_1 = 0.978197$
$H_2 = 0.579829$
$H_3 = -0.202354$

$$\bar{\mu}_1(\bar{T},\bar{\rho}) = \exp\left[\bar{\rho}\sum_{i=0}^{5}\sum_{j=0}^{6} H_{ij}\,(\frac{1}{\bar{T}}-1)^i(\bar{\rho}-1)^j\right] \qquad \text{(S9.4-3)}$$

The coefficients H_{ij} are given in the Table S9.4.2

Table S9.4.2 COEFFICIENTS $\bar{H}_{ij}$ for $\bar{\mu}_1(\bar{T},\bar{\rho})$

j\i	0	1	2	3	4	5
0	0.5132047	0.3205656	0.000	0.000	-0.7782567	0.1885447
1	0.2151778	0.7317883	1.241044	1.476783	0.000	0.000
2	-0.2818107	-1.070786	-1.263184	0.000	0.000	0.000
3	0.1778064	0.4605040	0.2340379	-0.4924179	0.000	0.000
4	-0.0417661	0.000	0.000	0.1600435	0.000	0.000
5	0.000	-0.01578386	0.000	0.000	0.000	0.000
6	0.000	0.000	0.000	-0.003629481	0.000	0.000

For industrial use, the function $\bar{\mu}_2$ may be taken to be unity everywhere in the range of validity of the equation, as mentioned later.

For scientific use, the value of the function $\bar{\mu}_2$ is 1, except for a very narrow range near the critical range given by

$0.9970 \le \bar{T} \le 1.0082$ and $0.755 \le \bar{\rho} \le 1.290$

In the near critical region

$$\bar{\mu}_2 = 0.922\;\bar{\chi}_T^{\,0.0263}\;,\; if \quad \bar{\chi}_T \ge 21.93 \qquad \text{(S9.4-4)}$$

$$\bar{\mu}_2 = 1, \qquad if\;\; \bar{\chi}_T < 21.93 \qquad \text{(S9.4-5)}$$

where,

$$\bar{\chi}_T = \bar{\rho}\left(\frac{\partial\bar{\rho}}{\partial\bar{p}}\right)_{\bar{T}} \qquad \text{(S9.4-6)}$$

Range of validity:

$P \leq 500$ MPa for 0°C $\leq t \leq$ 150°C
$P \leq 350$ MPa for 150°C $\leq t \leq$ 600°C
$P \leq 300$ MPa for 600°C $\leq t \leq$ 900°C

The reference constants are:

$T^* = 647.27$ K, $\mu^* = 55.071$ μPa-s
$\rho^* = 317.763$ kg/m^3, $P^* = 22.115$ MPa

Density values used in the calculation of viscosity are calculated according to IAPS-84 Formulation for the Thermodynamic properties of ordinary water substance for Scientific and General use.

S9.5. SATURATION PROPERTIES OF LIGHT WATER

A computer program was developed to calculate the vapor pressure as well as density, specific enthalpy and specific entropy of the saturated vapor and liquid for a given value of temperature. The equations used here are described in the supplementary release on the saturation properties of ordinary water substance by IAPS [5]. The equations are as follows:

Vapor pressure:

$$\ln\left(\frac{P}{P_c}\right) = \left(\frac{T_c}{T}\right)\left(a_1\tau + a_2\tau^{1.5} + a_3\tau^3 + a_4\tau^{3.5} + a_5\tau^4 + a_6\tau^{7.5}\right) \qquad \text{(S9.5-1)}$$

with

$a_1 = -7.85823$; $a_3 = -11.7811$; $a_5 = -15.9393$
$a_2 = 1.83991$; $a_4 = 22.6705$; $a_6 = 1.77516$

Densities:

Density of saturated liquid:

$$\frac{\rho}{\rho_c} = 1 + b_1\tau^{1/3} + b_2\tau^{2/3} + b_3\tau^{5/3} + b_4\tau^{16/3} + b_5\tau^{43/3} + b_6\tau^{110/3} \qquad \text{(S9.5-2)}$$

with

$b_1 = 1.99206$; $b_3 = -0.512506$; $b_5 = -45.4485$
$b_2 = 1.10123$; $b_4 = -1.75263$; $b_6 = -6.75615\times10^5$

Density of saturated vapor:

$$\ln\left(\frac{\rho''}{\rho_c}\right) = c_1\tau^{2/6} + c_2\tau^{4/6} + c_3\tau^{8/6} + c_4\tau^{18/6} + c_5\tau^{37/6} + c_6\tau^{71/6} \qquad \text{(S9.5-3)}$$

with

$c_1 = -2.02957$; $c_4 = -17.3151$
$c_2 = -2.68781$; $c_5 = -44.6384$
$c_3 = -5.38107$; $c_6 = -64.3486$

Specific Enthalpy and Entropy:

Auxiliary Equations:

$$\frac{\alpha}{\alpha_o} = d_\alpha + d_1\theta^{-19} + d_2\theta + d_3\theta^{4.5} + d_4\theta^{5} + d_5\theta^{54.5} \qquad \text{(S9.5-4)}$$

$$\frac{\phi}{\phi_o} = d_\phi + \frac{19}{20}d_1\theta^{-20} + d_2\ln\theta + \frac{9}{7}d_3\theta^{3.5} + \frac{5}{4}d_4\theta^{4} + \frac{109}{107}d_5\theta^{53.5} \qquad \text{(S9.5-5)}$$

with

$d_1 = -5.71756\times10^{-8}$; $d_5 = 9.68874\times10^{-1}$
$d_2 = 2.68981\times10^{+3}$; $d_\alpha = -1.135481615639\times10^{+3}$
$d_3 = 1.29889\times10^{+2}$; $d_\phi = 2.3189142\times10^{+3}$
$d_4 = -1.37181\times10^{+2}$

Specific enthalpy of saturated liquid

$$h' = \alpha + \frac{T}{\rho}\left(\frac{dP}{dT}\right) \qquad \text{(S9.5-6)}$$

Specific enthalpy of saturated vapor

$$h'' = \alpha + \left(\frac{T}{\rho''}\right)\left(\frac{dP}{dT}\right) \qquad \text{(S9.5-7)}$$

Specific entropy of saturated liquid

$$s' = \phi + \left(\frac{1}{\rho'}\right)\left(\frac{dP}{dT}\right) \qquad \text{(S9.5-8)}$$

Specific entropy of saturated vapor

$$s'' = \phi + \left(\frac{1}{\rho''}\right)\left(\frac{dP}{dT}\right) \qquad \text{(S9.5-9)}$$

The reference constants are:

$\alpha_0 = 1000.00$ J/kg; $\rho_c = 322.00$ kg/m^3
$T_c = 647.14$ K; $\phi_0 = \alpha_0/T_c$
$P_c = 22.064$ MPa

Considering the same equation as given for vapor pressure (i.e. equation S9.5.1), a subroutine was also developed to calculate saturation temperature for a given value of pressure.

Range of validity:

$$273.16 \text{ K} \leq T \leq 647.14 \text{ K}$$

S9.6. RESULTS AND DISCUSSIONS ON LIGHT WATER PROPERTIES

The thermophysical properties of light water have been calculated using the programs developed as described earlier. The calculated values are in excellent agreement with the values given in the corresponding references.

Nomenclature to Supplement S9

A : Helmholtz function, dimensionless
C_P : specific heat at constant pressure, J/(kg·K)
C_V : specific heat at constant volume, J/(kg·K)
G : specific Gibbs function, dimensionless
h : enthalpy, J/kg
P : pressure, MPa
s : specific entropy, J/(kg·K)
T : temperature, K
t : temperature,°C
w : speed of sound, m/s
ρ : density, kg/m^3
λ : thermal conductivity, W/(m·K)
μ : viscosity of light water, Pa·s
θ : T/T_c
τ : $1 - \theta$
χ_T : isothermal compressibility (symmetrized)

Subscripts:

c : critical point
sat : saturation property

Superscripts:

$'$: saturated liquid
$''$: saturated vapor
\- : dimensionless
* : reference value
** : derived referenced value

References to Supplement S9

[1] J. KESTIN, J.V. SENGERS, J. Phys. Chem. Ref. Data, 15, 1, 305 (1986)

[2] L. HAAR, J. S. GALLAGHEr, G.S.KELL, in Proceedings of the 8th Symposium on Thermophysical Properties, edited by J.V, Sengers (American Society of Mechanical Engineers, New York, 1982), Vol. II p. 198

[3] L. HAAR, J.S. GALLAGHER, and G.S. KELL, NBS/NRC Steam Tables (Hemisphere, Washington, 1984)

[4] J. V. SENGERS et al., "Improved international formulations for the viscosity and thermal conductivity of water substance", J. Phys. Chem. Ref. Data, Vol. 15, p. 1291 (1986)

[5] A. SAUL and W. WAGNER, "International equations for the saturation properties of ordinary water substance", J. Phys. Chem. Ref. Data, 16, 4, 893 (1987)

[6] J. R. COOPER, "Expressions for the thermodynamic properties of water in the ideal-gas limit", Int. J. Thermophysics, Vol. 3, p. 35 (1982)

[7] R. TUFEU et al., "Comparison of thermal conductivities of H_2O & D_2O", Int. J. of Thermophysics, Vol.7, p. 663 (1986)

[8] A. LAESECKE et al., "The MIDAS data-bank system for the transport properties of fluids", Int. J. of Thermophysics, Vol.7, p. 973 (1986)

[9] R. TUFEU et al., "Thermal conductivity of steam from 250 to 510°C at pressures up to 95 MPa including critical region", Int. J. of Thermophysics, Vol. 8, p. 283 (1987)

[10] W. V. WILDING et al., "Thermodynamic properties and vapor pressures of polar fluids from a four-parameter corresponding states method", Int. J. of Thermophysics, Vol. 8, p. 717 (1987)

[11] G.R. SOMAYAJULU, "A generalized equation for surface tension from triple point to the critical point", Int. J. of Thermophysics, Vol. 9, p. 559 (1988)

[12] "New equations for enthalpy of vaporization from the triple point to the critical point", G. R. Somayajulu, Int. J. of Thermophysics, Vol. 9, p. 567 (1988)

[13] G. A. OLCHOWY, "A simplified representation for the thermal conductivity of fluids in the critical region", Int. J. of Thermophysics, Vol. 10, p. 417 (1989)

[14] T. MAKITA, "A data base system for the thermophysical properties of 400 pure fluids & their binary mixtures", Int. J. of Thermophysics, Vol. 10, p. 727 (1989)

[15] B.A. GRIGORYEV, "Research on thermophysical properties of fluids at the Grozny Petroleum Institute (USSR)", Int. J. of Thermophysics, Vol. 11, p. 237 (1990)

[16] K. J. OKESON et al., "A four parameter corresponding states method for prediction of Newtonian, pure component viscosity", Int. J. of Thermophysics, Vol. 12, No. 1, p. 119 (1991)

[17] J. M. H. LEVELT SENGERS, W. L. GREER and J. V. SENGERS, "Scaled equation of state parameters for gases in the critical region", J. Phys. Chem. Ref. Data, Vol. 5, p. 1 (1976)

[18] J. T. R. WATSON, R. BASU and J. V. SENGERS, "An improved representative equation for the dynamic viscosity of water substance", J. Phys. Chem. Ref. Data, Vol. 9, p. 1255 (1980)

[19] P. G. HILL et al., "A fundamental equation of state for heavy water", J. of Physical and Chemical Reference Data, Vol. 11, p. 1 (1982)

[20] J. M. H. LEVELT SENGERS et al., "Thermodynamic properties of steam in the critical region", J. of Physical and Chemical Reference Data, Vol. 12, p. 1 (1983)

[21] B. KAMGAR-PARSI et al., "Thermodynamic properties of D2O in critical region", J. of Physical and Chemical Reference Data, Vol. 12, p. 513 (1983)

[22] N. B. VARGAFTIK et al., "International tables of the surface tension of water", J. of Physical and Chemical Reference Data, Vol. 12, p. 817 (1983)

[23] J. Kestin et al., "Thermophysical properties of fluid H_2O", J. of Physical and Chemical Reference Data, Vol. 13, p. 175 (1984)

[24] J. V. SENGERS and B. KAMGAR-PARSI, "Representative equations for the viscosity of water substance", J. Phys. Chem. Ref. Data, Vol. 13, p. 185 (1984)

[25] J. KESTIN et al., "Thermophysical properties of fluid D_2O", J. Phys. Chem. Ref. Data, Vol. 13, p. 601 (1984)

[26] J. V. SENGERS et al., "Representative equations for the thermal conductivity of water substance", J. Phys. Chem. Ref. Data, Vol. 13, p. 893 (1984)

[27] J. M. H. LEVELT SENGERS et al., "Assessment of critical parameter values of H_2O and D_2O", J. Phys. Chem. Ref. Data, Vol. 14, p. 193 (1985)
[28] J. KESTIN et al., "New international formulations for the thermodynamic properties of light and heavy water", J. Phys. Chem. Ref. Data, Vol. 15, p. 305 (1986)
[29] C. A. NIETO DE CASTRO, "Standard reference data for the thermal conductivity of liquids", J. Phys. Chem. Ref. Data, Vol. 15, p. 1073 (1986)
[30] SAUL,A., et al., "International equations for the saturation properties of ordinary water substance", J. Phys. Chem. Ref. Data, Vol. 16, p. 893 (1987)
[31] R. A. DOBBINS et al., "Pressure and density series equations of state for steam as derived from the Haar-Gallagher-Kell formulation", J. Phys. Chem. Ref. Data, Vol. 17, p. 1 (1988)
[32] H. SATO et al., "New international skeleton tables for the thermodynamic properties of water substance", J. Phys. Chem. Ref. Data, Vol. 17, p. 1439 (1988)
[33] A. SAUL et al., "A fundamental equation for water covering the range from melting line to 1273 K at pressures up to 25000 MPa", J. Phys. Chem. Ref. Data, Vol. 18, p. 1537 (1989)
[34] PHILIP G. Hill, "A unified fundamental equation for the thermodynamic properties of H_2O", J. of Physical and Chemical Reference Data, Vol. 19, No. 5, p. 1233 (1990)
[35] W. GILDSETH, A. HABENSCHUSS and F. H. SPEDDING, "Precision measurements of densities and thermal dilation of water between 5 and 80°C", J. Chem. Eng. Data, Vol. 17, p. 402 (1972)
[36] L. A. GUILDNER, D. P. JOHNSON and F. E. JONES, "Vapor pressure of water at its triple point", Science, Vol. 191, p. 1261 (1976)
[37] P. T. EUBANK, L. L. JOFFRION, M. R. PATEL and W. WAROWNY, "Experimental densities and virial coefficients for steam from 348 to 498 K with correction by absorption effects", J. Chem. Thermodynamics, Vol. 20, p. 1009 (1988)
[38] G. A. CHAPELA and J. S. ROWLINSON, "Accurate representation of thermodynamic properties near the critical point", J. Chem. Soc. Faraday, Vol. 170, p. 584 (1974)
[39] O. C. BRIDGEMAN and E. W. ALDRICH, "A reappraisal of the critical constants for water", Trans. ASME J. Heat Transfer, Vol. 87, p. 266 (1965)
[40] P. G. HILL and R. D. C. MCMILLAN, "The properties of steam: Current status", Trans. ASME J. Heat Transfer, Vol. 110, p. 763 (1988)
[41] F. G. KEYES, "The second virial coefficient for steam", Int. J. Heat Mass Trans., Vol. 5, p. 137 (1962)
[42] J. JUZA, V. KMONICEK, O. SIFNER and K. SCHOVANEC, "A contribution to the problem of thermodynamic similarity of H_2O and D_2O", Physica, Vol. 32, p. 362 (1966)
[43] C. A. ANGELL, M. OGUNI, and W. J. SICHINA, "Heat capacity of water at extremes of supercooling and superheating", J. Phys. Chem., Vol. 86, p. 998 (1982)
[44] G. S. KELL, G. E. MCLAURIN and E. WHALLEY, "PVT properties of water. II: Virial coefficients in the range 150-450°C without independent measurement of vapor volumes", J. Chem. Phys., Vol. 48, p. 3805 (1968)
[45] G. S. KELL, G. E. MCLAURIN and E. HALLEY, "PVT properties of water. III: Virial coefficients of D2O in the range 150-500°C", J. Chem. Phys., Vol. 49, p. 2839 (1968)
[46] T. GRINDLEY and J. E. LIND Jr., "PVT properties of water and mercury", J. Chem. Phys., Vol. 54, p. 3983 (1971)
[47] R. A. FINE and F. J. MILLERO, "Compressibility of water as a function of temperature and pressure", J. Chem. Phys., Vol. 59, p. 5529 (1973)
[48] G. S. KELL and E. WHALLEY, "Reanalysis of the density of liquid water in the range 0-150°C and 0-1 kbar", J. Chem. Phys., Vol. 62, p. 3496 (1975)
[49] Ter MINASSIAN, L. P. PRUZAN and A. SOULARD, "Thermodynamic properties of water under pressure up to 5 kbar and between 28 and 128°C. Estimations in the supercooled region down to -40°C", J. Chem. Phys., Vol. 75, p. 3064 (1981)
[50] D. E. HARE and C. M. SORENSEN, "Densities of supercooled H2O and D2O in 25 micron glass capillaries", J. Chem. Phys., Vol. 84, p. 5085 (1986)
[51] A. EGERTON and G. S. CALLENDAR, "An experimental study of the enthalpy of steam", Phil. Trans. Roy. Soc. (London), Vol. 252 A, p. 133 (1960)

[52] G. S. KELL and E. WHALLEY, "The PVT properties of water. I. Liquid water in the temperature range 0-150°C and at pressures up to 1 kbar", Phil. Trans. Roy. Soc., (London), Vol. 258 A, p. 565 (1965)

[53] S. ANGUS and D. M. NEWITT, "The measurements of the specific enthalpy of steam at pressures of 60 to 1000 bar and temperatures of 400 to 700°C", Phil. Trans. Roy. Soc. (London), Vol. 259 A, p. 107 (1966)

[54] G.S. KELL, G.E. MCLAURIN and E. WHALLEY, "The PVT properties of water. V: The fluid up to 1 kbar at 350 to 500°C and along the saturation line from 150 to 350°C", Phil. Trans. Roy. Soc. (London), Vol. 315 A, p. 235 (1985)

[55] G. S. KELL, G. E. MCLAURIN and E. WHALLEY, "The PVT properties of water. VI: Deuterium oxide in the range 150 to 500°C and 0 to 100 MPa", Phil. Trans. Roy. Soc. (London), Vol. 315 A, p. 247 (1985)

[56] G. S. KELL, G. E. MCLAURIN and E. WHALLEY, "The PVT properties of water. IV: Liquid water in the range 150 to 350°C, from saturation to 1 kbar", Proc. Roy. Soc. (London), Vol. 360 A, p. 389 (1978)

[57] G. S. KELL, G. E. MCLAURIN and E. WHALLEY, "PVT properties of water - VII. Vapor densities of light and heavy water from 150-350°C", Proc. Roy. Soc. (London), Vol. 425 A, p. 49 (1989).

NEXT PAGE(S) left BLANK

ABBREVIATIONS

AC	aluminium oxide concrete
ALUSELECT	data base for the thermophysical properties of aluminium alloys at the Royal Institute of Technology, Stockholm
ANL	Argonne National Laboratory, USA
AWCR	advanced water cooled reactors
BARC	Bhabha Atomic Research Center, Mumbai, India
BMI	Batelle Memorial Institute, USA
CIAE	China Institute of Atomic Energy, Beijing, China
CINDAS	Center for Information and Data Analysis, West Laffayette, USA
DTA	differential thermal analysis
ETR	Engineering Test Reactor
FROAXI	a computer code, see Supplement S1
HEDRC	High Energy Density Research Center, Russian Academy of Sciences, Moscow, Russian Federation
HEMATIC	Material Properties Database Center, Institute of Physics and Power Engineering, Obninsk, Russian Federation
HMTR	High Flux Material Test Reactor
IAPS	International Association for Properties of Steam
IAPWS	International Association for Pure Water and Steam
IFC	International Formulation Committee
IKE	Institute for Nuclear Technology and Energy Systems at University of Stuttgart, Germany
INF	Institute of Nuclear Fuels, Zbarslav, Czech Republic
INIS	bibliographical data base for nuclear materials available at FIZ-Karlsruhe (Fachinformationszentrum Karlsruhe, Germany)
IPPE	Institute of Physics and Power Engineering, Obninsk, Russian Federation
IPTS	International Practical Temperature Scale
IVTAN	Institute of High Temperatures, Russian Academy of Sciences, Moscow
IWGATWR	International Working Group on Advanced Technologies for Water Cooled Reactors

MATPRO	Material Properties Data base
METADEX	bibliographical data base for metallic materials available by FIZ-Karlsruhe
MTR	Material Testing Reactor
NBS	National Bureau of Standards, USA; now NIST (National Institute of Standards and Technology, USA)
NPP	nuclear power plant
NRI	Nuclear Research Institute Řež, Czech Republic
ORNL	Oak Ridge National Laboratory, USA
PHWR	pressurized heavy water reactor
RMSE	root mean square error
SC	silicate concrete
THERSYST	data base for thermophysical properties at Stuttgart University, Germany
TPRC	Thermophysical Properties Research Centre, Pudure University, West Laffayette, USA
TPSYS	data base for thermophysical properties in China
URD	US Utility Requirements Document
VISAR	laser differential interferometer
WWER-1000	water-water energy reactor type 1000, Russian Federation
ZDC	zirconium dioxide concrete

CONTRIBUTORS TO DRAFTING AND REVIEW

Belovsky, L.	Nuclear Research Institute, Řež, Czech Republic
Bobkov, V.P.	Head of HEMATIC Centre, Institute of Physics and Power Engineering Obninsk, Russian Federation
Boehm, A.	Universität Stuttgart, Institut für Kernenergetik und Energiesysteme, Stuttgart, Germany
Cleveland, J.	International Atomic Energy Agency
Dolas, P.K.	Bhabha Atomic Research Centre, Mumbai, India
Fink, J.K.	Argonne National Laboratory, Argonne, Illinois, USA
Fokin, L.R.	Institute for High Temperatures, Academy of Sciences, IVTAN Moscow, Russian Federation
Fortov, V.E.	High Energy Density Research Centre & Academy of Sciences, Moscow, Russian Federation
Hu, Chuanwen	Institute of Atomic Energy, Beijing, China
Ivashkevich, A.A.	Institute of Physics and Power Engineering Obninsk, Russian Federation
Jakab, J.	Nuclear Research Institute, Řež, Czech Republic
Jaroma-Weiland, G.	Universität Stuttgart, Institut für Kernenergetik und Energiesysteme, Stuttgart, Germany
Kanel, G.I.	High Energy Density Research Centre & Academy of Sciences, Moscow, Russian Federation
Kataoka, K.	International Atomic Energy Agency
Krett, V.	International Atomic Energy Agency
Li, Xiaohua	Institute of Atomic Energy, Beijing, China
Lu, Bin	Institute of Atomic Energy, Beijing, China
Lusternic, V.E.	Institute for High Temperatures, Academy of Sciences, IVTAN, Moscow, Russian Federation
Mitrofanova, T.V.	Institute of Physics and Power Engineering Obninsk, Russian Federation
Neuer, G.	Universität Stuttgart, Institut für Kernenergetik und Energiesysteme, Stuttgart, Germany
Onufriev, S.V.	High Energy Density Research Centre & Academy of Sciences, Moscow, Russian Federation
Pakhomov, E.P.	High Energy Density Research Centre & Academy of Sciences, Moscow, Russian Federation

Pesochin, V.R.	High Energy Density Research Centre & Academy of Sciences, Moscow, Russian Federation
Petukhov, V.A.	High Energy Density Research Centre & Academy of Sciences, Moscow, Russian Federation
Popov, V.N.	Moscow Energetic Institute, Moscow, Russian Federation
Preston, S.D.	AEA Technology, Risley, Warrington, Cheshire WA3 6AT, United Kingdom
Saha, D.	Bhabha Atomic Research Centre, Mumbai, India
Shestakov, E.N.	High Energy Density Research Centre & Academy of Sciences, Moscow, Russian Federation
Sinha, G.K.	Bhabha Atomic Research Centre, Mumbai, India
Smogalev, I.P.	Institute of Physics and Power Engineering Obninsk, Russian Federation
Raj, Venkat V.	Bhabha Atomic Research Centre, Mumbai, India
Vinogradov, V.N.	Institute of Physics and Power Engineering Obninsk, Russian Federation
Xu, Hanming	Institute of Atomic Energy, Beijing, China
Ye, Changyuan	Institute of Atomic Energy, Beijing, China
Zhang, Lili	Institute of Atomic Energy, Beijing, China
Zhong, Jianguo	Institute of Atomic Energy, Beijing, China

97-01671